



Aalborg Universitet

AALBORG UNIVERSITY  
DENMARK

## MODELLING AND CONTROL OF INTELLIGENT GLAZED FACADE

Liu, Mingzhe

*Publication date:*  
2014

*Document Version*  
Accepted author manuscript, peer reviewed version

[Link to publication from Aalborg University](#)

*Citation for published version (APA):*  
Liu, M. (2014). *MODELLING AND CONTROL OF INTELLIGENT GLAZED FACADE.*

### General rights

Copyright and moral rights for the publications made accessible in the public portal are retained by the authors and/or other copyright owners and it is a condition of accessing publications that users recognise and abide by the legal requirements associated with these rights.

- Users may download and print one copy of any publication from the public portal for the purpose of private study or research.
- You may not further distribute the material or use it for any profit-making activity or commercial gain
- You may freely distribute the URL identifying the publication in the public portal -

### Take down policy

If you believe that this document breaches copyright please contact us at [vbn@aub.aau.dk](mailto:vbn@aub.aau.dk) providing details, and we will remove access to the work immediately and investigate your claim.

# MODELLING AND CONTROL OF INTELLIGENT GLAZED FACADE

By

MINGZHE LIU



**AALBORG UNIVERSITY**  
DENMARK

**PhD Thesis**

**Defended in public at Aalborg University**

**Dissertation submitted 11/20/2014**

Thesis submitted: November 20, 2014  
PhD supervisor: Senior Researcher Kim B. Wittchen,  
Danish Building Research Institute (SBI), Aalborg University  
Assistant PhD supervisor: Prof. Per K. Heiselberg,  
Department of Civil Engineering, Aalborg University  
PhD committee: Associate Prof. Rasmus Lund Jensen, Aalborg University  
Prof. Arild Gustavsen, Norwegian University of Science and Technology-NTNU  
Senior Researcher Åke Blomsterberg, Lund University and WSP Environmental  
  
PhD Series: Faculty of TEK-NAT, Aalborg University

ISSN: xxxx- xxxx

ISBN: xxx-xx-xxxx-xxx-x

Published by:

Aalborg University Press

Skjernvej 4A, 2nd floor

DK – 9220 Aalborg Ø

Phone: +45 99407140

aauf@forlag.aau.dk

© Copyright by author

Printed in Denmark by Rosendahls, 2014

# CURRICULUM VITAE

## Personal Details

Name: Mingzhe Liu  
Date of Birth: 1984-08-18  
Nationality: Chinese  
Phone: +45-71438528  
Email: [whitelmz@hotmail.com](mailto:whitelmz@hotmail.com)  
Availability : From: 1st Sep 2014  
Legal status Working permit of Denmark  
Credentials: LEED AP, LEED GA



## Professional Experience

2011.10 – Current Danish Building Research Institute (SBI) Aalborg University  
2012.01 – 2012.05 Shenzhen Yuezhong Green Building Sc-Tech Development, China  
2010.10 – 2011.10 Aalborg University Denmark --- Research assistant  
2009.12 – 2010.06 R&D Department of Permasteelisa Group, Scholdebouw The Netherlands --- Internship  
2009.09 – 2009.12 Technology University of Delft Design Competition, The Netherlands  
2007.06 – 2008.01 Architectural design institute of logistics department of Chinese Army--- Internship  
2006.06 – 2006.08 Cultural Heritage institute of Hunan Province, China

## Education

2011.10 – 2014.9 Aalborg University, Denmark --- PhD Fellowship  
2008.09 – 2010.06 Technology University of Delft, The Netherlands --- Master of Building Technology.  
2003.09 – 2008.08 Hunan University, China --- Bachelor of Architecture

## Certifications

LEED AP (BD+C), LEED GA

## Computer skills

Good knowledge of Microsoft office, EnergyPlus, BSim, ECOTECT, WIS, Optics5, AutoCAD, Rhino, SketchUp, Labview, Matlab, Trisco, Capsol,.

## Language Skill

English : Fluent

Danish: Danskuddannelse 3.3

Mandarin : Native

## ABSTRACT

An intelligent glazed facade is defined as having dynamic control of thermal and solar properties (U-value, g value, light transmittance, natural ventilation and night cooling) by using existing facade technologies (insulated shutter, venetian blind, control of opening and closing windows). Energy consumption and indoor comfort of buildings could be greatly reduced and optimized by proper and integrated control of intelligent facade together with building services (heating, cooling, lighting and ventilation) according to the outdoor microclimate and the requirements of indoor environment. However, it is necessary to be able to simulate the dynamic function in Danish building simulation tool (BSim) and building compliance tool (Be10) in order to demonstrate the advantages of intelligent glazed facade. There is also a need for developing control strategies for the intelligent facade and the building services using the facade technologies to comply with future energy requirements of the building regulations. Therefore, a simplified method has been developed for the intelligent glazed façade, which has been compared with both numerical tool (BSim) and empirical data. Additionally, control strategies of intelligent facade with building services which mainly focus on office buildings have been developed and tested.

The simplified method calculates the thermal and solar properties of the facade under a defined control strategy. In order to investigate the influence of the facade on the performance of the entire building, a room model is also involved in the method according to the simple hour method by ISO EN 13790. The simplified method is compared with the Danish building simulation tool BSim in an hourly calculation with the weather data of the Danish reference year. Results show good correlation in indoor air temperature and solar transmittance and acceptable correlation in illuminance level, energy demands of heating, cooling, lighting and ventilation between the simplified method and BSim.

Integrated control strategies of the intelligent facade and building services have been developed taking both the indoor comfort and energy performance into consideration. The results show that the yearly primary energy demand of an office building with an intelligent glazed facade can be reduced by around 60 % compared with the same room without the intelligent facade. Together with the improvement of the thermal properties and efficiencies of other building elements, the building with the intelligent glazed facade can comply with the energy requirements of the Building Class 2020, which cannot be fulfilled by the building with the static facade. The comfort performance of the building can also be improved by the intelligent glazed facade. Buildings can also increase their ratio of glazing on the facade by using the intelligent facade without compromising the energy need or the indoor climate. The facade glazing ratio with the lowest energy consumption is increased to around 45 % for the building with the intelligent glazed facade compared to that of 20 % for the building with a static facade. At a glazing ratio of 90 %, the building with the intelligent facade still complies with the energy requirement of Low Energy Class 2015 with an energy consumption of 38 kWh/m<sup>2</sup>/year.

An experiment has been conducted to evaluate the simplified method and to test the control strategies of the intelligent facade. According to the results of the comparison, the calculated air temperature has good agreements with the measurements in Danish climate, with R<sup>2</sup> value of 0.8. Additionally, the total cooling energy consumption calculated by the simplified method is 13.6 % higher than the measured cooling energy consumption. The experiment also points out that the holistic control strategy integrating intelligent facade together with building services works as expected.

## DANSK RESUMÉ

En intelligent glasfacade defineres ved at have dynamisk styring af termiske og optiske egenskaber (U-værdi, g-værdi, lystransmittans, naturlig ventilation og nat køling) ved hjælp af eksisterende facade teknologier (isoleret skodde, persienne, styring af åbning og lukning af vinduer). Energiforbruget og indeklimaet i bygninger kan reduceres og optimeres betragteligt ved korrekt og integreret styring af intelligente facader sammen med bygningens servicesystemer (opvarmning, køling, belysning og ventilation) ud fra udendørs mikroklima og kravene for indendørsklima. Men det er nødvendigt at simulere den dynamiske funktion i et værktøj til dynamisk simulering af bygningens termiske indeklima, BSim, og i værktøjet, Be10 – til vurdering, at bygningen overholder energikravene i Bygningsreglementet, for at kunne demonstrere fordelene ved intelligente glasfacader. Der er også et behov for at udvikle styringsstrategier til de intelligente facader og bygnings-servicesystemer der gør det muligt at udnytte facadeteknologierne til at overholde fremtidige energikrav. Derfor er en forenklet metode blevet udviklet til beregning af den intelligente glasfacade, som er blevet sammenlignet med både et numerisk værktøj (BSim) og empiriske data. Derudover er styringsstrategier for intelligente facader i samspil med bygningens servicesystemer, hovedsageligt med fokus på kontorbygninger, blevet udviklet og testet.

Den forenkledede metode beregner termiske og sol-transmissions egenskaber af facaden under en defineret styringsstrategi. For at undersøge facadens indflydelse på hele bygningens ydelse, er en rummodel også implementeret i metoden jf. den enkle time-metode beskrevet i ISO EN 13790. Den forenkledede metode sammenlignes med BSim i en simulering med timebaserede vejrdata for det danske referenceår. Resultaterne viser god korrelation i indendørs lufttemperatur og soltransmittans og en acceptabel korrelation for niveauet af belysningsstyrke, energibehov til opvarmning, køling, belysning og ventilation mellem den forenkledede metode og BSim.

Integrerede styringsstrategier for intelligente facader og en bygnings energimæssige ydeevne er blevet udviklet med både indendørs komfort og energieffektivitet taget i betragtning. Resultaterne viser, at det årlige behov for primær energi i et rum i en kontorbygning med intelligente glasfacader kan reduceres med omkring 60 % sammenlignet med samme rum, uden intelligente facader. Sammen med forbedringen af de termiske egenskaber og effektiviteten af andre bygningsdele, kan bygningen med intelligent glasfacade opfylde energikravene til Bygningsklasse 2020, hvilket ikke kan opfyldes af en bygning med en statisk facade. Den termiske komfort i bygningen kan samtidig forbedres med en intelligent glasfacade. Det er også muligt at øge bygningens andel af glas i facaden ved brug af intelligente facader uden at kompromittere energibehovet eller indeklimaet. I bygningen med intelligente facader opnås det laveste energibehov ved en andel af facadevinduer omkring 45 % hvorimod det laveste energibehov opnås for 20 % facadevinduer i bygningen med en statisk facade. Ved en vinduesandel på 90 %, kan bygningen med den intelligente facade stadig overholde energikravet for Lavenergiklasse 2015 med et energiforbrug på 38 kWh/m<sup>2</sup>/år.

Et eksperiment er blevet udført for at vurdere den forenkledede metode og for at afprøve styringsstrategierne for den intelligente facade. Ifølge resultaterne fra sammenligningen, er den beregnede lufttemperatur i god overensstemmelse med målingerne fra et rum udsat for det danske klima, med en R<sup>2</sup>-værdi på 0,8. Dog er det samlede energiforbrug til køling beregnet af den forenkledede metode 30 % højere end det målte. Eksperimentet påpeger også, at den helhedsorienterede styringsstrategi der integrerer en intelligent facade sammen med bygningens servicesystemer fungerer som forventet.

## NOMENCLATURE

$E_{ref}$	energy gain of window	[kWh / m <sup>2</sup> ]
$g_w$	total solar energy transmittance of the window	[-]
$U_w$	thermal transmission coefficient of the window	[W/(m <sup>2</sup> K)]
$g_t$	total solar energy transmittance of the glazing with external solar protection device	[-]
$\tau_{e,B}$	solar transmittance of the solar protection device	[-]
$g$	total solar transmittance of glazing	[-]
$\alpha_{e,B}$	the solar absorptance of the solar protection device	[-]
$G_1$	equals to 5	[W/(m <sup>2</sup> K)]
$G_2$	equals to 10	[W/(m <sup>2</sup> K)]
$\beta$	angle between the slat and the horizontal plan.	[°]
$\alpha$	solar altitude angle	[°]
$H$	distance between the slats	[mm]
$W$	width of the slats	[mm]
$\Phi_{facade}$	heat flow through the facade	[W/m <sup>2</sup> ]
$\Phi_{sol}$	solar radiation on the glazed facade	[W/m <sup>2</sup> ]
$g_g$	solar transmittance of the facade	[-]
$U_g$	U-value of the glazing facade	[W/(m <sup>2</sup> K)]
$T_i$	indoor air temperature	[°C]
$T_o$	outdoor air temperature	[°C]
$g_{g+shutter}$	solar transmittance of the glazing together with the shutter	[-]
$U_{g+shutter}$	U-value of the glazing together with the shutter	[W/(m <sup>2</sup> ·K)]

# CONTENTS

MODELLING AND CONTROL OF INTELLIGENT GLAZED FACADE .....	1
ABSTRACT .....	1
DANSK RESUMÉ .....	2
NOMENCLATURE .....	3
CONTENTS .....	4
PREFACE.....	6
INTRODUCTION .....	7
1. INTELLIGENT GLAZED FACADE VS STATIC FACADE.....	7
1.1 SIMULATION TOOLS FOR INTELLIGENT FACADE .....	8
1.2 CONTROL STRATEGIES OF INTELLIGENT FACADE .....	8
1.3 OBJECTIVES AND RESEARCH QUESTIONS .....	9
1.4 METHODOLOGY .....	10
1.5 THESIS OUTLINE.....	11
PART I – SIMPLIFIED METHOD OF INTELLIGENT GLAZED FACADE .....	12
2. DEVELOPMENT OF SIMPLIFIED METHOD FOR INTELLIGENT GLAZED FACADE .....	13
2.1 SIMPLIFIED MODELLING OF DOUBLE GLAZING UNIT .....	13
2.2 SIMPLIFIED MODELLING OF GLAZED FACADE WITH NIGHT INSULATION .....	14
2.3 SIMPLIFIED MODELLING OF SOLAR SHADING .....	15
2.4 MODELLING OF ROOM AND BUILDING SERVICES ACCORDING TO EN 13790 .....	16
2.5 CONCLUSION AND ADVANTAGES OF THE SIMPLIFIED METHOD .....	16
3. VERIFICATION OF THE SIMPLIFIED METHOD WITH BSIM .....	17
3.1 COMPARISON BETWEEN THE SIMPLIFIED METHOD AND BSIM .....	17
3.2 CONCLUSION.....	20
4. VERIFICATION OF THE METHOD WITH EXPERIMENTAL MEASUREMENTS .....	20
4.1 EXPERIMENT SETUP .....	20
4.2 MEASUREMENTS AND UNCERTAINTY .....	23
4.3 CONTROL OF FACADE AND BUILDING SERVICES .....	25
4.4 COMPARISON: SIMPLIFIED METHOD AND EXPERIMENTAL MEASUREMENT .....	27
4.5 CONCLUSION.....	34
5. CONCLUSION OF PART I.....	35
PART II - CONTROL STRATEGIES OF THE INTELLIGENT GLAZED FACADE .....	36
6. CONTROL STRATEGIES: OFFICE BUILDINGS WITH INTELLIGENT GLAZED FACADE .....	37
6.1 DEVELOPMENT OF CONTROL STRATEGIES FOR DIFFERENT FACADE ELEMENTS... ..	37
6.2 CASE STUDY.....	41
6.3 SENSITIVITY ANALYSIS OF CONTROL STRATEGIES--- BASED ON DIFFERENT BUILDING DESIGN.....	46
6.4 CONCLUSION.....	51
7. TEST OF THE CONTROL STRATEGIES IN THE FULL-SCALE TEST FACILITY (CUBE).....	51



8. CONCLUSION OF PART II .....	51
CONCLUSION OF THE THESIS .....	52
FUTURE WORK .....	53
REFERENCES .....	54
PUBLICATIONS .....	57

## PREFACE

This thesis represents a part of the fulfilment for acquiring the PhD degree. The thesis will be presented at Aalborg University, Denmark.

The PhD study is carried out as part of the Strategic Research Centre for Zero-energy-buildings at Aalborg University and financed by Danish aluminium section of the Danish Construction Association, Aalborg University and The Danish Council for Strategic Research (DSF), the Programme Commission for Sustainable Energy and Environment. This PhD project is supervised by Senior Researcher Kim Wittchen, Danish Building Research Institute (SBI) and Professor Per Heiselberg, Department of Civil Engineering both at Aalborg University, Denmark.

The project is divided into two larger sections. The first section contains development of a simplified method and control strategies of intelligent glazed facade. The second section presents the experimental results performed during this research.

I would like to thank both Kim Wittchen and Per Heiselberg for their continuous guidance, their inspiring and fruitful discussions and their support and faith in me. Also, I want to thank Rasmus Lund Jensen for his guidance and constructive comments. Additionally, I would like to express my thanks to all my colleagues from the Indoor Environmental Engineering Research Group, Strategic Research Centre on ZEBs, and others at the Department of Civil Engineering.

Finally, I would like to thank my family and friends for believing in me and for supporting me through the rough patches that turn up on the road once in a while.

Mingzhe Liu

September 2014

# INTRODUCTION

In the European Union, buildings are responsible for 40 % of the total energy consumption and for 36 % of CO<sup>2</sup> emissions. The energy performance of buildings is the key to achieving the EU Climate and Energy objectives, namely the reduction of 20 % of the greenhouse gases emissions and 20 % energy savings by 2020 (based on the level of 2005) [1]. Future energy regulations in Denmark aim at reducing the energy demand in new buildings by 25% (to approx. 73 kWh/m<sup>2</sup> per year<sup>1</sup>) in 2010, 50% (to approx. 42 kWh/m<sup>2</sup> per year<sup>1</sup>) in 2015 and 75% (to 25 kWh/m<sup>2</sup> per year) in 2020 compared with the energy regulations of 2008 (95 kWh/m<sup>2</sup> per year) [2]. To successfully achieve this goal it is necessary to identify and develop innovative building and energy technologies and solutions for medium and long-term periods.

The main parameter influencing the building energy-performance is the facade [3]. At present, there is a trend of increased use of glazed facades for office building because of the requirement of higher light transmittance and better views by users, but its thermal properties need serious improvement. The objective of this thesis is to develop a simplified method and holistic control strategy for the intelligent glazed facade integrated with building services in order to minimize the energy consumption and optimize the indoor comfort of office buildings.

The first part will introduce general information about the different methods and control strategies of dynamic facade. Additionally, a literature review gave an overview of the current knowledge in this field.

## 1. INTELLIGENT GLAZED FAÇADE VS STATIC FAÇADE

There are two trends involving glazing and facade development: 1) advances based on new materials science breakthroughs at the scale of microstructures and 2) simultaneous development and interest in full-scale facades where solar control, daylight redirection and ventilation air are all supplied by the new envelope systems [4]. This PhD project focuses on the full-scale intelligent glazed facade with single skin (double glazing and triple glazing). The controlled technologies are developed in following areas:

- Control of solar shading (venetian blind)
- Control of heat transport (glazing and night shutter)
- Control of mass transport (natural ventilation and night cooling)
- Control of building services (heating, cooling, lighting and ventilation)

The envelope systems should react sensibly to the changes in the exterior climate and adjust solar loads, day lighting, heat loss, ventilation, and venting to the changing needs of the occupants and the building.

Previous studies show that the introduction of dynamic facade solutions to regular office buildings can reduce the entire energy demand significantly and fulfil the energy requirements in the Danish Building Regulations for Building Class 2020 [5]. The results from the study on static solutions of facade show that the energy demand cannot be reduced significantly simply by optimizing technologies.

In connection with the enhanced requirements in Danish Building Regulations (BR10) [2] it has been decided to require energy labelled window systems with energy surplus i. e. a positive  $E_{ref}$ :

$$E_{ref} = 196,4 \times g_w - 90,36 \times U_w \quad (1)$$

Where:

$g_w$ : Total solar energy transmittance of the window.

$U_w$ : Thermal transmission coefficient of the window.

It is required that all buildings complying with Building Class 2020 should at least have an  $E_{ref}$  value of 0 kWh/m<sup>2</sup> per year. However, studies shows that energy consumptions of office buildings do not decrease with the increase of  $E_{ref}$  value [6, 7], which means energy consumption of buildings cannot be reduced by simply improving static properties (U-value and g value) of the facade. Lower U-values are for example helpful in reducing the heating demand, and lower g-values are helpful in reducing the cooling demand. Focusing only on one of these energy demands will result in higher energy demand of the other energy demand and not necessarily a reduction of the total energy demand. Focus should be put on design and control of the facade in correlation with the usage of the building and the microclimate as well as the architecture.

---

<sup>1</sup> For a non-residential building with 1000 m<sup>2</sup> heated gross floor area.

## 1.1 SIMULATION TOOLS FOR INTELLIGENT FACADE

The ability of an architect or engineer to accurately predict the performance of an advanced facade system is much better than in the past but there are still significant limitations that impede widespread use of the intelligent facade systems [4].

Different calculation methods have been developed to model one or more properties of the intelligent facade:

- Some stand-alone calculation methods have been developed to simulate some of the aspects for glazed facade, blind, insulation and ventilation [8, 9].
- A two-dimensional numerical model for single story multiple-skin facades with mechanical as well as natural ventilation was developed. But the use of model is restricted to multiple-skin facades with roller blinds [10].
- A method presented in [11] can be used to investigate the impact of different control strategies for shading devices on energy demand and visual comfort. With the help of the method, the cut-off control strategy seemed to be a good compromise in summer for the balance between solar loads and visual comfort requirements. However, the secondary heat gains caused by the absorption of solar energy in the slats of the venetian blind were missing.
- Methods for realistic performance evaluation of solar control properties of facades with solar shading or other solar control systems were developed by [12-14]. They contributed to the determination of the angular dependent total solar transmittance and calculation of effective monthly or hourly g-values. The models were more accurate than other methods and could be used to improve the formulas given in the European Standard EN13363 [15, 16].
- A simplified building simulation tool presented in [17, 18] was to evaluate the energy demand and the thermal indoor environment in the early stages of the building design. The tool gave reliable results compared to detailed tools and needs only few input data to perform a calculation.
- The simplified methods for double glazing units and glazed facades with night shutter were developed by our research group [19-21]. They showed good agreement with experiment data, which made them part of the simplified method to simulate the entire performance of the intelligent facade.
- Approaches for estimating daylight and lighting energy savings with daylighting schemes were presented in [22]. The work was helpful to compute accurately the interior daylight illuminance and to determine the long-term energy use of internal spaces with appropriate daylight-linked lighting controls.

Some simulation tools like BSim [23] and EnergyPlus [24] have the function of quantifying the impact of controlled facade on energy and comfort performance of buildings. However, the control strategies included in the tools are limited and defined by the tools, so they are not flexible enough to investigate different control strategies for facades designed by the users.

In Denmark, all the features of facades in the building compliance programme (Be10) [25] are still static at present; the programme is not sophisticated enough to estimate and evaluate the performance of future intelligent glazed facades in the design and certification stages.

The intelligent facade is capable of controlling different facade elements together with building services. Since most of the methods above are for a single element of the facade and the complex tools are not flexible enough, the properties of the intelligent facade and its influence on the indoor environment cannot be fully covered in these methods. It is necessary to realize a holistic method for a building with intelligent facade, which is flexible enough to accept different control strategies, by integrating the existing strategy or by developing new calculation algorithms of different facade elements. Therefore, the first part of this thesis (Part I) will focus on developing a simplified method to investigate the influence of the intelligent glazed facade on the energy and comfort performance of office rooms. A room model is also included in the method according to the simple hourly method in ISO EN 13790 [26] to achieve the purpose

## 1.2 CONTROL STRATEGIES OF INTELLIGENT FACADE

Facade systems in buildings, ranging from single windows to complete glass facades, share some common performance requirements. These requirements are often in conflict with each other and they often change over short and long time frames [4]. Facades provide view but must control glare. They admit daylight but must control solar transmittance to reduce cooling needs. They provide a degree of connection with the outdoors or

psychological comfort but they must also maintain physical comfort in the face of temperature and solar extremes. They provide natural ventilation but admit undesired air leakage and can create drafts. Most glazing and windows themselves are intrinsically static but they must respond over a wide range of climate and use conditions [4]. Therefore, all the functions of a facade system need to be controlled to realize a trade-off strategy in different conditions and to optimize comfort and energy performance. Smarter building operation is necessary to meet the goal of lower energy consumption and better indoor comfort, and control systems need to integrate strategies that support all aspects of complex facade functions [4, 27].

- Some control strategies have been developed for glazed facade systems [11, 28], but most of them are stand-alone control systems only for one facade function or not in relation to building services.
- Existing models of control patterns for occupant-shading interactions in office buildings and their influence in terms of energy demand are reviewed in [29]. Energy performance and visual comfort are investigated for eleven control strategies.
- The potential of dynamic solar shading is quantified in [30] with the simulated results from an investigation of three different solar shading types. The annual energy demand can be reduced by 16 % for a south-facing facade using dynamic shading.
- The difference between static and dynamic control of interior and exterior blind systems in office buildings is addressed in [31]. Optimal control can achieve energy savings of 7 -17 % compared with manual control and without blind control. Additionally, the energy performance of blind systems can be significantly improved by applying daylight control.
- The impact of glazing area, shading device properties and shading control on building cooling and lighting energy use in perimeter spaces are evaluated in [32]. Shading control accounted for a 50 % decrease in annual cooling energy demand compared with the case without shading. Although electric lighting demand is increased, the total annual energy demand is still reduced by 12%.
- The impact of management strategies for external mobile shading and cooling by natural ventilation is focused on in [33]. The control modes have to be carefully selected with regard to building's characteristics and local weather conditions.
- A comprehensive analysis is presented in [34] studying the balance between daylighting benefits and energy requirements in perimeter office spaces with interior roller shades considering glazing properties, shading properties and control together with window size, climate and orientation integrating daylight and thermal needs. The analysis reveals that windows occupying 30-50 % of the facade can actually result in lower total energy consumption for most cases with automated shading [34]. The analysis also points out the best designs for each orientation and location based on both daylighting and thermal results.
- In [35] both cooling energy and fan electrical energy are saved with the help of well-designed natural ventilation systems compared with mechanical cooling and ventilation. It is possible to save cooling energy between 13 and 44 kWh/m<sup>2</sup> per year at Stuttgart, Turin and Istanbul, and additionally savings in fan ventilation electrical energy can be around 4 kWh/m<sup>2</sup> per year.

The previous studies focus on the investigation of the controlling of one or more of the facade elements separately. It is necessary to conduct investigations on a holistic control of both facade system and building services. Therefore, the second part of the thesis (Part II) focuses on the development of the control strategies of the intelligent glazed facade together with building services. The influence of the control strategies is evaluated on both the energy consumption and the indoor comfort level.

### 1.3 OBJECTIVES AND RESEARCH QUESTIONS

In order to support the advantages of the intelligent facade and demonstrate its influence on the energy and comfort performance of office buildings, it is necessary to develop a calculation method to be integrated into the Danish building simulation tool (BSim) and the compliance checking tool (Be10). Additionally, proper and holistic control strategies of intelligent facade and building services will enhance its influence on the saving of energy and improvement of comfort.

This study is based on both simulations and full-scale experiments. Experiments are useful to validate the numerical method and also obtain more details about the control strategies.

The objectives of the thesis are to:

- Provide models for the intelligent glazed facades to be used in simulation tools BSim and Be10 for the design and certification of future low energy buildings.
- Develop holistic control strategies for the intelligent facade and building services (heating, cooling, ventilation, and lighting) to optimize the energy performance and indoor environment in office buildings.
- Compare the simplified method and Danish building simulation tool BSim.
- Conduct experimental verification of the model and test of control strategies.
- Estimate the energy savings and indoor climate improvements of the future low energy buildings with intelligent glazed facades.

The simplified method integrates the existing and newly developed algorithms to fulfil the requirements. It includes both the facade model and the room model. The facade model consists of the algorithms of glazing, glazing with external insulation, glazing with venetian blind, and it also calculates the internal surface temperature of the glazing to evaluate the thermal comfort. Both the algorithms of glazing and blind take the solar incident angle into consideration. The room model is developed according to ISO EN 13790, considering the change of the facade elements (insulation, blind, natural ventilation and night cooling) and the operation of the building services. The simplified method is compared with BSim on the calculation of indoor air temperature and yearly total energy demands.

The verification of the simplified method is conducted by comparing the calculated and measured internal surface temperature, indoor air temperature, energy loads and total energy consumptions during the experiment period. The influence of insulated shutter on the heating demand is not verified in the experiment due to the warm weather during the experiment period. The energy consumption of ventilation is calculated and verified by simulation tool but not the experimental measurements.

The evaluation of the indoor comfort by numerical calculation focuses on the visual comfort (glare check on eye level and the illuminance level on the working plane) and the thermal comfort (operative temperature of the room).

#### 1.4 METHODOLOGY

The simplified method requires integrated properties of different facade technologies to achieve reliable calculations of energy and comfort performance under variable façade control strategies. In addition, it also needs capability of conducting hourly calculation for one year with acceptable computation time. Part I of the study was the development of the simplified method. The method was divided into two main parts: 1--- the method of intelligent façade, which includes model of double glazing unit, model of night shutter and model of venetian blind; 2--- the method of entire building or room, which is an one-zone hourly model built according to EN 13790 [26].

The model of double glazing unit was built utilising algorithms from EN 410 [36] and EN 673 [37] for calculating solar and thermal properties, which was the same as the principle in software WIS. Additionally, in order to simulate indoor comfort in terms of internal surface temperature of façade, the model was integrated with finite volume energy balance equations as the principle described by Clarke [38]. Detail description of the model can be found in Paper 1 and 3 [19, 21].

The calculation of glazed facade with night shutter was created based on the model of double glazing unit by considering one more insulation layer and infiltration through the cavity between the glazing and the insulation. Detail information of the model is described in Paper 2 [20].

The calculation of glazed façade with venetian blind was implemented by integrating the model of double glazing unit and the model of venetian blind. The model of venetian blind was built based on the algorithms described in EN 13363 [15, 16].

The one-zone building model took thermal properties of all the building elements and building services into account, including the control strategies of natural ventilation and night cooling of the intelligent façade.

The simplified method was first verified by Danish building simulation tool BSim (Paper 4 [39]). Then experiment measurements were performed in the test facility “The Cube” at Aalborg University with two purposes: verification on the accuracy of the simplified method and test of performance of the control strategies. Paper 5 describes detail of the verification [40].

The full literature review of the method and experiment is to be found in the papers. Only the most central papers and methods are referred in the thesis.

## 1.5 THESIS OUTLINE

The thesis is divided into two parts. Part I---- Chapter 2, 3, 4 and 5, presents the development and the verification of the simplified method of intelligent glazed facade. Part II ---- Chapters 6, 7 and 8, presents the development and the test of the control strategies of intelligent glazed façade.

Chapter 2 presents calculation models of different façade technologies including double glazing unit (Paper 1 and Paper 3), glazed façade with insulation (Paper 2) and solar shading. Modelling of other parts of a room is also described in this chapter (Paper 4). Combining above models, a simplified method is created for simulating the performance of buildings with intelligent glazed façade.

Chapter 3 presents the verification of simplified method and Danish building simulation tool BSim (Paper 4). Calculations are conducted by both simplified method and BSim. Results are compared between the two methods in terms of calculating energy consumptions and thermal properties.

In Chapters 4, the verification of the simplified method with experimental measurements is presented. Paper 1, 2, 3 and 5 describe details of the verification.

Chapter 5 concludes Part I.

Chapter 6 elaborates controlling strategies of intelligent glazed façade and the performance of buildings utilising intelligent façade with a case study. Paper 6 provides further details.

Chapter 7 explains the experiment measurements applied on the test of the control strategies and the results of the test.

Chapter 8 concludes Part I.

Finally, conclusions of the entire project are drawn, and recommendations for future research are presented.

**PART I – SIMPLIFIED METHOD OF INTELLIGENT  
GLAZED FACADE**



## 2. DEVELOPMENT OF SIMPLIFIED METHOD FOR INTELLIGENT GLAZED FACADE

Figure 1 shows a sample office room installed with intelligent glazed facade. With the control of different facade elements, the energy demand can be minimized without sacrificing indoor comfort.

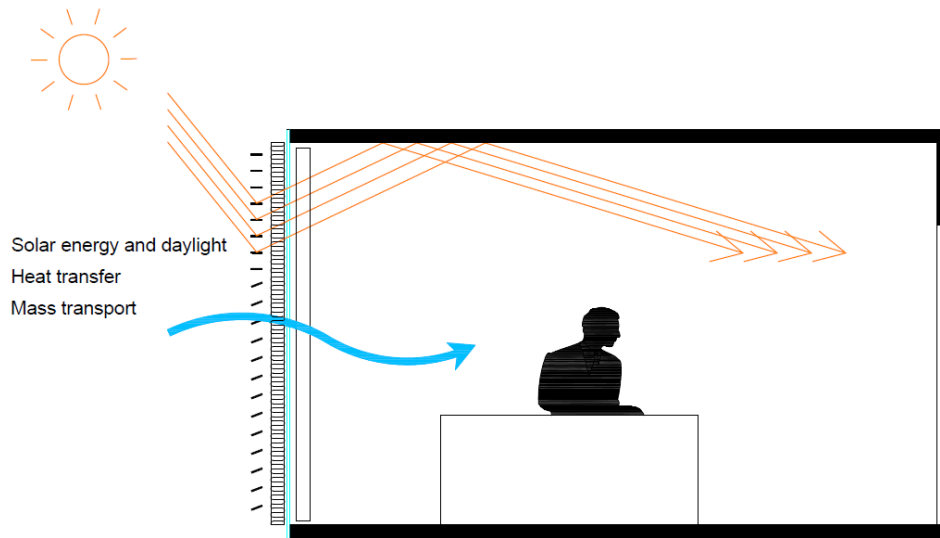


Figure 1: Room model with intelligent glazed facade

Figure 2 shows the structure of the simplified method. The core part of the method is the algorithms of facade elements (red dashed frame), which contains algorithms of different facade elements: double glazing unit (triple glazing unit), insulated shutter, solar shading (venetian blind), natural ventilation and night cooling. The one-zone room model based on the hourly simple method in ISO EN 13790 is integrated in order to demonstrate the influence of the intelligent facade on the energy and comfort performance of buildings. By setting the input of weather data and indoor comfort requirements, the parameters of energy demand, thermal comfort and visual comfort will be calculated. The method is flexible in evaluating different control strategies.

This chapter describes the details of the method.

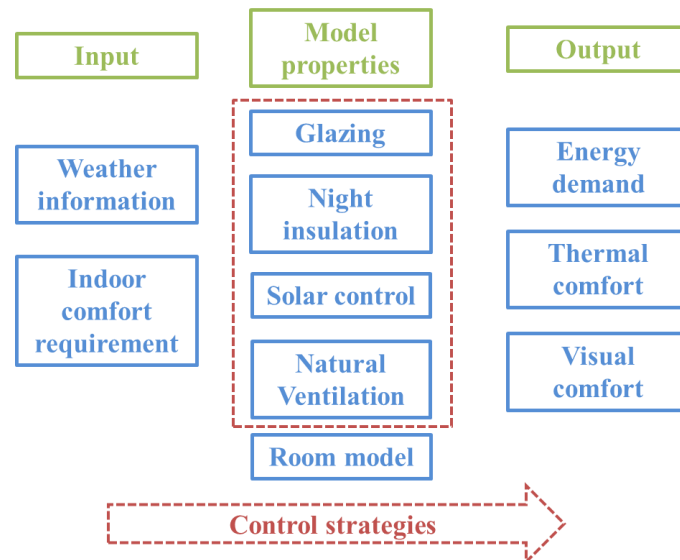


Figure 2: Structure of the simplified method.

### 2.1 SIMPLIFIED MODELLING OF DOUBLE GLAZING UNIT

The method is developed to calculate the performance of the double glazing facade. The known U-value of the glazing is input to the method, while the internal surface temperature of the glazing is calculated according to the properties of the glazing by solving the heat balance equations of two variables (the internal glazing surface

temperature  $T_{is}$  and the external glazing surface temperature  $T_{os}$ ). Figure 3 illustrates the heat balance of the variables and the thermal connection between different thermal parameters inside and outside the room [38].

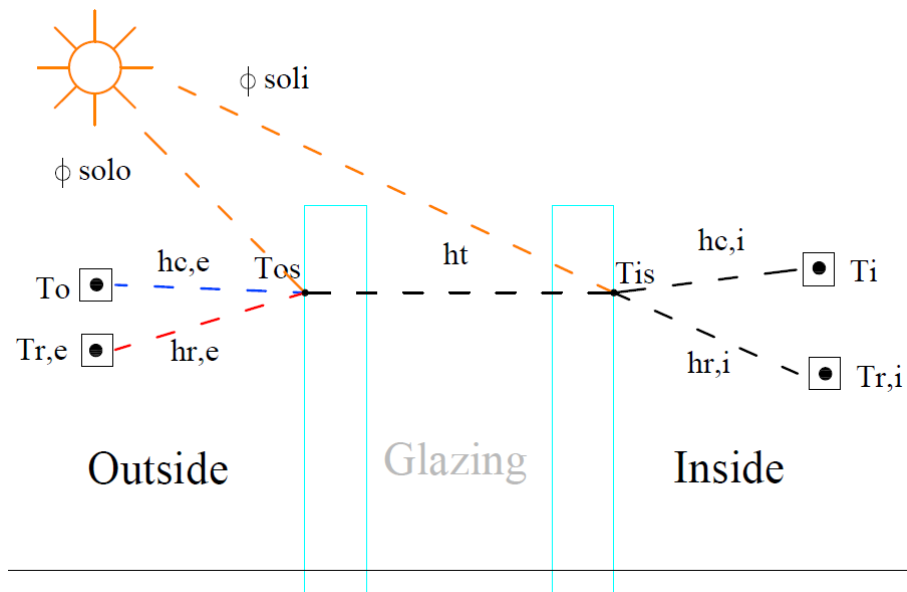


Figure 3: The heat balance of the variables and the thermal connection between different thermal parameters inside and outside the room.

The method of glazing is implemented by making use of the finite volume energy balance equations by Clarke [38] to calculate the temperature of internal and external surfaces, taking into account of the thermal mass of the glass, the spectral and angle dependence of the solar radiation [14, 36, 41]. The two variable nodes in the equations represent the surface temperatures of the internal and the external glass. It is assumed that the temperature of glass is homogeneous. The method takes both implicit and explicit conditions into account [38], considering the boundary conditions of both the present and previous time steps to increase the accuracy of the result.

For further information and detail calculations of the different parameters, please refer to Paper 3: “Development and sensitivity study of a simplified and dynamic method for double glazing facade and verified by a full-scale facade element.”

## 2.2 SIMPLIFIED MODELLING OF GLAZED FAÇADE WITH NIGHT INSULATION

The method of glazing with insulated shutter is implemented to calculate the comfort and thermal properties of the facade by determining the internal surface temperature of the glazing and the U-value of the entire glazing with the shutter. The determination of the internal surface temperature is based on finite volume energy balance equations by Clarke [38]. In order to simplify the calculation, there are two variable nodes in the equations representing the internal and the external glazing surface temperature with the volume of a quarter of the thickness of the pane. It is assumed that the temperature of glass in the volume is homogeneous. The method is developed by solving the equations and calculating the surface temperatures at different time steps. In addition, the equations take both implicit and explicit conditions into account [38] considering the boundary conditions of both the present and previous time steps to increase the accuracy of the result. Furthermore, the method considers the thermal mass of the glass and the infiltration through the cavity between the glazing and the insulated shutter.

Figure 4 illustrates the heat balance of the variables and the thermal connection between different thermal parameters inside and outside the room [38].

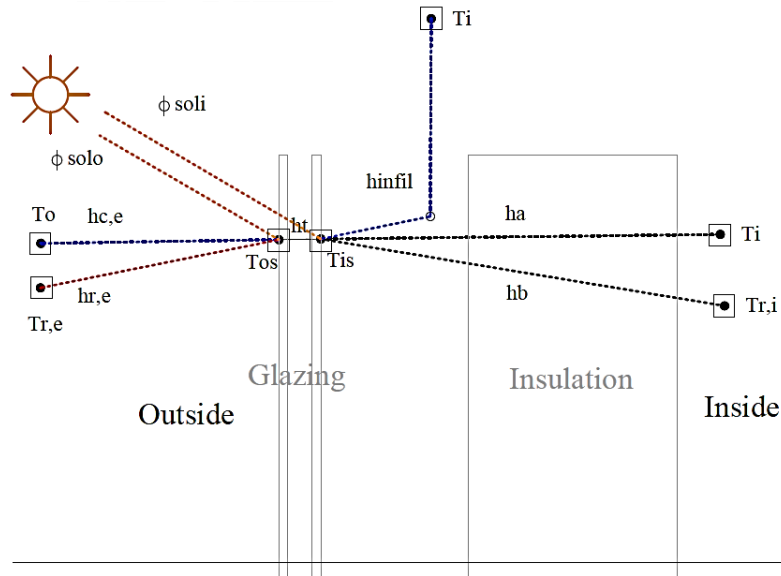


Figure 4: Layout of the facade system and the heat balance of the variable nodes in the simplified model (on the internal and external surfaces of glazing).

For further information and detail calculation process, please refer to Paper 2: “Development of a simplified and dynamic method for double glazing facade with night insulation and validated by full-scale facade element.”

### 2.3 SIMPLIFIED MODELLING OF SOLAR SHADING

This section describes the calculation method for the mode when the blind is activated. The method calculates the solar properties of the venetian blind considering the incident angle of the solar radiation and the slat angle of the blind. The calculation is conducted in 2D (Figure 5 [15, 16]), assuming that the reflection of the solar radiation along the slats is neglected. Therefore, only the solar altitude angle is taken into account and there is no reflectance along the slat length of the blind.  $H$  is the distance between the slats;  $W$  is the width of the slats;  $\alpha$  is the solar altitude angle;  $\beta$  is the tilt angle of the slats; the numbers 1-6 stand for different solar surfaces used to calculate the view factors [15, 16]. Both the total solar energy transmittance  $g_t$  and the direct solar transmittance  $\tau_{e,t}$  of the double glazing with external blind are calculated by the equations shown in Paper 4. Direct solar transmittance  $\tau_{e,t}$  will be used to compare with the calculated results by BSim.

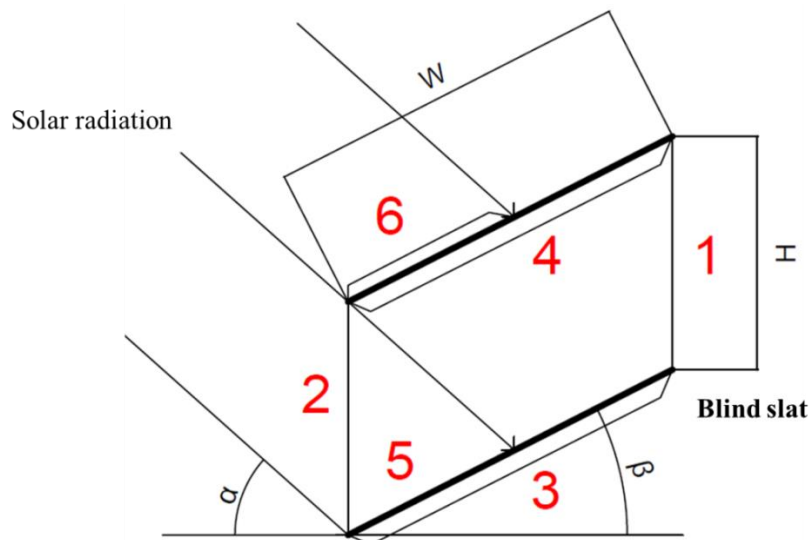


Figure 5: Illustration of solar radiation irradiating on the blind (surface 1 is the space between two slats on the opposite side of solar radiation, surface 2 is the space between two slats facing solar radiation, surface 3 is back side of the lower slat, surface 4 is back side of the upper slat, surface 5 is the part of the top side of the lower slat that is under direct solar radiation, surface 6 is the part of the top side of the upper slat that is under direct solar radiation).

The total solar energy transmittance of the glazing with external solar protection device is given by equation (2) [15, 16]:

$$g_t = \tau_{e,B}g + \alpha_{e,B} \frac{G}{G_2} \tau_{e,B}(1-g) \frac{G}{G_1} \quad (2)$$

Where  $\tau_{e,B}$  is the solar transmittance of the solar protection device,  $g$  is the total solar transmittance of glazing,  $\alpha_{e,B}$  is the solar absorptance of the solar protection device,  $G_1$  equals to  $5W/(m^2K)$  and  $G_2$  equals to  $10W/(m^2K)$  [15, 16].

For further information and detail calculation process, please refer to Paper 4: “Development of a simplified method for intelligent glazed facade design under different control strategies and verified by building simulation tool BSim.”

## 2.4 MODELLING OF ROOM AND BUILDING SERVICES ACCORDING TO EN 13790

In order to investigate the influence of the facade on the energy and comfort performance of the entire building, the method also includes the room model according to the simple hourly model in EN 13790 [26]. Therefore, the simplified method is able to calculate the energy demands (heating, cooling, lighting and ventilation) and the indoor environment (indoor air temperature, solar transmittance through the facade and the indoor illuminance level at a chosen point) of the room with different control strategies of the facade.

Figure 6 [26] shows the network and heat flow of the simulated zone. Full sets of equations for the simple hourly method are shown in EN 13790 [26].

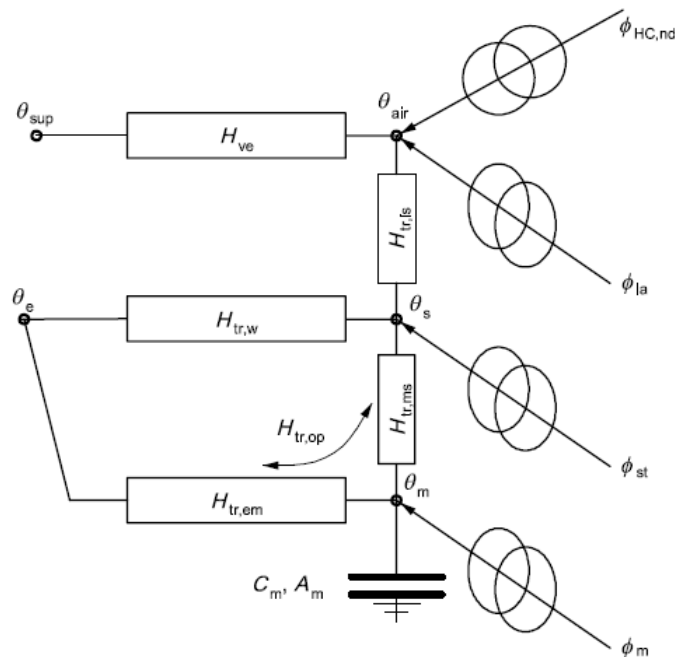


Figure 6: Analogue electrical network of heat flow of the simulated zone.

## 2.5 CONCLUSION AND ADVANTAGES OF THE SIMPLIFIED METHOD

The simplified method for intelligent glazed facade is developed to calculate the energy and comfort performance of buildings with intelligent facade controlling insulated shutter, venetian blind, natural ventilation and night cooling. Energy consumption (heating, cooling, lighting and ventilation) and indoor operative temperature are calculated by the method. The method is planned to be integrated into BSim and Be10, but it can also work independently with the interface shown in Figure 7. Capability of hourly calculation of an office room in the whole reference year and flexibility of modelling new control strategies make the method a great advantage in the design and certification of buildings with intelligent facade.

BUILDING INFORMATION 2020			FACADE INFORMATION			
<b>Building construction</b>	Area (m <sup>2</sup> )	U-value	Orientation	0		
Wall West	15	0	Total Facade Area (m <sup>2</sup> )	7.59		
Wall East	15	0	Ratio Of Glazed Facade (%)	40.00%		
Wall North	9	0	Glazed Facade (m <sup>2</sup> )	4.32	1.2	0.3
Ceiling	9.9	0	Facade Frame (m <sup>2</sup> )	0	1.2	
Floor	9.9	0	Opaque Part Of The Facade (m <sup>2</sup> )	3.174	0.09	
Heat Exchange Rate	0.85		Glazing Type	1		
			Insulation Position	1		
			Blind Position	1		
<b>Building Services</b>			CONTROL STRATEGIES			
Area (m <sup>2</sup> )	9.936		On/Off	Indoor set-point (°C)	Outdoor set-point (°C)	
Internal Load (W)	99.36		Control Mode	0		
Heating Set-Point (°C)	20		Control Blind	1	24	
Cooling Set-Point (°C)	25		Control Insulation	1		
Working Time	8	17	Glare	1		
Mechanical Ventilation (l/s per m <sup>2</sup> )	1.2		Natural Ventilation	1	23	12
Infiltration Rate (l/s per m <sup>2</sup> )	0.03		Night Cooling	1	18	12
			Lighting	1		

Figure 7: Interface of the simplified method.

### 3. VERIFICATION OF THE SIMPLIFIED METHOD WITH BSIM

#### 3.1 COMPARISON BETWEEN THE SIMPLIFIED METHOD AND BSIM

After development of the method, the calculation results were compared with simulation results from the Danish building simulation tool BSim. The purpose of this was to evaluate the accuracy of the simplified method in terms of calculating the different energy and comfort parameters of the test room. Hourly calculations were conducted through a whole year with weather data of the Danish Design Reference Year (DRY) [23].

The test room was modelled in both the simplified method and the BSim programme to compare the calculated parameters. The modelled office room is a south-facing office room with the dimension of 3m × 3m × 5 m (H×W×D). The facade system faces south and measures 3 m×3 m. The glazing area of the facade system is 4.08 m<sup>2</sup>. The glazing type used in the simulation is a double glazing unit with a 15 mm argon-filled cavity and low-E coating on the internal pane. Table 1 shows the detailed specification of all the other building elements except glazed facade. It is assumed that there is no heat transfer through all the other enclosures in order to make the heat balance of the room dominated by the facade. The total infiltration rate used in both the simplified method and BSim is 1.6 l/s.

Table 1 shows the input values of the thermal loads and set-points for the indoor conditions for both the simplified method and BSim. Both the heating and cooling loads are assumed to be 100 % convective, and the indoor illuminance level is calculated at the working plane (height of 0.85 m) 0.5 m from the facade on the centreline of the room.

Building Component	U-Value (W/m <sup>2</sup> k)	Thickness (mm)	Area (m <sup>2</sup> )
External wall (south)	0.000001	126	4.92
Glazed facade (south)	1.4	23	4.08
Wall (east/west)	0.000001	126	15
Roof	0.000001	120	15
Floor	0.000001	226	15
Wall (north)	0.000001	126	9

Table 1: Specification of building elements.

Internal load of people	150 W
Lighting power (on/off)	105W
Set point for the heating	20 °C
Set point for the cooling	25 °C
Mechanical ventilation rate (office hour)	1.2 l/m <sup>2</sup>
Set point of lighting	300 lux

Table 2: Setup of building services and indoor conditions.

The comparisons on the results between the simplified method and BSim were performed under four different conditions: facade without control, facade with control of insulated shutter, facade with control of solar shading, and facade with control of natural ventilation. There are some simple and fixed control strategies of facades in BSim. In order to unify the inputs of the simplified method and BSim, the control strategies of the four conditions are chosen from the existing control strategies in BSim:

- The facade is not controlled according to the indoor and outdoor environment.
- External shutter is installed and activated to cover the glazed facade outside the office hour; Table 3 shows the layout and the properties of the glazing with external insulated shutter.
- External venetian blind is installed and activated to shade the glazed facade when the solar transmittance through the facade into the room is above 200W/m<sup>2</sup>. The solar transmittance of the shading is 0.1.
- Control of the natural ventilation, the facade is open when the indoor temperature exceeds 23 °C.

Position	Material	Conductivity	IR Emissivity Outdoor	IR Emissivity Indoor
Outside	Polystyren 100mm	0.05 W/mK	0.09	0.09
Cavity	Air 110mm	-	-	-
Middle	Planilux 4 mm SGG	1 W/mK	0.837	0.837
Cavity	Argon 15 mm	0.017 W/mK	-	-
Inside	PITutran 4 mm SGG	1 W/mK	0.04	0.837

Table 3: Layout and material of the facade with external night insulation.

After the simulations of the four control conditions, energy and indoor environment parameters (indoor air temperature, daylight illuminance on the reference point and energy demand of heating, cooling, lighting and ventilation) are calculated and compared with the BSim software.

Figure 8 and Figure 9 show the comparison between the simplified method and BSim on the yearly energy demand under the four control conditions. According to the figures, compared with BSim, the energy demands for heating calculated by the simplified method are overestimated for all four control conditions. The heating demand under the control of the natural ventilation calculated by the simplified method has the biggest difference of approximately 2.4 % compared with that calculated by BSim.

Compared with BSim, the energy demands for cooling are overestimated by the simplified method under all the four control conditions except control of shutter. The cooling demands calculated by the simplified method under the control of solar shading have the biggest difference of around 6.8 % compared with that calculated by BSim. The differences can be explained by the different inputs of heating and cooling loads calculated according to different principles of the two methods. For instance, BSim does not take the infiltration between the shutter and glazing into account under the control of insulated shutter.

The energy demand for lighting under all the control conditions is underestimated by the simplified method, with the difference of up to -8.3 % compared with BSim. The difference is bigger than that of the heating, cooling and ventilation, because it is difficult to have quite similar prediction of daylight level around the set-point of artificial lighting (300 lux). The lighting devices being turned on or off can be significantly influenced by the prediction of the daylight level at the reference point.

The total energy demand and the energy demand for ventilation between the two methods are similar with the difference of less than  $\pm 2\%$ .

Paper 4 presents the detailed comparisons on calculation of indoor air temperature, solar transmittance and daylight illuminance.

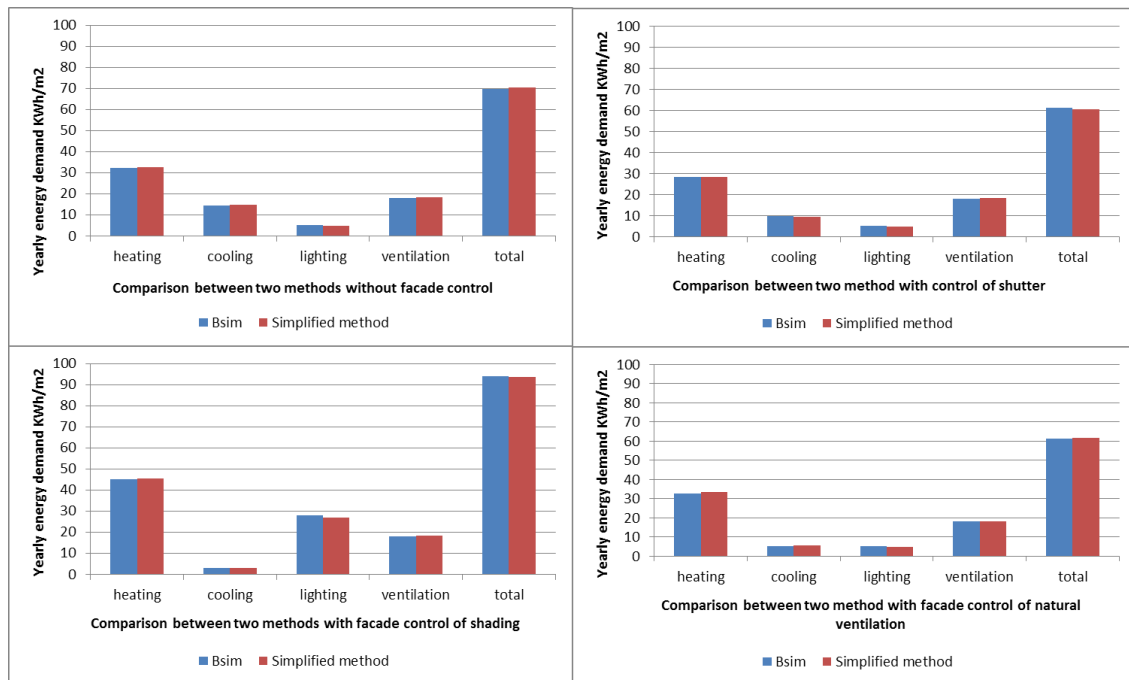


Figure 8: Comparisons of energy demand of the room on the four control conditions.

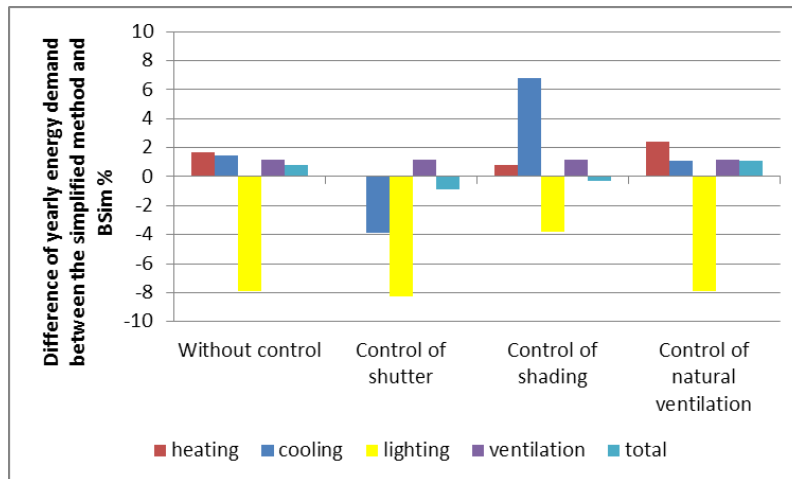


Figure 9: Difference of energy demand on the four control conditions between the two methods.

The simplified method is exclusively developed for evaluating the performance of intelligent or controlled facade design for office buildings. Therefore, the inputs and simulation possibilities for control strategies of facade can be made as detailed as possible according to the design of facades. The method is also open to be updated to fulfil different properties of design. It is possible to change the parameters of the remaining parts of the building except the facade to users' needs. Otherwise, they are set as normal office conditions with pre-inputted parameters and set points, which make it simple and less time consuming to investigate only the properties of building facade.

### 3.2 CONCLUSION

The simplified method is compared with Danish building simulation tool BSim on calculating the yearly energy demand (heating, cooling, lighting and ventilation) and indoor environment parameters (indoor air temperature, solar transmittance and daylight level on the reference point) under different control strategies. According to all the comparisons, the correlation between the results of the simplified method and that of BSim is relatively high. The difference in energy calculation between the two methods is below 10 %, and the average  $R^2$  value of the calculated indoor air temperature, solar transmittance and daylight level is higher than 0.94. In general the simplified method is acceptable for further simulations.

For further information, please refer to Paper 4: "Development of a simplified method for intelligent glazed facade design under different control strategies and verified by building simulation tool BSim."

## 4. VERIFICATION OF THE METHOD WITH EXPERIMENTAL MEASUREMENTS

An experimental test has been designed and implemented specifically for evaluating the accuracy of the simplified method, which is necessary for future application of the method for predicting the influence of intelligent facade on the energy and comfort performance of buildings. The verification of the simplified method is conducted by the measurements performed in the test facility "The Cube" at Aalborg University [42, 43], which is described in this chapter together with the setup, instruments, procedure and the results of the experiment. Parameters (indoor air temperature, activation of blind, illuminance level on the working plane and eye position, power and energy consumption of heating, cooling and artificial lighting) were measured and compared with the calculation by the simplified method. The measurements were conducted during a period at the end of June and in the middle of August 2014 under control of natural ventilation and night cooling and at the end of August 2014 without the control of natural ventilation and night cooling. The calculations by the simplified method were conducted throughout the period in order to be compared with the measurements.

### 4.1 EXPERIMENT SETUP

The measurements were implemented in the full-scale test facility (The Cube at Aalborg University [42, 43]) (Figure 10) consisting of one south-facing test room with the internal dimensions of 2.76 m × 2.7 m × 3.65 m (H×W×D). The glazed facade system faces south and measures 2.76×1.6 m<sup>2</sup>. All the enclosures of the test room except the south facade are surrounded by a guarded zone in order to minimize heat transfer through the enclosures. The heat capacity of the entire test room is 1700 kJ/K (47Wh/Km<sup>2</sup>).

The glazing type used in the experiments is a double glazing unit with a 12 mm argon-filled cavity and solar control coating on the external pane. The air-tightness between the test room and outdoor has been tested by



performing a blower door test, using both over and under pressure. The layout of the double glazing unit is shown in Table 4.

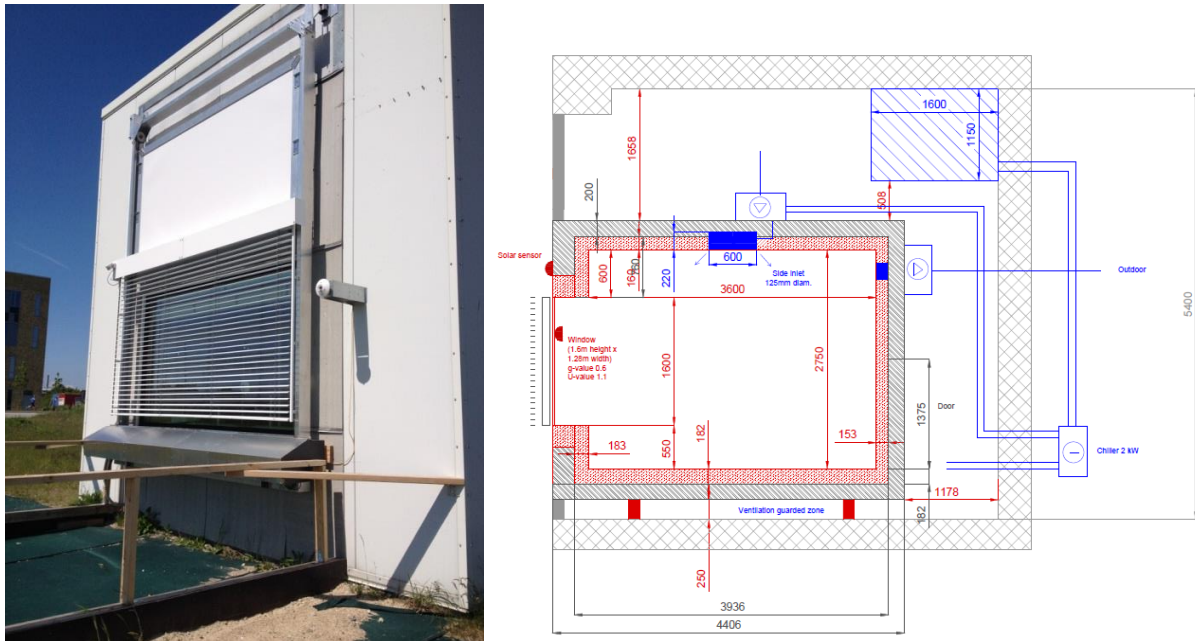


Figure 10: Full-scale test facility in Aalborg University-Cube. (Left: test facility, Right: section).

Element	Thickness (mm)	$\lambda$ (W/m.K)	$\rho$ (kg/m <sup>3</sup> )	$C_p$ (J/kg.K)	$\epsilon_1$ LW (-)	$\epsilon_2$ LW (-)
Outer Pane	5.9	1.0	2300	840	0.84	0.03
Cavity	12.0	0.017	1.64	522	-	-
Inner Pane	5.9	1.0	2300	840	0.84	0.84

Table 4: Layout and material properties of the double glazing façade, incl. uncertainty.

The surrounding internal surfaces of the room are made of 15 mm plywood and are painted white, apart from the floor, which is made of 150 mm concrete. The infiltration is minimized to 0.09l/s per square meter at a pressure difference of 50 Pa by sealing all joints with silicon. The internal heat loads are from a thermal manikin (around 80 W during the office hour) and artificial lighting (maximum 60 W), which is described in detail later together with heating and cooling system.

The data collection and device control in the experiment were realized by using NI Labview. Figure 11 shows the setup of the entire system to collect measured data from different sensors and to control different elements and devices. All the instruments can be integrated and controlled according to measurements from different sensors in the system. The system is flexible and offers the possibility in implementing different control strategies.

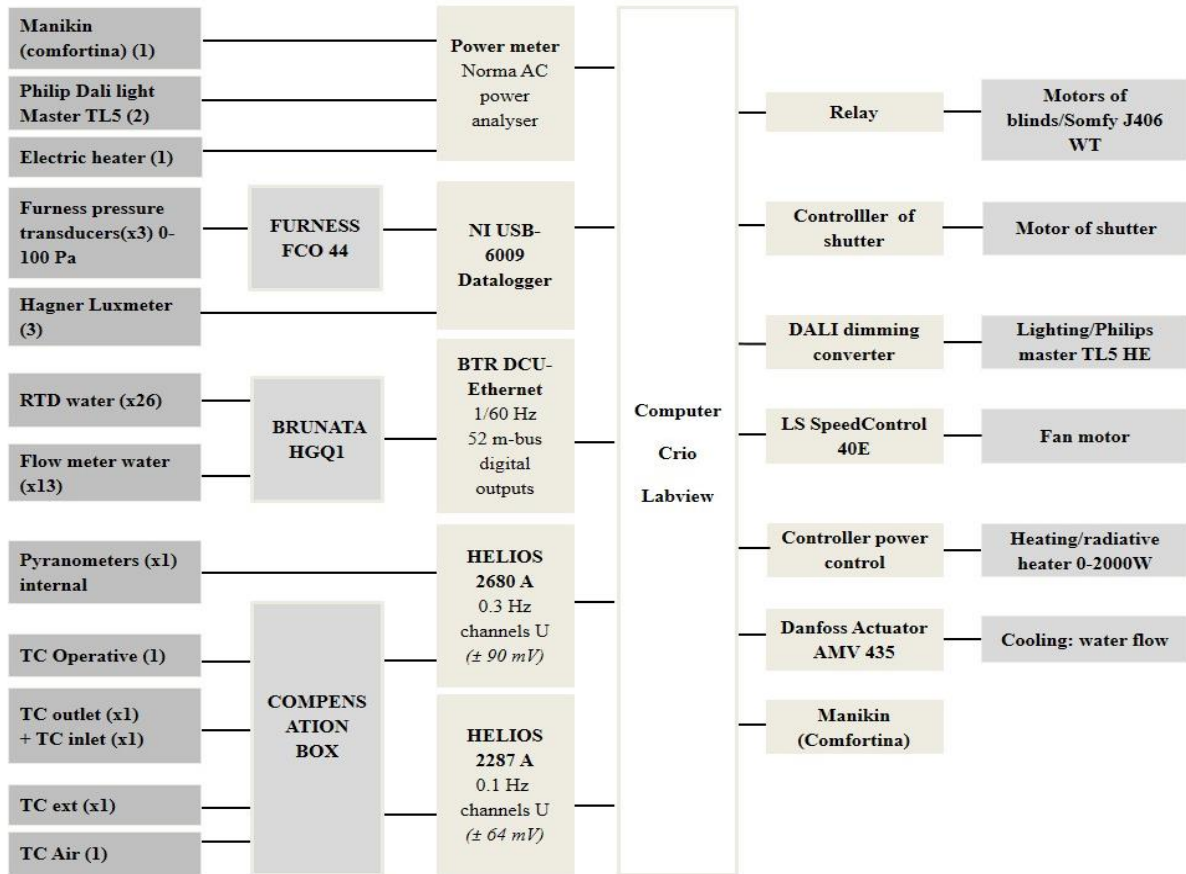


Figure 11: Experiment setup and structure of the connection of measurement instruments and control devices.



Figure 12: Pictures of the test room.

#### 4.2 MEASUREMENTS AND UNCERTAINTY

Table 5 shows the parameters measured by different sensors that are used to calculate the heating and cooling energy needs. All the measured data is averaged every 10 minutes.

Description	Measurements From Sensors
Internal Heat Load (Manikin+ Artificial Lighting)	Power meters of manikin and artificial lighting
Solar Heat Gain Into The Room	Pyranometer inside CM21
Air Flow Rate	Orifice plate
Inlet Air Temperature	Thermocouple (inlet position)
Outdoor Air Temperature	Thermocouple (outdoor)
Heating Or Cooling Load (+Heating; -Cooling)	Heating: Power meter; Cooling: Water temperature sensor and flow meter

Table 5: Measurements of the parameters used in the simplified method.

- Air temperature

To measure the air temperature in the room, five columns of thermocouples have been installed in the test room: one in the middle of the room and one at the centre of each wall (60 cm away from the south and north wall, and 25 cm away from the west and east wall). Temperatures are measured using thermocouples type K, which are calibrated with a reference thermocouple. The temperatures are logged using Helios data logger connected to an ice point reference. All the thermocouples are connected to a compensating box in order to increase accuracy in measurements [42, 44]. The thermocouples measure the air temperature at 0.1, 0.6, 1.1, 1.7 and 2.65 m high above the floor with an accuracy of  $\pm 0.1$  K. In order to decrease the influence of radiation on the measurement of air temperature, the thermocouples are silver-coated and protected by a mechanically ventilated silver shield.

- Irradiance

Outside irradiance is measured using two CM21-pyranometers and one CM22-pyranometer. CM22 is placed on the top of the cube to measure the global irradiance on a horizontal surface. The CM21 pyranometers are placed inside and outside the glazing respectively, measuring irradiance on the vertical surface both on the external facade and in the test room. Prior to the installation, the pyranometers are calibrated in reference to CM21, which is calibrated in sun simulator and corrected by Kipp&Zonen B.V [42].

- Air flow rate

The measurement of the air flow through the ventilation system is performed using an orifice plate located before the inlet (accuracy of the air flow rate:  $\pm 7.5\%$ ) [42, 43].

- Water flow rate and water temperature for cooling

The cooling power released by the active chilled beam is measured by a combination of flow meters and temperature sensors. Cooling load of the active chilled beam can be calculated according to the water flow rate and the temperature difference between the forward and return water flow. The accuracy of the measurement has been estimated to  $\pm 0.9$  L/h for the flow meters and  $\pm 0.057$  K for the Pt-500 sensors [43].

- Illuminance

The lighting is controlled according to the illuminance of the test room measured by Hagner Luxmeters which are placed on the height of working plane (0.85m) in the centre of the room. There is also one luxmeter, which is used to evaluate the glare control, fixed at the eye position 1m away from the facade.

- Pressure difference

Pressure difference between the test room and the guarded zone is measured by Furness pressure transducer. The measurement is used to control an outlet fan to keep the pressure difference at 0 and minimize the infiltration of the air from the guarded zone to the test room.

- Power meter

The heats released from the manikin, the artificial lighting and the electrical heater are all measured by power meters, which are used in the calculation and verification as the internal load from people, lighting and heating.

An uncertainty analysis has been performed to assess the accuracy and the precision of the measurements. This analysis is based on the measured heat balance in the experiment. By comparing the difference between the heat balance of the room and the heat balance to the thermal mass of the room (air, equipment and construction), it is possible to estimate the error on the heat balance and, therefore, the uncertainty on the measurements (Figure 13).

The analysis has been performed for calculation interval of 10 minutes during experiment period 18<sup>th</sup>-22<sup>nd</sup> June. The uncertainty on the internal thermal mass is  $\pm 20\%$ . This uncertainty did not show any correlation with the intensity of solar radiation.

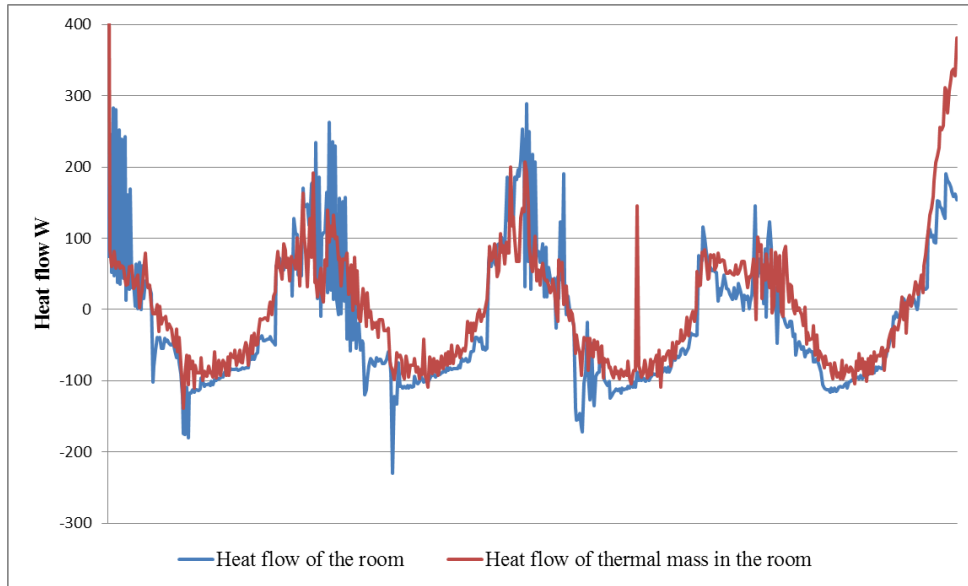


Figure 13: Comparison between the heat balance to the test room and heat balance to the thermal mass in the room.

### 4.3 CONTROL OF FACADE AND BUILDING SERVICES

A blind is used to prevent glare problems and to reduce the extra solar transmittance through the facade. The tilt angle of the blind depends on its functions. During occupied hours, the angle is calculated by equation (3) [39] to cut the direct solar radiation, which both improve the visual comfort and maximize the daylight transmittance into the room. During unoccupied hours, the blind is controlled to be closed if the indoor air temperature is above 24 °C. The blind is scrolled up if it is not set at a cut-off angle or in a closed position.

$$\beta = \arccos \left[ \frac{\frac{H}{W} \times \tan \alpha + \sqrt{\tan^2 \alpha - \left(\frac{H}{W}\right)^2 + 1}}{\tan^2 \alpha + 1} \right] \quad (3)$$

Where  $\beta$  is the angle between the slat and the horizontal plan.  $\alpha$  is the solar altitude angle.  $H$  is the distance between the slats.  $W$  is the width of the slats.

The glazed facade is open when the indoor temperature exceeds 23 °C, which is lower than the set point of the control of a closed blind so that the room cools down by natural ventilation first without sacrificing the import of daylight by the closed blind. The control is active only when the outdoor temperature is lower than the indoor temperature and the outdoor temperature is above 12 °C, preventing cold draft in the room. In the real situation, the natural ventilation rate is determined according to wind speed, wind direction, temperature difference between indoor and outdoor and some other parameters, which is not focused in this work. The ventilation rate is assumed to be 2 l/s per m<sup>2</sup>, which is equal to around 2.6 air change rate per hour (ACH) assuming the height of the room is 2.7m [45].

The night cooling control is active during unoccupied hours in terms of opening the window if the average outdoor air temperature between 12:00 and 17:00 is above 18 °C [46] and if the indoor air temperature is higher than the outdoor air temperature. It is turned off when the indoor air temperature is lower than 20 °C during night. The control of night cooling can precool the room and help to balance the cooling peak during day time.

Heating and cooling installations are controlled in order to secure the set-point temperature in the office space. However, it is not possible to predict heating and cooling needs when the heating and cooling are under PI control according to set-point of indoor air temperature. In order to compare with the calculation, heating and cooling needs released to the room are calculated according to the same approach as the simplified method. Therefore, they are under PI control according to the set-points of heating and cooling needs but not the indoor air temperature, which can also avoid the delay of adjusting the temperature to the requirement. The heating and cooling needs for the office room in every time step (hour) can be calculated by the simplified model according to hourly heat gain and heat lost to keep the room temperature between 20 °C and 25 °C. Detailed equations for calculating the heating and cooling needs are shown in the EN 13790 [26]. It needs to be noticed that the way the

heating and cooling are controlled is only feasible in experimental environment, where all the boundary conditions and environmental parameters are measurable. In practice, it is realistic to control buildings according to indoor temperature. The room is heated by a maximum 2 kW electrical heater controlled to heat indoor air. Output of the heating power is calculated by the simplified method and realized by PI control from computer and Compact RIO. There are other internal heat sources like artificial lighting and manikin in the room. The test room is cooled down using the active chilled beam with an efficiency of 0.85. The unit is located in the middle of the ceiling with dimensions of 0.6 m × 0.6 m. The cooling is controlled using the Danfoss AME435 actuator. The achieved indoor air temperature is between 20 °C and 25 °C.

Artificial lighting of the office building has dimming control during occupied hours according to the illuminance level at the working plane mentioned before. The set point of the lighting is 300 Lux. There are two DALI dimming light (Philips Master TL5 HE) installed under the ceiling and on the centre line of the test room, which are controlled by 0-10 V through a DALI converter to fulfil the required illuminance of the room. The electricity power of the lighting are measured and accounted as internal heat source. Correlation between the voltage output of artificial lighting and the illuminance compensation from the lamps has been found by a test at night when there is no daylight in the room. Figure 14 shows the correlation equation between the illuminance and analog output to the lamps. In order to calculate the daylight level during the time when the artificial lightings are on, the correlation between the measured power of lamps and the output illuminance from them on the working plane is found in Figure 15. The real daylight level can be calculated by subtracting the contribution from the artificial lighting from the total measured illuminance.

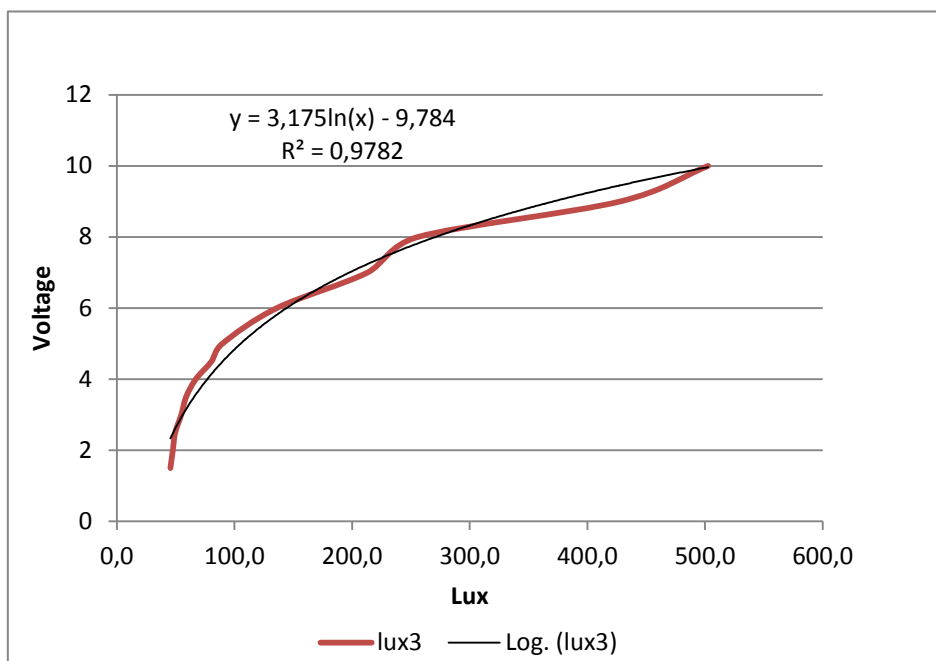


Figure 14: Correlation between the needed illuminance and the analog output to the lamps.

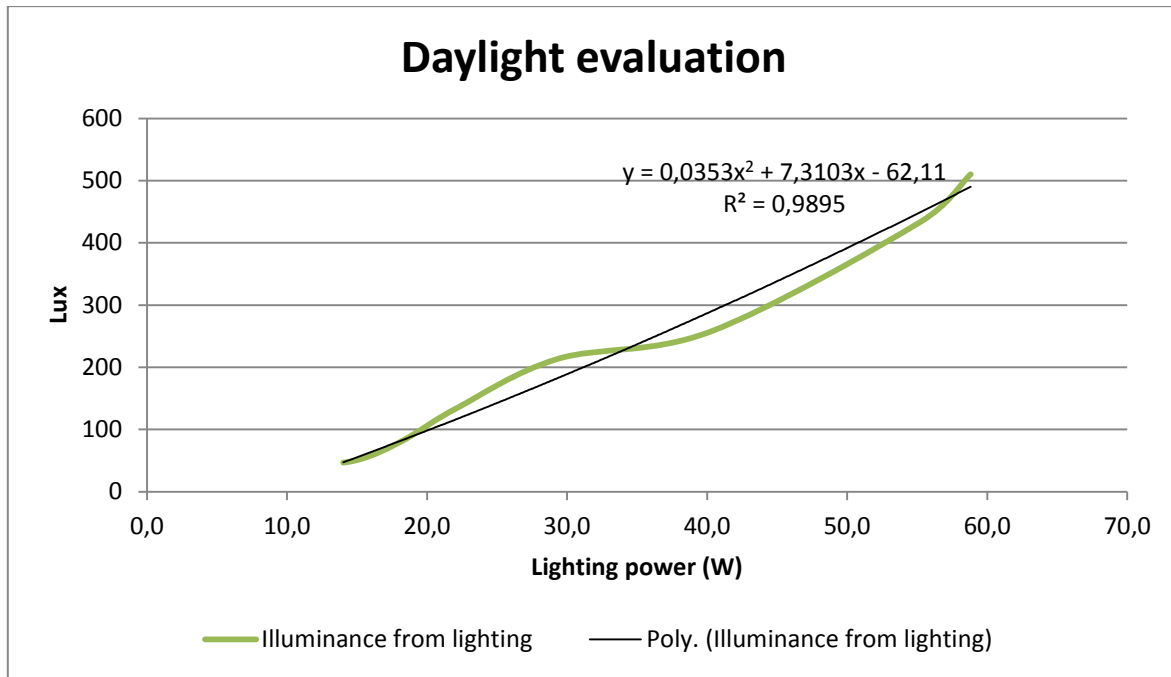


Figure 15: Correlation between the power of lamps and their output illuminance.

The fresh air is provided from the guarded zone through the same unit as the active chilled beam. When the cooling is performed by the active chilled beam, the inlet consequently has two functions (cooling and ventilation inlet). The air change rate can vary between 1 up to 4 ACH controlled according to the speed of the fan. A circular outlet is located at the top of the north wall (diameter 125 mm). The extraction rate of the outlet is controlled so that there is no over or under pressure between the guarded zone and the experimental room.

In order to know the cooling amount exactly from the control of natural ventilation and night cooling, these are not activated by importing air from outside but rather by the chilled beam. When the natural ventilation or night cooling is needed, the amount of cooling load caused by them is calculated according to the assumed air flow rate and the temperature difference between indoor and outdoor and outputted by controlling the chilled beam. Therefore, the total cooling power measured is the sum of natural cooling (natural ventilation or night cooling) and mechanical cooling.

In order to simulate an office worker, a thermal manikin has been placed close to the south wall, in an open chair. The manikin is made of a fibreglass shell covered with 0.3 mm diameter nickel wires, which are sequentially used to heat the manikin (accuracy on the heat flow  $\pm 1\%$ ) and to measure and control the skin temperature (accuracy  $\pm 0.2$  K). The thermal manikin corresponds to a 1.7 m tall woman and is divided into 17 parts, which can be controlled and measured individually (Comfortina [43]).

#### 4.4 COMPARISON: SIMPLIFIED METHOD AND EXPERIMENTAL MEASUREMENT

Comparisons between the simplified method and the measurements are conducted on the results of indoor air temperature, illuminance on eye position and working plane, activation of blind, cooling power, total energy consumption of cooling, lighting power and total energy consumption of lighting.

In order to make it comparable between the calculation and the measurements of lighting, the lighting dimming correlation between the needed illuminance at the working plane and the output lighting power are found by measurements based on the specific positions of the lamps and lux meter in the test room. The equation is used in the simplified method for calculating the lighting power.

Figure 16 (chart 4) shows the comparison between the measured and calculated heating and cooling powers during the experiment period, where a positive value means heating and a negative value means cooling. The calculated results of cooling power generally have the same tendency as the measurements but with some fluctuations. However, the simplified method overestimates the cooling power compared with the measurements during some periods. The reason for this is the disagreement between the calculated and measured indoor air temperature around 23 °C, which causes the overestimation of cooling by activation of natural ventilation in the calculation (Figure 16, charts 3 and 4). The calculated indoor air temperature drops with the activation of the natural ventilation. The difference between the calculated and measured cooling load is also caused by the slow

reaction of the system. Figure 16 (chart 4) shows the calculated cooling load by the simplified method (red line), the measured cooling load in the experiment (blue line) and the requested cooling load which is calculated during the experiment by the control system (green line). During some periods the measured cooling load cannot reach the amount of the requested cooling load before the requested drops, which results in the overestimation of cooling load and the total cooling consumption by the simplified method.

Apart from this, the disagreement could be caused by different reasons. The calculation is conducted assuming homogenous thermal mass in the test room, but the real situation is that half of the thermal mass is contributed by the tiles lying on the floor. The efficiency of the chilled beam and the difference between the calculation and measurement on the solar transmittance could also influence the calculation of the heat balance. The shield factor of the facade caused by the external frame holding the blind and insulation could also influence the calculation of the solar heat gain.

The calculated and measured heating powers are different, which is because of the experiment system. During the night time, there is always low heating power due to the slightly higher forward water temperature than the return water temperature through the chilled beam. It is because the chilled beam actually heats the indoor air when the indoor air temperature is lower than the forward water temperature, which was unexpected.

Figure 16 shows the measured illuminance at the eye level according to the activation of blind, position of blind, internal loads and solar radiation on external vertical facade surface. The comparisons between the calculated and measured lighting power (chart 8) and illuminance (chart 5 blue and red line) at the working plane are also shown in Figure 16. When the blind is not covering the glazed facade, the calculated and measured light levels are more similar. When the blind is covering the facade, the method underestimates the illuminance at the working plane most of the time, which could be due to the fact that the blind angle is not exactly the same as controlled resulting from the wind and also there are gaps at the edges of the window causing unexpected light leakage or reflection.

Figure 16 (chart 5 grey and black dashed line) shows the calculated and measured illuminance at the eye level which is what the glare control reacts according to. In the simplified method, the glare control is based on the illuminance caused only by the direct solar radiation, but it is not possible for the lux meter to tell the difference between the illuminance from the direct solar radiation and the diffuse solar radiation. Therefore, the measured illuminance is higher than the calculated one when the blind is not activated.

The comparisons on the indoor air temperature, cooling power and illuminance at the working plane are evaluated by the  $R^2$ -value [47]. This value indicates the comparison between the measured and the calculated results at each time step and evaluates the level of accuracy of the method. The  $R^2$  value is not only a measure of how well the pattern of the model follows the pattern of the measurements, but also a measure of accuracy determining error at each time step.

Figure 19 shows the linear regression of the calculation results of heating, cooling power and indoor air temperature by the simplified method. According to the figure, the comparison between the calculation results and the measurements is expressed with  $R^2$  value, which is 0.8 for air temperature and 0.34 for cooling power, respectively.



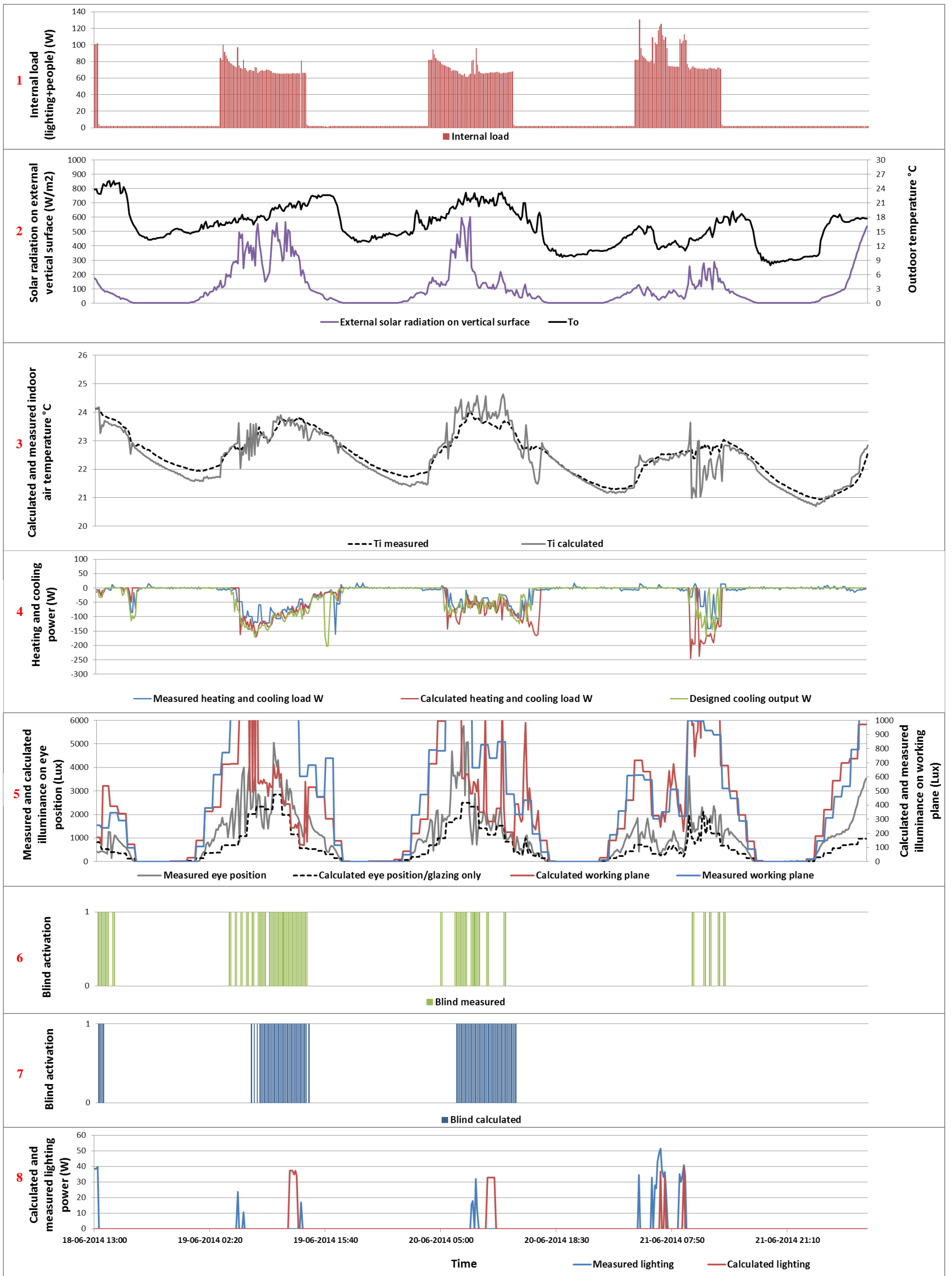


Figure 16: Experiment results under the control strategy of natural ventilation and night cooling (18<sup>th</sup>-22<sup>nd</sup> June).

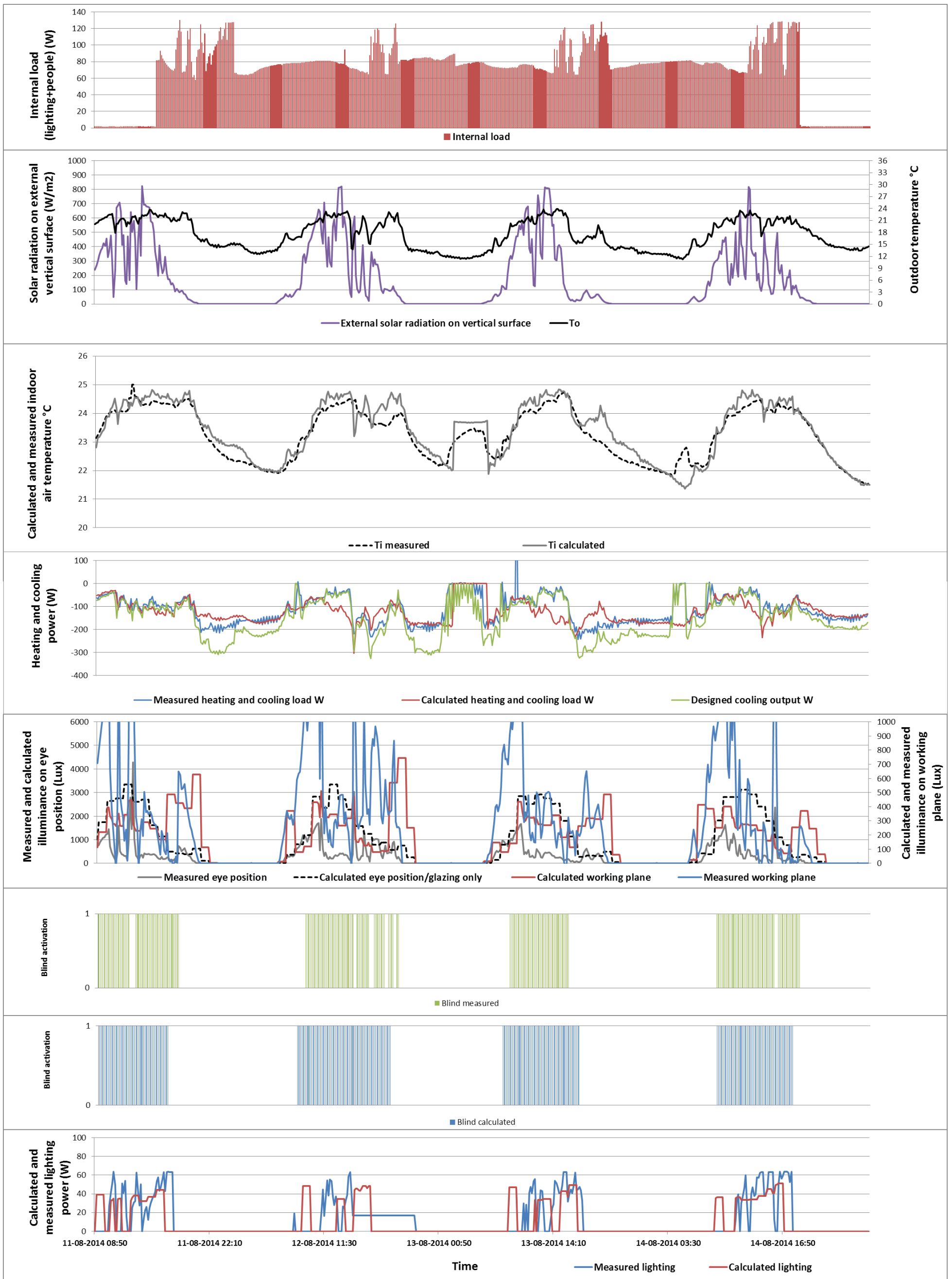


Figure 17: Experiment results under the control strategy of natural ventilation and night cooling (11<sup>th</sup>-14<sup>th</sup> August).

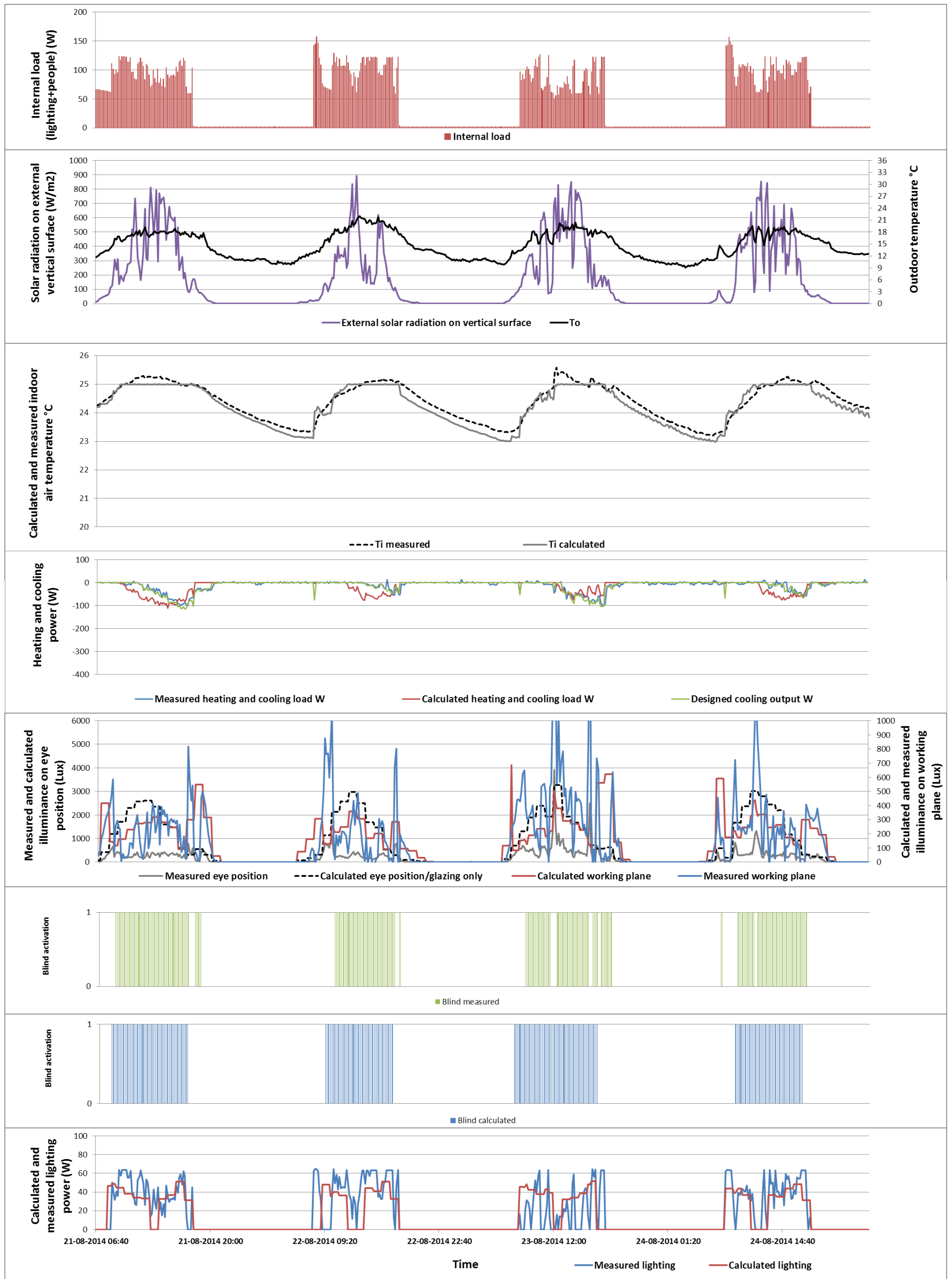


Figure 18: Result of experiment without control of natural ventilation and night cooling.

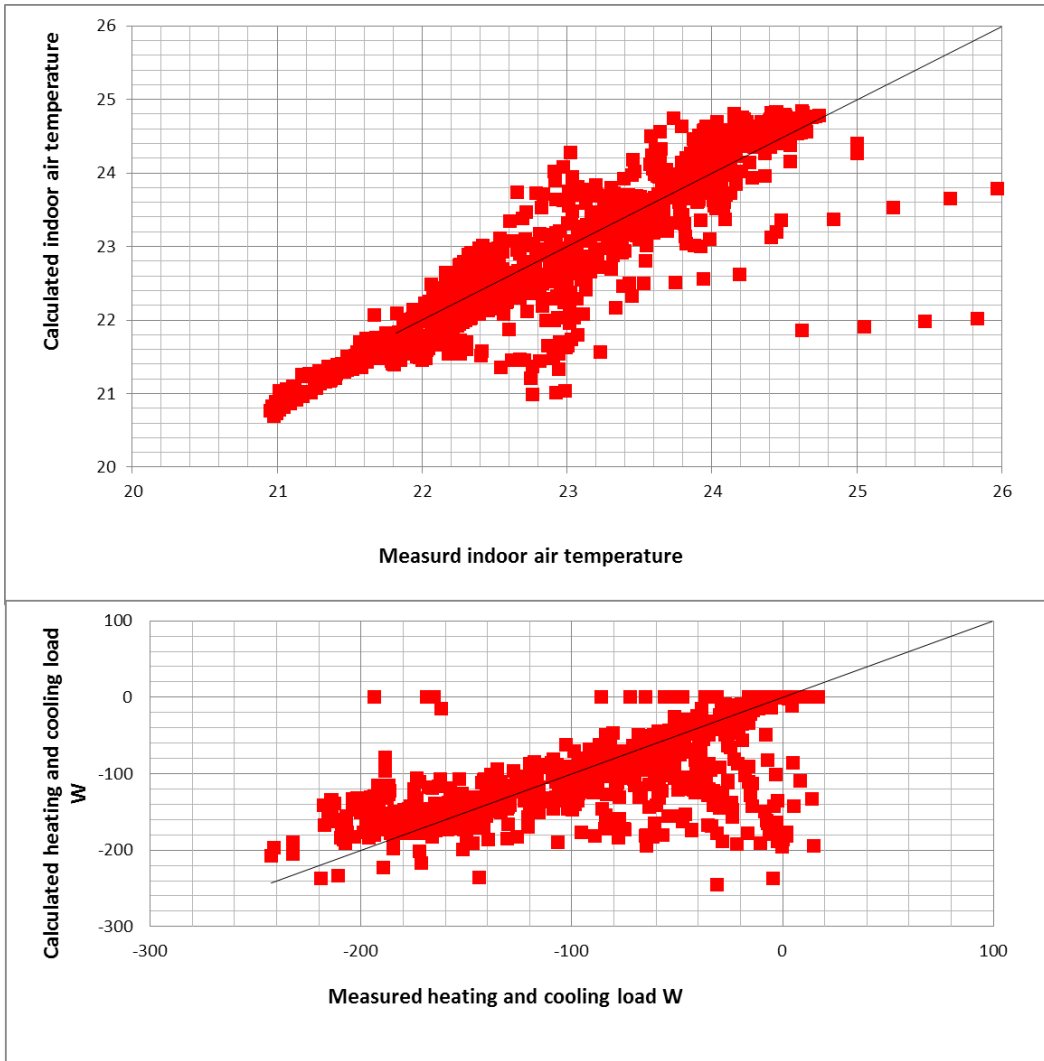


Figure 19: Comparison between measured and calculated heating and cooling power and indoor air temperature.

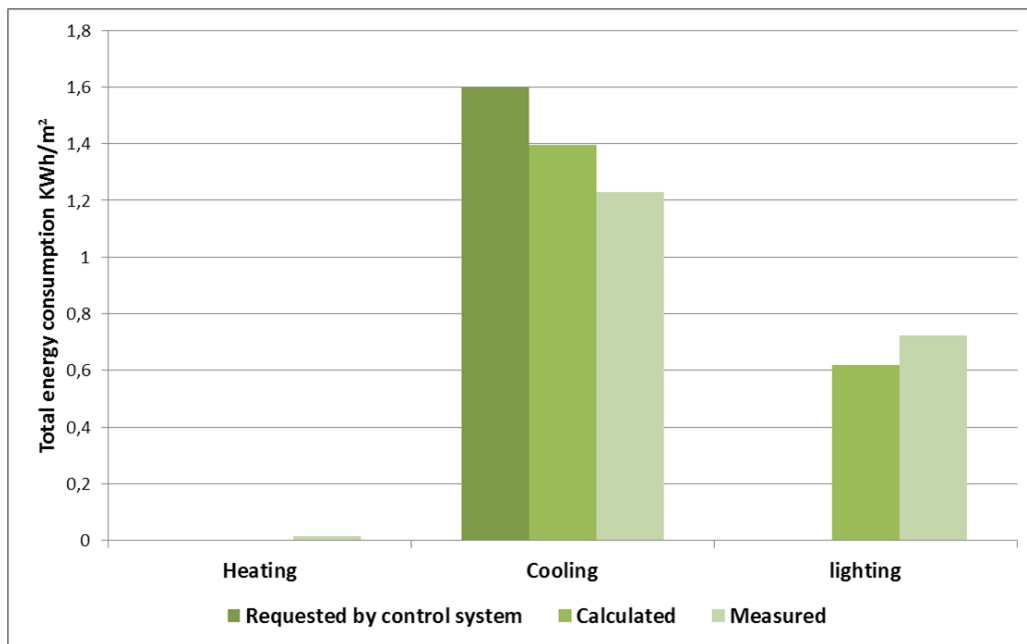


Figure 20: Comparison between the calculated and measured energy consumption under the control of natural ventilation and night cooling.

Figure 20 shows the comparisons between the measured and calculated total energy consumptions of heating, cooling and lighting in the test room during the entire experimental period. The simplified method underestimates the cooling energy consumption by 12.7 % compared with the requested cooling output calculated by the control system and overestimates it by 13.6 % compared with the measured cooling output. The measured heating energy consumption is almost 100% higher than the calculated which is closed to 0 because of the unexpected output from the experiment system and can be neglected. The method underestimates the energy consumption of lighting by around 14.3 % compared with the measurements.

The disagreement between the calculated and measured energy consumption is within the uncertainty of the heat balance in the experiment ( $\pm 20\%$  for ten minutes) which is calculated in section 4.2. Uncertainty is calculated by comparing the total heat balance of the test room and the thermal media in the room.

Comparison without control of natural ventilation and night cooling

A comparison has been conducted between the calculation and measurements on the energy consumption of cooling under the control of natural ventilation and night cooling. However, the cooling released in the room is to replace the cooling from natural ventilation and night cooling in order to know the exact cooling amount of them. In practice, this part of cooling does not come from the mechanical cooling device that consumes energy. According to the previous experiment results, the cooling demand of the room can be fulfilled by natural cooling in most of the experiment time. Therefore, an extra experiment was conducted without the control of natural ventilation and night cooling to investigate the correspondence between the calculation and measurement on mechanical cooling energy consumption.

Figure 21 shows that the total cooling energy consumption calculated by the simplified method is 8.4 % higher than the requested cooling consumption calculated by the control system and around 8 % higher than the measured cooling consumption. The calculated total energy consumption of lighting is 9.5 % lower than the measured.

Figure 22 shows the linear regression of the calculation results of heating, cooling power and indoor air temperature by the simplified method. According to the figure, the comparison between the calculation results and the measurements is expressed with  $R^2$  value, which is 0.32 for energy power and 0.88 for air temperature, respectively.

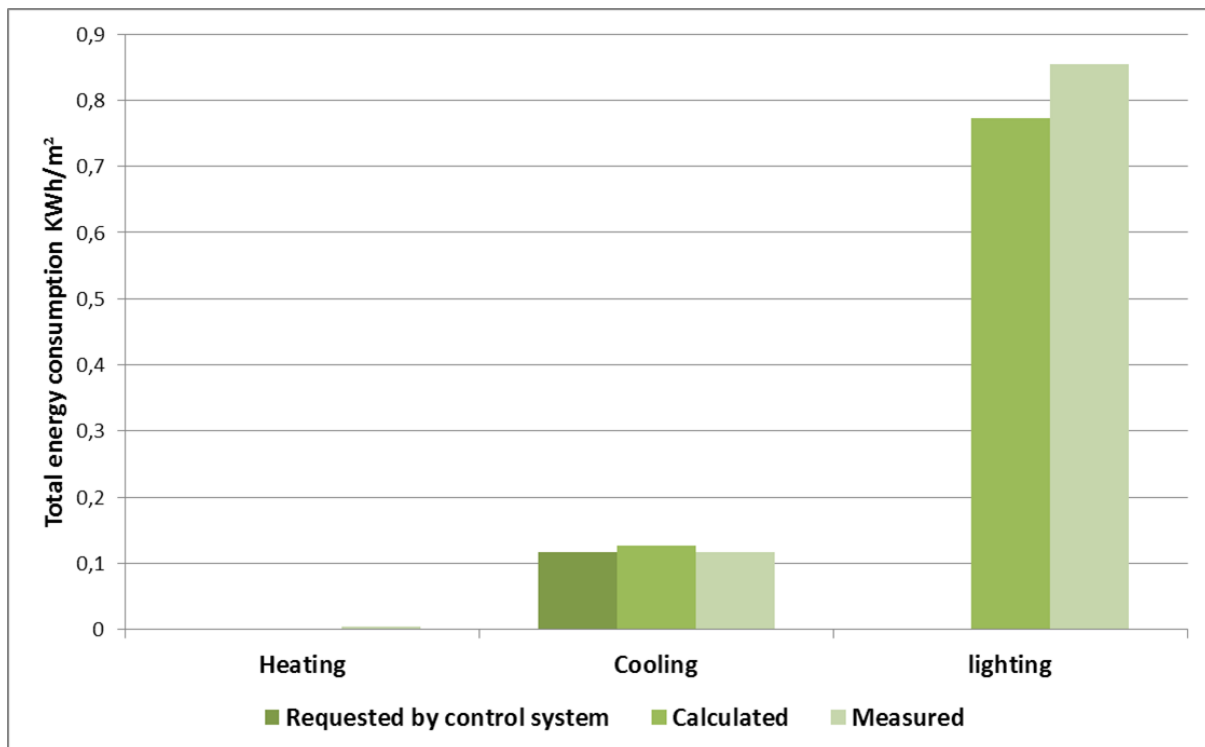


Figure 21: Energy comparison between calculation and measurement without control of natural ventilation and night cooling.

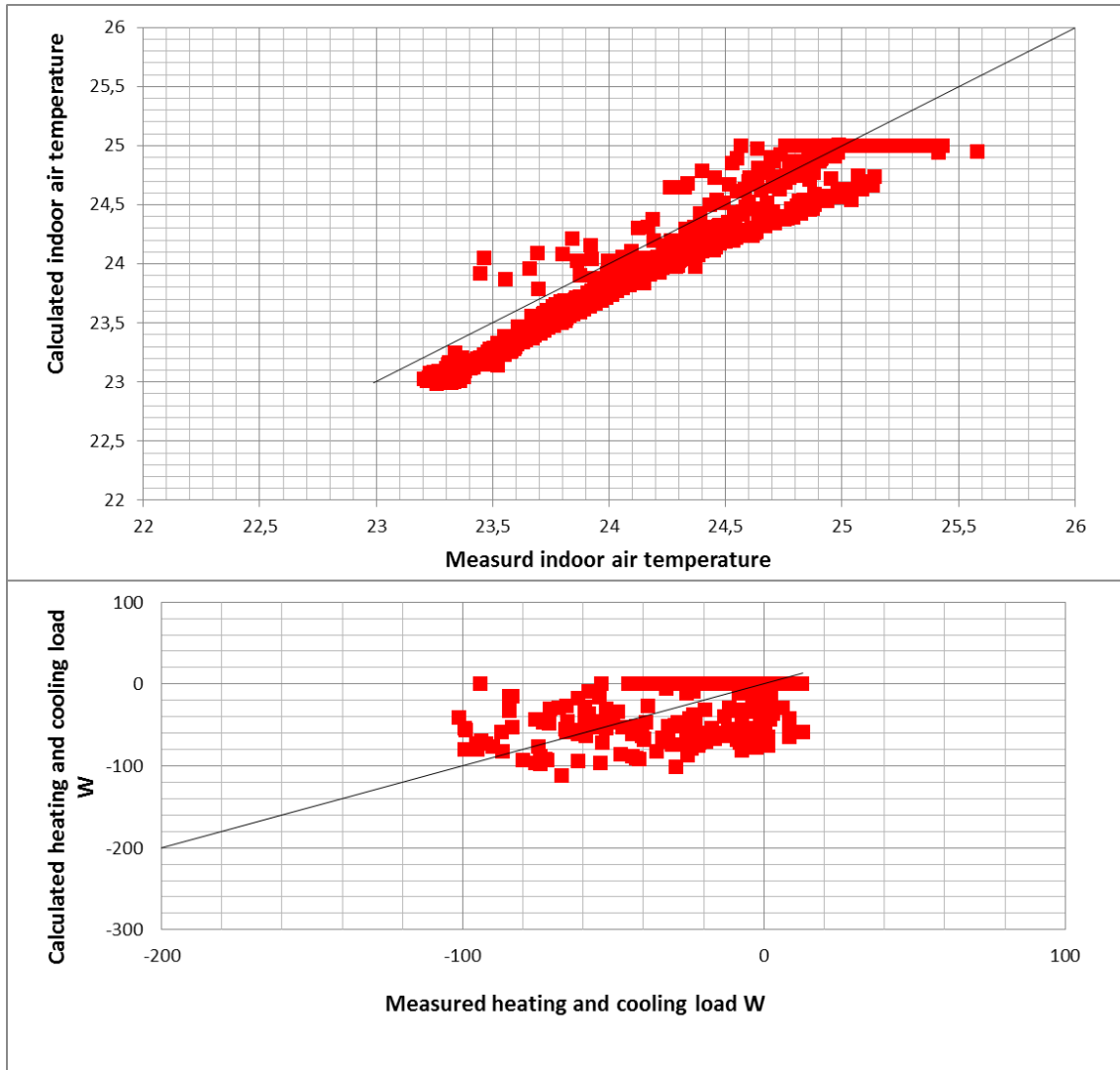


Figure 22: Comparison between measured and calculated heating and cooling power and indoor air temperature without control of natural ventilation and night cooling.

#### 4.5 CONCLUSION

According to the results of the comparison, the calculated air temperature is in good agreement with the measurements, with  $R^2$  value of 0.8. Additionally, the total cooling energy consumptions calculated by the simplified method are 12.7 % lower than the requested by the control system and around 13.6 % higher than the measured. The calculated total energy consumption of lighting is 14.3 % lower than the measured. The disagreement between the calculated and measured illuminance on the working plane on which the lighting is controlled is bigger when the blind is down.

During the experiment without control of natural ventilation and night cooling the total cooling energy consumption calculated by the simplified method is 8.4 % higher than the requested by the control system and around 8 % higher than the measured. The calculated total energy consumption of lighting is 9.5 % lower than the measured. The  $R^2$  value between the calculated and measured indoor air temperature is 0.88.

The experiment method and setup are sufficiently advanced to be implemented in complex experiments that require the integration of different measurement instruments and building services into a holistic system, especially when the measured data is needed to control other devices.

## 5. CONCLUSION OF PART I

The simplified method is compared with Danish building simulation tool BSim in the calculation of the yearly energy consumption (heating, cooling, lighting and ventilation) and indoor environment parameters (indoor air temperature, solar transmittance and daylight level on the reference point) under different control strategies. According to all the comparisons, the correlation between the results of the simplified method and that of BSim is relatively high. The difference in energy calculation between the two methods is below 10 %, and the average  $R^2$  value of the calculated indoor air temperature, solar transmittance and daylight level is higher than 0.94. In general, the method is acceptable for further simulations.

According to the results of the comparison between the simplified method and experiment measurements, the calculated air temperature is in good agreement with the measurements, with  $R^2$  value of 0.8. Additionally, the total cooling energy consumptions calculated by the simplified method are 12.7 % lower than the requested by the control system and around 13.6 % higher than the measured. The calculated total energy consumption of lighting is 14.3 % lower than the measured. The disagreement between the calculated and measured illuminance on the working plane on which the lighting is controlled is bigger when the blind is down.

During the experiment without control of natural ventilation and night cooling the total cooling energy consumption calculated by the simplified method is 8.4 % higher than the requested by the control system and around 8 % higher than the measured. The calculated total energy consumption of lighting is 9.5 % lower than the measured. The  $R^2$  value for indoor air temperature is 0.88.

**PART II - CONTROL STRATEGIES OF THE  
INTELLIGENT GLAZED FACADE**



## 6. CONTROL STRATEGIES: OFFICE BUILDINGS WITH INTELLIGENT GLAZED FACADE

The chapter demonstrates the development of appropriate and holistic control strategies for the intelligent glazed facade containing different functions (solar shading, window shutter, natural ventilation and night cooling (Figure 23) and integrated with building services (heating, cooling, ventilation and lighting) to optimize the comfort performance and minimize the energy demand of buildings. The chapter shows the development of the optimized control strategies for intelligent facades and their improvement on the indoor comfort and energy performance. A numerical case study of an office building with intelligent facade will be demonstrated in this chapter, showing the energy and comfort improvements of the building by different control strategies of the facade. Additionally, this chapter also presents the sensitivity analysis of the influence of building design on the performance of intelligent facades.

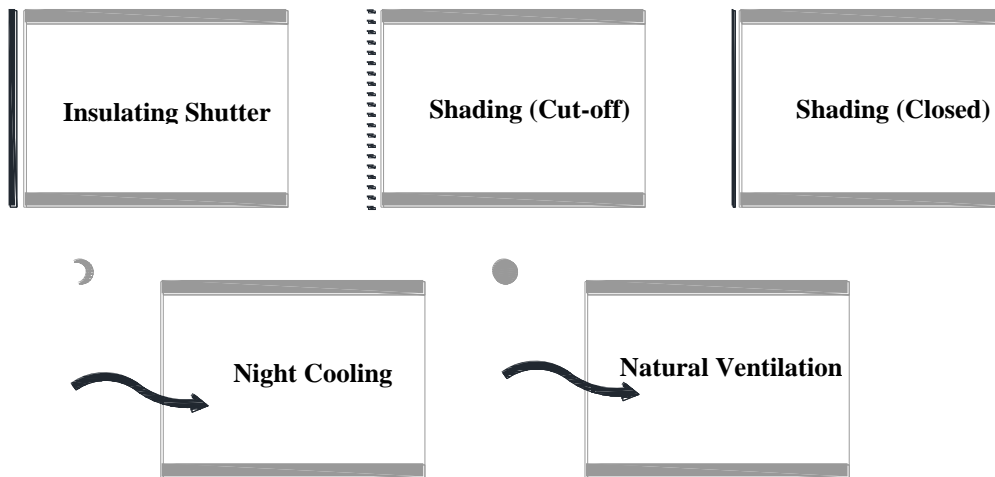


Figure 23: Control of different facade technologies.

### 6.1 DEVELOPMENT OF CONTROL STRATEGIES FOR DIFFERENT FACADE ELEMENTS

Figure 24 and Figure 25 show the developed control strategies of the intelligent glazed facade for all the controlling technologies during both the occupied and unoccupied hours.

The detailed information of the different control technologies are described below.

- External shutter

An external shutter is installed and activated to cover the glazed facade outside office hours. Table 3 (Page 18) shows the layout and the properties of glazing with the external shutter. The theoretical calculation is based on the thermal properties of the shutter, not considering the design and realization of construction.

The control of external shutter is active during the unoccupied hours when the indoor air temperature is below 21 °C. The shutter is controlled as a function of the energy balance across the facade. The evaluation in the calculation is performed by the heat loss and the solar gains through the facade, excluding infiltration (Equation (4)). In order to realize the evaluation of the external shutter control, it requires the measurement of internal and external temperature, incident irradiance, and the calculation of internal loads.

$$\phi_{facade} = \left[ \phi_{sol} \times g_g - U_g \times (T_i - T_o) \right] - \left[ \phi_{sol} \times g_{g+shutter} - U_{g+shutter} \times (T_i - T_o) \right] < 0 \quad (4)$$

Where  $\phi_{facade}$  is heat flow through the facade.  $\phi_{sol}$  is the solar radiation on the glazed facade.  $g_g$  is the solar transmittance of the window, which is 0.4.  $U_g$  is the U-value of the window, which is 1.1 W/(m<sup>2</sup>K).  $T_i$  is the indoor air temperature.  $T_o$  is the outdoor air temperature.  $g_{g+shutter}$  is the solar transmittance of the glazing together with the shutter, which is 0.  $U_{g+shutter}$  is the U-value of the glazing together with the shutter, which is lower than 0.5 W/(m<sup>2</sup>K).

- Glare and solar control by blind

A blind is used to prevent glare problems during the occupied hours and to reduce the solar transmittance through the facade during both the occupied and the unoccupied hours. The tilt angle of the blind depends on its functions. During occupied hours, the angle is calculated by equation (3) from previous research [39] to cut the direct solar radiation, which both improves the visual comfort and maximizes the daylight transmittance into the room.

During unoccupied hours, the blind is controlled to be closed if the indoor air temperature is above 24 °C. The blind is scrolled up if it is not set at a cut-off angle or in a closed position.

- Natural ventilation

The glazed facade is open when the indoor temperature exceeds 23 °C during the occupied hours. The control is active only when the outdoor temperature is lower than the indoor temperature and the outdoor temperature is above 12 °C [46], preventing cold draft in the room. In the real situation, the natural ventilation rate is calculated according to wind speed, wind direction, temperature difference between indoor and outdoor and some other parameters. The calculation is not focus in this chapter. The ventilation rate is assumed to be 1 l/s per m<sup>2</sup>, which is equal to around 1.5 air change rate per hour (ACH) assuming the height of the room is 2.7m [45].

- Night cooling

The night cooling control is active during unoccupied hours in terms of opening the window if the average outdoor air temperature between 12:00 and 17:00 is above 18 °C and if the indoor air temperature is higher than the outdoor air temperature. The control of night cooling can precool the room and help to balance the cooling peak during the next day.

- Heating and cooling

Heating and cooling installations are under PI control to secure the indoor air temperature in the office space between 20 °C and 25 °C.

- Lighting

Artificial lighting of the office building has on-off control during occupied hours according to the illuminance level at the reference point mentioned before. The lighting control is included in all the cases. The set point of the lighting is 300 Lux. The calculation of the illuminance level at the reference point is described in a previous paper [39].

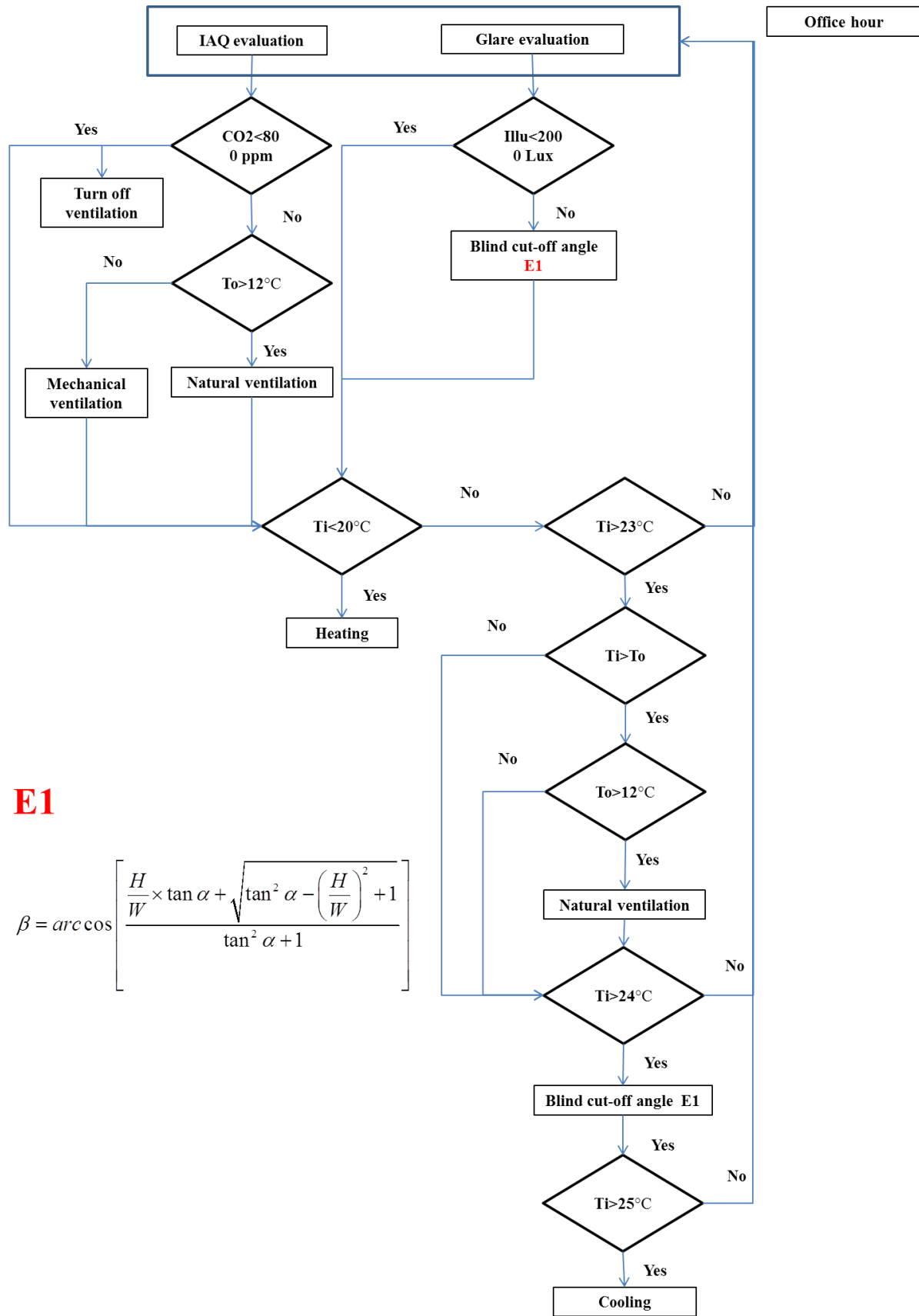


Figure 24: Control strategies of facade for office buildings in occupied hours.

Outside office hour

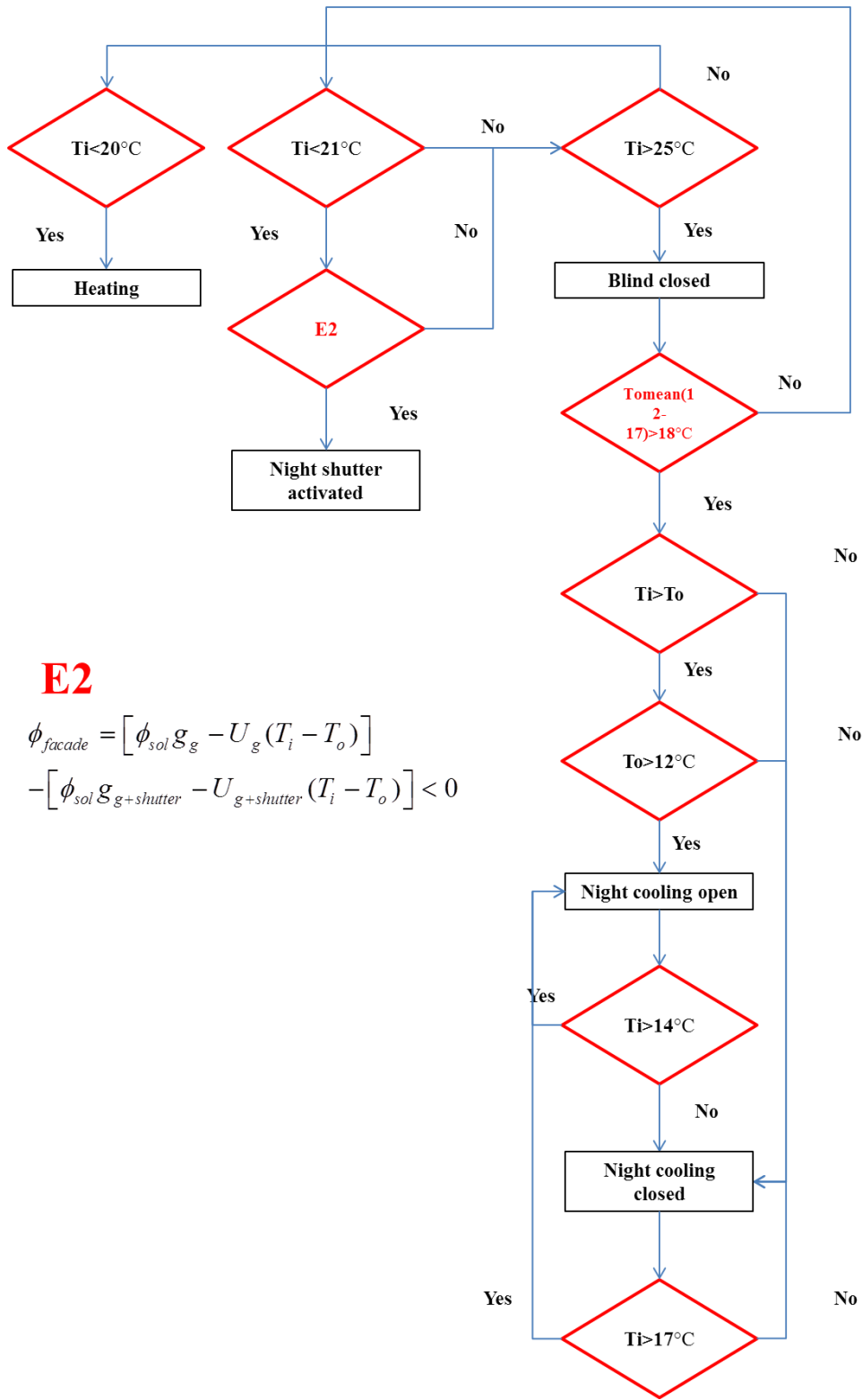


Figure 25: Control strategies of facade for office buildings in unoccupied hours.

## 6.2 CASE STUDY

### Performance Of An Office Building With Intelligent Facade Under Different Control Strategies

The final control strategies are selected after evaluating their influences on the energy and comfort performance of buildings. The influences of the different control strategies on an office building are investigated by the simplified calculation method [39]. The comfort performance is evaluated by operative temperature according to the comfort classes given in EN 15251 [48]. The office building used as example was built in Buddinge Denmark in 2013 with a total heated floor area of around 7400 m<sup>2</sup> and glazing ratio of the entire facade of around 40 % (Figure 26).

Figure 27 shows one floor plan of the building. The window areas towards south, north east and west facades are 514 m<sup>2</sup>, 661 m<sup>2</sup>, 339 m<sup>2</sup> and 376 m<sup>2</sup>, respectively. The glazing type used in the building is a double glazing unit with a 15 mm argon-filled cavity and low-E coating on the internal pane. The total infiltration rate used in the simplified method is 0.06 l/(sm<sup>2</sup>). Table 6 shows the input values of the setups and indoor conditions for the simplified method. Both the heating and cooling loads are assumed to be released 100% convectively to the indoor air, and the indoor illuminance level is measured at the reference point on the working plane (height of 0.85m) which is 1 m from the facade on the centreline of the room. The lighting of the entire room is controlled by this sensor.



Figure 26: Pictures of case study building.

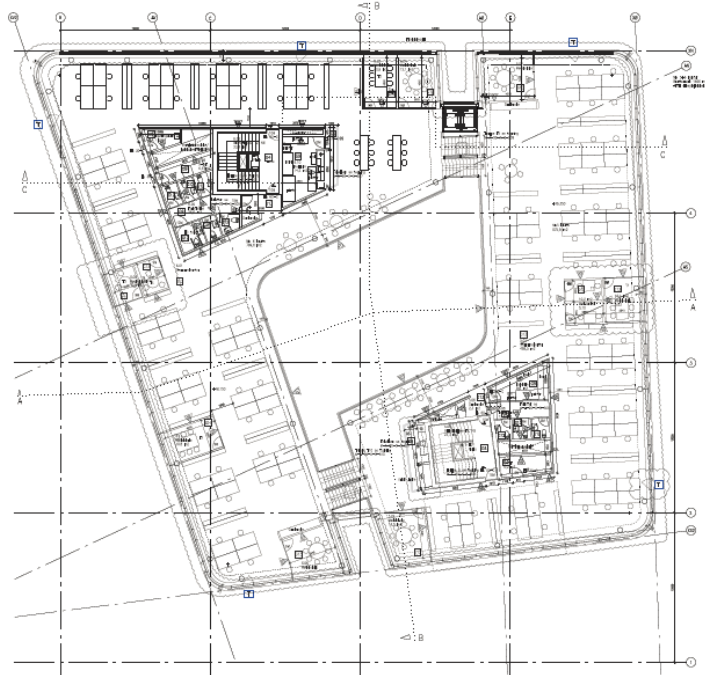


Figure 27: Floor plan of the building in Buddings used as case study.

<b>Internal Loads Of People And Equipment</b>	10 W/m <sup>2</sup>
<b>Lighting Power (On/Off)</b>	7W/m <sup>2</sup>
<b>Setpoint For The Heating</b>	20 °C
<b>Setpoint For The Cooling</b>	25 °C
<b>Mechanical Ventilation Rate (Office Hour)</b>	1.2 l/(sm <sup>2</sup> )
<b>Setpoint Of Lighting</b>	300 lux

Table 6: Setup of building services and indoor conditions.

The study is conducted theoretically and numerically with the help of the simplified method described previously [19-21, 39]. The method can calculate the dynamic properties of different elements of the facade and is also integrated with the hourly model calculating the performance of whole building according to EN 13790 [26]. Therefore, the simplified model is able to calculate the energy demands (heating, cooling, lighting and ventilation) and the indoor environment (indoor air temperature, solar transmittance through the facade and the indoor illuminance level at a chosen point) of the building with a facade of different control strategies. The hourly calculations are conducted throughout the whole year with the weather data of Danish Reference Year (DRY) [23].

Influence of different control strategies and compliance of future building regulation

The calculations on the energy and comfort performance of the office building are conducted for different control conditions:

- Facade without any control (present).
- Control of insulated shutter.
- Control of insulated shutter+ control of solar shading.
- Control of insulated shutter+ control of solar shading+ control of natural ventilation.
- Control of insulated shutter+ control of solar shading+ control of natural ventilation+ control of night cooling.
- Control of insulated shutter+ control of solar shading+ control of natural ventilation+ control of night cooling+ control of lighting.

The control strategies of the different technologies are added one by one to show the improvement in the energy and comfort performance step by step.

The building showed previously was designed to comply with the Danish building regulation of BR10 with a primary energy consumption lower than 72 kWh/m<sup>2</sup> per year [2]. The Danish Government has fixed energy requirements for future new buildings. They are defined as Low Energy Class 2015 and Building Class 2020 [2] with yearly primary energy demand of around 41kWh/m<sup>2</sup>and 25kWh/m<sup>2</sup>, respectively. A study is conducted to investigate if the building after the design changes complies with the future Building Class 2020 [2]. Design changes include improving the thermal properties or using intelligent glazed facade. Table 7 shows the thermal properties of the present and improved building assumed to comply with standards of BR10 and Building Class 2020. They are not required specifically by the standards but taken as the levels within the limitations that fulfil each standard.

The primary energy demand of the building is reduced from approximately 72kWh/m<sup>2</sup>/year to 63kWh/m<sup>2</sup>/year by improving the building from standard of BR10 to Building Class 2020 but still using the static facade (Figure 28). However, the energy performance is still far from the requirement of Building Class 2020. With the help of the control of night shutter, the heating energy is reduced by 10kWh/m<sup>2</sup>/year, lowering the total energy demand by 17 % compared with that of the building without any control strategies. The cooling energy is greatly reduced by 24kWh/m<sup>2</sup>/year by adding the control of the blind. The total energy demand of the facade with the control for night shutter and blind is 32kWh/m<sup>2</sup>/year, which is 9kWh/m<sup>2</sup>/year lower than the requirement of Low Energy Class 2015. The energy performance of the building is optimized further by adding the control for natural ventilation and night cooling. The annual energy demand of the building under all the control strategies reaches approximately 25kWh/m<sup>2</sup>/year, which is 40% of the energy use of the building without any facade control. The energy demand for mechanical ventilation could potentially be reduced by conducting the control of natural ventilation, which was not counted in the simulation.

	BR10	2020
Area (m <sup>2</sup> )	7405	7405
Heat Capacity (Wh/Km <sup>2</sup> )	120	120
Office Hour	8-17	8-17
Internal Load (W/m <sup>2</sup> )	10	10
Heating Temp (°C)	20	20
Cooling Temp (°C)	25	25
Ventilation (l/sm <sup>2</sup> ) (On office hour)	1,2	1,2
Lighting (W/m <sup>2</sup> ) (on/off 250Lux)	7	4
U-Value Opaque Wall (W/m <sup>2</sup> K)	0,13	0,09
Fan Efficiency (kJ/m <sup>3</sup> )	2	0,5
Heat Exchange	0,85	0,85
Infiltration (l/sm <sup>2</sup> )	0,06	0,03

Table 7: Properties difference of building for both BR10 and Building Class 2020.

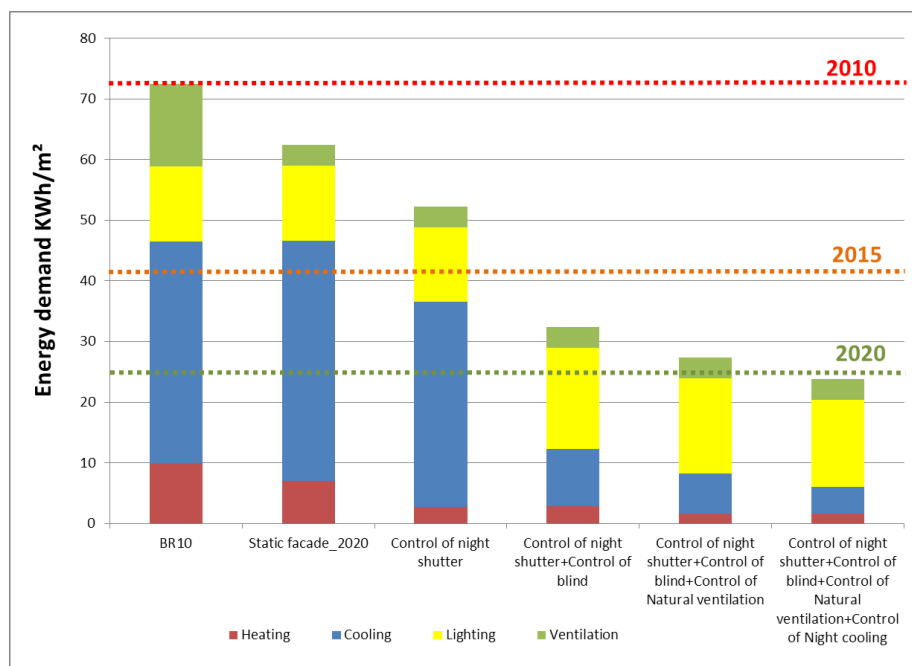


Figure 28: Energy demand of the office building under different control strategies.

The comfort performance of the building was also improved using different control strategies compared with the static facade. Figure 29 shows the time percentage of the different comfort classes specified according to EN 15251. The total time percentage of comfort class I and class II is increased from 21 % to 64 % of the occupied hours by applying control strategies. In addition, the comfort class IV, which is not recommended for indoor comfort, was decreased to 7 % of the occupied hours. The indoor set points of air temperature are set at the same value for the different control strategies, so the operative temperature of the office is optimized by using facade control strategies.

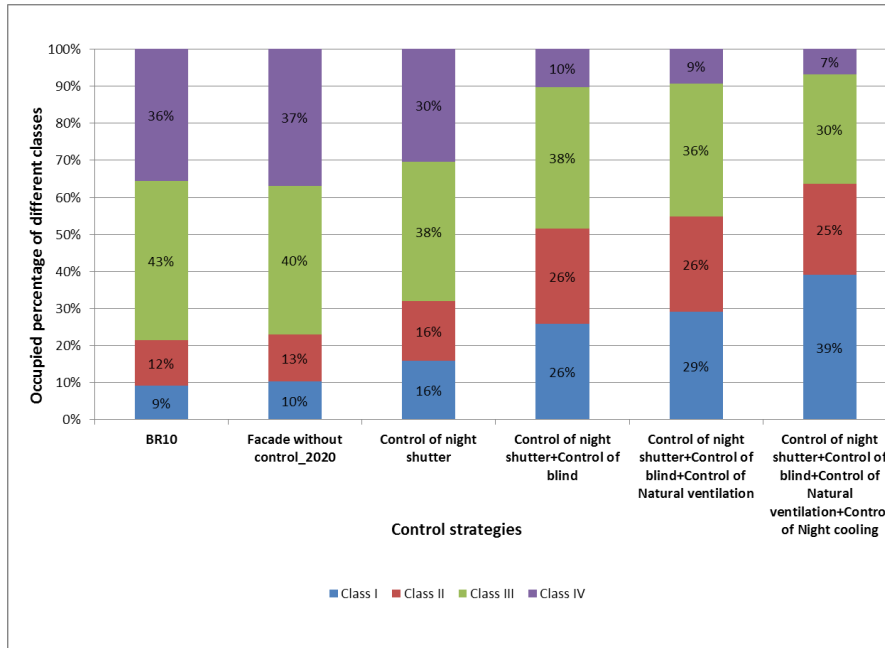


Figure 29: Percentage of different comfort classes of different control strategies.

Even though the properties of all other building elements (U-value of walls, infiltration rate of the building and fan efficiency) but the façade are improved from the standards of BR10 to 2020, the energy performance of the building does not comply with the requirements of total energy demand of 2020 with the static facade (Figure 30). The energy demand of the BR10 building with the intelligent glazed facade is lower than that of the 2020 building with the static facade. The building complies with the Building Class 2020 with both the improved thermal properties from BR10 to 2020 and the intelligent facade. It is reasonable that the energy demand for lighting will increase when the blind control is introduced, because the blind makes the light transmittance of the facade lower than one without the blind.

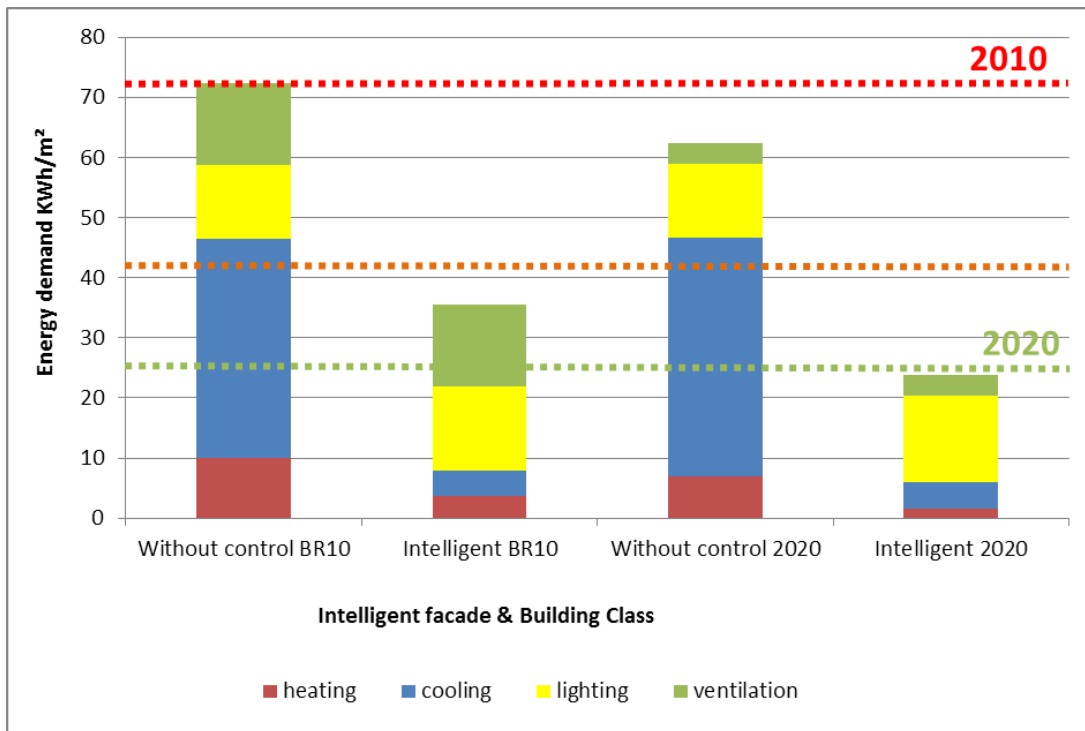


Figure 30: Energy consumptions of the building under different building conditions and different types of facade.



Investigation Of Influence Of Glazing Ratio On The Energy Consumption

Influences from the glazing share ratio of the entire facade on the energy performance are studied for the office building with both a static facade solution and intelligent glazed facade solution. The glazing ratio of facades is limited because there should be a certain fraction of frame. However, theoretical calculations are conducted for the ratio of glazed facade from 20 % to nearly 100 % (fully glazed).

Figure 31 and Figure 32 show the energy performances of the building with different glazing ratios for both the static facade and the intelligent facade. The less the glazing ratio of the static facade is, the better the energy performance. The building with a 20 % glazing ratio of the static glazed facade has the lowest energy demand approximately 50kWh/m<sup>2</sup>/year. With the intelligent glazed facade, the glazing ratio with the lowest energy demand is 40 %. Additionally, even with 100% of glazing in the facade, it still has significantly lower energy demand compared to the static facade with a glazing ratio of 20 %. The building with an intelligent glazed facade with glazing ratio of 90 % complies with the energy requirement of 2015. The advantages of the intelligent glazed facade make it possible for modern office buildings to have higher glazing ratios of the facade without increasing the energy demand significantly, which is preferred because of the good daylight conditions and the better view.

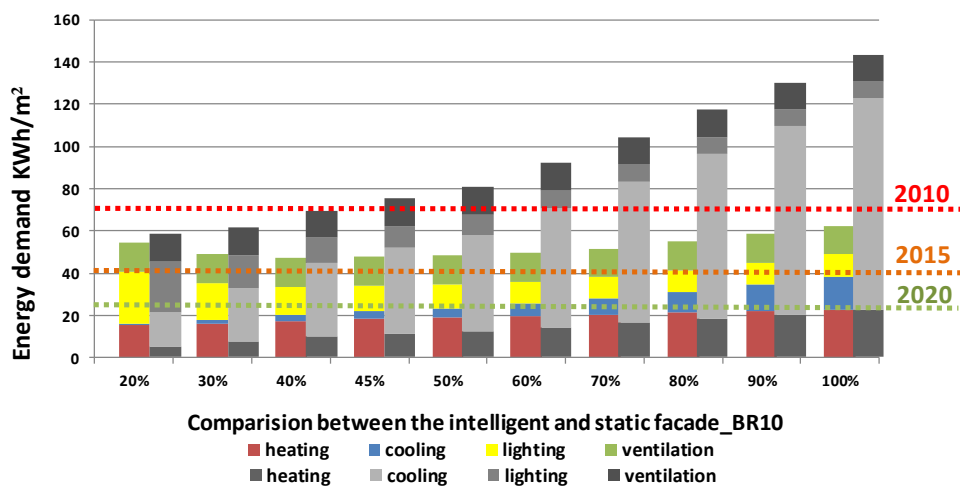


Figure 31: Energy performance of intelligent glazed facade (coloured column) static facade (grey column) with different ratio of glazing share under building standard of BR10.

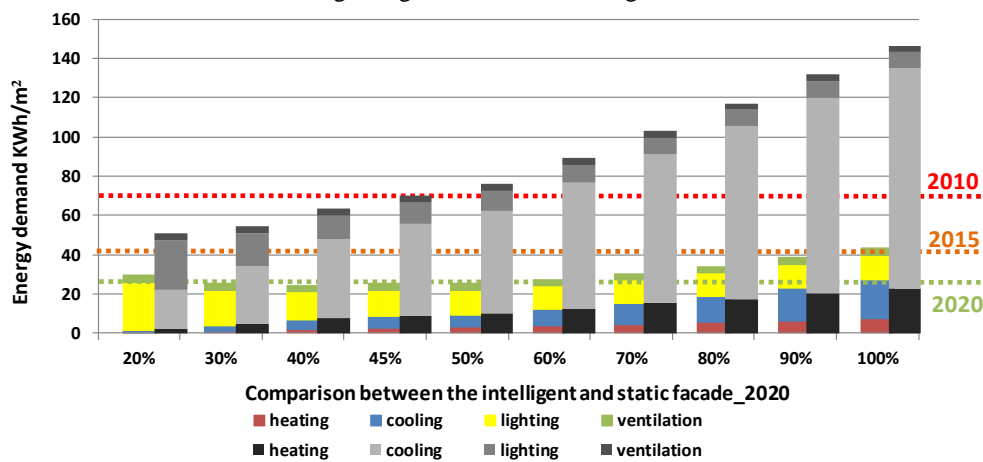


Figure 32: Energy performance of intelligent glazed facade (coloured column) static facade (grey column) with different ratio of glazing share under building standard of 2020.

### 6.3 SENSITIVITY ANALYSIS OF CONTROL STRATEGIES--- BASED ON DIFFERENT BUILDING DESIGN

Analyses have been conducted on how the architectural design of the building affects the performance of the control strategies. Calculations have been implemented for buildings with different features (building quality/building orientation/internal load/thermal mass/weekly office hour).

Table 8 shows the detailed information of different features. Calculations have been conducted with information of buildings under different features. E/W means that the building plan is rectangle with bigger façade area on eastern and western sides. N/S means bigger façade area on northern and southern sides. Equal means that the building plan is square. The assumption is that the buildings in E/W, N/S and Equal have the same total area and the building in Equal has an atrium in the middle causing more external facade area (Figure 33).

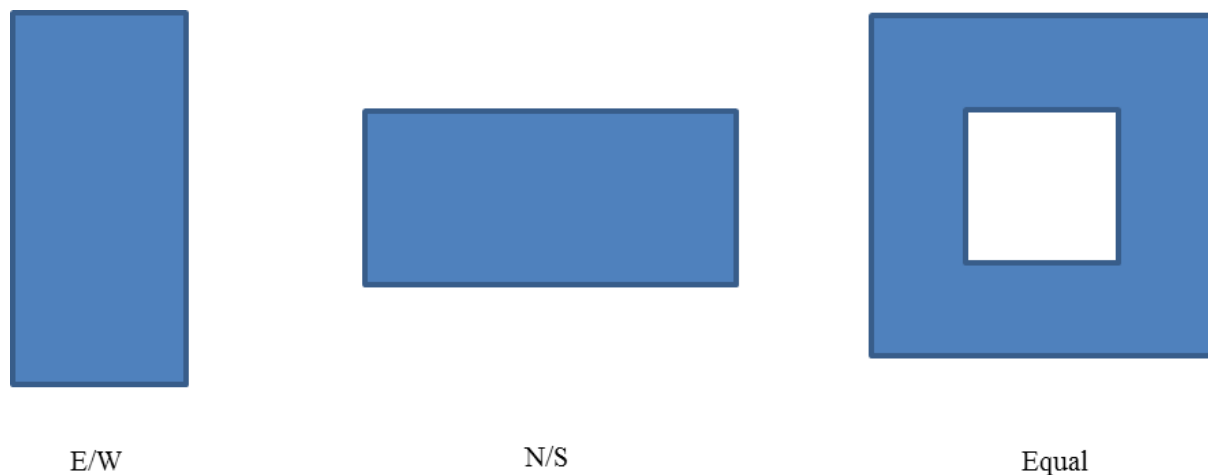


Figure 33: Different building orientations.

Figure 34 shows the influence of the number of weekly office hours and the thermal mass of buildings on the energy consumption of the building. It is obvious that the total energy consumption will increase with longer weekly office hours, which is because the operation time of the building is longer. However, the energy consumption of heating is lower because of the longer period of internal heat load. As the thermal mass increases, the total energy consumption is slightly decreased in a building with intelligent facade. Figure 35 shows the influence of the internal load and building quality on the energy consumption of buildings. It is reasonable that the increase of internal load will cause decrease of the heating consumption and increase of cooling consumption, respectively. Additionally, the energy consumption of lighting also increases because the higher indoor temperature caused by the higher internal load results in more activation of the blind. Figure 36 demonstrates the influence of the building orientation on its energy consumption. It is shown that the total energy consumption of a building with intelligent facade is decreased by almost 50 % by improving the quality of building from 2015 to 2020. The total energy consumptions of buildings in the orientation of E/W and N/S are almost the same. The Equal building has more energy consumption because of more external facade area with the atrium. Figure 37 shows the overview of all the results combining different features.

MODELLING AND CONTROL OF INTELLIGENT GLAZED FAÇADE----- MINGZHE LIU

	Internal load (W/m <sup>2</sup> )			Thermal mass (Wh/Km <sup>2</sup> )			Weekly Office hour (h)			Orientation of building			Building quality	
	5	10	15	60	90	120	30	45	60	E/W	N/S	Equal	2015	2020
<b>Internal Load (W/m<sup>2</sup>)</b>	5	10	15											
<b>Heat Capacity (Wh/Km<sup>2</sup>)</b>				60	90	120								
<b>Office Hour Start</b>							9	8	6					
<b>Office Hour End</b>							14	17	18					
<b>Total Facade Area North (m<sup>2</sup>)</b>										648	1645	1620		
<b>Total Facade Area South (m<sup>2</sup>)</b>										648	1645	1620		
<b>Total Facade Area East (m<sup>2</sup>)</b>										1645	648	1620		
<b>Total Facade Area West (m<sup>2</sup>)</b>										1645	648	1620		
<b>Skylight Over Atrium (m<sup>2</sup>)</b>										0	0	236		
<b>Area Of Roof (m<sup>2</sup>)</b>										1062	1062	826		
<b>Area Of Basement (m<sup>2</sup>)</b>										1062	1062	1062		
<b>Lighting (W/m<sup>2</sup>)</b>													4	7
<b>U-Value of Wall/Roof/Basement (W/Km<sup>2</sup>)</b>													0.13	0.09
<b>Fan Efficiency (kJ/m<sup>3</sup>)</b>													2	0.5
<b>Infiltration (l/sm<sup>2</sup>)</b>													0.06	0.03
<b>Eref (kWh/m<sup>2</sup>)</b>													-17	0
<b>gg</b>													0.61	0.67
<b>ff</b>													0.85	0.9
<b>Uw (W/Km<sup>2</sup>)</b>													1.3	1.3
<b>Light Transmittance</b>													0.78	0.8
<b>Area (m<sup>2</sup>)</b>	7405	7405	7405	7405	7405	7405	7405	7405	7405	7405	7405	7405	7405	7405
<b>Heating Temp (°C)</b>	20	20	20	20	20	20	20	20	20	20	20	20	20	20
<b>Cooling Temp (°C)</b>	25	25	25	25	25	25	25	25	25	25	25	25	25	25
<b>Ventilation (l/sm<sup>2</sup>)</b>	1.2	1.2	1.2	1.2	1.2	1.2	1.2	1.2	1.2	1.2	1.2	1.2	1.2	1.2
<b>Heat Exchange</b>	0.85	0.85	0.85	0.85	0.85	0.85	0.85	0.85	0.85	0.85	0.85	0.85	0.85	0.85

Table 8: Parameters of different building features.

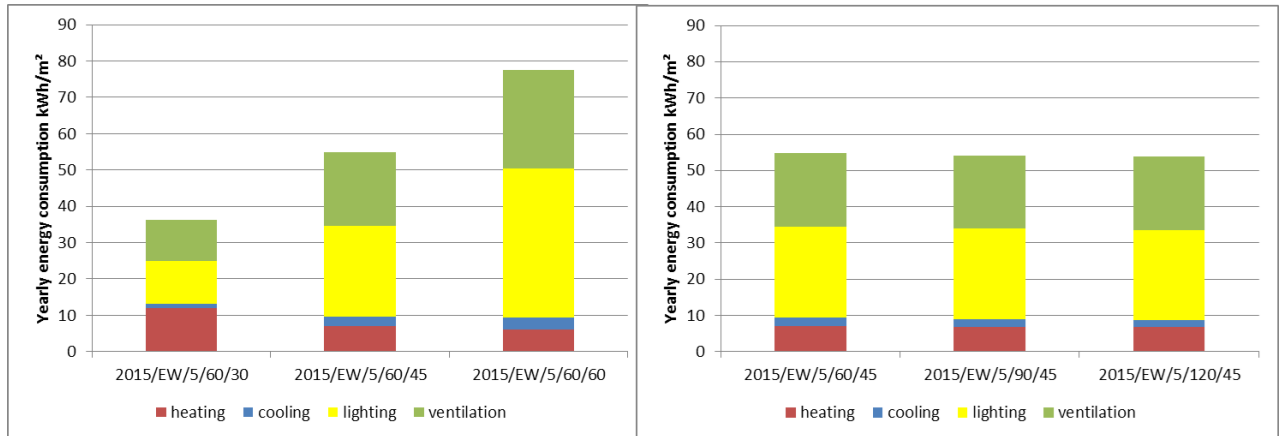


Figure 34: Investigation on the influence of office hour and thermal mass of buildings on the energy consumption (2015/EW/5/60/30 means Building with 2015 level/Orientation of EW/Internal load 5 W/m<sup>2</sup>/Thermal mass 60Wh/Office hours 30 per week).

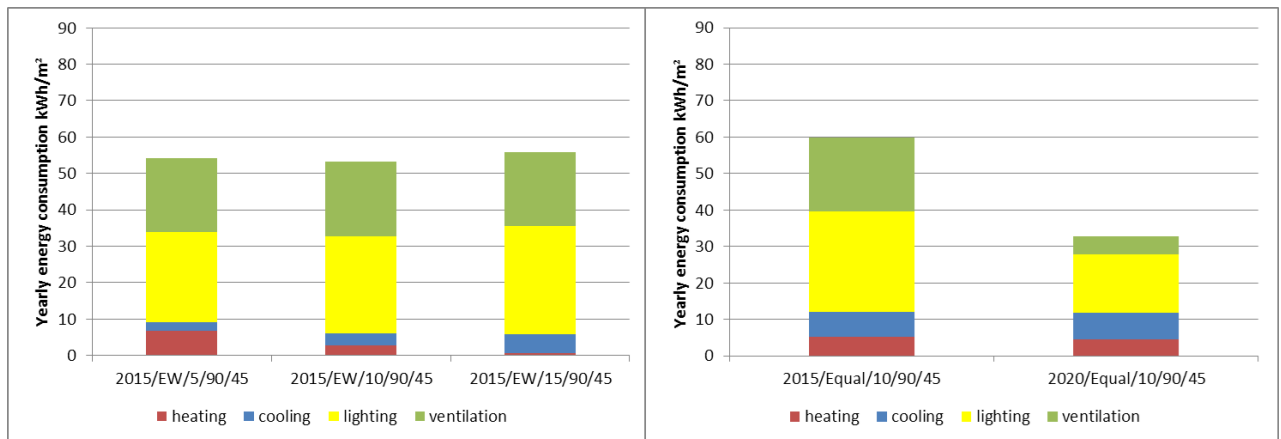


Figure 35: Investigation on the influence of internal heat load and quality of buildings on the energy consumption.

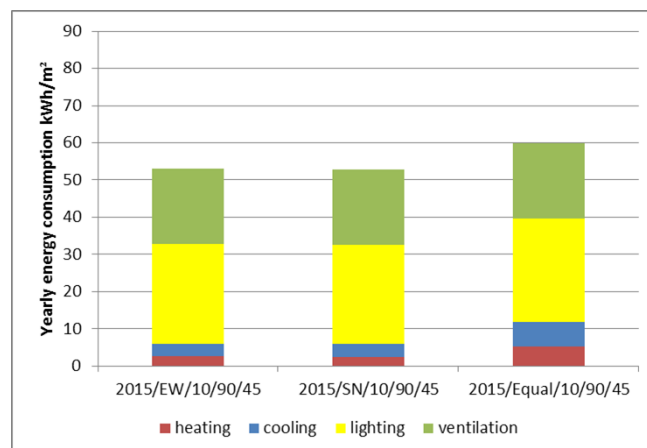


Figure 36: Investigation on the influence of building orientations on the energy consumption.



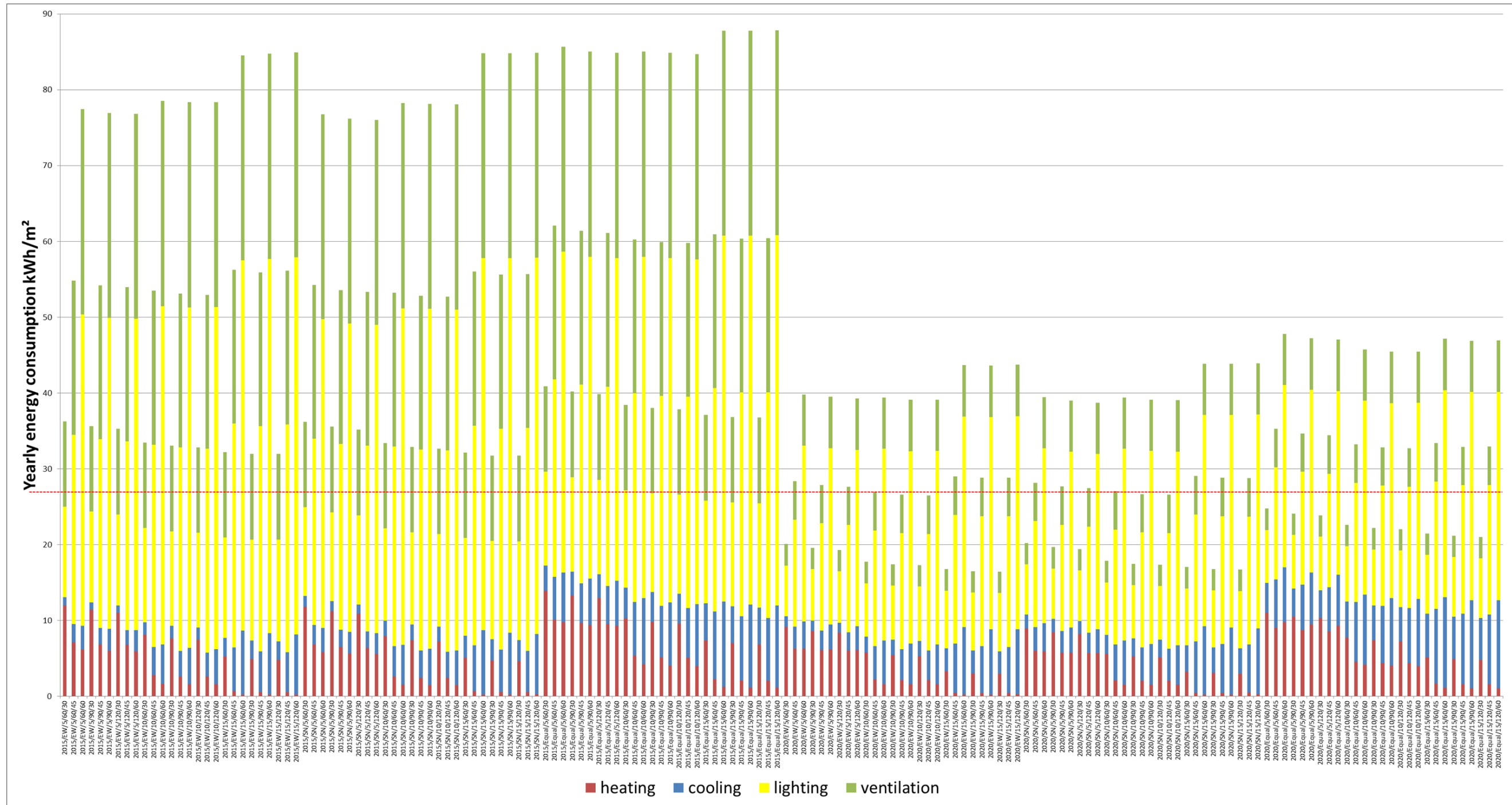


Figure 37 : Overview of the energy consumption of building under different features.

## 6.4 CONCLUSION

The energy consumption of the given building is greatly reduced by approximately 60 % when using the intelligent glazed facade instead of a static facade in the Danish climate. The intelligent glazed facade also improves the indoor comfort by increasing the comfort class I and II from 21 % of the occupied hour to 64 % in the given building.

Together with the improvement of the thermal properties of other building elements, the building installed with the intelligent glazed facade can comply with the energy requirements of the Building Class 2020 with energy consumption of around 25kWh/m<sup>2</sup>/year, which cannot be fulfilled by the building with the static facade.

The facade glazing ratio with the lowest energy consumption increases to around 40 % for the building with the intelligent glazed facade compared with that of 20 % for the building with a static facade. At a glazing ratio of 90 %, the building with the intelligent facade still complies with the energy requirement of Low Energy Class 2015 with an energy consumption of 38kWh/m<sup>2</sup>/year.

## 7. TEST OF THE CONTROL STRATEGIES IN THE FULL-SCALE TEST FACILITY (CUBE)

Control strategies with different set-points for natural ventilation, night cooling and blind have been realized in the control system in the test facility to investigate how they work precisely and their influence on the energy and comfort performance of the room during a period with hot summer days. Since there is only one test room in the test facility, it is not possible to compare the control strategies at the same time with the same weather condition. Therefore, the comparison can only be implemented by conducting the control strategies in different but similar hot summer days with high solar radiation and similar outdoor temperatures.

Two strategies are picked from the experiments. The first is between 18<sup>th</sup> and 19<sup>th</sup> June 2014 with set-points of natural ventilation, night cooling and blind at 23 °C, 23 °C and 24 °C, respectively (Figure 38). The second is between 11<sup>th</sup> and 12<sup>th</sup> August 2014 with set points of natural ventilation, night cooling and blind at 23 °C, 20 °C and 23 °C, respectively (Figure 39).

In the first strategy, lighting energy consumption is reduced because of a higher set-point of blind (24 °C). The control of natural ventilation and blind is capable of covering the heat gain and keeping the indoor air temperature around 24 °C without activating the mechanical cooling. The night cooling is not activated because its set-point is higher than the indoor air temperature during the unoccupied hour, which lessens its effect of reducing the cooling load on the next day. The room temperature reaches around 22 °C during the night without night cooling.

In the second strategy, lighting energy consumption is increased compared with the first strategy because the blind is activated at 23 °C. There is also no need of activating the mechanical cooling in the room. The set-point of night cooling is reduced to 20 °C to even cool down the room temperature during unoccupied hour. The room temperature at night is cooled down to 21 °C, which reduces the potential cooling energy consumption during the next day.

One defect of the glare control of the blind is that the sensor can only check the illuminance on the position of the eyes after the blind is scrolled up, which results in the risk that there is still glare problem when the blind is up. The defect could cause glare problem during one hour (depending on the time step that the system checks the data) and a high frequency of movement of the blind. It is suggested to calculate the illuminance on the eyes' position according to the outdoor solar radiation to avoid the problem.

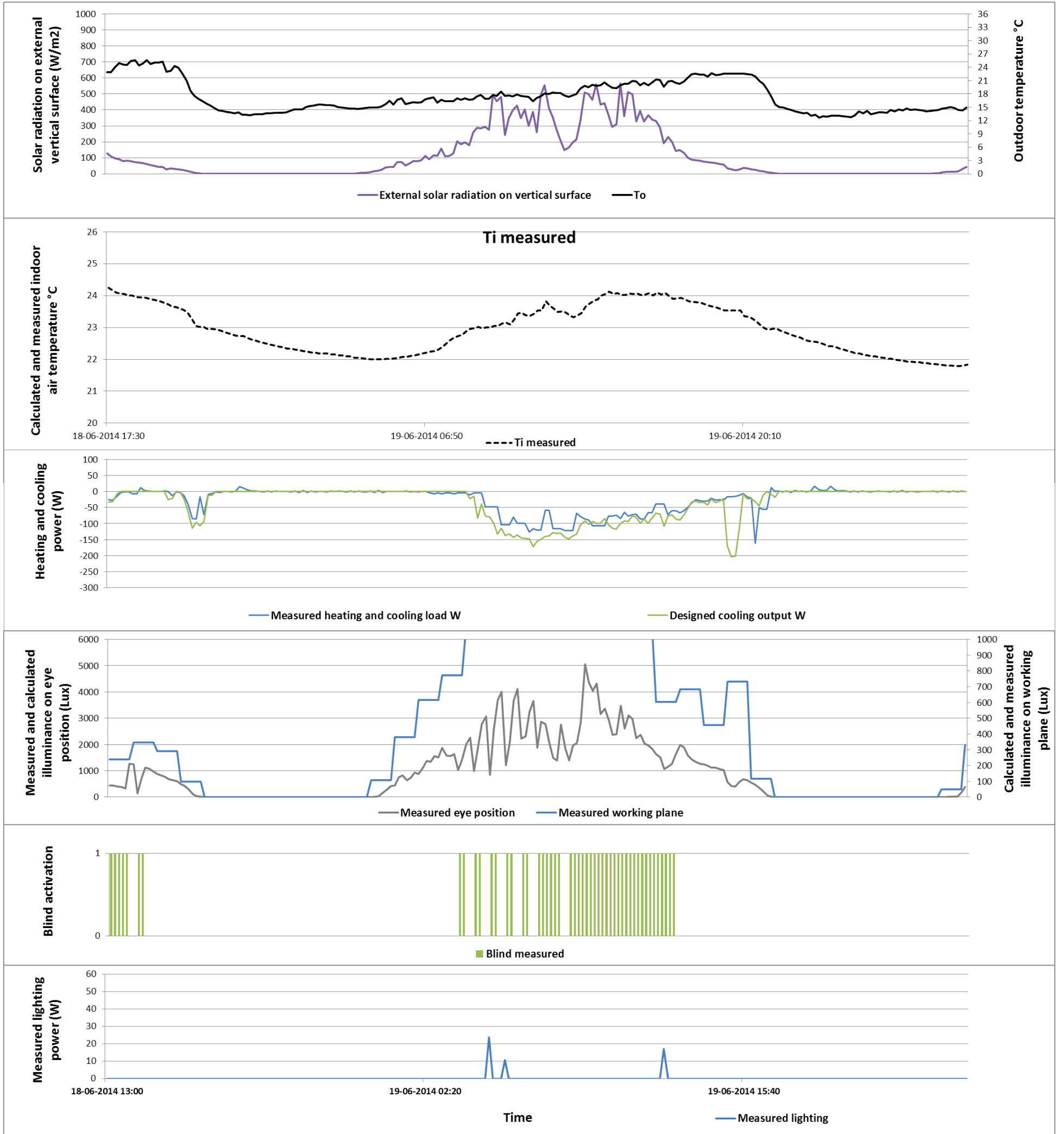


Figure 38: Result of control strategy between 18<sup>th</sup> and 19<sup>th</sup> June. (Natural ventilation 23 °C; Night cooling 23 °C; Blind 24 °C)



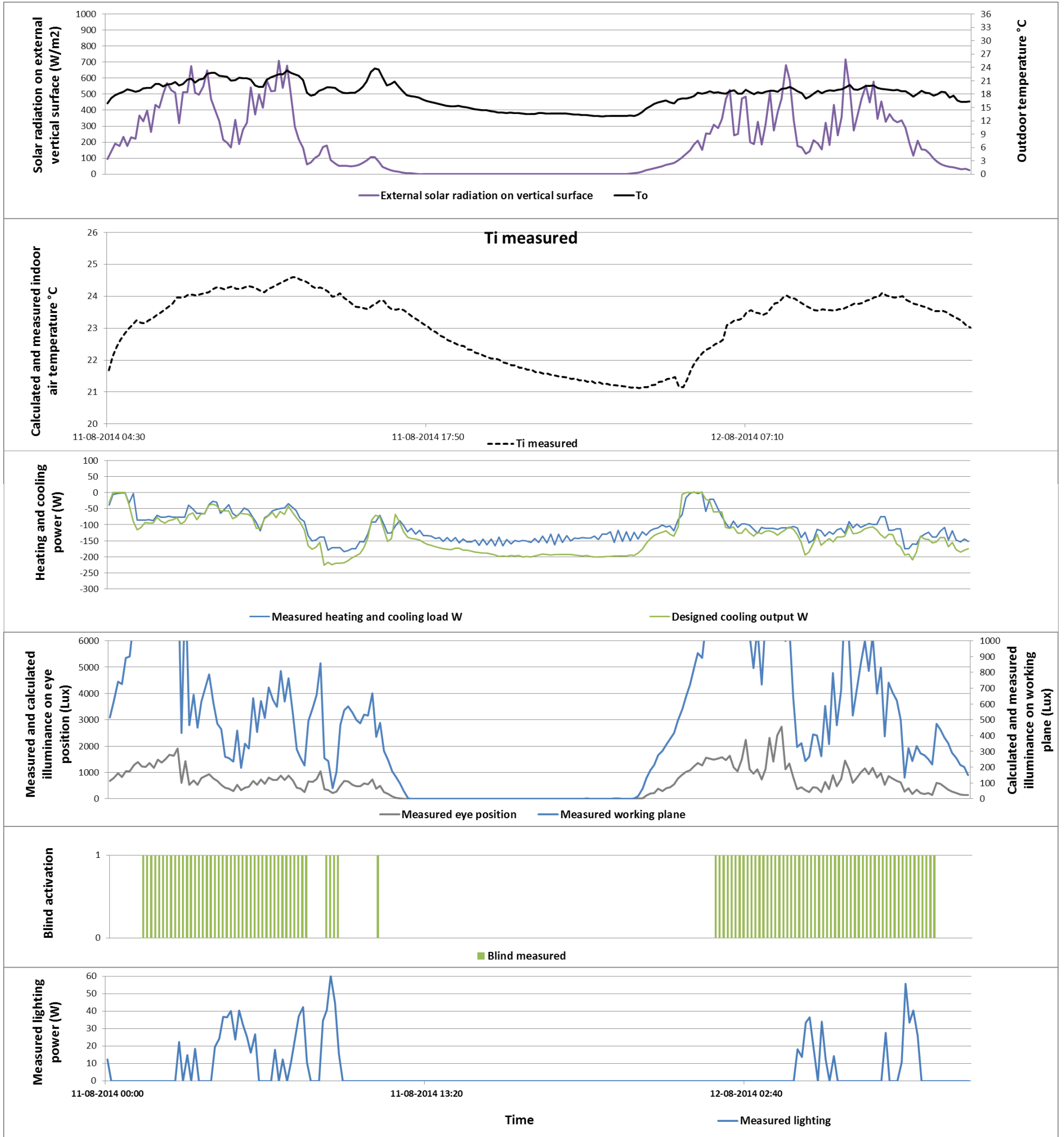


Figure 39: Result of control strategy between 11<sup>th</sup> and 12<sup>th</sup> August. (Natural ventilation 23 °C; Night cooling 20 °C; Blind 23 °C)

## 8. CONCLUSION OF PART II

The energy consumption of the building is greatly reduced by approximately 60 % when using the intelligent glazed facade instead of a static facade in the Danish climate.

Together with the improvement of the thermal properties of other building elements, the building installed with the intelligent glazed facade can comply with the energy requirements of the Building Class 2020, which cannot be fulfilled by the building with the static facade.

The facade glazing ratio with the lowest energy consumption is increased to around 40 % for the building with the intelligent glazed facade compared with that of 20 % for the building with a static facade. At a glazing ratio of 90 %, the building with the intelligent facade still complies with the energy requirement of Low Energy Class 2015 with an energy consumption of 38kWh/m<sup>2</sup>/year.

It is suggested to use higher blind set-point to reduce the energy consumption of lighting if the natural ventilation is enough to cool down the room. The set-point of night cooling is better to be set lower but within the comfort range in order to reduce the potential cooling energy consumption. In practice, the set-point of glare control needs to be calculated according to external solar radiation but not measured in the room, avoiding the risk of glare problems and frequent movements of the blind.

## CONCLUSION OF THE THESIS

Intelligent (or dynamic) facades are implemented more and more in modern buildings. They have the potential of reducing the energy consumption and improving indoor comfort in buildings. In order to support their performance, it is important to have functions in the building simulation and the compliance tools simulating the properties of an intelligent facade. Proper control strategies of facade elements can strengthen the performance of intelligent facade; otherwise, the energy consumption of buildings might even increase. This thesis presents a simplified calculation method and control strategies developed for the intelligent glazed facade. This work has focused on the energy performance in terms of primary energy. The analysis was based on both numerical studies and full-scale experiments of office rooms. Building services were also controlled holistically along with the controlled facade elements (insulated shutter, venetian blind, natural ventilation and night cooling). The heating case has only been investigated numerically but not in the experiment.

Calculation methods of different facade elements were developed to be integrated into the Danish building simulation and compliance tools BSim and Be10 or to work independently.

The comparison between the simplified method and the BSim tool are expressed by the calculations of different thermal and visual properties. The comparison between the indoor air temperature, solar transmittance and illuminance level are presented by average  $R^2$  values of 0.935, 0.993 and 0.947, respectively. Additionally, the simplified method has average difference of 1.2 %, 1.1 %, 7 % and 1.1 % in the calculations of energy demands of heating, cooling, lighting and ventilation compared with BSim (Figure 9). Some differences are caused by the different inputs of heating and cooling needs that are calculated according to different principles of the two methods. In general, the accuracy of the method is acceptable for further simulations.

The simplified calculation method was verified by experiment measurements in the full-scale test facility at Aalborg University. The experiment method and setup is advanced enough to be implemented in complex experiments that require the integration of different measurement instruments and building services into a holistic system, especially when the measured data is needed to control other devices. According to the comparison results, the calculated indoor air temperature generally correlates with the measurements, with the  $R^2$  value of 0.8. Additionally, the total cooling energy consumptions calculated by the simplified method are 8 % higher than the measured cooling consumption. This supports the application of the simplified method in simulation and evaluation of the performance of buildings with intelligent glazed facades in Denmark.

Control strategies for facades and building services were developed for both occupied and unoccupied hours, considering both energy efficiency and indoor comfort. The energy and comfort performance of the given building with the control strategies were calculated by the simplified method with acceptable accuracy. The energy consumption of the given building is reduced by approximately 60 % when using the intelligent glazed facade instead of a static facade in the Danish climate (Figure 28). Together with the improvement of the entire building quality, the building installed with the intelligent glazed facade can comply with the energy requirements of the Building Class 2020, which cannot be fulfilled by the building with the static facade. The facade glazing ratio with the lowest energy consumption is increased to around 40 % for the building with the intelligent glazed facade compared with that of 20 % for the building with a static facade. At a glazing ratio of 90 %, the building with the intelligent glazed facade still complies with the energy requirement of Low Energy Class 2015 with an energy consumption of 38kWh/m<sup>2</sup>/year (Figure 32).

Tests of the control strategies were also conducted in the test facility (Cube) at Aalborg University. According to the test, it is suggested to use higher blind set-point to reduce the energy consumption of lighting if the natural ventilation is enough to cool down the room. The set-point of night cooling is better to be lower within the comfort range to reduce the potential cooling energy consumption. In realistic practice, the set-point of glare control needs to be calculated according to external solar radiation but not measured in the room, to avoid the risk of glare problem and frequent movement of blind.

However, there are some limitations in the method and the experiment. The verification can only present the accuracy of the method in a one-zone building. More work needs to be done for multi-zone buildings to evaluate the influences of heat and mass transfer between different zones. The accuracy of verification of the method is limited because of the homogenous room model. Additionally, the test facility is categorised as a light building, which could limit the verification of the method. More work need to be done in buildings with different levels of heat capacity. The facade of the test facility faces south, more tests on other orientation need to be done. The test was conducted in a short summer period, which limits the verification on the yearly energy calculation and accuracy of the method in other seasons.

Additionally, the user needs to be careful when using water system in the chilled beam to cool down test room. The forward water temperature should be controlled not to be higher than the air temperature of the test room when there is no cooling need in the test room, otherwise the chilled beam will release heating to the test room, which could influence the accuracy of the result.

## FUTURE WORK

The heating case is missing in the full-scale test due to the weather condition during the experiment. It is necessary to investigate the heating consumptions with the activation of insulated shutter.

In the future, the performance of the intelligent glazed facade together with the control of building services needs to be investigated in real office buildings. Additionally, it can also be used for residential buildings, in which the control strategies need to be modified according to different requirement and time schedule, since the building type is heating-dominated in the Danish climate in contrast to the office building which is cooling-dominated. The occupied hours in resident buildings are opposite to the office hours in office buildings.

Moreover, the verifications only present the accuracy of the method in a one-zone building. More work need to be done for multi-zone buildings in order to be able to evaluate the influences of heat and mass transfer between different zones. Additionally, the test facility is categorised as a light building, which could limit the verification of the method. More work need to be done in buildings with different levels of heat capacity.

The study conducted in the project focused on the energy and comfort performances required by the standard but not on the extent of satisfaction and feelings from users. A survey needs to be implemented to evaluate user behaviour in buildings with intelligent facade and the reactions to the control strategies.

In the test, there was only one room in which the control strategies were applied. Control strategies were tested and compared in picked weather conditions that were similar but not exactly the same. Different control strategies could also be compared simultaneously in two test rooms to investigate the different influences under the same conditions.

Heating and cooling were controlled based on the actual heating and cooling needs calculated according to the heat losses and gains resulted from all the facades and operation of building services. It is important to compare the influences on the energy and comfort performance of buildings between this control strategy and the ordinary control of the indoor air temperature.

The operation of natural ventilation during office hour can also reduce the energy consumption of mechanical ventilation by providing fresh air. Therefore, it is important to investigate the influence of the natural ventilation on the indoor air quality and then the reduced operation of the mechanical ventilation.

The infiltration rate of the system is an important parameter in the method as it influences the accuracy of the performance significantly. Therefore, in a practical situation, it is important for the manufacturers to provide an accurate value of the infiltration rate according to the weather data in order to maximize the accuracy of the calculation result.

## REFERENCES

- [1] Communication from the Commission. Action Plan for Energy Efficiency, Realizing the Potential, EC (European Commission) (2006).
- [2] The Danish Ministry of Economic and Business Affairs, Danish Enterprise and Construction Authority, Building Regulations (BR10) (2010).
- [3] H. Poirazis, Single Skin Glazed Office Buildings-Energy Use and Indoor Climate Simulations, Report EBD-T--05/4 (2005).
- [4] S.E. Selkowitz, Integrating advanced facades into high performance buildings (2001).
- [5] F.V. Winther, P. Heiselberg, R.L. Jensen, Intelligent glazed facades for fulfilment of future energy regulations, Passivhus Norden 2010: Towards 2020-Sustainable Cities and Buildings (2010).
- [6] T.R. Nielsen, S.A.H. Svendsen, K. Duer, J.M. Schultz, M.M. Mogensen, Ruder og vinduers energimæssige egenskaber. Kompendium 1: Grundlæggende energimæssige egenskaber, 1999.
- [7] Navid Sidiqi, The influence of window systems on energy performance and indoor environment in low energy office buildings (2012).
- [8] B.A. Lomanowski, J.L. Wright, Modeling fenestration with shading devices in building energy simulation: a practical approach (2009).
- [9] T.E. Kuhn, Solar control: A general evaluation method for facades with venetian blinds or other solar control systems, Energy Build. 38 (2006) 648-660.
- [10] D. Saelens, Energy performance assessment of single storey multiple-skin facades, PhD, KATHOLIEKE UNIVERSITEIT LEUVEN, Leuven (2002).
- [11] J. Wienold, Dynamic simulation of blind control strategies for visual comfort and energy balance analysis (2007) 1197-1204.
- [12] M.G. Gomes, A. Santos, A.M. Rodrigues, Solar and visible optical properties of glazing systems with venetian blinds: Numerical, experimental and blind control study, Build. Environ. 71 (2014) 47-59.
- [13] T.E. Kuhn, C. Bühler, W.J. Platzer, Evaluation of overheating protection with sun-shading systems, Solar Energy. 69 (2001) 59-74.
- [14] J. Karlsson, A. Roos, Modelling the angular behaviour of the total solar energy transmittance of windows, Solar Energy. 69 (2000) 321-329.
- [15] EN, 13363-1, Solar protection devices combined with glazing-Calculation of solar and light transmittance-Part 1: Simplified method (2007).
- [16] EN, 13363-2, Solar protection devices combined with glazing-Calculation of total solar energy transmittance and light transmittance-Part2: Detailed calculation method (2005).
- [17] M.V. Nielsen, S. Svendsen, L.B. Jensen, Quantifying the potential of automated dynamic solar shading in office buildings through integrated simulations of energy and daylight, Solar Energy. 85 (2011) 757-768.
- [18] J. Wong, H. Li, Development of a conceptual model for the selection of intelligent building systems, Build. Environ. 41 (2006) 1106-1123.

- [19] M. Liu, K.B. Wittchen, P.K. Heiselberg, F.V. Winther, Development of simplified and dynamic model for double glazing unit validated with full-scale façade element (2012).
- [20] M. Liu, K.B. Wittchen, P.K. Heiselberg, F.V. Winther, Development of a simplified and dynamic method for double glazing façade with night insulation and validated by full-scale façade element, *Energy Build.* (2012).
- [21] M. Liu, K.B. Wittchen, P.K. Heiselberg, F.V. Winther, Development and sensitivity study of a simplified and dynamic method for double glazing facade and verified by a full-scale façade element, *Energy Build.* 68 (2014) 432-443.
- [22] D.H. Li, A review of daylight illuminance determinations and energy implications, *Appl. Energy.* 87 (2010) 2109-2118.
- [23] K.B. Wittchen, K. Johnsen, K. Grau, *BSIM User's guide*, Danish Building Research Institute, Hørsholm, Denmark (2005).
- [24] U. DOE, *EnergyPlus, Input Output Reference: The Encyclopedic Reference to EnergyPlus Input and Output*, USA, Department of Energy (2010).
- [25] S. Aggerholm, K. Grau, *Bygningers energibehov-SBi-anvisning 213*, Building Research Institute, Aalborg University, Hørsholm, Denmark (2008).
- [26] E. ISO, 13790: Energy performance of buildings–Calculation of energy use for space heating and cooling (EN ISO 13790: 2008), European Committee for Standardization (CEN), Brussels (2008).
- [27] S. Selkowitz, O. Aschehoug, E.S. Lee, *Advanced Interactive Facades-Critical Elements for Future Green Buildings?* (2003).
- [28] D. Kim, C. Park, Manual vs. optimal control of exterior and interior blind systems (2009) 1663-1670.
- [29] P.C. da Silva, V. Leal, M. Andersen, Influence of shading control patterns on the energy assessment of office spaces, *Energy Build.* 50 (2012) 35-48.
- [30] M.V. Nielsen, S. Svendsen, L.B. Jensen, Quantifying the potential of automated dynamic solar shading in office buildings through integrated simulations of energy and daylight, *Solar Energy.* 85 (2011) 757-768.
- [31] D. Kim, C. Park, Manual vs. optimal control of exterior and interior blind systems (2009) 1663-1670.
- [32] A. Tzempelikos, A.K. Athienitis, The impact of shading design and control on building cooling and lighting demand, *Solar Energy.* 81 (2007) 369-382.
- [33] G. van Moeseke, I. Bruyère, A. De Herde, Impact of control rules on the efficiency of shading devices and free cooling for office buildings, *Build. Environ.* 42 (2007) 784-793.
- [34] H. Shen, A. Tzempelikos, Daylighting and energy analysis of private offices with automated interior roller shades, *Solar Energy.* 86 (2012) 681-704.
- [35] T. Schulze, U. Eicker, Controlled natural ventilation for energy efficient buildings, *Energy Build.* (2012).
- [36] E. CEN, 410, *Glass in building–Determination of luminous and solar characteristics of glazing*. Bruxelles (1998).
- [37] B. EN, 673: 1998 *Glass in building-Determination of thermal transmittance (U value)–Calculation method*, British Standards Institution, London, ISBN. 580 (1998) 8.
- [38] J.A. Clarke, *Energy simulation in building design*, Routledge, 2001.

- [39] M. Liu, K.B. Wittchen, P.K. Heiselberg, Development of a simplified method for intelligent glazed façade design under different control strategies and verified by building simulation tool BSim, *Build. Environ.* 74 (2014) 31-38.
- [40] M. Liu, K.B. Wittchen, P.K. Heiselberg, Verification of a simplified method for intelligent glazed façade design under different control strategies in a full-scale façade test facility—Preliminary results of a south facing single zone experiment for a limited summer period, *Build. Environ.* 82 (2014) 400-407.
- [41] T.E. Kuhn, C. Bühler, W.J. Platzer, Evaluation of overheating protection with sun-shading systems, *Solar Energy.* 69 (2001) 59-74.
- [42] O. Kalyanova, P. Heiselberg, , Experimental Set-up and Full-scale measurements in the 'Cube' (2008).
- [43] J. Le Dreau, , Energy flow and thermal comfort in buildings: Comparison of radiant and air-based heating & cooling systems.
- [44] N. Artmann, R. Vonbank, R.L. Jensen, , Temperature Measurements Using Type K Thermocouples and the Fluke Helios Plus 2287A Datalogger (2008).
- [45] T.S. Larsen, P. Heiselberg, Single-sided natural ventilation driven by wind pressure and temperature difference, *Energy Build.* 40 (2008) 1031-1040.
- [46] A. Martin, Control of natural ventilation, BSRIA, 1996.
- [47] D.C. Montgomery, Design and Analysis of Experiments, John Wiley & Sons, 2008.
- [48] C.E. de Normalisation, EN 15251: indoor environmental input parameters for design and assessment of energy performance of buildings addressing indoor air quality, thermal environment, lighting and acoustics, Thermal Environment, Lighting and Acoustics, CEN, Brussels (2007).

## PUBLICATIONS

- 1) Liu M, Wittchen KB, Heiselberg P, Winther FV. Development of Simplified and Dynamic Model for Double Glazing Unit Validated with Full-Scale Facade Element. PLEA 2012 Lima Peru-Opportunities, Limits & Needs.
- 2) Liu M, Wittchen KB, Heiselberg PK, Winther FV. Development of a simplified and dynamic method for double glazing facade with night insulation and validated by full-scale facade element. Energy and Buildings 58 (2013) 163–171
- 3) Liu M, Wittchen KB, Heiselberg PK, Winther FV. Development and sensitivity study of a simplified and dynamic method for double glazing facade and verified by a full-scale facade element. Energy and Buildings 68 (2014) 432–443
- 4) Liu M, Wittchen KB, Heiselberg PK. Development of a simplified method for intelligent glazed facade design under different control strategies and verified by building simulation tool BSim. Building and Environment 2014; 74:31-38.
- 5) Liu M, Wittchen KB, Heiselberg PK. Verification of a simplified method for intelligent glazed facade design under different control strategies in a full-scale facade test facility--- Preliminary results of a south-facing single zone experiment for a limited summer period. Building and Environment 2014; 82:400-407.
- 6) “Control strategies for intelligent glazed facade and their influence on energy and comfort performance of office buildings in Denmark”, Submitted to Journal of Applied Energy.
- 7) “Investigation of configurations of a ventilated window to optimize both the energy balance and the thermal comfort”, submitted to International journal of sustainable built environment.

1.	Modelling and control of intelligent glazed facade
2.	Mingzhe Liu
3.	Kim B. Wittchen, Senior researcher; Per K. Heiselberg, Professor.
4.	<p>List of published and submitted papers:</p> <ul style="list-style-type: none"> <li>• <i>Liu M, Wittchen KB, Heiselberg P, Winther FV. Development of Simplified and Dynamic Model for Double Glazing Unit Validated with Full-Scale Facade Element. PLEA 2012 Lima Peru-Opportunities, Limits &amp; Needs.</i></li> <li>• <i>Liu M, Wittchen KB, Heiselberg PK, Winther FV. Development of a simplified and dynamic method for double glazing facade with night insulation and validated by full-scale facade element. Energy and Buildings 58 (2013) 163–171</i></li> <li>• <i>Liu M, Wittchen KB, Heiselberg PK, Winther FV. Development and sensitivity study of a simplified and dynamic method for double glazing facade and verified by a full-scale facade element. Energy and Buildings 68 (2014) 432–443</i></li> <li>• <i>Liu M, Wittchen KB, Heiselberg PK. Development of a simplified method for intelligent glazed facade design under different control strategies and verified by building simulation tool BSim. Building and Environment 2014; 74:31-38.</i></li> <li>• <i>“Verification of a simplified method for intelligent glazed facade design under different control strategies in a full-scale facade test facility--- Preliminary results of a south-facing single zone experiment for a limited summer period”, published online in journal of Building and environment.</i></li> <li>• <i>“Control strategies for intelligent glazed facade and their influence on energy and comfort performance of office buildings in Denmark”, Submitted to Journal of Applied Energy.</i></li> <li>• <i>“Investigation of configurations of a ventilated window to optimize both the energy balance and the thermal comfort”, submitted to International journal of sustainable built environment.</i></li> </ul>
5.	<p>This thesis has been submitted for assessment in partial fulfilment of the PhD degree. The thesis is based on the submitted or published scientific papers which are listed above. Parts of the papers are used directly or indirectly in the extended summary of the thesis. As part of the assessment, co-author statements have been made available to the assessment committee and are also available at the Faculty. The thesis is not in its present form acceptable for open publication but only in limited and closed circulation as copyright may not be ensured.</p>



# Development of Simplified and Dynamic Model for Double Glazing Unit Validated With Full-Scale Façade Element

MINGZHE LIU<sup>1</sup>, KIM B. WITTCHE<sup>1</sup>, PER KVOLS HEISELBERG<sup>2</sup> AND FREDERIK VILDBRAD WINTHER<sup>2</sup>

<sup>1</sup>Danish Building Research Institute (SBI), Aalborg University, Hørsholm, Denmark

<sup>2</sup>Department of Civil Engineering, Aalborg University, Aalborg, Denmark

*ABSTRACT: The project aims at developing simplified calculation methods for the different features that influence energy demand and indoor environment behind “intelligent” glazed façades. This paper describes how to set up simplified model to calculate the thermal and solar properties (U and g value) together with comfort performance (internal surface temperature of the glazing) of a double glazing unit. Double glazing unit is defined as 1D model with nodes representing different layers of material. Several models with different number of nodes and position of these are compared and verified in order to find a simplified method which can calculate the performance as accurately as possible. The calculated performance in terms of internal surface temperature is verified with experimental data collected in a full-scale façade element test facility at Aalborg University (DK).*

*The advantage of the simplified method is that the models are based on the standards EN 410 and EN 673 taking the thermal mass of the glazing into account. In addition, angle and spectral dependency of solar characteristic will also be considered during the calculation. Using the method, it is possible to calculate the whole year performance with different time steps, e.g. in simple energy and comfort compliance checking tools.*

*Keywords: simplified method, double glazing unit, dynamic, surface temperature, energy*

## INTRODUCTION

Glazed façades are more and more popular for office buildings because of the requirement of higher light transmittance and better view by users; however there are drawbacks of these facades as more glazing gives a higher cooling and heating demand. Furthermore results from static solutions of glazed façade shows that the energy demand cannot be reduced significantly simply by optimizing technologies [1].

In order to minimize the energy demand of glazed office buildings, “intelligent” glazed façades has already been developed, which can react dynamically according to the environment and take advantage of the microclimate to provide optimum indoor environment and minimum building energy demand. Research has been done to evaluate the performance of the “intelligent” glazed façade [1]. Since this concept is still relatively new and some existing simulation tools are either too detailed or not accurate enough to be used for energy analysis in design stage of building design. An on-going PhD project is currently developing simplified calculation model for the “intelligent” glazed facades to accurately calculate its performance in terms of energy use and indoor environment in the building.

The expected output of the simplified calculation model is the energy needed to maintain an optimal comfort level of the room. Thermal comfort will also be evaluated, which means the internal surface temperature of façades should be one of the outputs. Together with other parameters of indoor environment, it contributes to comfort level described in the criteria [2].

Some simulation tools, standards and calculation methods has already been developed to simulate double glazing unit [3, 4, 5, 6, 7], but they either require much time and professional knowledge from the users to build the model and get the result or are not detailed and accurate enough to calculate the performance. In the method developed in the BESTFACADE project [3] a continuous procedure for calculating the impact of Double Skin Façade (DSF) constructions on the overall energy demand of buildings is applied. However, the calculation method is only suitable for double skin façade with ventilated cavity but not for single skin façade like double glazing unit. It cannot calculate the surface temperature of glazing. WIS software [4] can calculate the U-value and g value together with the internal surface temperature of different kind of glazing unit, but the method in WIS Software considers only steady state condition and it can only calculate performance in one time step, which results in much time

consuming to calculate the performance of whole year. Using the methods defined in ISO 15099 [5] one can calculate the surface temperature of glazing. But the methods do not take the thermal mass of glass and temperature of cavity into account in its heat balance. Danish simulation tool BSim [6] and compliance checking tool Be10 [7] are simplified calculation tools to calculate the energy demand of building and internal surface temperature of glazing, but their glass models are not detailed and accurate enough to calculate the surface temperature taking into dynamic features of facade.

So a simplified though dynamic calculation method that can predict the energy and comfort performance of double glazing unit with acceptable accuracy needs to be developed for used in the early design stage of building and façade. This paper describes part of the simplified calculation method, focusing on the development of the simplified calculation method of the basic element of the “intelligent” glazed façade, i.e. the double glazing unit.

**METHOD**

Simplified calculation method is developed to calculate the internal surface temperature of double glazing unit together with the energy exchange through it. The performance of the simplified calculation method is compared with WIS software and evaluated by measurements performed at the test facility “The Cube” at Aalborg University. The purpose of this is to see how the simplified calculation method performs in terms of determination of internal surface temperatures. Internal surface temperatures of the double glazing unit are measured every 6 minutes from 15:00 24<sup>th</sup> January 2011 to 14:00 31<sup>st</sup> January 2011. The calculation by the simplified calculation method is conducted through all the time when temperatures are measured. But because of its time consuming, the calculation of WIS software is only conducted in 28<sup>th</sup> and 30<sup>th</sup>, representing a cloudy day and a clear day.

By calculating the internal surface temperature, the heat exchange through the double glazing unit can be calculated by the simplified calculation method. Together with the solar transmittance through the glazing, the total heating or cooling energy demand caused by the façade can be predicted.

**GRID SENSITIVITY OF THE METHOD**

In order to test the grid sensitivity of the simplified method, models with the same principle and heat balance equations but different number of variable nodes are constructed in matrices calculating the internal surface temperature. Figure 1 shows the layout of the double glazing unit and an example of node positions and numbers in model 3\_1\_3 (3 variable nodes in the external

pane, 1 node in the cavity and 3 variable nodes in the internal pane). Calculations are conducted from model 3\_1\_3 to model 129\_1\_129, where number of nodes increases step by step in external pane and internal pane of the double glazing unit.

Figure 2 shows the calculated results and deviation of different models compared with model 129\_1\_129 in terms of internal surface temperature in one time step. The last four models (2\_0\_2 surfaces, 1\_0\_1 surfaces, 1\_1\_1 middle and 1\_0\_1 middle) are potential simple models from which the simplified method is chosen.

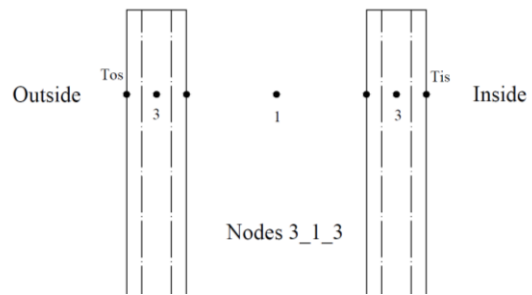


Figure 1: Example of model with nodes 3\_1\_3 (number of nodes in external pane\_ number of nodes in cavity\_ number of nodes in internal pane).

The result shows that all the four simple models have good accuracy with deviation of under 0.2 % compared with model 129\_1\_129. But model 2\_0\_2 surfaces and model 1\_0\_1 surfaces are better than the other two simple models. Considering the complexity and time consumption of solving equations with four variables, model 1\_0\_1 surfaces is chosen.

According to Figure 2, the deviation of the 1\_0\_1 surface model is around 0.02 %, which is adequately accurate for the simplified calculation method. The 1\_0\_1 surface model can be used to calculate the internal surface temperature with only two nodes, which are located on the internal surface and external surface of the double glazing unit. In time step 1, calculation is taken as steady state. After time step 1 calculation is conducted dynamically taking thermal mass of glass into account.

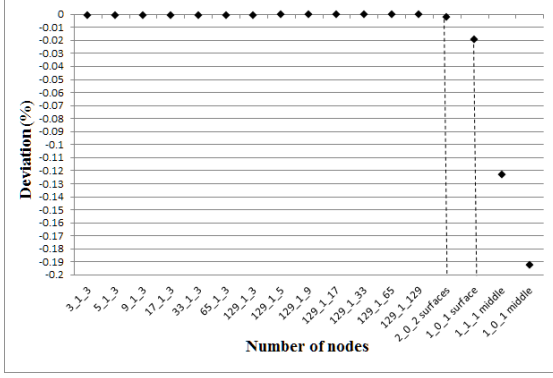


Figure 2: Deviation of different models compared with model 129\_1\_129 in terms of internal surface temperature (2\_0\_2 surfaces means two nodes on surfaces of internal and external pane but there is no node in the cavity).

### SIMPLIFIED CALCULATION METHOD

According to the comparison of grid sensitivity, the 1\_0\_1 surface model is finally chosen as the simplified model. The simplified calculation method is implemented making use of finite volume energy balance equations by Clarke [8] to calculate the temperature of internal and external surfaces, taking into account of the thermal mass of the glass, spectral and angle dependence of the solar radiation [10, 11]. There are two variable nodes in the equations representing the internal and external surface temperature with the volume of  $\frac{1}{4}$  of the thickness of glass. It is assumed that the temperature of glass in the volume is homogeneous. The equations take both implicit and explicit conditions into account [8] considering the boundary conditions of both the present and previous time steps to increase the accuracy of the result.

The following equations are the results of the method calculating the temperatures of internal and external surface of the glazing.

Internal and external surface temperatures for time step 1 can be calculated by equations (1) and (2):

$$T_{is1} = \frac{[(T_{o1}h_{c,e1} + T_{r,e1}h_{r,e1} + \Phi_{solo1})h_{t1} + (T_{i1}h_{c,i1} + T_{r,i1}h_{r,i1} + \Phi_{soli1})(h_{t1} + h_{c,e1} + h_{r,e1})]}{[(h_{t1} + h_{c,i1} + h_{r,i1})(h_{t1} + h_{c,e1} + h_{r,e1}) - h_{t1}^2]} \quad (1)$$

$$T_{os1} = \frac{[(T_{o1}h_{c,e1} + T_{r,e1}h_{r,e1} + \Phi_{solo1})(h_{t1} + h_{c,i1} + h_{r,i1}) + (T_{i1}h_{c,i1} + T_{r,i1}h_{r,i1} + \Phi_{soli1})h_{t1}]}{[(h_{t1} + h_{c,i1} + h_{r,i1})(h_{t1} + h_{c,e1} + h_{r,e1}) - h_{t1}^2]} \quad (2)$$

Internal and external surface temperatures for time step  $(t + \delta t)$  can be calculated by equations (3) and (4):

$$T_{is(t+\delta t)} = [(T_{o(t+\delta t)}h_{c,e(t+\delta t)} + T_{r,e(t+\delta t)}h_{r,e(t+\delta t)} + \Phi_{solo(t+\delta t)} + a)h_{t(t+\delta t)} + (T_{i(t+\delta t)}h_{c,i(t+\delta t)} + T_{r,i(t+\delta t)}h_{r,i(t+\delta t)} + \Phi_{soli(t+\delta t)} + b)] \quad (3)$$

$$\cdot \left( h_{t(t+\delta t)} + h_{c,e(t+\delta t)} + h_{r,e(t+\delta t)} + \frac{2C_p\rho V}{\delta t} \right) / \left[ (h_{t(t+\delta t)} + h_{c,i(t+\delta t)} + h_{r,i(t+\delta t)} + \frac{2C_p\rho V}{\delta t})(h_{t(t+\delta t)} + h_{c,e(t+\delta t)} + h_{r,e(t+\delta t)} + \frac{2C_p\rho V}{\delta t}) - h_{t(t+\delta t)}^2 \right]$$

$$T_{os(t+\delta t)} = [(T_{o(t+\delta t)}h_{c,e(t+\delta t)} + T_{r,e(t+\delta t)}h_{r,e(t+\delta t)} + \Phi_{solo(t+\delta t)} + a) \cdot \left( h_{t(t+\delta t)} + h_{c,i(t+\delta t)} + h_{r,i(t+\delta t)} + \frac{2C_p\rho V}{\delta t} \right) + (T_{i(t+\delta t)}h_{c,i(t+\delta t)} + T_{r,i(t+\delta t)}h_{r,i(t+\delta t)} + \Phi_{soli(t+\delta t)} + b)h_{t(t+\delta t)}] / \left[ (h_{t(t+\delta t)} + h_{c,i(t+\delta t)} + h_{r,i(t+\delta t)} + \frac{2C_p\rho V}{\delta t})(h_{t(t+\delta t)} + h_{c,e(t+\delta t)} + h_{r,e(t+\delta t)} + \frac{2C_p\rho V}{\delta t}) - h_{t(t+\delta t)}^2 \right] \quad (4)$$

$$a = (T_{is(t)} - T_{os(t)})h_{t(t)} + (T_{o(t)} - T_{os(t)})h_{c,e(t)} + (T_{r,e(t)} - T_{os(t)})h_{r,e(t)} + \Phi_{solo(t)} + \frac{2C_p\rho V}{\delta t}T_{os(t)} \quad (5)$$

$$b = (T_{os(t)} - T_{is(t)})h_{t(t)} + (T_{i(t)} - T_{is(t)})h_{c,i(t)} + (T_{r,i(t)} - T_{is(t)})h_{r,i(t)} + \Phi_{soli(t)} + \frac{2C_p\rho V}{\delta t}T_{is(t)} \quad (6)$$

After calculating the internal surface temperature, the total energy exchange between inside and outside can be calculated by equation (7):

$$Q_{total} = Q_{tr} - Q_{sol} \quad (8)$$

$$Q_{sol} = \tau_{e,gzg}Q_{dir} + \tau_{e,dif}Q_{dif} \quad (9)$$

$$Q_{tr} = (T_i - T_{is})h_{c,i} + (T_{r,i} - T_{is})h_{r,i} \quad (10)$$

$$(11)$$

By inputting the results of the variables and parameters of subsystems in excel, the simplified calculation method can be realised. This method can be used in the early design stage of building and façade to predict the energy and comfort performance of double glazing unit. Compared with software like ESP-r and WIS, it requires less time and professional knowledge to input the parameters and build the model. The method can also be implemented in calculations using any number of time steps, saving much time compared with WIS software which can only calculate the performance of one time step.

### Dynamic heat transfer coefficient in subsystems

This method not only takes into account the thermal mass of the glass, but also dynamic properties of the convective and radiative heat transfer coefficients. The present heat transfer coefficients decided by temperature difference are calculated using the results of surface temperature of previous time step.

Convective heat transfer

Interior surface convective heat transfer coefficient [8]:

$$h_{c,i} = \left\{ \left[ 1.5 \left( \frac{\Delta T}{H} \right)^{0.25} \right]^6 + [1.23(\Delta T)^{0.33}]^6 \right\}^{\frac{1}{6}} \text{ (W/(m}^2 \cdot \text{K))} \quad (12)$$

Dynamic solution can be realized in (11) [8], calculating  $h_{c,i}$  with the parameters of previous time step:

$$h_{c,i(t+\delta t)} = \left\{ \left[ 1.5 \left( \frac{T_{is(t)} - T_{i(t)}}{H} \right)^{0.25} \right]^6 + [1.23(T_{is(t)} - T_{i(t)})^{0.33}]^6 \right\}^{\frac{1}{6}} \text{ (W/(m}^2 \cdot \text{K))} \quad (13)$$

Exterior surface convective heat transfer coefficient can be calculated by (12) [8]:

$$h_{c,e} = 5.678 \left[ a + b \left( \frac{V}{0.3048} \right)^n \right] \text{ (W/(m}^2 \cdot \text{K))} \quad (14)$$

If  $V < 4.88$  m/s then  $a=0.99$ ,  $b=0.21$ , and  $n=1$ .

If  $4.88$  m/s  $< V < 30.48$  m/s then  $a=0$ ,  $b=0.5$ , and  $n=0.78$ .

For climate of Aalborg, the average wind speed in January 2011 according to Windfinder [15] is taken as 5.5 m/s.

Long-wave radiative heat transfer

Longwave radiative heat transfer coefficient between internal surface and internal walls is calculated as described in the following.

The internal radiative heat transfer coefficient of time step 1 is 4.4 W/(m<sup>2</sup> · K) according to EN 673 [9].

After time step 1, dynamic solution can be realized in (13), calculating  $h_{r,i}$  with the parameters of previous time step.

$$h_{r,i(t+\delta t)} = \frac{\epsilon_i \epsilon_{r,i} \sigma (A_i T_{is(t)}^4 f_{i \rightarrow r,i} - A_{r,i} T_{r,i(t)}^4 f_{is \rightarrow r,i})}{A_i (T_{is(t)} - T_{r,i(t)}) [1 - (1 - \epsilon_i)(1 - \epsilon_{r,i}) f_{is \rightarrow r,i} f_{r,i \rightarrow i}]} \quad (15)$$

Long-wave radiative heat transfer between external surface and surroundings can be calculated by (14) and (15) [8]:

In time step 1,  $h_{r,e}$  can be calculated by (14) assuming the mean temperature of  $T_{r,e}$  and  $T_{os}$  is outdoor air temperature  $T_o$ .

$$h_{r,e1} = 4\epsilon\sigma T_o^3 \quad (16)$$

After time step 1, dynamic solution can be realized in (15), calculating  $h_{r,e}$  with the parameters of previous time step.

$$h_{r,e(t+\delta t)} = \frac{\epsilon\sigma(T_{r,e}^4 - T_{os}^4)}{T_{r,e} - T_{os}} \quad (17)$$

## VERIFICATION OF SIMPLIFIED METHOD

The model is verified by empirical data of internal surface temperature from experiments. The measurement is implemented in the full-scale test facility of façade and room (The Cube at Aalborg University) (figure 3). The test facility has two identical rooms facing south, with the internal dimension of  $5.66 \times 2.46 \times 1.65$  m<sup>3</sup> (H×W×D). The entire window systems face south and each has a size of  $1.5 \times 4$  m<sup>2</sup>. There are two operable windows, one large window in the middle and a filling at top of the window system. The operable windows has a size of  $1.5 \times 0.5$  m<sup>2</sup> including frame area, and the middle window has a size of  $1.5 \times 2.2$  m<sup>2</sup>. The filling at the top of the window system has a size of  $1.5 \times 0.8$  m<sup>2</sup>. The measurements for the double glazing unit were conducted in one of the rooms in the end of January 2011 with low outdoor temperature.

The glazing type used in the experiments is a double glazing unit with a 22 mm argon-filled cavity and low-e coating on the internal pane. The layout of the double glazing unit is showed in table 1.

The thermocouples, used for measuring the internal surface temperatures of the glazing were shielded from the outside to prevent solar irradiance from influencing the measurements [16]. The vertical gradient of the room temperature was measured at 0.91 m, 1.82 m and 2.73 m above the floor in the room.

Table 1: Layout and glass type of double glazing unit used in the simplified method and WIS.

Position	Material
Outside	Planilux 4 mm SGG
Cavity	Argon 22 mm
Inside	PIUturan 4 mm SGG



Figure 3: Full-scale façade element test facility.

Figure 4 shows the overall results of simplified method compared with the measured performance during all the days when the measurements are conducted. It shows that during night or daytime with less solar radiation the simplified method overestimates the internal surface temperature with the deviation less than 1°C. While during sunny days it underestimates the internal surface temperature probably because it underestimates the solar absorption of the internal pane.

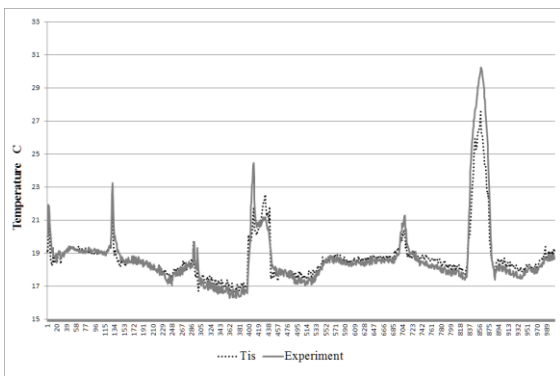


Figure 4: Comparison between calculated and measured internal surface temperature.

The calculation results of the simplified method are compared with the performance calculated by WIS software. Because it takes much time to do calculation of different time steps, calculations from WIS software are only conducted on 28<sup>th</sup> and 30<sup>th</sup> of January. The 28<sup>th</sup> of January is a typical overcast day with less solar radiation

while the 30<sup>th</sup> of January is a typical sunny day with high solar radiation. The calculations conducted in WIS use the same input of external and internal air and surrounding temperatures as the simplified method. The heat transfer coefficients used in WIS calculation are taken from EN673 [9]. Figure 5 and 6 show the internal surface temperature calculated by the simplified method and WIS compared with the measured in the test facility. The results show that during the time with no or less solar radiation, both simplified and WIS overestimate the internal surface temperature. But the simplified method is closer to the measured performance compared with WIS, with a deviation less than 0.5°C. During the time with high solar radiation, the simplified method underestimates the internal surface temperature, possibly because of the underestimation of the solar absorption of internal pane, while WIS overestimates the performance during most of the time. The reason for the difference between the results of the simplified method and experiments could also be the tolerance of the convective and radiative heat transfer coefficient. Internal convective and radiative heat transfer coefficient significantly influent the calculated temperature. The reason for the overestimation of WIS software during the overcast day could probably be the overestimation of the internal convective heat transfer coefficient (3.6W/m2K) according to EN673 [9]. It could also be the overestimation of the default emissivity of in internal surround surface  $\epsilon_{r,i}$  used in WIS resulting in more heat exchange between the internal glazing surface and the internal surroundings. The reason for the overestimation of WIS software during the sunny day could probably be the overestimation of the angle-dependent solar absorption. The calculated internal surface temperature by WIS is almost the same under different incident angle of solar radiation.

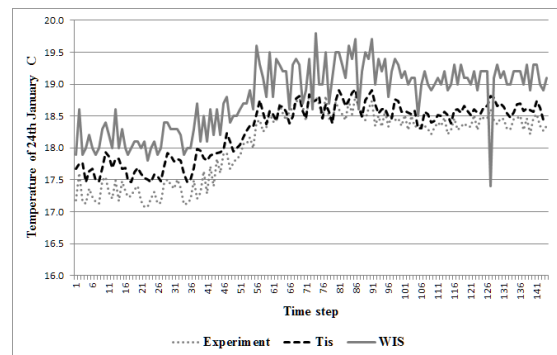


Figure 5: Temperature Comparison between simplified method, WIS and measurement on 28<sup>th</sup> January 2011.

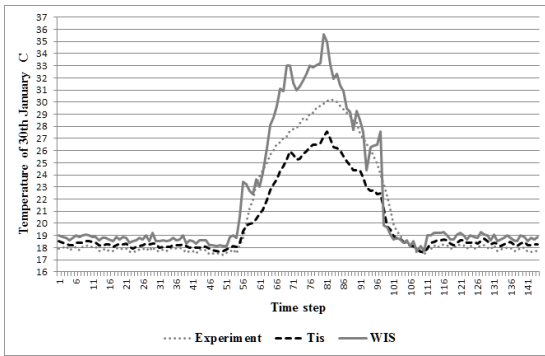


Figure 6: Temperature Comparison between simplified method, WIS and measurement on 30<sup>th</sup> January 2011.

## CONCLUSION

A new simplified calculation method is developed to calculate the heat exchange and internal surface temperature of double glazing unit. Together with the state of art method of calculating solar transmittance [12, 13], the total energy exchange through the façade between inside and outside can be calculated. Furthermore the internal surface temperature can be calculated with reasonable accuracy according to the measurements conducted in the test facility. The method is a dynamic calculation method which can be used for whole year energy performance calculations considering angle of incidence and spectral dependence of solar radiation. From the calculation and verification, it shows that the simplified calculation method has better performance of calculating the internal surface temperature than WIS during the two select days.

## FUTURE WORK

This method can stand alone for calculating the performance of the double glazing unit. But it is taken as a basic model to calculate the performance of “intelligent” glazed façade. Properties of other features like external shutter, blind and natural ventilation will be added to the method and validated by the measurements from the experiments in full-scale test facility.

## NOMENCLATURE

Simplified calculation method:

- $T_{is}$  internal surface temperature of glazing;
- $T_{os}$  external surface temperature of glazing;
- $T_i$  indoor air temperature;
- $T_o$  outdoor air temperature;
- $T_{r,i}$  internal surface equivalent temperature;
- $T_{r,e}$  external surrounding equivalent temperature;
- $h_t$  total thermal conductance of glazing;
- $h_{c,e}$  external convective heat transfer coefficient;
- $h_{c,i}$  internal convective heat transfer coefficient;

- $h_{r,i}$  indoor radiative heat transfer coefficient between glazing and other surfaces;
- $h_{r,e}$  outdoor radiative heat transfer coefficient between glazing and surroundings;
- $\Phi_{solo}$  absorption of solar radiation in external layer of glazing;
- $\Phi_{soli}$  absorption of solar radiation in internal layer of glazing;
- $C_p$  heat capacity of glass;
- $\rho$  density of glass;
- $V$  volume of glass per square meter;
- $\delta t$  time step;
- $Q_{total}$  is the total heat exchange from inside to outside ( $W/m^2$ );
- $Q_{sol}$  is the solar radiation to the inside ( $W/m^2$ );
- $Q_{tr}$  is the heat transfer from inside to outside ( $W/m^2$ );
- $Q_{dir}$  is the direct solar radiation ( $W/m^2$ );
- $Q_{dif}$  is the diffuse solar radiation ( $W/m^2$ );
- $\tau_{e,gzg}$  is the angle dependent direct solar transmittance;
- $\tau_{e,dif}$  is the diffuse solar transmittance;
- $\Delta T$  is the temperature difference between the wall and the ambient air (K) (for time step 1,  $\Delta T$  is assumed as 293 K);
- $H$  is the wall height (m);
- $\epsilon_i$  is the emissivity of in internal glazing surface;
- $\epsilon_{r,i}$  is the emissivity of in internal surround surface;
- $T_n$  is the mean absolute temperature of internal glazing surface and internal wall surface;
- $A_i$  is the area of internal glazing;
- $A_{r,i}$  is the area of total internal wall;
- $f_{is \rightarrow r,i}$  and  $f_{r,i \rightarrow is}$  are the view factor between internal glazing surface and internal wall surface, which are assumed as 1 in the simplified method for whole room.

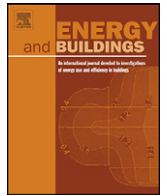
## ACKNOWLEDGEMENTS

This paper is based on research conducted in a PhD project supervised by Senior Researcher Kim Wittchen, Danish Building Research Institute (SBI) and Professor Per Heiselberg, Department of Civil engineering both at Aalborg University, Denmark. The PhD is part of the Strategic Research Centre for Zero Energy Buildings at Aalborg University and financed by the Danish aluminium section of The Danish Construction Association, Aalborg University and The Danish Council for Strategic Research, under the Programme Commission for Sustainable Energy and Environment.

## REFERENCES

1. Winther, F. V., Per, H. & Jensen, R. L., (2010). *Intelligent glazed facades for fulfilment of future energy regulations.* s.l., 3rd Nordic Passive House Conference.
2. EN ISO 7730, (2005). *Ergonomics of the thermal environment-Analytical determination and interpretation of thermal comfort using calculation of the PMV and PPD indices and local thermal comfort criteria.*

3. Erhorn, H. et al., (2007). *WP 4 Report "Simple calculation method"*, s.l.: Fraunhofer-Institut für Bauphysik – IBPBstfacade, Germany.
4. Dijk, D. v. & Goulding, J., (1996). *Wis Reference Manual-Advanced Windows Information System*.
5. ISO15099, November (2003). *Thermal performance of windows, doors and shading devices-Detailed calculations*.
6. Wittchen, K. B., Johnsen, K. & Grau, K., (2000-2011). *BSim – User's Guide*, Hørsholm, Denmark: Danish Building Research Institute, Aalborg University.
7. Aggerholm, S. & Grau, K., (2008). *Bygningers energibehov- SBI-anvisning 213*. Hørsholm, Denmark: Building Research Institute, Aalborg University.
8. Clarke, J., (2001). *Energy Simulation in Building Design*. Electronic edition red. s.l.:Butterworth-Heinemann.
9. EN673, (1997). *Glass in building-Determination of thermal transmittance (U value)-Calculation method*.
10. EN410, (1998). *Glass in building-Determination of luminous and solar characteristics of glazing*.
11. ISO9050, (1990). *Glass in Building-Determination of light transmittance, solar direct transmittance, total solar energy transmittance, ultraviolet transmittance and realated glazing factors*, s.l.: International organisation for Standardisation.
12. J.Karlsson & A.Roos, (2000). Modelling the angular behaviour of the total solar energy transmittance of windows. *Solar Energy*, Årgang 69, pp. 321-329.
13. Kuhn, T. E., (2006). Solar control: A general evaluation method for facades with venetian blinds or other solar control systems. *Energy and Buildings*, Årgang 38, pp. 648-660.
14. Duffie, J. & Beckman, W. A., (1991). *Solar Engineering of Thermal Processes*. 2nd Ed red. s.l.:John Wiley & Sons.
15. [http://www.windfinder.com/windstats/windstatistic\\_aalborg.htm](http://www.windfinder.com/windstats/windstatistic_aalborg.htm)
16. Kalyanova, O, Heiselberg, P, (2008), Experimental Set-up and Full-scale measurements in "The Cube", DCE Technical Reports, nr. 034, Aalborg University, Department of Civil Engineering, Aalborg



# Development of a simplified and dynamic method for double glazing façade with night insulation and validated by full-scale façade element

Mingzhe Liu<sup>a,\*</sup>, Kim Bjarne Wittchen<sup>a</sup>, Per Kvols Heiselberg<sup>b</sup>, Frederik Vildbrad Winther<sup>b</sup>

<sup>a</sup> Danish Building Research Institute (SBI), Aalborg University, Dr. Neergaards vej 15, 2970 Hørsholm, Denmark

<sup>b</sup> Department of Civil Engineering, Aalborg University, Sohngaardsholmsvej 57, 9000 Aalborg, Denmark

## ARTICLE INFO

### Article history:

Received 4 September 2012

Received in revised form

25 November 2012

Accepted 27 November 2012

### Keywords:

Simplified method

Double glazing

Night insulation

$U$ -value

Dynamic

Surface temperature

Façade

## ABSTRACT

The study aims to develop a simplified calculation method to simulate the performance of double glazing façade with night insulation. This paper describes the method to calculate the thermal properties ( $U$ -value) and comfort performance (internal surface temperature of glazing) of the double glazing façade with the night insulation. The calculation result of the internal glazing surface temperature has been validated with experimental data collected in a full-scale façade element test facility at Aalborg University (DK). With the help of the simplified method, dynamic  $U$ -value of the facade with night insulation is calculated and compared with that of the facade without the night insulation.

Based on standards EN 410 and EN 673, the method takes the thermal mass of glazing and the infiltration between the insulation layer and glazing into account. Furthermore it is capable of implementing whole year calculation at different time steps. Acceptable accuracy and simplicity inputs are also the advantages of the method, which make it a suitable tool to evaluate the performance of night insulation during the design stage of buildings. The result calculated by the method proves that the facade with the night insulation performs much better than that without the night insulation.

© 2012 Elsevier B.V. All rights reserved.

## 1. Introduction

Glazed façades are more and more popular for office buildings because of users' requirement of higher light transmittance and better view. However, this kind of façade has drawbacks, one of which is that more glazing provides higher heating demand and unsatisfied thermal comfort. Night insulation is one of the solutions to provide the optimum indoor environment and minimum heat energy demand for glazed buildings [1]. It can decrease the energy loss and improve the indoor comfort during the night time when natural light is not available from the outside and/or needed in the room. Research and experimental study have been carried out showing the energy and comfort benefit of making use of the night insulation [1–4]. Therefore, it is important to simulate the performance of the façade with the night insulation accurately and fast, which can contribute to performance prediction in the design stage of the buildings.

Some modelling work has already been done before. Calculation methods solving some problems (e.g. dynamic effects of the thermal shutters and the air flow through the cracks) of the thermal shutters have been implemented [5,6]. However, they cannot

simulate the performance of the complete system considering all the features. Some standards and calculation methods have already been developed to calculate the glazed facade [7–19], but the features of the night insulation are not integrated with them. It is possible to analyze night insulation with some simulation tools (BSim [20], ESP-r [21] and Be10 [22]), but they either require much time and professional knowledge from the users or are not detailed and accurate enough to calculate the performance.

Therefore, a simplified though dynamic calculation method that can predict the energy and comfort performance of the double glazing façade with the night insulation needs to be developed. Together with the help of the state of art method of calculating solar properties [9–14], the output of the model is the amount of the energy consumption of the façade to maintain an optimal comfort level of indoor environment and the comfort performance in terms of the internal surface temperature. The method must have acceptable accuracy and be suitable for using in the early design stage of buildings and façades.

This paper describes not only the simplified method calculating the performance of the façade with the night insulation but also the validation of the method by measurements. Additionally, with the help of the simplified method, the difference of the thermal performances will be calculated and compared between the facade with the night insulation and that without the night insulation. The comparisons are implemented in terms of both the  $U$ -value and the

\* Corresponding author. Tel.: +45 99407234.

E-mail address: [ml@civil.aau.dk](mailto:ml@civil.aau.dk) (M. Liu).



## Nomenclature

$T_{is}$	temperature of the internal pane [°C]
$T_{os}$	temperature of the external pane [°C]
$T_i$	indoor air temperature [°C]
$T_o$	outdoor air temperature [°C]
$T_{r,i}$	indoor surface equivalent temperature [°C]
$T_{r,e}$	outdoor surrounding equivalent temperature [°C]
$h_t$	equivalent heat transfer coefficient between the internal pane and the external pane [10] [W/(m <sup>2</sup> K)]
$h_{c,e}$	external convective heat transfer coefficient [W/(m <sup>2</sup> K)]
$h_{c,i}$	internal convective heat transfer coefficient [W/(m <sup>2</sup> K)]
$h_{r,i}$	internal radiative heat transfer coefficient between the internal pane and indoor surfaces [W/(m <sup>2</sup> K)]
$h_{r,e}$	external radiative heat transfer coefficient between the external pane and outdoor surroundings [W/(m <sup>2</sup> K)]
$h_{c,cavity}$	convective heat transfer coefficient in the cavity [W/(m <sup>2</sup> K)]
$h_{r,cavity}$	radiative heat transfer coefficient between the insulation and the internal pane [W/(m <sup>2</sup> K)]
$h_{infil}$	infiltration heat transfer coefficient between the internal pane and the indoor air through cavity [W/(m <sup>2</sup> K)]
$h_a$	equivalent heat transfer coefficient between the internal pane and the indoor air through the insulation [W/(m <sup>2</sup> K)]
$h_b$	equivalent heat transfer coefficient between the internal pane and the indoor surface through the insulation [W/(m <sup>2</sup> K)]
$d_l$	thickness of night insulation [m]
$\lambda_l$	heat conductivity of night insulation [W/(m <sup>2</sup> K)];
$I_{dir}$	direct solar radiation [W/m <sup>2</sup> ]
$I_{dif}$	diffuse solar radiation [W/m <sup>2</sup> ]
$\phi_{solo}$	absorption of solar radiation of the external pane [W/m <sup>2</sup> ]
$\phi_{soli}$	absorption of solar radiation of the internal pane [W/m <sup>2</sup> ]
$C_p$	heat capacity of glass [J/(kg K)]
$\rho$	density of glass [kg/m <sup>3</sup> ]
$V$	volume of glass per square metre [m <sup>3</sup> /m <sup>2</sup> ]
$C_{p,air}$	heat capacity of air [J/(kg K)];
$\rho_{air}$	density of air [kg/m <sup>3</sup> ]
$V_{air}$	infiltration rate through the cavity [m <sup>3</sup> /s]
$\delta t$	time step [s]
$U_{total}$	total $U$ -value of the glazing with insulation [W/(m <sup>2</sup> K)]
$T_{iequivalent}$	is the indoor equivalent temperature [°C]
$T_{oequivalent}$	is the outdoor equivalent temperature [°C]
$T_{insulation}$	is the internal surface temperature of the night insulation calculated by the method
$\Delta T$	is the temperature difference between the wall and the ambient air (K) (at time step 1, $\Delta T$ is assumed as 293 K)
$H$	is the wall height [m]
$\varepsilon_i$	is the emissivity of in internal glazing surface [–]
$\varepsilon_{r,i}$	is the emissivity of in internal surround surface [–]
$T_n$	is the mean absolute temperature of internal glazing surface and internal wall surface [K]
$A_i$	is the area of internal glazing [m <sup>2</sup> ]

$A_{r,i}$  is the area of total internal wall [m<sup>2</sup>]  
 $f_{is \rightarrow r,i}$  and  $f_{r,i \rightarrow is}$  are the view factor between internal glazing surface and internal wall surface, which are assumed as 1 in the simplified method for whole room [–]

internal surface temperature of the façade (the internal insulation surface of the façade with the insulation, and the internal glazing surface of the façade without the insulation).

## 2. Description and research method

The first part of the study was the development of the simplified method. The façade system was built up with double glazing unit facing outside and night insulation fixed inside the glazing (Fig. 1). The method was developed to calculate the performance when the night insulation was covering the glazing. The result of the method was to calculate two variables (the internal glazing surface temperature  $T_{is}$  and the external glazing surface temperature  $T_{os}$ ) by solving the heat balance equations of them. Fig. 1 illustrates the heat balance of the variables and the thermal connection between different thermal parameters inside and outside the room.

After the development of the method, its performance was validated by the measurements performed in the test facility “The Cube” at Aalborg University. The purpose of this was to evaluate the accuracy of the method in terms of calculating the internal glazing surface temperatures. The internal surface temperatures of the glazing were measured every 10 min during a winter period of one week and the calculation by the simplified method was conducted through all the time the temperatures were measured.

After the validation of the method, an equivalent  $U$ -value of the façade system can be predicted according to the result of the temperatures  $T_{is}$  and  $T_{os}$ .

### 2.1. Experiment setup

The method was validated by the empirical data of the internal surface temperatures measured in the experiments. The measurements were implemented in the full-scale test facility consisting of façades and rooms (The Cube at Aalborg University [23]) (Figs. 2 and 3). The test facility had two identical south-facing rooms with the internal dimension of 5.66 m × 2.46 m × 1.65 m

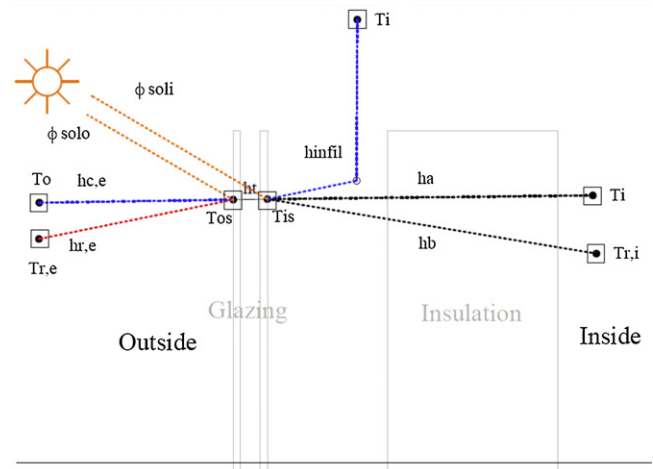
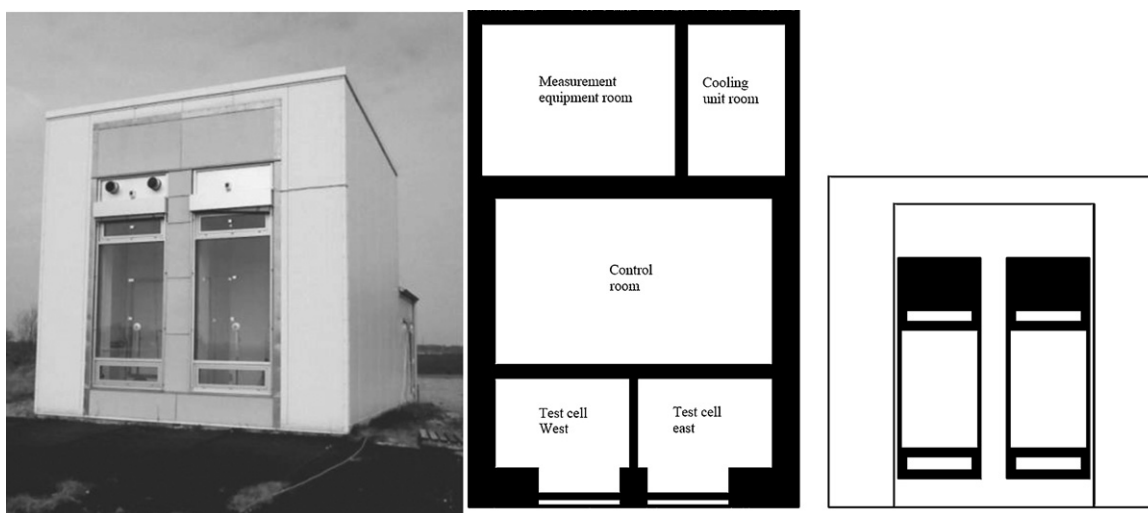


Fig. 1. Layout of the façade system and the heat balance of the variable nodes in the simplified model (on the internal and external surfaces of glazing).



Figs. 2 and 3. Full-scale façade element test facility.

**Table 1**  
Layout and material of the façade.

Position	Material
Outside	Planilux 4 mm SGG
Cavity	Argon 22 mm
Middle	PI/Tutran 4 mm SGG
Cavity	Air 110 mm
Inside	Polystyren 100 mm

**Table 2**  
Material properties of the insulation.

Properties	Insulation
Thickness	0.1 m
Conductivity	0.05 W/m <sup>2</sup> K
Heat resistance	2 m <sup>2</sup> K/W

(H × W × D). Both of the façade systems faced south and each had a dimension of 1.5 m × 4 m. There were one large window in the middle, two operable windows and a filling at top of the window system. The operable windows had a dimension of 1.5 m × 0.5 m including frame area, and the window in the middle had a dimension of 1.5 m × 2.2 m. The filling at the top of the window system had a dimension of 1.5 m × 0.8 m (Figs. 2 and 3).

The glazing type used in the experiments was a double glazing unit with a 22 mm argon-filled cavity and low-e coating on the internal pane. The glazing in the west cell was fitted with polystyrene on the internal side of the window, generating a cavity between the glazing system and the polystyrene of 110 mm. On the other hand, the façade in the east cell was not fitted with the night insulation. The layout of the double glazing unit with night insulation is shown in Table 1, and the material properties of the night insulation in Table 2. The measurements of the internal surface temperature of the glazing in both the west and the east room were conducted in the middle of February 2011 when the outdoor temperature was low. However, the data measured in the east cell is not used in this paper. This paper focuses on the method and the validation of the method. Detailed comparison between the performance of the façade with the insulation and that without the insulation will be implemented in the future work.

The surrounding internal surfaces were built up of 15 mm plywood and were painted white, apart from the floor, which was made of 150 mm concrete. The heat loss due to infiltration was minimized to a minimum by sealing all joints with silicon.

Temperatures were measured using thermocouples type K, which were calibrated with a reference thermocouple at reference temperatures of 10 °C, 20 °C and 30 °C. The temperature was logged using Helios data logger connected to an ice point reference. The calibration of the thermocouples was done using a reference thermometer with an accuracy of 0.01 °C, insuring an accuracy of 0.6 °C for the thermocouples. All thermocouples were connected to a compensating box in order to increase accuracy in measurements [24]. The thermocouples measured internal surface temperatures of the glazing, shielded from the outside to prevent solar irradiance from influencing the measurements [23]. The temperature gradient was measured at 0.91 m, 1.82 m and 2.73 m heights in the room.

The room was heated by 1 kW electrical convective heating system heating the air to keep the air temperature stable. There was no other internal heat source in the room. The temperature was controlled using Danfoss Devireg™ 535. The achieved temperature was 22 °C.

Irradiance was measured using CM21-pyranometer, CM11-pyranometer, Wilhelm Lambrecht pyranometer and BF3-pyranometer. BF3 and Wilhelm Lambrecht were placed externally measuring the diffuse and global irradiance on a horizontal surface. CM21 and CM11 pyranometers were placed in each of the test cells, measuring transmitted irradiance through the glazing system. The pyranometers were prior to the installation calibrated in reference to CM21, which was calibrated in sun simulator and corrected by Kipp&Zonen B.V. [23].

### 3. Simplified calculation method

#### 3.1. Development of the simplified method

The simplified calculation method was implemented to calculate the temperature of internal and external glazing surfaces making use of finite volume energy balance equations by Clarke [9]. In order to simplify the calculation, there were two variable nodes in the equations representing the internal and the external glazing surface temperature with the volume of 1/4 the thickness of the pane. It was assumed that the temperature of glass in the volume was homogeneous. The method was developed by solving the equations and calculating the surface temperatures at different time steps. In addition, the equations took both implicit and explicit conditions into account [9] considering the boundary conditions of both the present and previous time steps to increase the accuracy of the result. Furthermore, the method took into account

of the thermal mass of the glass and the infiltration through the cavity between the glazing and the night insulation.

The following equations show the calculation process of the internal and the external temperatures of the glazing.

At the first time step, equations were built statically. The heat balances of the nodes standing for the internal and the external surfaces of the glazing were built in Eqs. (1) and (2). The internal and external surface temperatures at time step 1 can be calculated by solving the equations:

$$(T_{os1} - T_{is1}) \times h_{t1} + (T_{i1} - T_{is1}) \times h_{a1} + (T_{i1} - T_{is1}) \times h_{infil1} + (T_{r,i1} - T_{is1}) \times h_{b1} + \phi_{soli1} = 0 \tag{1}$$

$$(T_{is1} - T_{os1}) \times h_{t1} + (T_{o1} - T_{os1}) \times h_{c,e1} + (T_{r,e1} - T_{os1}) \times h_{r,e1} + \phi_{solo1} = 0 \tag{2}$$

The internal and external glazing surface temperatures at time step 1 were calculated in Eqs. (3) and (4):

$$T_{os1} = \frac{(T_{i1}h_{a1} + T_{i1}h_{infil1} + T_{r,i1}h_{b1} + \phi_{soli1}) \times h_{t1} + (T_{o1}h_{c,e1} + T_{r,e1}h_{r,e1} + \phi_{solo1}) \times (h_{t1} + h_{a1} + h_{infil1} + h_{b1})}{(h_{t1} + h_{a1} + h_{infil1} + h_{b1}) \times (h_{t1} + h_{c,e1} + h_{r,e1}) - h_{t1}^2} \tag{3}$$

$$T_{is1} = \frac{(T_{i1}h_{a1} + T_{i1}h_{infil1} + T_{r,i1}h_{b1} + \phi_{soli1}) \times (h_{t1} + h_{c,e1} + h_{r,e1}) + (T_{o1}h_{c,e1} + T_{r,e1}h_{r,e1} + \phi_{solo1}) \times h_{t1}}{(h_{t1} + h_{a1} + h_{infil1} + h_{b1}) \times (h_{t1} + h_{c,e1} + h_{r,e1}) - h_{t1}^2} \tag{4}$$

After the first time step, equations were built dynamically taking the thermal mass of glazing into account. During the calculation of dynamic conditions, explicit and implicit conditions were considered [9] and added together in order to increase the accuracy of the results. Then Eqs. (5) and (6) were resulted to build the heat balance standing for the nodes of the internal and the external surfaces at time step  $t + \delta t$ :

$$\begin{aligned} &(T_{os(t)} - T_{is(t)}) \times h_{t(t)} + (T_{i(t)} - T_{is(t)}) \times h_{a(t)} + (T_{i(t)} - T_{is(t)}) \\ &\times h_{infil(t)} + (T_{r,i(t)} - T_{is(t)}) \times h_{b(t)} + \phi_{soli(t)} + (T_{os(t+\delta t)} - T_{is(t+\delta t)}) \\ &\times h_{t(t+\delta t)} + (T_{i(t+\delta t)} - T_{is(t+\delta t)}) \times h_{a(t+\delta t)} + (T_{i(t+\delta t)} - T_{is(t+\delta t)}) \\ &\times h_{infil(t+\delta t)} + (T_{r,i(t+\delta t)} - T_{is(t+\delta t)}) \times h_{b(t+\delta t)} + \phi_{soli(t+\delta t)} \\ &= \frac{2C_p\rho V}{\delta t} \times (T_{is(t+\delta t)} - T_{is(t)}) \end{aligned} \tag{5}$$

$$\begin{aligned} &(T_{is(t)} - T_{os(t)}) \times h_{t(t)} + (T_{o(t)} - T_{os(t)}) \times h_{c,e(t)} + (T_{r,e(t)} - T_{os(t)}) \\ &\times h_{r,e(t)} + \phi_{solo(t)}(T_{is(t+\delta t)} - T_{os(t+\delta t)}) \times h_{t(t+\delta t)} \\ &+ (T_{o(t+\delta t)} - T_{os(t+\delta t)}) \times h_{c,e(t+\delta t)} + (T_{r,e(t+\delta t)} - T_{os(t+\delta t)}) \\ &\times h_{r,e(t+\delta t)} + \phi_{solo(t+\delta t)} = \frac{2C_p\rho V}{\delta t} \times (T_{os(t+\delta t)} - T_{os(t)}) \end{aligned} \tag{6}$$

The time step was 600 s, which was the same as the measurements.

By solving Eqs. (5) and (6), the temperatures of internal and external glazing surfaces at time step  $t + \delta t$  can be calculated in Eqs. (7) and (8):

$$T_{os(t+\delta t)} = \frac{\left[ (T_{i(t+\delta t)}h_{a(t+\delta t)} + T_{i(t+\delta t)}h_{infil(t+\delta t)} + T_{r,i(t+\delta t)}h_{b(t+\delta t)} + \phi_{soli(t+\delta t)} + a) \times h_{t(t+\delta t)} + (T_{o(t+\delta t)}h_{c,e(t+\delta t)} + T_{r,e(t+\delta t)}h_{r,e(t+\delta t)} + \phi_{solo(t+\delta t)} + b) \times (h_{t(t+\delta t)} + h_{a(t+\delta t)} + h_{infil(t+\delta t)} + h_{b(t+\delta t)} + (2C_p\rho V/\delta t)) \right]}{[(h_{t(t+\delta t)} + h_{a(t+\delta t)} + h_{infil(t+\delta t)} + h_{b(t+\delta t)} + (2C_p\rho V/\delta t)) \times (h_{t(t+\delta t)} + h_{c,e(t+\delta t)} + h_{r,e(t+\delta t)} + (2C_p\rho V/\delta t)) - h_{t(t+\delta t)}^2]} \tag{7}$$

$$T_{is(t+\delta t)} = \frac{\left[ (T_{i(t+\delta t)}h_{a(t+\delta t)} + T_{i(t+\delta t)}h_{infil(t+\delta t)} + T_{r,i(t+\delta t)}h_{b(t+\delta t)} + \phi_{soli(t+\delta t)} + a) \times (h_{t(t+\delta t)} + h_{c,e(t+\delta t)} + h_{r,e(t+\delta t)} + (2C_p\rho V/\delta t)) + (T_{o(t+\delta t)}h_{c,e(t+\delta t)} + T_{r,e(t+\delta t)}h_{r,e(t+\delta t)} + \phi_{solo(t+\delta t)} + b) \times h_{t(t+\delta t)} \right]}{[(h_{t(t+\delta t)} + h_{a(t+\delta t)} + h_{infil(t+\delta t)} + h_{b(t+\delta t)} + (2C_p\rho V/\delta t)) \times (h_{t(t+\delta t)} + h_{c,e(t+\delta t)} + h_{r,e(t+\delta t)} + (2C_p\rho V/\delta t)) - h_{t(t+\delta t)}^2]} \tag{8}$$

Where parameters a and b were calculated in Eqs. (9) and (10):

$$a = (T_{os(t)} - T_{is(t)}) \times h_{t(t)} + (T_{i(t)} - T_{is(t)}) \times h_{a(t)} + (T_{i(t)} - T_{is(t)}) \times h_{infil(t)} + (T_{r,i(t)} - T_{is(t)}) \times h_{b(t)} + \phi_{soli(t)} + \frac{2C_p\rho V}{\delta t} T_{is(t)} \tag{9}$$

$$b = (T_{is(t)} - T_{os(t)}) \times h_{t(t)} + (T_{o(t)} - T_{os(t)}) \times h_{c,e(t)} + (T_{r,e(t)} - T_{os(t)}) \times h_{r,e(t)} + \phi_{solo(t)} + \frac{2C_p\rho V}{\delta t} \times T_{os(t)} \tag{10}$$

where

$$\frac{1}{h_a} = \frac{1}{h_{c,i}} + \frac{d_l}{\lambda_l} + \frac{1}{(h_{c,cavity} + h_{r,cavity})} \tag{11}$$

$$\frac{1}{h_b} = \frac{1}{h_{r,i}} + \frac{d_l}{\lambda_l} + \frac{1}{(h_{c,cavity} + h_{r,cavity})} \tag{12}$$

$$\frac{1}{h_{infil}} = \frac{1}{2h_{c,cavity}} + \frac{1}{C_{p,air}\rho_{air}V_{air}} \tag{13}$$

After calculating the temperature of the internal and the external glazing surfaces, the total U-value of the system can be calculated by Eq. (14):

$$U_{total} = \frac{(T_{is} - T_{os}) \times h_t}{T_{iequivalent} - T_{oequivalent}} \tag{14}$$

where

$$T_{iequivalent} = \frac{T_i h_{c,i} + T_{r,i} h_{r,i}}{h_{c,i} + h_{r,i}} \tag{15}$$

$$T_{oequivalent} = \frac{T_o h_{c,e} + T_{r,e} h_{r,e}}{h_{c,e} + h_{r,e}} \tag{16}$$

The internal surface temperature of the night insulation  $T_{insulation}$  can also be calculated according to the internal and the external surface temperatures of the glazing (17):

$$T_{insulation} = \frac{(1/(1/(h_{c,cavity} + h_{r,cavity}) + (d/\lambda))) \times T_{is} + T_i \times h_{c,i} + T_{r,i} \times h_{r,i}}{(1/(1/(h_{c,cavity} + h_{r,cavity}) + (d/\lambda))) + h_{c,i} + h_{r,i}} \tag{17}$$

By inputting the results of the variables (calculated in Eqs. (2), (3), (7) and (8) and the parameters of subsystems in excel, the simplified calculation method can be realized.

### 3.2. Thermal parameters used to calculate the result

The internal and the external surface temperature of the glazing  $T_{is}$  and  $T_{os}$  can be calculated by the method. All the other parameters in the equations were already known. Some of the known parameters were measured in the experiment at each time step, e.g.,

the indoor and the outdoor air temperatures  $T_i$  and  $T_o$ , the direct and the diffuse solar radiation  $I_{dir}$  and  $I_{dif}$ , the indoor equivalent surface temperature  $T_{r,i}$  and the infiltration rate through the cavity  $V_{air}$ . The outdoor surrounding equivalent temperature  $T_{r,e}$  was calculated according to the outdoor air temperature  $T_o$  [9]. Furthermore, the absorption of the solar radiation by the internal and the external pane  $\phi_{soli}$  and  $\phi_{solo}$  were the function of the amount of the solar radiation and the solar incident angle [11,13,14]. The measurements of these parameters have been described in the part of the experiment setup. The convective and the radiative heat transfer coefficients are calculated according to Clarke [9].

### 3.2.1. Dynamic heat transfer coefficient

The method not only takes into account of the thermal mass of the glass, but also the dynamic properties of the convective and radiative heat transfer coefficients. The present heat transfer coefficients decided by temperature difference are calculated using the results of the surface temperature of previous time step.

3.2.1.1. Convective heat transfer coefficient. Interior surface convective heat transfer coefficient [9]:

$$h_{c,i} = \left\{ \left[ 1.5 \left( \frac{\Delta T}{H} \right)^{0.25} \right] + [1.23(\Delta T)^{0.33}]^6 \right\}^6 \quad (18)$$

Dynamic solution can be realized in (19) [9], calculating  $h_{c,i}$  with the parameters of previous time step:

$$h_{c,i(t+\delta)} = \left\{ \left[ 1.5 \left( \frac{T_{is(t)} - T_{i(t)}}{H} \right)^{0.25} \right]^6 + [1.23(T_{is(t)} - T_{i(t)})^{0.33}]^6 \right\}^{1/6} \quad (19)$$

Exterior surface convective heat transfer coefficient can be calculated by (20) [9]:

$$h_{c,e} = 5.678 \left[ a + b \left( \frac{V}{0.3048} \right)^n \right] \quad (20)$$

where  $V$  is the wind speed; if  $V < 4.88$  m/s then  $a = 0.99$ ,  $b = 0.21$ , and  $n = 1$ .

If  $4.88$  m/s  $< V < 30.48$  m/s then  $a = 0$ ,  $b = 0.5$ , and  $n = 0.78$ .

For climate of Aalborg, the average wind speed during the test period according to Windfinder [25] is taken as 5.5 m/s.

3.2.1.2. Long-wave radiative heat transfer coefficient. Long-wave radiative heat transfer coefficient between internal surface and internal walls is calculated as described in the following.

The internal radiative heat transfer coefficient of time step 1 is  $4.4$  W/(m<sup>2</sup> K) according to EN 673 [10].

After time step 1, dynamic solution can be realized in (21), calculating  $h_{r,i}$  with the parameters of previous time step.

$$h_{r,i(t+\delta t)} = \frac{\varepsilon_i \varepsilon_r \sigma \times (A_i T_{is(t)}^4 f_{r,i \rightarrow is} - A_{r,i} T_{r,i(t)}^4 f_{is \rightarrow r,i})}{A_i \times (T_{is(t)} - T_{r,i(t)}) [1 - (1 - \varepsilon_i)(1 - \varepsilon_r) f_{is \rightarrow r,i} f_{r,i \rightarrow is}]} \quad (21)$$

Long-wave radiative heat transfer between external surface and surroundings can be calculated by (22) and (23) [9]:

At time step 1,  $h_{r,e}$  can be calculated by (22) assuming the mean temperature of  $T_{r,e}$  and  $T_{os}$  is outdoor air temperature  $T_o$ .

$$h_{r,e1} = 4\varepsilon\sigma T_o^3 \quad (22)$$

After the first time step, dynamic solution can be realized in (23), calculating  $h_{r,e}$  with the parameters of previous time step.

$$h_{r,e(t+\delta t)} = \frac{\varepsilon\sigma(T_{r,e}^4 - T_{os}^4)}{T_{r,e} - T_{os}} \quad (23)$$

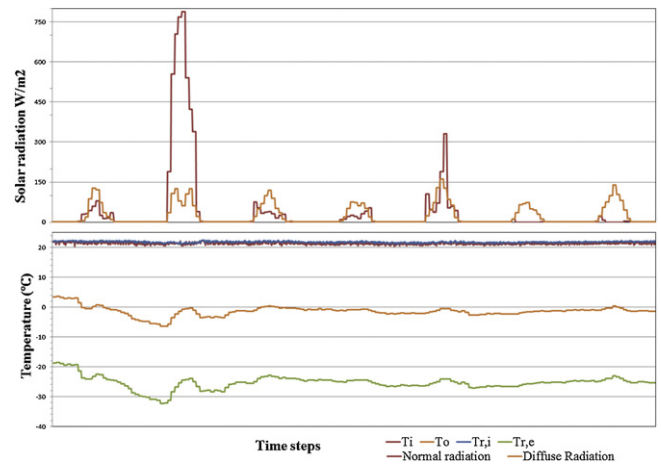


Fig. 4. Indoor and outdoor thermal parameters used to calculate the variables.

### 3.2.2. Outdoor weather data and indoor environment

3.2.2.1. Temperature and solar radiation. Fig. 4 shows the indoor and the outdoor environment data measured in the experiments. If the method is used in practice project, the outdoor weather data should be the reference weather data of the locations or defined by the users. The indoor environment temperature could be set by the users according to the requirement of the buildings. In order to simulate the façade in different orientations, the global solar radiation should be converted for different orientations [26].

3.2.2.2. Infiltration rate through the cavity. The value of the infiltration rate used in the calculation method was the same as the measured in the experiment. Fig. 5 shows the result of infiltration rate through the cavity measured in the test facility. When used in the real building design practice, the value of the infiltration rate could be preferably provided by the facade manufacturer according to different weather conditions (temperatures and wind speed, etc.). The infiltration rate depends on the tightness of the connection between glazing and the night insulation.

To measure the infiltration rate through the cavity a tracer gas system was used. The tracer gas, CO<sub>2</sub>, was applied with a constant amount to the cavity between the glazing and the insulation. The CO<sub>2</sub> was applied through a perforated rubber hose placed along the edge of the window (Fig. 6). The placement of the hose was to ensure mixing between the applied CO<sub>2</sub> and the air in the cavity. Four symmetrically fixed rubber hoses were placed in the cavity, each connected to the tracer gas analyser to measure the CO<sub>2</sub>-level in the cavity, which were marked with red in Fig. 6. Based on the setup the infiltration rate in the cavity was calculated.

## 4. Result and validation of the simplified method

Fig. 7 shows the comparison on the internal surface temperatures from the simplified method and that from the experiments. It shows that during the sunny days the simplified method underestimates the internal surface temperature of the glazing, which is probably because it underestimates the solar absorption of the internal pane and it does not take the solar radiation absorbed by the insulation into account. However, in practice situation the insulation is mostly used at night time when there is little or even no solar radiation and low outdoor temperature, therefore the tolerance of the method during the time of high solar radiation does not influence the accuracy of the simplified method so much.

During the time with little or no solar radiation, the calculation results of the simplified method have acceptable accuracy compared with the measurements with an average deviation of around

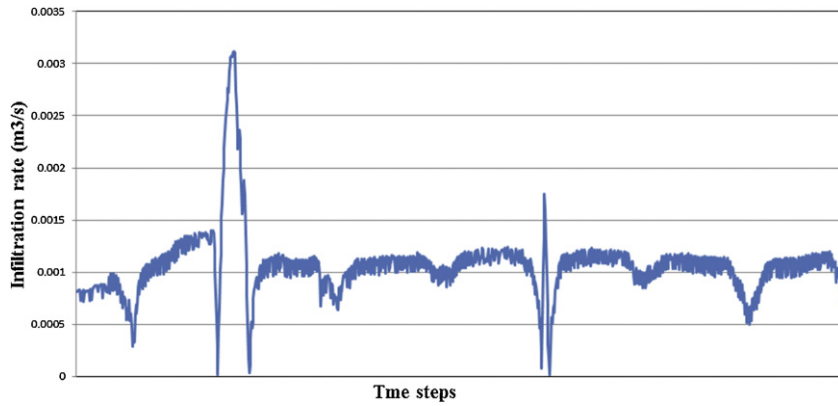


Fig. 5. Infiltration rate measured through the cavity between the glazing and the night insulation.

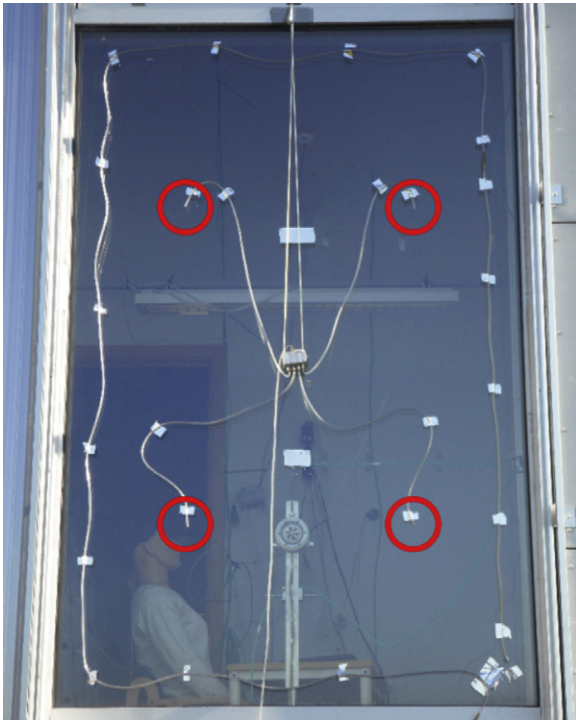


Fig. 6. Measurement setup of the infiltration.

1 °C. At some time steps, the deviation is around 2 °C which is probably because of the tolerance of the measured infiltration rate. The infiltration rate is difficult to be measured accurately and it could influence the result significantly.

4.1. Validation of the method

The accuracy of the model is validated through the  $R^2$ -value [27]. This value indicates how accurate the method fits the measurements, by comparing the values of each time step to each other and determining the level of accuracy as an evaluation of the overall differences between them. The  $R^2$ -value is not only a measure of how well the pattern of the model follows the pattern of the measurements, but also a measure of accuracy determining the error at each time step.

Eqs. (24)–(26) show the calculation of the  $R^2$ -value. Where  $y_i$  is the measured value;  $f_i$  is the calculated value;  $\bar{y}$  is the mean of the measured value. The calculation result is  $R^2 = 0.806387101$ .

$$R^2 = 1 - \frac{SS_{err}}{SS_{tot}} \tag{24}$$

$$SS_{err} = \sum_i^n (y_i - f_i)^2 \tag{25}$$

$$SS_{tot} = \sum_i^n (y_i - \bar{y})^2 \tag{26}$$

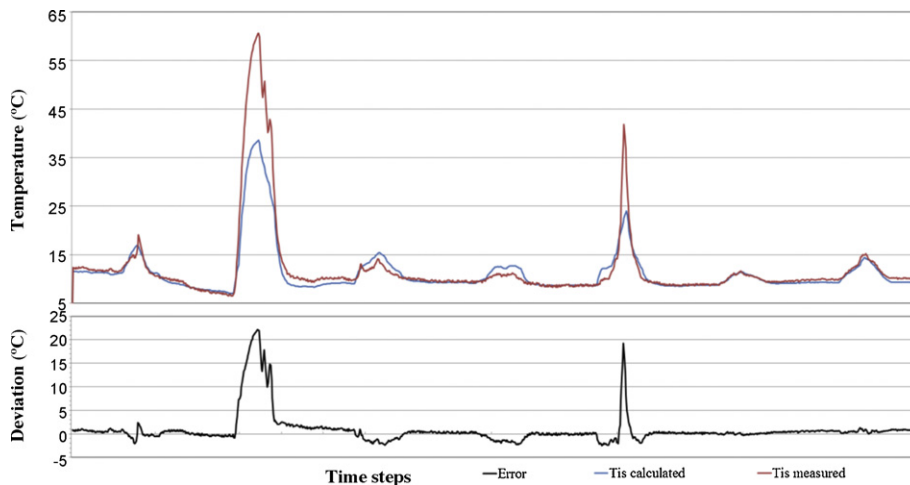


Fig. 7. Calculated and measured internal surface temperature of the glazing in the west cell and the deviation between them.

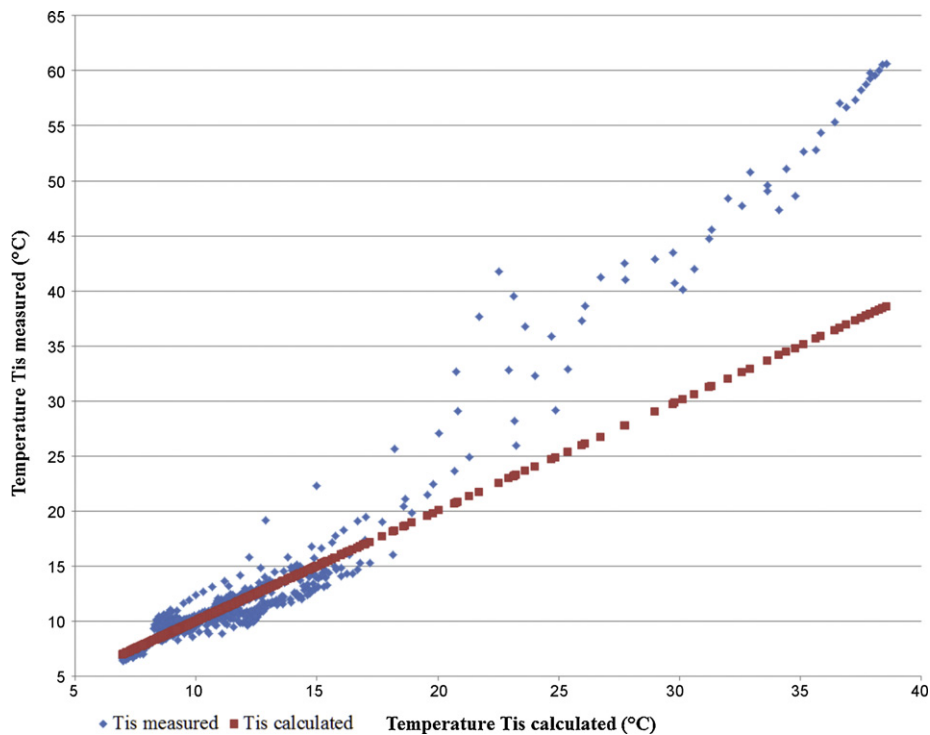


Fig. 8. Comparison on the internal surface temperature of the glazing between the calculation and the measurements in the west cell.

Fig. 8 shows the linear regression of the data. As it was shown in Fig. 7, the temperature calculated by the simplified method corresponds with the measurements much better when it is below 20 °C (there is little or no solar radiation).

**5. Comparison on the U-value between glazing with night insulation and glazing without night insulation**

With the help of the developed method, the total U-value of the glazing with night insulation and that of glazing without night insulation are calculated at different time steps. The results calculated every 10 min are shown in Fig. 9. By implementing the night insulation inside the glazing, the total U-value of the façade can be decreased from around 1.1 to below 0.8 which is an improvement

of about 30%. The improvement depends on the thickness of the insulation, the heat conductivity of the insulation material and the infiltration of the cavity between the insulation and the glazing.

Fig. 10 shows the internal surface temperatures of the glazing of the façade without night insulation and the internal surface temperature of the insulation of the façade with the night insulation. The glazing surface temperature shown is calculated by the simplified method developed for double glazing [12]. The insulation surface temperature shown is calculated by the simplified method developed in this paper. Both of the calculations use the same weather data and boundary conditions. The comparison shows that the façade with the night insulation has better thermal comfort than that without the insulation. The temperature difference between them is approximately 4 °C.

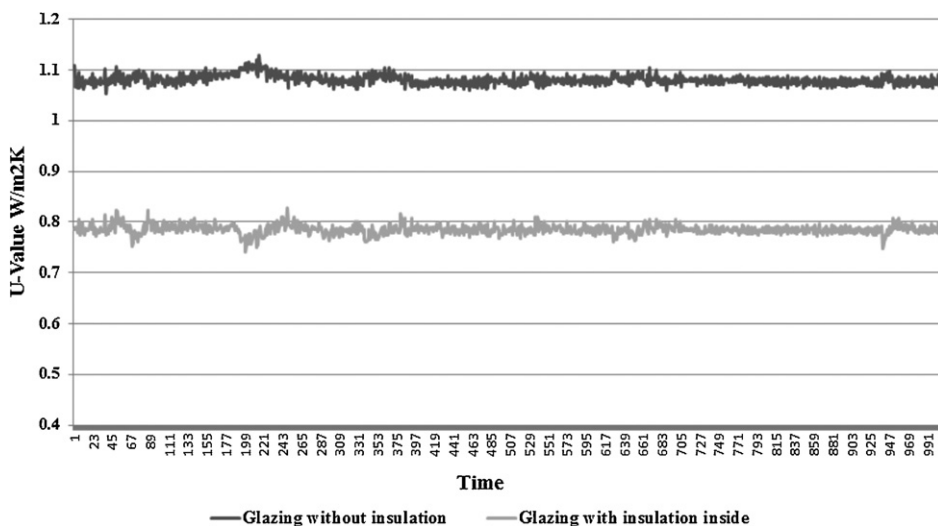


Fig. 9. Comparison on U-value between glazing with night insulation and that without night insulation.

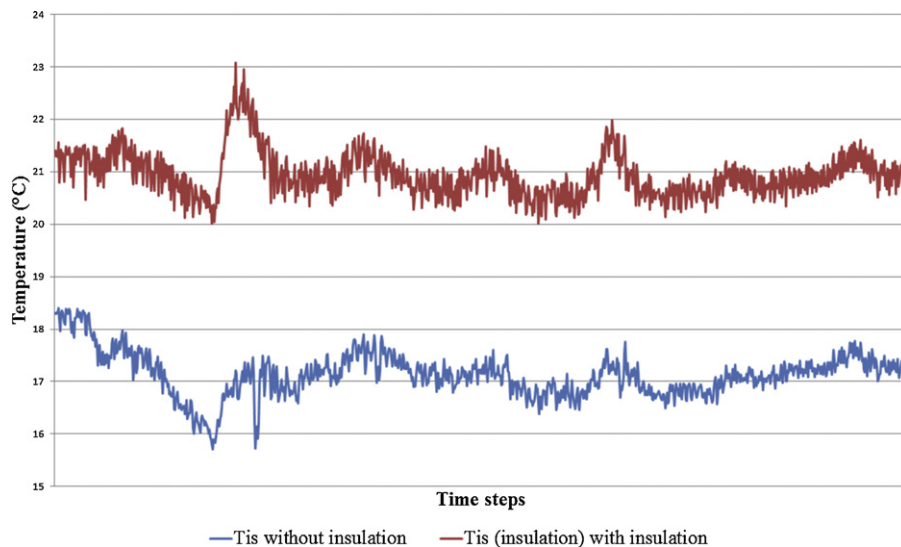


Fig. 10. Comparison on the internal surface temperatures between the glazing in the west cell and that in the east cell.

## 6. Conclusion and future work

A new simplified calculation method has been developed to predict the energy and comfort performance of the double glazing with the night insulation. It can make whole year simulation at different time steps. The validation shows that the method has acceptable accuracy in terms of calculating the internal surface temperature. Compared with other simulation tools, it requires less time and professional knowledge to input parameters and implement the simulation. Danish building simulation tool BSim [20] is capable of simulating the energy performances of buildings with effect of night insulating shutters, but it costs much time to input data and it cannot calculate the internal surface temperature of the façade. Tools like ESP-r [21] can do the job, but it requires much knowledge and input work. Danish building compliance checking tool Be10 [22] is not detailed and accurate enough to simulate the performance of night insulation. Therefore the simplified method is efficient and accurate which makes it a suitable tool to be used in the early design stage of façade.

Infiltration rate of the system is an important parameter in the method as it influences the accuracy of the performance significantly. Therefore, in practice situation, it is important for the manufacturers to provide accurate value of infiltration rate according to the weather data in order to maximize the accuracy of the calculation result.

Calculation result by the method shows that the equivalent  $U$ -value of the double glazing façade with the night insulation is around 30% lower than that of the facade without the night insulation.

Fitted inside the glazing, the night insulation may cause (depending on the  $U$ -value of the glazing) a problem with condensation on the glazing when the insulation is removed in the morning after a cold night, which has to be checked and avoided in a practice situation.

The glazing was covered by the insulation over the whole test period. In practice situation, the insulation is movable and only covers the glazing during the night in the winter. Therefore, the dynamic effect in the morning and night is also important to the performance of the insulation. The method needs to be tested for this condition as well in the future.

The development of the method for the façade with the night insulation outside the glazing and its validation should also be implemented in the future. The comparison between the accuracy

of the simplified method and the other softwares (BSim or ESP-r) should be implemented in the future.

## Acknowledgements

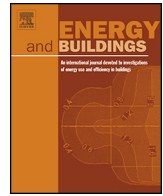
This paper is based on research conducted in a PhD project supervised by Senior Researcher Kim Wittchen, Danish Building Research Institute (SBI) and Professor Per Heiselberg, Department of Civil engineering both at Aalborg University, Denmark. The PhD is part of the Strategic Research Centre for Zero Energy Buildings at Aalborg University and financed by the Danish aluminium section of The Danish Construction Association, Aalborg University and The Danish Council for Strategic Research, under the Programme Commission for Sustainable Energy and Environment.

## References

- [1] F.V. Winther, P.K. Heiselberg, R.L. Jensen, Intelligent glazed facades for fulfilment of future energy regulations. s.l., 3rd Nordic Passive House Conference, 2010.
- [2] J.M. Schult, Isolerende Skodder (Insulating shutters), Danish with a summary in English. Report no. 202, Technical University of Denmark, Thermal Insulation Laboratory, 1990.
- [3] J. Winter, Practical assessment of window shutters for night insulation and solar shading for domestic buildings, New Zealand.
- [4] K. Nicol, The thermal effectiveness of various types of window coverings, *Energy and Buildings* 9 (1986) 231–237.
- [5] M. Zaheer-Uddin, Dynamic effects of thermal shutters, *Building and Environment* 25 (1) (1990) 33–35.
- [6] P.H. Baker, S. Sharples, I.C. Ward, Air flow through cracks, *Building and Environment* 22 (4) (1987) 293–304.
- [7] D.V. Dijk, J. Goulding, WIS Reference Manual—Advanced Windows Information System, 1996.
- [8] D. Saelens, Energy Performance assessment of multiple-skin facades, Ph.D. dissertation, Laboratory for Building Physics, K.U. Leuven, Leuven, 2002.
- [9] J. Clarke, *Energy Simulation in Building Design*. Electronic edition red. s.l.: Butterworth-Heinemann, 2001.
- [10] EN673, Glass in building—determination of thermal transmittance ( $U$  value)—Calculation method, 1997.
- [11] EN410, Glass in building—determination of luminous and solar characteristics of glazing, 1998.
- [12] M. Liu, K.B. Wittchen, P.K. Heiselberg, F.V. Winther, Development of simplified and dynamic model for double glazing unit validated with full-scale façade element, PLEA2012, 28th conference, Lima, 2012.
- [13] J. Karlsson, A. Roos, Modelling the angular behaviour of the total solar energy transmittance of windows, *Solar Energy* 69 (2000) 321–329.
- [14] T.E. Kuhn, Solar control: a general evaluation method for facades with venetian blinds or other solar control systems, *Energy and Buildings* 38 (2006) 648–660.
- [15] S. Pal, B. Roy, S. Neogi, Heat transfer modelling on windows and glazing under the exposure of solar radiation, *Energy and Buildings* 41 (2009) 654–661.

- [16] F. Noh-Pat, J. Xamán, G. Álvarez, Y. Chávez, J. Arce, Thermal analysis for a double glazing unit with and without a solar control film(SnS–CuxS) for using in hot climates, *Energy and Buildings* 43 (2011) 704–712.
- [17] J. Breitenbach, S. Lart, I. LaËngle, J.L.J. Rosenfel, Optical and thermal performance of glazing with integral Venetian blind, *Energy and Buildings* 33 (2001) 433–442.
- [18] M.C. Singh, S.N. Garg, An empirical model for angle-dependent g-values of glazings, *Energy and Buildings* 42 (2010) 375–379.
- [19] R. Hart, H. Goudey, D. Arasteh, D.C. Curcija, Thermal performance impacts of center-of-glass deflections in installed insulating glazing units, *Energy and Buildings* 54 (2012) 453–460.
- [20] K.B. Wittchen, K. Johnsen, K. Grau, BSIm – User’s Guide, Hørsholm, Denmark: Danish Building Research Institute, Aalborg University, 2000–2011.
- [21] <http://www.esru.strath.ac.uk/Programs/ESP-r.htm>
- [22] S. Aggerholm, K. Grau, Bygningers energibehov- SBI-anvisning 213, Building Research Institute, Aalborg University, Hørsholm, Denmark, 2008.
- [23] O. Kalyanova, P. Heiselberg, Experimental Set-up and Full-scale measurements in “The Cube”, DCE, Technical Reports, nr. 034, Aalborg University, Department of Civil Engineering, Aalborg, 2008.
- [24] N. Artmann, R. Vonbank, R.L. Jensen, Temperature Measurements Using Type K Thermocouples and the Fluke Helios Plus 2287A Datalogger, DCE Technical Reports, nr. 52, Aalborg University. Department of Civil Engineering, Aalborg, 2008.
- [25] <http://www.windfinder.com/windstats/windstatistic.aalborg.htm>
- [26] J. Duffie, W.A. Beckman, *Solar Engineering of Thermal Processes*, 2nd ed., John Wiley & Sons, New York, 1991.
- [27] D.C. Montgomery, *Design and Analysis of Experiments*, 7th ed., John Wiley & Sons, Hoboken, N.J., 2009.





# Development and sensitivity study of a simplified and dynamic method for double glazing facade and verified by a full-scale façade element



Mingzhe Liu<sup>a,\*</sup>, Kim Bjarne Wittchen<sup>a</sup>, Per Kvols Heiselberg<sup>b</sup>, Frederik Vildbrad Winther<sup>b</sup>

<sup>a</sup> Danish Building Research Institute (SBI), Aalborg University, A.C. Meyers Vænge 15, 2450 København SV, Denmark

<sup>b</sup> Department of Civil Engineering, Aalborg University, Sohngaardsholmsvej 57, 9000 Aalborg, Denmark

## ARTICLE INFO

### Article history:

Received 17 January 2013

Received in revised form 5 March 2013

Accepted 10 March 2013

### Keywords:

Simplified method  
Double glazing facade  
U-value  
Dynamic  
Surface temperature  
Energy

## ABSTRACT

The research aims to develop a simplified calculation method for double glazing facade to calculate its thermal and solar properties ( $U$  and  $g$  value) together with comfort performance (internal surface temperature of the glazing). Double glazing is defined as 1D model with nodes representing different layers of material. Several models with different numbers of nodes or in different positions are compared and verified in order to find a simplified method which can calculate the performance as accurately as possible. The performance calculated in terms of internal surface temperature is verified with experimental data collected in a full-scale façade element test facility at Aalborg University (DK). Comparison was conducted between the simplified method and WIS software on the accuracy of calculating internal surface temperature of double glazing facade.

The method is based on standards EN410 and EN673, taking the thermal mass of the glazing into account. In addition, angle and spectral dependency of solar characteristic is also considered during the calculation. By using the method, it is possible to calculate whole year performance at different time steps, which makes it a time economical and accurate tool in design stage of double glazing façade.

© 2013 Elsevier B.V. All rights reserved.

## 1. Introduction

Double glazing facades are widely used in modern buildings. Its solar and thermal properties have a significant effect on both the energy consumption and indoor thermal comfort. Both the energy ( $U$ -value) and the comfort (internal surface temperature) performances of the double glazing façade are dynamic and vary according to the change of both indoor environment and outdoor weather conditions. In addition, it is preferred by architects to evaluate the whole year performance of the facade with hourly dynamic simulation at the beginning stage of the building design.

Therefore, it is important to develop a method which must have following qualities:

- Simulation is performed hourly for the whole year (thus 8760 h);
- Capable of simulating energy and comfort performance with dynamic properties;
- Set of requirement of indoor environment for both winter and summer;
- To be fast and user-friendly with simple input.

Some simulation tools, standards and calculation methods have already been developed to simulate the double glazing facade [1–6], but they either require much time and professional knowledge from the users to build the model and get the result or are not detailed and accurate enough to calculate the performance. In the methods developed in the BESTFACADE project [1] and by Saelens [2] continuous procedure for calculating the impact of Double Skin Facade (DSF) constructions on the overall energy demand of buildings was applied. However, the calculation methods were only suitable for double skin façade with ventilated cavity but not for single skin façade like double glazing unit. It cannot calculate the surface temperature of glazing. WIS software [3] can calculate the  $U$ -value,  $g$  value and the internal surface temperature of different kind of double glazing unit, but the method in WIS software considers only steady state condition.

\* Corresponding author. Tel.: +45 99407234.

E-mail address: [ml@civil.aau.dk](mailto:ml@civil.aau.dk) (M. Liu).

## Nomenclature

### Simplified calculation method

$T_{is}$	internal surface temperature of glazing [°C]
$T_{os}$	external surface temperature of glazing [°C]
$T_i$	indoor air temperature [°C]
$T_o$	outdoor air temperature [°C]
$T_{r,i}$	internal surface equivalent temperature [°C]
$T_{r,e}$	external surrounding equivalent temperature [°C]
$h_t$	equivalent heat transfer coefficient between the internal pane and the external pane [9] [W/(m <sup>2</sup> K)]
$h_{c,e}$	external convective heat transfer coefficient [W/(m <sup>2</sup> K)]
$h_{c,i}$	internal convective heat transfer coefficient [W/(m <sup>2</sup> K)]
$h_{r,i}$	indoor radiative heat transfer coefficient between glazing and other surfaces [W/(m <sup>2</sup> K)]
$h_{r,e}$	outdoor radiative heat transfer coefficient between glazing and surroundings [W/(m <sup>2</sup> K)]
$\phi_{solo}$	absorption of solar radiation in external layer of glazing [W/m <sup>2</sup> ]
$\phi_{soli}$	absorption of solar radiation in internal layer of glazing [W/m <sup>2</sup> ]
$C_p$	heat capacity of glass [J/(kg K)]
$\rho$	density of glass [kg/m <sup>3</sup> ]
$V$	volume of glass per square meter [m <sup>3</sup> ]
$\delta t$	time step [s]
$Q_{total}$	total heat exchange from inside to outside [W/m <sup>2</sup> ]
$Q_{sol}$	solar radiation to the inside [W/m <sup>2</sup> ]
$Q_{tr}$	heat transfer from inside to outside [W/m <sup>2</sup> ]
$Q_{dir}$	direct solar radiation [W/m <sup>2</sup> ]
$Q_{dif}$	diffuse solar radiation [W/m <sup>2</sup> ]
$\lambda$	thermal conductivity of glass [W/(m·K)]
$d$	thickness of the glass [m]
$h_r$	radiative heat transfer coefficient between two panes [W/m <sup>2</sup> ]
$h_g$	convective heat transfer coefficient in the cavity [W/m <sup>2</sup> ]
$\sigma$	Stefan–Boltzmann's constant [W/(m <sup>2</sup> K <sup>4</sup> )]
$T_m$	mean absolute temperature of the gas space [K]
$\varepsilon_1$ and $\varepsilon_2$	corrected emissivities of the internal surface of the outer pane and the external surface of the inter pane at $T_m$ [dimensionless]
$s$	width of the space [m]
$\lambda_{gas}$	thermal conductivity of the gas in the cavity [W/(m K)]
$Nu$	Nusselt number of the gas in the cavity [dimensionless]
$Gr$	Grashof number of the gas in the cavity [dimensionless]
$Pr$	Prandtl number of the gas in the cavity [dimensionless]
$\Delta T$	temperature difference between glass surfaces bounding the gas space (fixed to 15 K in the calculations) [K]
$\rho$	density of the gas in the cavity [kg/m <sup>3</sup> ]
$\mu$	dynamic viscosity of the gas in the cavity [kg/m s]
$c$	specific heat capacity of the gas in the cavity [J/(kg K)]
<b>For vertical glazing</b>	
$A$	0.035 [dimensionless]
$n$	0.38 [dimensionless]
$\tau_{e,gzg}$	angle dependent direct solar transmittance [dimensionless]
$\tau_{e,dif}$	diffuse solar transmittance [dimensionless]
$\Delta T$	temperature difference between the wall and the ambient air (K) (for time step 1, $\Delta T$ is assumed as 293 K)
$H$	wall height [m]
$\varepsilon_i$	emissivity of in internal glazing surface [dimensionless]
$\varepsilon_{r,i}$	emissivity of in internal surround surface [dimensionless]
$T_n$	mean absolute temperature of internal glazing surface and internal wall surface [K]
$A_i$	area of internal glazing [m <sup>2</sup> ]
$A_{r,i}$	area of total internal wall [m <sup>2</sup> ]
$f_{is \rightarrow r,i}$ and $f_{r,i \rightarrow is}$	view factor between internal glazing surface and internal wall surface, which are assumed as 1 in the simplified method for whole room [dimensionless]
$\alpha_{e1}$	direct angle dependent solar absorption coefficient of external pane [W/m <sup>2</sup> ]
$\alpha_{e1,dif}$	diffuse solar absorption coefficient of external pane [dimensionless]
$\alpha_{e1,dir}$	direct solar absorption coefficient of external pane [dimensionless]
$\alpha_{e2}$	direct angle dependent solar absorption coefficient of internal pane [W/m <sup>2</sup> ]
$\alpha_{e2,dif}$	diffuse solar absorption coefficient of internal pane [dimensionless]
$\alpha_{e2,dir}$	direct solar absorption coefficient of internal pane [dimensionless]

**Table 1**  
Layout and glass type of double glazing unit used in the simplified method and WIS.

Position	Material
Outside	Planilux 4 mm SGG
Cavity	Argon 22 mm
Inside	PI Tutran 4 mm SGG

Furthermore, it can only perform the calculation of one time step each time, which makes it quite time consuming to simulate the whole year performance of the facade. Using the method defined in ISO 15099 [4], people can calculate the surface temperature of glazing. However, the methods do not take the thermal mass of glass into account. Danish simulation tool BSim [5] and compliance checking tool Be10 [6] are simplified calculation tools to calculate the energy demand of building and internal surface temperature of glazing, but their glass models are not detailed and accurate enough to calculate the surface temperature taking into dynamic features of facade.

Therefore, it is necessary to develop a simplified though dynamic calculation method that can predict the energy and comfort performance of the double glazing facade at the early design stage of building and facade. The study aims to develop the simplified calculation method to accurately calculate the performance of the double glazing facade in terms of energy consumption and thermal comfort. The result of the method has already been shown in [7], but the detail development and the sensitivity analysis of the thermal mass of the glazing need to be shown. A method with the same principle used to simulate the facade with night insulation was shown in [8]. This paper describes the simplified calculation method and its validation by the full-scale facade element at Aalborg University. Comparisons on the calculated results between the method and WIS programme are also shown in this paper.

## 2. Description and research method

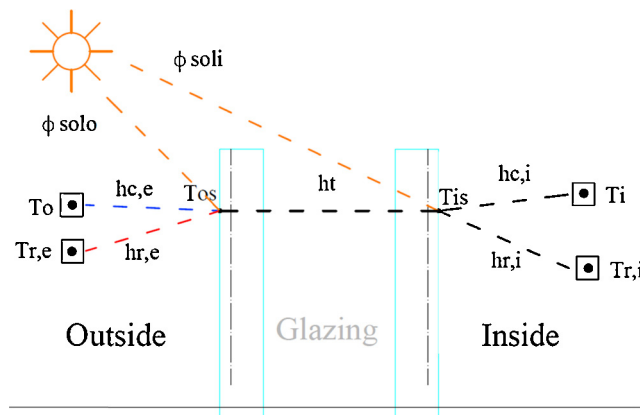
The first part of the study was the development of the simplified method. The method was developed to calculate the performance of the double glazing facade. The results of the method were two variables (the internal glazing surface temperature  $T_{is}$  and the external glazing surface temperature  $T_{os}$ ), which were calculated by solving the heat balance equations of them. Fig. 1 illustrates the heat balance of the variables and the thermal connection between different thermal parameters inside and outside the room [9].

After the development of the method, its results were validated by the measurements performed in the test facility “The Cube” at Aalborg University. The purpose of this was to evaluate the accuracy of the method in terms of calculating the internal glazing surface temperatures. In addition, the performance of the method was compared with that of WIS programme. The internal surface temperatures of the glazing were measured every 10 min during a winter period of one week in 2011, and the calculations by the simplified method were conducted through all the time the temperatures were measured. Because it was time consuming to conduct the calculation in WIS, WIS calculations were only implemented on two days of the week, i.e., one cloudy day on 28th of January and one sunny day on 30th of January. The sensitivity on the thermal mass of the glazing was also analysed for the simplified method. The result of the method calculated considering the heat capacity of the internal and the external panes was compared with that calculated without considering the heat capacity of the panes.

After the validation of the method, the heat exchange through the facade can be predicted according to the result of the temperatures  $T_{is}$  and  $T_{os}$ . Together with the solar transmittance through the glazing [10–12], the total heating or cooling energy demand caused by the facade can be predicted.

### 2.1. Experiment setup

The method was validated by the empirical data of the internal surface temperatures of the glazing measured in the experiments. The measurements were implemented in the full-scale test facility consisting of facades and rooms (The Cube at Aalborg University [13]) (Fig. 2 [7,8]). The test facility had two identical south-facing rooms with the internal dimension of 5.66 m × 2.46 m × 1.65 m ( $H \times W \times D$ ). Both of the facade systems faced south and had a dimension of 1.5 m × 4 m. The measurements of the double glazing facade were conducted in the west room of the facility.



**Fig. 1.** The heat balance of the variables and the thermal connection between different thermal parameters inside and outside the room.

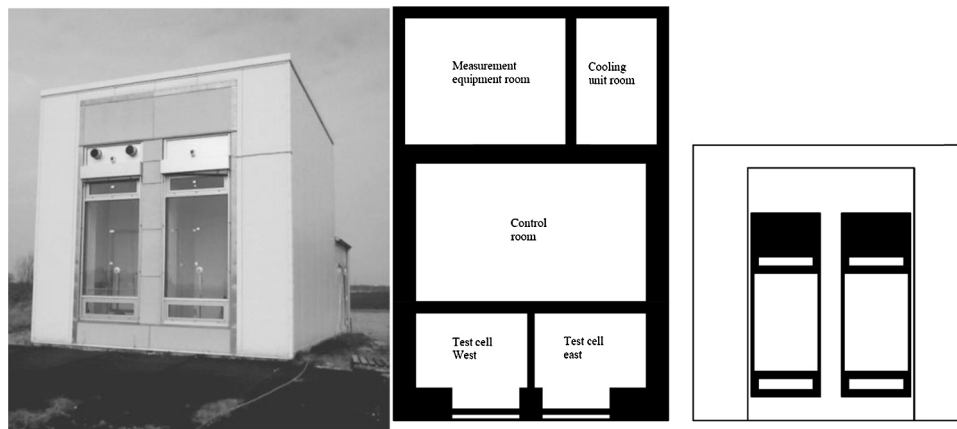


Fig. 2. Full-scale façade element test facility (left: test facility, middle: top view, right: front view).

The glazing type used in the experiments was a double glazing unit with a 22 mm argon-filled cavity and low-E coating on the internal pane. The facade in the west cell where the measurements were conducted was the double glazing facade. The layout of the double glazing unit is shown in Table 1. The measurements of the internal surface temperature on the glazing of the west room were conducted in the end of January 2011 (winter condition). The experiment is time consuming, therefore only the double glazing with low-E coating was tested in this experiment. Glazing with other type of coating (like solar control) needs to be investigated in the future work.

The surrounding internal surfaces of the room were built up of 15 mm plywood and were painted white, apart from the floor, which was made of 150 mm concrete. The heat loss due to infiltration was minimized to a minimum by sealing all joints with silicon.

Temperatures were measured using thermocouples type K, which were calibrated with a reference thermocouple at reference temperatures of 10 °C, 20 °C and 30 °C. The temperature was logged using Helios data logger connected to an ice point reference. The calibration of the thermocouples was done using a reference thermometer with an accuracy of 0.01 °C, insuring an accuracy of 0.6 °C for the thermocouples. All thermocouples were connected to a compensating box in order to increase accuracy in measurements [14]. The thermocouples measured internal surface temperatures of the glazing, shielded from the outside to prevent solar irradiance from influencing the measurements [13]. The temperature gradient was measured at 0.91 m, 1.82 m and 2.73 m heights in the room.

The room was heated by 1 kW electrical convective heating system heating the air to keep the air temperature stable. There was no other internal heat source in the room. The indoor air temperature was controlled using Danfoss Devireg™ 535. The achieved temperature was 22 °C.

Irradiance was measured using CM21-pyranometer, CM11-pyranometer, Wilhelm Lambrecht pyranometer and BF3-pyranometer. BF3 and Wilhelm Lambrecht were placed externally measuring the diffuse and global irradiance on a horizontal surface. CM21 and CM11 pyranometers were placed in each of the test cells, measuring transmitted irradiance through the glazing system. The pyranometers were prior to the installation calibrated in reference to CM21, which was calibrated in sun simulator and corrected by Kipp&Zonen B.V [13].

### 3. Simplified calculation method

#### 3.1. Choice and grid sensitivity of the method

In order to improve the accuracy of the simplified method, grid sensitivity of models were tested. The matrices of models with the same principle and heat balance equations but different number of variable nodes were constructed to calculate the internal surface temperature. Fig. 3 shows the layout of one double glazing unit example showing the positions and numbers of nodes in model 3.1.3 (3 variable nodes in the external pane, 1 node in the cavity and 3 variable nodes in the internal pane). Calculations were conducted from model 3.1.3 to model 129.1.129, where number of nodes increases step by step in the external pane and the internal pane of the double glazing unit.

In addition, four potentially simplified models were also chosen to perform the calculations in order to find a simplified method with fewer variable nodes and acceptable accuracy. The four simplified models were 2.0.2 surfaces, 1.0.1 surfaces, 1.1.1 middle and 1.0.1 middle, shown in Fig. 4. The simplified method was chosen among the four models.

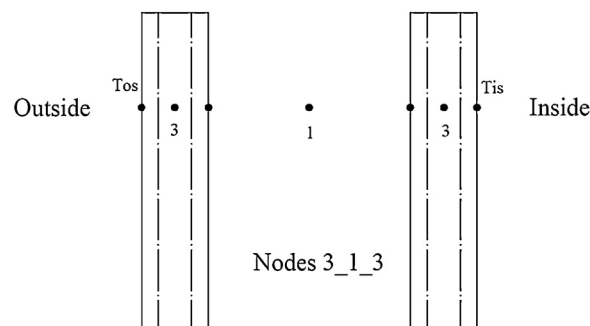


Fig. 3. The Layout of model with nodes 3-1-3 (number of nodes in external pane\_number of nodes in cavity\_number of nodes in internal pane).

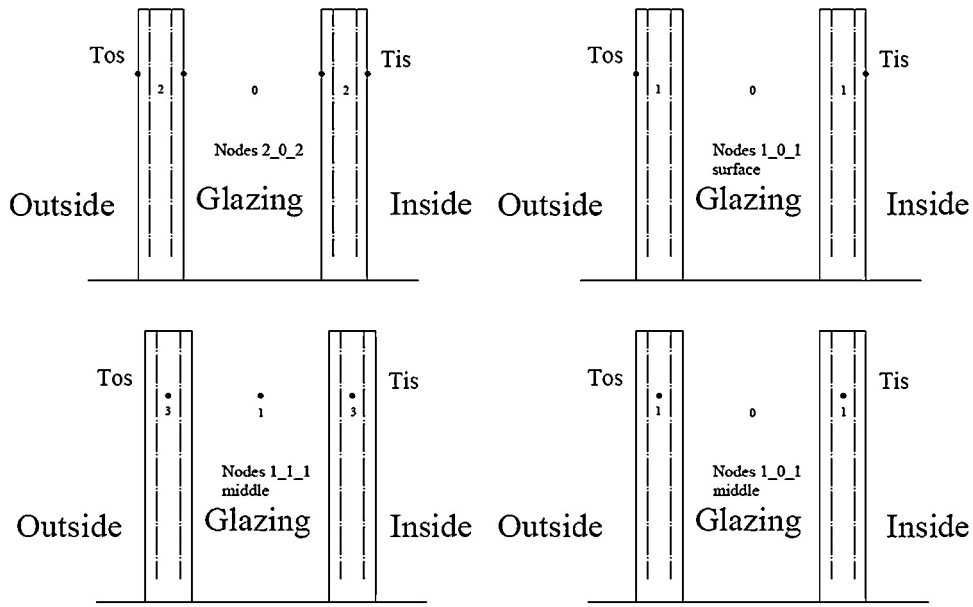


Fig. 4. The four potentially simplified models.

Fig. 5 shows the calculation results and the deviation of all the different models compared with model 129.1.129 in terms of internal surface temperature at one time step. The result shows that all the four simple models have good accuracy with deviation of under 0.2% compared with model 129.1.129. However, model 2.0.2 surfaces and model 1.0.1 surfaces are better than the other two simple models. Considering the complexity and time consumption of solving equations with four variables, the 1.0.1 surfaces model was more suitable than the model 2.0.2. According to the Fig. 5, the deviation of the 1.0.1 surfaces model is around 0.02%, which is adequately accurate for the simplified method. Therefore, the 1.0.1 surfaces model was chosen to calculate the internal surface temperature with only two nodes, which are located on the internal surface and external surface of the double glazing unit.

3.2. Development of simplified method

According to the comparison of the different models, the 1.0.1 surface model was finally chosen as the simplified model. The simplified calculation method was implemented making use of finite volume energy balance equations by Clarke [9] to calculate the temperature of internal and external surfaces, taking into account of the thermal mass of the glass, the spectral and angle dependence of the solar radiation [10–12]. There were two variable nodes in the equations representing the internal and external surface temperature with the volume of ¼ of the thickness of glass. It was assumed that the temperature of glass in the volume was homogeneous. The equations took both implicit and explicit conditions into account [9] considering the boundary conditions of both the present and previous time steps to increase the accuracy of the result.

Following equations are the procedure of the development and the results of the method calculating the temperatures of internal and external surface of the glazing.

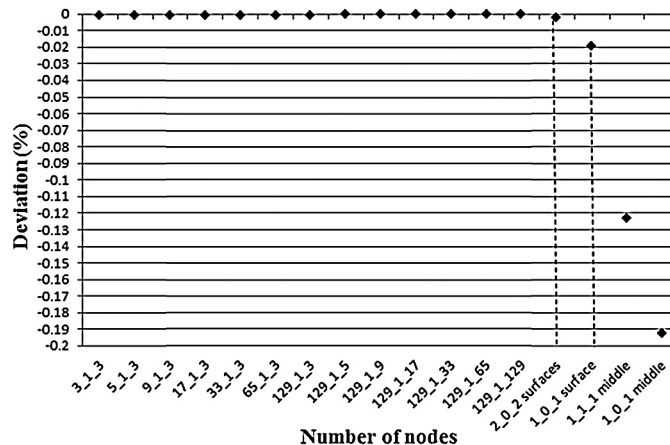


Fig. 5. The deviation of different models compared with model 129.1.129 in terms of internal surface temperature.

At the first time step, equations were developed for steady state conditions. The heat balances of the nodes standing for the internal and the external surfaces of the glazing were built in Eqs. (1) and (2). The internal and external surface temperatures at the first time step can be calculated by solving the equations:

$$(T_{is1} - T_{os1}) \times h_{t1} + (T_{o1} - T_{os1}) \times h_{c,e1} + (T_{r,e1} - T_{os1}) \times h_{r,e1} + \phi_{solo1} = 0 \quad (1)$$

$$(T_{os1} - T_{is1}) \times h_{t1} + (T_{i1} - T_{is1}) \times h_{c,i1} + (T_{r,i1} - T_{is1}) \times h_{r,i1} + \phi_{soli1} = 0 \quad (2)$$

The internal and external surface temperatures at the first time step were calculated in Eqs. (3) and (4):

$$T_{is1} = \frac{(T_{i1}h_{c,i1} + T_{r,i1}h_{r,i1} + \phi_{soli1}) \times (h_{t1} + h_{c,e1} + h_{r,e1}) + (T_{o1}h_{c,e1} + T_{r,e1}h_{r,e1} + \phi_{solo1}) \times h_{t1}}{(h_{t1} + h_{c,i1} + h_{r,i1}) \times (h_{t1} + h_{c,e1} + h_{r,e1}) - h_{t1}^2} \quad (3)$$

$$T_{os1} = \frac{(T_{i1}h_{c,i1} + T_{r,i1}h_{r,i1} + \phi_{soli1}) \times h_{t1} + (T_{o1}h_{c,e1} + T_{r,e1}h_{r,e1} + \phi_{solo1}) \times (h_{t1} + h_{c,i1} + h_{r,i1})}{(h_{t1} + h_{c,i1} + h_{r,i1}) \times (h_{t1} + h_{c,e1} + h_{r,e1}) - h_{t1}^2} \quad (4)$$

After the first time step, equations were built dynamically taking the thermal mass of the glazing into account. During the calculation of the dynamic conditions, explicit and implicit conditions were considered [9]: The explicit condition:

$$(T_{is(t)} - T_{os(t)}) \times h_{t(t)} + (T_{o(t)} - T_{os(t)}) \times h_{c,e(t)} + (T_{r,e(t)} - T_{os(t)}) \times h_{r,e(t)} + \phi_{solo(t)} = \frac{C_p \rho V}{\delta t} \times (T_{os(t+\delta t)} - T_{os(t)}) \quad (5)$$

$$(T_{os(t)} - T_{is(t)}) \times h_{t(t)} + (T_{i(t)} - T_{is(t)}) \times h_{c,i(t)} + (T_{r,i(t)} - T_{is(t)}) \times h_{r,i(t)} + \phi_{soli(t)} = \frac{C_p \rho V}{\delta t} \times (T_{is(t+\delta t)} - T_{is(t)}) \quad (6)$$

The implicit condition:

$$(T_{is(t+\delta t)} - T_{os(t+\delta t)}) \times h_{t(t+\delta t)} + (T_{o(t+\delta t)} - T_{os(t+\delta t)}) \times h_{c,e(t+\delta t)} + (T_{r,e(t+\delta t)} - T_{os(t+\delta t)}) \times h_{r,e(t+\delta t)} + \phi_{solo(t+\delta t)} = \frac{C_p \rho V}{\delta t} \times (T_{os(t+\delta t)} - T_{os(t)}) \quad (7)$$

$$(T_{os(t+\delta t)} - T_{is(t+\delta t)}) \times h_{t(t+\delta t)} + (T_{i(t+\delta t)} - T_{is(t+\delta t)}) \times h_{c,i(t+\delta t)} + (T_{r,i(t+\delta t)} - T_{is(t+\delta t)}) \times h_{r,i(t+\delta t)} + \phi_{soli(t+\delta t)} = \frac{C_p \rho V}{\delta t} \times (T_{is(t+\delta t)} - T_{is(t)}) \quad (8)$$

In order to increase the accuracy of the results, explicit and implicit conditions were added together. Then Eqs. (9) and (10) were resulted to build the heat balance standing for the nodes of the internal and the external surfaces at time step  $t + \delta t$ :

$$(T_{is(t)} - T_{os(t)}) \times h_{t(t)} + (T_{o(t)} - T_{os(t)}) \times h_{c,e(t)} + (T_{r,e(t)} - T_{os(t)}) \times h_{r,e(t)} + \phi_{solo(t)} (T_{is(t+\delta t)} - T_{os(t+\delta t)}) \times h_{t(t+\delta t)} + (T_{o(t+\delta t)} - T_{os(t+\delta t)}) \times h_{c,e(t+\delta t)} + (T_{r,e(t+\delta t)} - T_{os(t+\delta t)}) \times h_{r,e(t+\delta t)} + \phi_{solo(t+\delta t)} = \frac{2C_p \rho V}{\delta t} \times (T_{os(t+\delta t)} - T_{os(t)}) \quad (9)$$

$$(T_{os(t)} - T_{is(t)}) \times h_{t(t)} + (T_{i(t)} - T_{is(t)}) \times h_{c,i(t)} + (T_{r,i(t)} - T_{is(t)}) \times h_{r,i(t)} + \phi_{soli(t)} (T_{os(t+\delta t)} - T_{is(t+\delta t)}) \times h_{t(t+\delta t)} + (T_{i(t+\delta t)} - T_{is(t+\delta t)}) \times h_{c,i(t+\delta t)} + (T_{r,i(t+\delta t)} - T_{is(t+\delta t)}) \times h_{r,i(t+\delta t)} + \phi_{soli(t+\delta t)} = \frac{2C_p \rho V}{\delta t} \times (T_{is(t+\delta t)} - T_{is(t)}) \quad (10)$$

The time step was 600 s, which was the same as the measurements.

By solving the Eqs. (9) and (10), the internal and external glazing surface temperatures at time step  $t + \delta t$  can be calculated by Eqs. (11) and (12):

$$T_{is(t+\delta t)} = \frac{\left[ (T_{i(t+\delta t)}h_{c,i(t+\delta t)} + T_{r,i(t+\delta t)}h_{r,i(t+\delta t)} + \phi_{soli(t+\delta t)} + b) \times (h_{t(t+\delta t)} + h_{c,e(t+\delta t)} + h_{r,e(t+\delta t)} + \frac{2C_p \rho V}{\delta t}) + (T_{o(t+\delta t)}h_{c,e(t+\delta t)} + T_{r,e(t+\delta t)}h_{r,e(t+\delta t)} + \phi_{solo(t+\delta t)} + a) \times h_{t(t+\delta t)} \right]}{\left[ (h_{t(t+\delta t)} + h_{c,i(t+\delta t)} + h_{r,i(t+\delta t)} + \frac{2C_p \rho V}{\delta t}) \times (h_{t(t+\delta t)} + h_{c,e(t+\delta t)} + h_{r,e(t+\delta t)} + \frac{2C_p \rho V}{\delta t}) - h_{t(t+\delta t)}^2 \right]} \quad (11)$$

$$T_{os(t+\delta t)} = \frac{\left[ (T_{i(t+\delta t)}h_{c,i(t+\delta t)} + T_{r,i(t+\delta t)}h_{r,i(t+\delta t)} + \phi_{soli(t+\delta t)} + b) \times h_{t(t+\delta t)} + (T_{o(t+\delta t)}h_{c,e(t+\delta t)} + T_{r,e(t+\delta t)}h_{r,e(t+\delta t)} + \phi_{solo(t+\delta t)} + a) \times (h_{t(t+\delta t)} + h_{c,i(t+\delta t)} + h_{r,i(t+\delta t)} + \frac{2C_p \rho V}{\delta t}) \right]}{\left[ (h_{t(t+\delta t)} + h_{c,i(t+\delta t)} + h_{r,i(t+\delta t)} + \frac{2C_p \rho V}{\delta t}) \times (h_{t(t+\delta t)} + h_{c,e(t+\delta t)} + h_{r,e(t+\delta t)} + \frac{2C_p \rho V}{\delta t}) - h_{t(t+\delta t)}^2 \right]} \quad (12)$$

where

$$a = (T_{is(t)} - T_{os(t)}) \times h_{t(t)} + (T_{o(t)} - T_{os(t)}) \times h_{c,e(t)} + (T_{r,e(t)} - T_{os(t)}) \times h_{r,e(t)} + \phi_{solo(t)} + \frac{2C_p \rho V}{\delta t} T_{os(t)} \quad (13)$$

$$b = (T_{os(t)} - T_{is(t)}) \times h_{t(t)} + (T_{i(t)} - T_{is(t)}) \times h_{c,i(t)} + (T_{r,i(t)} - T_{is(t)}) \times h_{r,i(t)} + \phi_{soli(t)} + \frac{2C_p \rho V}{\delta t} T_{is(t)} \quad (14)$$

After calculating the internal surface temperature, the total energy exchange between inside and outside can be calculated by Eq. (15):

$$Q_{total} = Q_{tr} + Q_{sol} \quad (15)$$

where

$$Q_{sol} = \tau_{e,gzg} Q_{dir} + \tau_{e,dif} Q_{dif} \quad (16)$$

$$Q_{tr} = (T_{os} - T_{is}) \times h_t \quad (17)$$

By inputting the results of the variables and the parameters of subsystems in excel, the simplified calculation method can be realised.

### 3.3. Thermal parameters used in the method

The internal and the external surface temperature of the glazing  $T_{is}$  and  $T_{os}$  can be calculated by the method. All the other parameters in the equations were already known. Some of the known parameters were measured in the experiment at each time step, e.g., the indoor equivalent surface temperature  $T_{r,i}$ , the indoor and the outdoor air temperatures  $T_i$  and  $T_o$ , the direct and the diffuse solar radiation  $I_{dir}$  and  $I_{dif}$ . The outdoor surrounding equivalent temperature  $T_{r,e}$  was calculated according to the outdoor air temperature  $T_o$  [9]. Furthermore, the absorption of the solar radiation by the internal and the external pane  $\phi_{soli}$  and  $\phi_{solo}$  were the function of the amount of the solar radiation and the solar incident angle [10–12,15,16]. The convective and the radiative heat transfer coefficients are calculated according to Clarke [9].

#### 3.3.1. Thermal transfer coefficient of the double glazing unit

Equivalent heat transfer coefficient between the internal pane and the external pane  $h_t$  can be calculated according to EN673 [17]:

$$\frac{1}{h_t} = \frac{1}{h_s} + \frac{2d}{\lambda} \quad (18)$$

$$h_s = h_r + h_g \quad (19)$$

where the radiative heat transfer coefficient  $h_r$  between two panes is given by:

$$h_r = 4\sigma \left( \frac{1}{\varepsilon_1} + \frac{1}{\varepsilon_2} - 1 \right)^{-1} T_m^3 \quad (20)$$

According to EN673 [17], standardized boundary condition for the mean temperature of gas space  $T_m$  is used as 283 K at the first time step.

According to EN673  $h_r$  is constant in all the time steps. Dynamic solution can be realized in Eq. (21) [9], calculating  $h_r$  making use of the parameters at the previous time step.

$$h_{r(t+\delta t)} = \frac{\varepsilon_2 \varepsilon_1 \sigma \times (A_1 T_{is(t)}^4 f_{1 \rightarrow 2} - A_2 T_{os(t)}^4 f_{2 \rightarrow 1})}{A_1 \times (T_{is(t)} - T_{os(t)}) [1 - (1 - \varepsilon_1)(1 - \varepsilon_2) f_{1 \rightarrow 2} f_{2 \rightarrow 1}]} \quad (21)$$

According to EN673 [17] the convective heat transfer coefficient in the cavity  $h_g$  is given by Eq. (22):

$$h_g = Nu \frac{\lambda_{gas}}{s} \quad (22)$$

where

$$Nu = A(G_r P_r)^n \quad (23)$$

$$G_r = \frac{9.81s^3 \Delta T \rho^2}{T_m \mu^2} \quad (24)$$

$$P_r = \frac{\mu C}{\lambda} \quad (25)$$

#### 3.3.2. Dynamic heat transfer coefficient

The method not only takes into account of the thermal mass of the glass, but also the dynamic properties of the convective and radiative heat transfer coefficients. The present heat transfer coefficients decided by temperature difference are calculated using the results of the surface temperature of previous time step.

##### 3.3.2.1. Convective heat transfer coefficient. Interior surface convective heat transfer coefficient [9]:

$$h_{c,i} = \left\{ \left[ 1.5 \left( \frac{\Delta T}{H} \right)^{0.25} \right]^6 + \left[ 1.23 (\Delta T)^{0.33} \right]^6 \right\}^{1/6} \quad (26)$$

Dynamic solution can be realized in Eq. (27) [9], calculating  $h_{c,i}$  with the parameters of previous time step:

$$h_{c,i(t+\delta t)} = \left\{ \left[ 1.5 \left( \frac{T_{is(t)} - T_{i(t)}}{H} \right)^{0.25} \right]^6 + \left[ 1.23 (T_{is(t)} - T_{i(t)})^{0.33} \right]^6 \right\}^{1/6} \quad (27)$$

Exterior surface convective heat transfer coefficient can be calculated by Eq. (28) [9]:

$$h_{c,e} = 5.678 \left[ a + b \left( \frac{V}{0.3048} \right)^n \right] \quad (28)$$

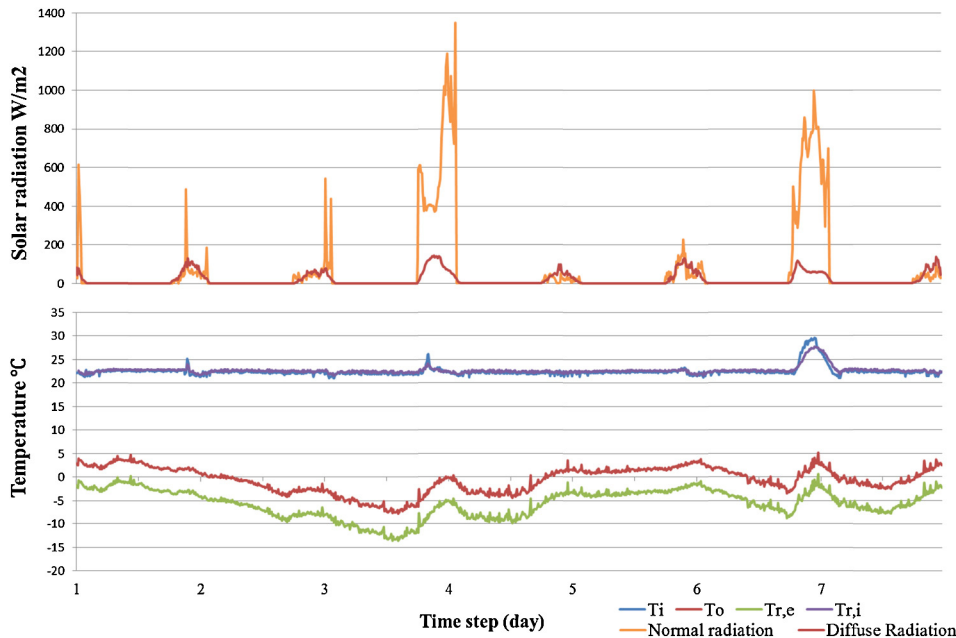


Fig. 6. Indoor and outdoor thermal parameters used to calculate the variables.

where  $V$  is the wind speed: If  $V < 4.88$  m/s then  $a = 0.99$ ,  $b = 0.21$ , and  $n = 1$ .

If  $4.88$  m/s  $< V < 30.48$  m/s then  $a = 0$ ,  $b = 0.5$ , and  $n = 0.78$ .

For climate of Aalborg, the average wind speed during the test period according to Windfinder [18] is taken as 5.5 m/s.

3.3.2.2. Long-wave radiative heat transfer coefficient. Long-wave radiative heat transfer coefficient between internal surface and internal walls is calculated as described in the following.

The internal radiative heat transfer coefficient of time step 1 is  $4.4$  W/(m<sup>2</sup> K) according to EN673 [17].

After time step 1, dynamic solution can be realized in Eq. (29), calculating  $h_{r,i}$  with the parameters of previous time step.

$$h_{r,i(t+\delta t)} = \frac{\varepsilon_i \varepsilon_{r,i} \sigma \times (A_i T_{is(t)}^4 f_{r,i \rightarrow is} - A_{r,i} T_{r,i(t)}^4 f_{is \rightarrow r,i})}{A_i \times (T_{is(t)} - T_{r,i(t)}) [1 - (1 - \varepsilon_i)(1 - \varepsilon_{r,i}) f_{is \rightarrow r,i} f_{r,i \rightarrow is}]} \quad (29)$$

Long-wave radiative heat transfer between external surface and surroundings can be calculated by Eqs. (30) and (31) [9]:

At time step 1,  $h_{r,e}$  can be calculated by Eq. (30) assuming the mean temperature of  $T_{r,e}$  and  $T_{os}$  is outdoor air temperature  $T_o$ .

$$h_{r,e1} = 4\varepsilon\sigma T_o^3 \quad (30)$$

After the first time step, dynamic solution can be realized in Eq. (31), calculating  $h_{r,e}$  with the parameters of previous time step.

$$h_{r,e(t+\delta t)} = \frac{\varepsilon\sigma(T_{r,e}^4 - T_{os}^4)}{T_{r,e} - T_{os}} \quad (31)$$

### 3.3.3. Temperature and solar radiation

Fig. 6 shows the indoor and the outdoor environment data measured in the experiments. If the method is used in practice project, the outdoor weather data should be the reference weather data of the locations or defined by the users. The indoor environment temperatures could be set by the users according to the requirement of the buildings. In order to simulate the façade in different orientations, the global solar radiation should be converted for different orientations [16].

Sky temperature can be calculated as following:

$$T_{r,e} = 0.05532 T_o^{1.5} \quad (32)$$

The solar absorption  $\phi_{solo}$  and  $\phi_{soli}$  of the external and the internal glazing layers can be calculated by Eqs. (33) and (34).

$$\phi_{solo} = \alpha_{e1} Q_{dir} + \alpha_{e1,dif} Q_{dif} \quad (33)$$

$$\phi_{soli} = \alpha_{e2} Q_{dir} + \alpha_{e2,dif} Q_{dif} \quad (34)$$

According to EN410 [12]  $\alpha_{e1}$  and  $\alpha_{e2}$  are calculated by Eqs. (35) and (36) in double glazing unit. Spectral properties of glazing can be obtained from ISO9050 [15] and WIS [4].

$$\alpha_{e1} = \frac{\sum_{300 \text{ nm}}^{2500 \text{ nm}} S_\lambda \left\{ \alpha_1(\lambda) + \frac{\alpha'_1(\lambda)\tau_1(\lambda)\rho_2(\lambda)}{1 - \rho'_1(\lambda)\rho_2(\lambda)} \right\} \Delta(\lambda)}{\sum_{300 \text{ nm}}^{2500 \text{ nm}} S_\lambda \Delta(\lambda)} \quad (35)$$



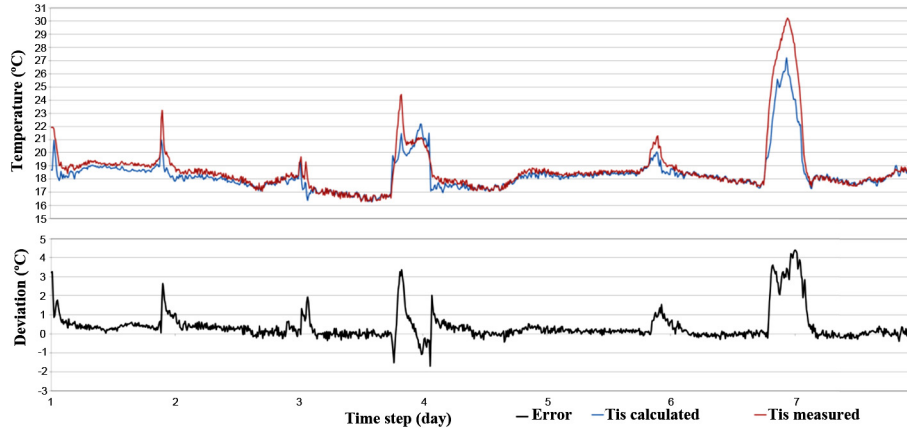


Fig. 7. The calculated and measured internal surface temperature of the glazing in the test cell and the deviation between them.

$$\alpha_{e2} = \frac{\sum_{300 \text{ nm}}^{2500 \text{ nm}} S_{\lambda} \left\{ \frac{\alpha_2(\lambda) \tau_1(\lambda)}{1 - \rho_1^x(\lambda) \rho_2(\lambda)} \right\} \Delta(\lambda)}{\sum_{300 \text{ nm}}^{2500 \text{ nm}} S_{\lambda} \Delta(\lambda)} \quad (36)$$

The solar absorption of different panes and solar transmittance of the whole glazing system are calculated taking incident angles of solar radiation into account. The solar absorption coefficients are calculated by Eq. (37) [11].

$$\alpha(\alpha_{in}) = 1 - \rho_{e, \text{g zg}}^x(\alpha_{in}) - \tau_{e, \text{g zg}}(\alpha_{in}) \quad (37)$$

where [10]

$$\tau_{e, \text{g zg}}[\alpha_{in}] \approx \tau_{e, \text{g zg}}[0^\circ] \left( 1 - a_{roos} \left( \frac{\alpha_{in}}{90^\circ} \right)^{\alpha_{roos}} - b_{roos} \left( \frac{\alpha_{in}}{90^\circ} \right)^{\beta_{roos}} - c_{roos} \left( \frac{\alpha_{in}}{90^\circ} \right)^{\gamma_{roos}} \right) \quad (38)$$

$$\rho_{e, \text{g zg}}^x[\alpha_{in}] \approx 1 - \tau_{e, \text{g zg}}[\alpha_{in}] - [1 - \rho_{e, \text{g zg}}^x(\alpha_{in} = 0^\circ) - \tau_{e, \text{g zg}}(\alpha_{in} = 0^\circ)], \quad \alpha_{in} \leq 75^\circ \quad (39)$$

$$\rho_{e, \text{g zg}}^x[\alpha_{in}] \approx 1 - \tau_{e, \text{g zg}}[\alpha_{in}] - \alpha^x(\alpha_{in} = 0^\circ) \frac{\alpha_{in} - 90^\circ}{15^\circ}, \quad \alpha_{in} > 75^\circ \quad (40)$$

where  $a_{roos}$ ,  $b_{roos}$ ,  $c_{roos}$ ,  $\alpha_{roos}$ ,  $\beta_{roos}$ ,  $\gamma_{roos}$  are calculated in [10].

The solar transmittance and reflectance under normal incident solar radiation can be calculated by Eqs. (41) and (42) [12].

$$\tau_{e, \text{g zg}}[0^\circ] = \frac{\sum_{300 \text{ nm}}^{2500 \text{ nm}} S_{\lambda} \tau(\lambda) \Delta(\lambda)}{\sum_{300 \text{ nm}}^{2500 \text{ nm}} S_{\lambda} \Delta(\lambda)} \quad (41)$$

$$\rho_{e, \text{g zg}}^x[0^\circ] = \frac{\sum_{300 \text{ nm}}^{2500 \text{ nm}} S_{\lambda} \rho(\lambda) \Delta(\lambda)}{\sum_{300 \text{ nm}}^{2500 \text{ nm}} S_{\lambda} \Delta(\lambda)} \quad (42)$$

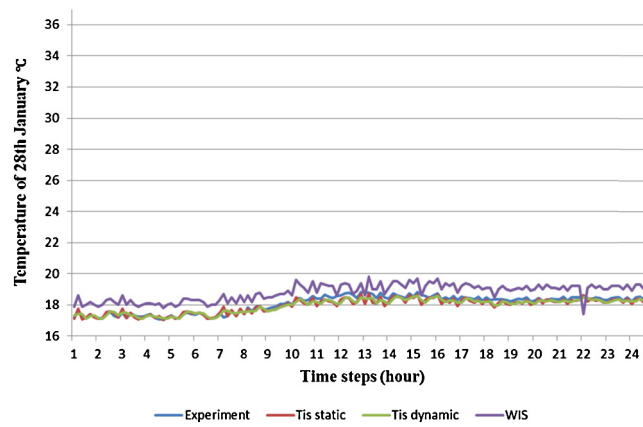
The solar incident angle at different time steps can be calculated according to the longitude and latitude angle of the sun and the orientation of the façade [16].

#### 4. Result

Fig. 7 shows the overall results of the simplified method compared with the measured performance during all the days when the measurements were conducted. It shows that when there is little or no solar radiation, the simplified method overestimates the internal surface temperature with a deviation of less than 1 °C. During sunny days it underestimates the internal surface temperature, which is probably because it underestimates the solar absorption of the internal pane.

The calculation results of the simplified method are compared with the performance calculated by WIS software. Because it is time consuming to carry out the calculation of different time steps, calculations in WIS software were only conducted on 28th and 30th of January. The 28th of January was a typical overcast day with little solar radiation while the 30th of January was a typical sunny day with high solar radiation. The calculations carried out in WIS used the same inputs of the external and the internal air temperature and the outdoor and the indoor surrounding temperatures as that of the simplified method. The heat transfer coefficients used in WIS calculations were taken from EN673 [17]. Figs. 8 and 9 show the internal surface temperatures calculated by the simplified method and WIS programme [7]. The temperatures were compared with that measured in the test facility.

The comparisons show that during the time of little or no solar radiation, the result of the simplified method was closer to the measured performance compared with that of the WIS software, with a deviation of approximately 0.5 °C. The reason for the overestimation of the internal surface temperature by WIS software during the cloudy day was probably the overestimation of the internal convective heat transfer coefficient (3.6 W/m<sup>2</sup>K) according to EN673 [17]. It could also be the overestimation of the default emissivity between the internal pane and the internal surround surfaces  $\varepsilon_{\tau, i}$  used in WIS, which could result in more heat exchange between the internal pane and the internal surroundings.



**Fig. 8.** Temperature comparison among WIS, measurement and the simplified method considering (Tis dynamic) and not considering (Tis static) thermal mass of glazing on 28th January 2011.

When the solar radiation was high, the simplified method underestimated the internal surface temperature, which was possibly because of the underestimation of the solar absorption of the internal pane. The reason for the difference between the results of the simplified method and the experiments could also be the tolerance of the internal convective and radiative heat transfer coefficient, which could significantly influence the calculation result. On the other hand, WIS overestimated the performance most of the time. The reason for the overestimation of WIS software during the sunny day was probably be the overestimation of the angle-dependent solar absorption of the panes. The internal surface temperature calculated by WIS was almost the same under solar radiation at different incident angles.

The sensitivity on the thermal mass of the glazing was also analysed for the simplified method. The result calculated considering the heat capacity of the internal and the external pane (dynamic) was compared with that calculated without considering the heat capacity of the panes (static). Figs. 8 and 9 show the calculation results of “Tis dynamic” and “Tis static” on 28th and 30th January. According to the figures, it indicates that “Tis dynamic” has relatively gentler curve than “Tis static” as the change of indoor and outdoor environment. However, the difference between “Tis dynamic” and “Tis static” is not significant, which because the heat capacity of the glazing is not big enough.

#### 4.1. Validation of the simplified method

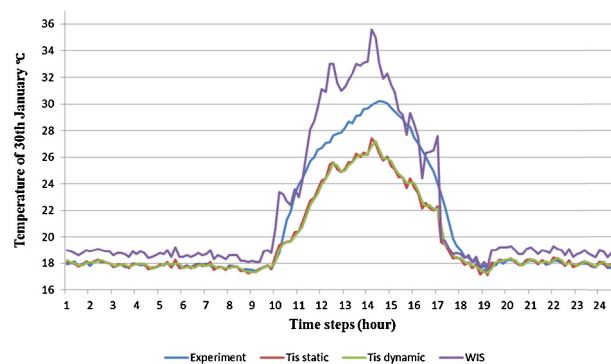
The accuracy of the model is validated through the  $R^2$ -value [19]. This value indicates how accurate the method and WIS programme fit the measurements, by comparing the values at each time step to the measurements and determining the level of accuracy as an evaluation of the overall differences between them. The  $R^2$  value is not only a measure of how well the pattern of the model follows the pattern of the measurements, but also a measure of accuracy determining the error at each time step.

Eqs. (43)–(45) show the calculation of the  $R^2$  value. Where  $y_i$  is the measured value;  $f_i$  is the calculated value;  $\bar{y}$  is the mean of the measured value.

$$R^2 = 1 - \frac{SS_{err}}{SS_{tot}} \quad (43)$$

$$SS_{err} = \sum_i^n (y_i - f_i)^2 \quad (44)$$

$$SS_{tot} = \sum_i^n (y_i - \bar{y})^2 \quad (45)$$



**Fig. 9.** Temperature Comparison among WIS, measurement and the simplified method considering (Tis dynamic) and not considering (Tis static) thermal mass of glazing on 30th January 2011.

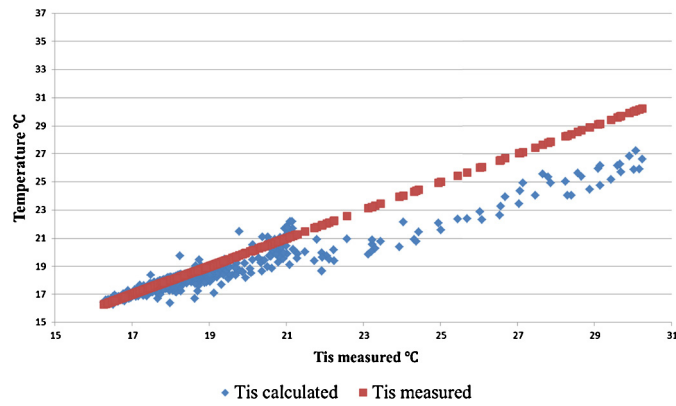


Fig. 10. Comparison on the internal surface temperature of the glazing among the simplified method, WIS programme and the measurements in the whole week.

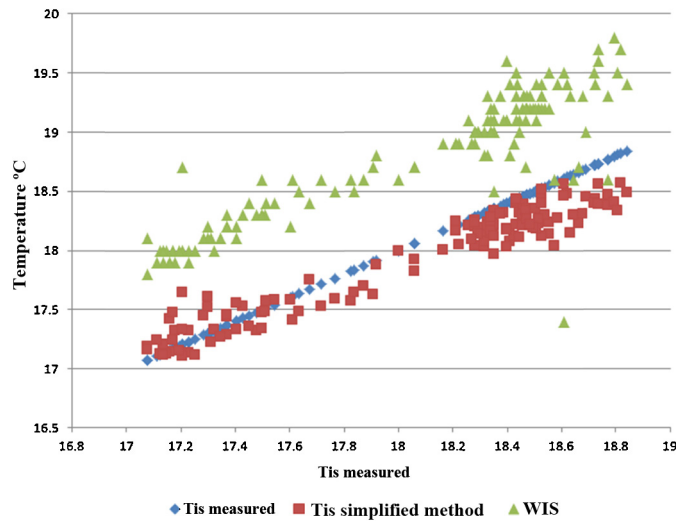


Fig. 11. Comparison on the internal surface temperature of the glazing between the calculation and the measurements on 28th January 2011.

The calculation result of the simplified method for the whole week is  $R^2 = 0.83$ .

Fig. 10 shows the linear regression of the calculation result by the simplified method in the whole week when the measurements were conducted. The temperature calculated by the simplified method corresponds with the measurements much better when it is below  $20^\circ\text{C}$  (when there was little or no solar radiation).

Figs. 11 and 12 show the linear regression of the calculation result by the simplified method and WIS programme on 28th and 30th January. According to the figures, the simplified method has better performance than WIS programme on cloudy days. Moreover, the

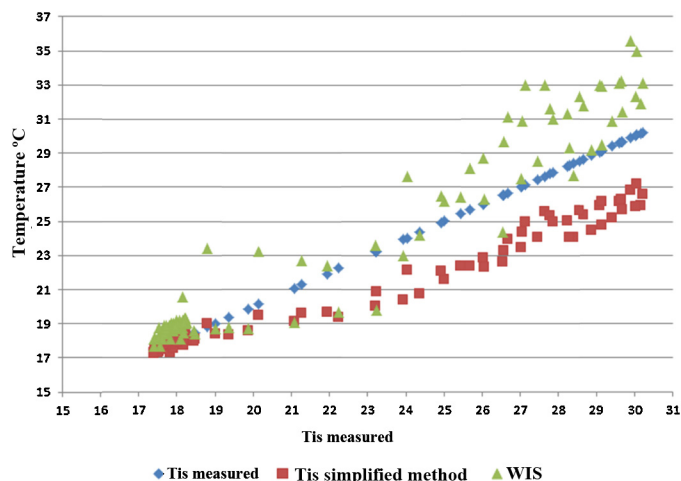


Fig. 12. Comparison on the internal surface temperature of the glazing between the calculation and the measurements on 30th January 2011.

simplified method underestimates the internal surface temperature when the solar radiation is high. WIS overestimates the internal surface temperature when the solar radiation is high.

The calculation result of the simplified method on 28th is  $R^2 = 0.85$ .

The calculation result of the WIS programme on 28th is  $R^2 = -1.14$ .

The calculation result of the simplified method on 30th is  $R^2 = 0.83$ .

The calculation result of the WIS programme on 30th is  $R^2 = 0.88$ .

## 5. Conclusion

A new simplified calculation method is developed to calculate the energy and comfort performance of the double glazing façade. The total energy exchange through the double glazing façade between inside and outside can be calculated. Furthermore the internal surface temperature can be calculated with reasonable accuracy according to the measurements conducted in the test facility. The method is a dynamic calculation tool which can be used for whole year energy performance calculations considering angle and spectral dependence of solar radiation. According to the calculation and the validation, it shows that the simplified calculation method has better performance in terms of calculating the internal surface temperature than WIS during the two select days.

This method can be used in the early design stage of building and façade to predict the energy and comfort performance of the double glazing façade. Compared with software like WIS, it requires less time and professional knowledge to input the parameters and build the model.

The method can also be implemented at any number of time steps, saving much time compared with WIS software which can only calculate the performance of one time step in each simulation.

Sensitivity analysis on the thermal mass of the glazing shows that the method including heat capacity of the glazing has slightly better accuracy than the static situation and slightly closer result to the reality.

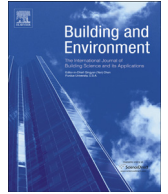
However, the validation was only for the double glazing with the pane of low-E coating. More work need to be done for the glazing with panes of other types like solar control, etc. According to the results, the method works better for cloudy days. And the experiments were conducted in a week in winter time only on the south façade. Therefore, the errors between the calculated results and the measurements can be greater in summer when the solar radiation is higher. Future work needs to be done for the façades on other directions of the building. In addition, more deep investigation about why these errors occurred when the solar radiation was high needs to be implemented.

## Acknowledgements

This paper is based on research conducted in a PhD project supervised by Senior Researcher Kim Wittchen, Danish Building Research Institute (SBI) and Professor Per Heiselberg, Department of Civil engineering both at Aalborg University, Denmark. The Ph.D. is part of the Strategic Research Centre for Zero Energy Buildings at Aalborg University and financed by the Danish aluminium section of The Danish Construction Association, Aalborg University and The Danish Council for Strategic Research, under the Programme Commission for Sustainable Energy and Environment.

## References

- [1] H. Erhorn, WP 4 Report "Simple calculation method", Fraunhofer-Institute for Building Physics – IBPBestfacade, Germany, 2007.
- [2] D. Saelens, Energy Performance assessment of multiple-skin facades, Laboratory for Building Physics, K.U. Leuven, Leuven, 2002 (Ph.D. dissertation).
- [3] D.V. Dijk, J. Goulding, WIS Reference Manual-Advanced Windows Information System, 1996.
- [4] ISO15099, Thermal Performance of Windows, Doors and Shading Devices-Detailed Calculations, 2003.
- [5] K.B. Wittchen, K. Johnsen, K. Grau, BSim – User's Guide, Danish Building Research Institute, Aalborg University, Hørsholm, 2000–2011.
- [6] S. Aggerholm, K. Grau, Building Energy Needs: Calculation Guidance – SBI-213, Danish Building Research Institute, Aalborg University, Hørsholm, 2008.
- [7] M. Liu, K.B. Wittchen, P.K. Heiselberg, F.V. Winther, Development of simplified and dynamic model for double glazing unit validated with full-scale façade element, in: PLEA2012, 28th Conference, Lima, 2012.
- [8] M. Liu, K.B. Wittchen, P.K. Heiselberg, F.V. Winther, Development of a simplified and dynamic method for double glazing façade with night insulation and validated by full-scale façade element, Energy and Buildings 58 (2013) 163–171.
- [9] J. Clarke, Energy Simulation in Building Design, Electronic edition red. s.l., Butterworth-Heinemann, 2001.
- [10] J. Karlsson, A. Roos, Modelling the angular behaviour of the total solar energy transmittance of windows, Solar Energy 69 (2000) 321–329.
- [11] T.E. Kuhn, Solar control: a general evaluation method for facades with venetian blinds or other solar control systems, Energy and Buildings 38 (2006) 648–660.
- [12] EN410, Glass in Building – Determination of Luminous and Solar Characteristics of Glazing, 1998.
- [13] O. Kalyanova, P. Heiselberg, Experimental Set-up and Full-scale measurements in "The Cube", DCE, Technical Reports, nr. 034, Aalborg University, Department of Civil Engineering, Aalborg, 2008.
- [14] N. Artmann, R. Vonbank, R.L. Jensen, Temperature Measurements Using Type K Thermocouples and the Fluke Helios Plus 2287A Datalogger, DCE Technical Reports, nr. 52, Aalborg University, Department of Civil Engineering, Aalborg, 2008.
- [15] ISO9050, Glass in building – determination of light transmittance, solar direct transmittance, total solar energy transmittance, ultraviolet transmittance and related glazing factors, International Organisation for Standardisation, 1990.
- [16] J. Duffie, W.A. Beckman, Solar Engineering of Thermal Processes, 2nd ed., John Wiley & Sons, New York, 1991.
- [17] EN673, Glass in building – determination of thermal transmittance (U value) – calculation method, 1997.
- [18] <http://www.windfinder.com/windstats/windstatistic.aalborg.htm>
- [19] D.C. Montgomery, Design and Analysis of Experiments, 7th ed., John Wiley & Sons, Hoboken, NJ, 2009.



# Development of a simplified method for intelligent glazed façade design under different control strategies and verified by building simulation tool BSim



Mingzhe Liu<sup>a,\*</sup>, Kim Bjarne Wittchen<sup>a</sup>, Per Kvols Heiselberg<sup>b</sup>

<sup>a</sup> Danish Building Research Institute (Sbi), Aalborg University, A.C. Meyers Vænge 15, 2450 København SV, Denmark

<sup>b</sup> Department of Civil Engineering, Aalborg University, Sohngaardsholmsvej 57, 9000 Aalborg, Denmark

## ARTICLE INFO

### Article history:

Received 16 October 2013

Received in revised form

3 January 2014

Accepted 5 January 2014

### Keywords:

Simplified method

Intelligent façade

Night shutter

Venetian blind

Natural ventilation

Indoor comfort

## ABSTRACT

The research aims to develop a simplified calculation method for intelligent glazed facade under different control conditions (night shutter, solar shading and natural ventilation) to simulate the energy performance and indoor environment of an office room installed with the intelligent facade. The method took the angle dependence of the solar characteristic into account, including the simplified hourly building model developed according to EN 13790 to evaluate the influence of the controlled façade on both the indoor environment (indoor air temperature, solar transmittance through the façade and the illuminance level on a chosen point) and the energy performance of the room.

The parameters calculated by the simplified method were compared with the Danish building simulation tool BSim in an hourly calculation with the weather data of the Danish reference year. By using the simplified method, it is possible to calculate the whole year performance of a room or building with intelligent glazed façade, which makes it a less time consuming tool to investigate the performance of the intelligent façade under different control strategies in the design stage with acceptable accuracy. Results showed good agreement between the simplified method and BSim in terms of simulating the energy and comfort performance of the room.

© 2014 Elsevier Ltd. All rights reserved.

## 1. Introduction

Given highly glazed facades are more and more popular in modern buildings, solar heat load and light transmittance through facades in summer and the heat transmittance through them in winter are of great importance to the energy consumption and indoor environment of high performance buildings. To decrease the energy demand and improve the indoor comfort of buildings, intelligent façades with controlled façade elements can be used. The appropriate control of all these technologies (night shutter, solar shading and natural ventilation, etc.) can greatly reduce the heating and cooling load and optimizes the visual and thermal comfort in a building. It would be beneficial if different control strategies could be compared and optimized in the early stage of building design. Therefore, it is important to develop a simplified method for the intelligent façade integrating all the controlled façade elements to calculate its performance under different control strategies in the beginning of the design stage [1,2].

A method which can be used to investigate the impact of different control strategies for shading devices on energy demand and visual comfort was shown in [3]. With the help of the method, the cut-off control strategy seemed to be a good compromise in summer for the balance between solar loads and visual comfort requirements. However, the secondary heat gains caused by absorption of solar energy in the slats of the venetian blind were missing. Methods for realistic performance evaluation of solar control properties of facades with sun-shading or other solar control systems were developed by [4–6]. They contributed to the determination of the angular dependent total solar transmittance and calculation of effective monthly or hourly  $g$ -values. It was shown that the models were more accurate than other methods and could be used to improve the formulas given in the European Standard EN13363 [7,8]. A method was developed by [9] to simulate predictive control of building systems operation in the early stages of building design. It can be used to determine an appropriate temperature set point and strategy for the control of the building systems in the present time step to prevent operative temperatures outside the comfort range in the future period. A simplified building simulation tool was presented in [10,11] to evaluate energy demand and the thermal indoor environment in

\* Corresponding author. Tel.: +45 99407234.

E-mail address: [ml@civil.aau.dk](mailto:ml@civil.aau.dk) (M. Liu).

the early stages of building design. It gave reliable results compared to detailed tools and needs only few input data to perform a calculation. The simplified methods for double glazing unit and glazed façade with night shutter were developed by our research group [12–14]. They showed good agreement with experiment data, which made them part of the simplified method to simulate the entire performance of the intelligent façade. Approaches for estimating daylight and lighting energy savings with daylighting schemes were presented in [15]. The work was helpful to compute accurately the interior daylight illuminance and to determine the long-term energy use of internal spaces with appropriate daylight-linked lighting controls.

However, most of the methods were for single element of the façade (like solar shading or window shutter, etc.). The intelligent façade is capable of control different façade elements together with building services. The properties of the intelligent façade and its influence on the indoor environment were not fully covered in these methods. Therefore, it is necessary to integrate the calculation algorithms of different façade elements and realize a holistic method for the intelligent façade. Additionally, the models of the façade and the other part of the room need to be connected together to calculate the influence of the controlled façade on the energy and comfort performance of the room.

Some simulation tools like BSim [16] and EnergyPlus [17] have function of quantifying the impact of controlled facade on energy and comfort performance of buildings. However, the control strategies included in the tools are limited and defined by the tools, so they are not flexible enough to investigate different control strategies of façade designed by the users. Sometimes it takes much time to input parameters in the tools and get results. Therefore, it is necessary to develop a simplified, though dynamic calculation method that can predict the energy and comfort performance of the façade with different control strategies.

The purpose of this article is to describe a simplified methodology that can make holistic calculation of an office room with the intelligent façade integrating the calculation of different facade elements together. It also calculates the influence of the façade under different control strategies on the energy and comfort performance of the room. Additionally, the method is flexible enough to accept modelling of different control strategies for external and internal shutters, external and internal solar shadings and natural ventilation, which makes it a suitable tool for the early stage of building design. Finally, the paper shows an evaluation of accuracy of the simplified method which has been implemented by comparing its predicted results with that of the Danish building simulation tool BSim.

## 2. Description and research method

The simplified method was developed for simulating the intelligent glazed façade design, focussing on the properties and control strategies of façade. It will be used on the investigation and optimization of different control strategies of façade and also will contribute during the design stage of buildings with intelligent façade design. It has the function of simulating the performance of whole building, but it is not advanced to investigate the rest parts of the building except façade. Parts of the method were described and presented in [12–14], solving the method for the glazing and the night shutter of the façade. The model of the solar shading and the entire building are presented in this paper.

The first part of the study was development of the simplified method to calculate the energy and comfort performance of the room with the controlled facade. The method can calculate the dynamic properties of different elements of the façade and it has also been integrated with the hourly model simulating the

performance of whole building according to EN 13790 [18]. Therefore, the simplified model is able to calculate the energy demands (heating, cooling, lighting and ventilation) and the indoor environment (indoor air temperature, solar transmittance through the façade and the indoor illuminance level on a chosen point) of the room with different control strategies of the facade.

After development of the method, its results were compared with simulation results from the Danish building simulation tool BSim. The purpose of this was to evaluate the accuracy of the simplified method in terms of calculating the different energy and comfort parameters of the test room. The hourly calculations were conducted through a whole year with weather data of the Danish Design Reference Year (DRY) [16].

The model used in both the simplified method and BSim programme was one south-facing office room with the dimension of  $3 \times 3 \times 5 \text{ m}^3$  ( $H \times W \times D$ ). The facade systems faced south and had a dimension of  $3 \times 3 \text{ m}^2$ . The glazing area of the façade system was  $4.08 \text{ m}^2$ . The glazing type used in the simulation was a double glazing unit with a 15 mm argon-filled cavity and low-E coating on the internal pane. It was assumed that there was no heat transfer through all the other enclosures in order to make the heat balance of the room dominated by that through the façade. The total infiltration rate used in both the simplified method and BSim was  $1.6 \text{ l/s}$ . Table 1 shows the input values of the thermal loads and set-points for the indoor conditions for both the simplified method and BSim. Both the heat and cooling loads were assumed to be 100% convective, and the indoor illuminance level was measured at the working plane (height of 0.85 m) 0.5 m from the façade on the centreline of the room.

The comparisons on the results between the simplified method and BSim were conducted in four different control conditions: façade without control; façade with control of night shutter; façade with control of solar shading; façade with control of natural ventilation. The reason of choosing these four control conditions was that the shutter, the solar shading and the natural ventilation were the most important controllable elements in order to develop intelligent façade design. However, the control strategies of different elements in BSim were limited. The purpose was to compare the simplified method with BSim under the basic control strategies in BSim to make sure the accuracy of the simplified method. After proving the simplified method by BSim with the basic control strategies, the simplified method can be updated with flexible and advanced control strategies that BSim does not have.

In order to unify the inputs of the simplified method and BSim, some normal set points of the different elements of the four control conditions were chosen for office buildings from the existing control strategies in BSim:

- The façade was not controlled according to the indoor and outdoor environment;
- The control of the night shutter, external shutter was installed and activated to cover the glazed façade outside the office hour; Table 2 shows the layout and the properties of the glazing with external night shutter;
- The control of the solar shading, external venetian blind was installed and activated to shade the glazed façade when the

**Table 1**  
Setup of building services and indoor conditions.

Internal load of people	150 W
Lighting power (on/off)	105 W
Setpoints for the heating	20 °C
Setpoints for the cooling	25 °C
Mechanical ventilation rate (office hour)	1.2 l/m <sup>2</sup>
Setpoint of lighting	250 lux

**Table 2**

Layout and material of the façade with night insulation outside.

Position	Material	Conductivity	IR emissivity outdoor	IR emissivity indoor
Outside	Polystyren 100 mm	0.05 W/mK	0.09	0.09
Cavity	Air 110 mm	–	–	–
Middle	Planilux 4 mm SGG	1 W/mK	0.837	0.837
Cavity	Argon 15 mm	0.017 W/mK	–	–
Inside	PITutran 4 mm SGG	1 W/mK	0.04	0.837

solar transmittance through the façade into the room was above 200 W/m<sup>2</sup>. The solar transmittance of the shading is 0.1;

- The control of the natural ventilation, the façade was open when the indoor temperature exceeded 23 °C.

After the simulations of the four control conditions, the predicted parameters (indoor air temperature, daylight illuminance on the reference point and energy demand of heating, cooling, lighting and ventilation) of the energy and indoor environment were calculated and compared with the BSim software. The accuracy of the simplified method was evaluated by calculating the mean bias error (MBE), root mean square error (RMSE) and the mean percentage error (MPE). Positive MBE showed overestimation while negative MBE indicated underestimation of the simplified method compared with BSim. The RMSE and MBE were also expressed as a percentage of the corresponding parameters. The MBE, RMSE and MPE were defined as in the following equations:

$$MBE = \left[ \sum (P_{i,simplified} - P_{i,BSim}) \right] / n \quad (1)$$

$$RMSE = \left\{ \left[ \sum (P_{i,simplified} - P_{i,BSim})^2 \right] / n \right\}^{1/2} \quad (2)$$

The coefficient of determination  $R^2$  of the results was also calculated [19]. The criteria with regards to the analysis utilized to determine the degree of agreement between the predicted parameters by the simplified method and that simulated by BSim was the closeness of magnitude of  $R^2$  to 1.

### 3. Simplified calculation method

#### 3.1. Simplified method of controlled façade

The simplified method of the façade contains algorithms of different elements: double glazing unit, night shutter, solar shading and natural ventilation. The detailed algorithms of the double glazing unit and the night shutter have been shown in [12–14]. In the comparison of this paper, the value of the natural ventilation rate of the window from the simulation of BSim is used in the simplified method. The algorithms of calculating the natural ventilation rate according to the opening of the window and the outdoor weather data is not involved in the simplified method for

now. However, it will be integrated in the method in the future. The detailed algorithms of the solar shading with venetian blind are shown below.

The algorithms of the façade with controlled blind contain two modes, one is when the blind is activated and the other one is when the blind is inactivated. When the blind is inactivated, the same as the method of the double glazing unit, the method calculates the solar heat gain of the double glazing unit by equation (3).

$$g = \tau_e + q_i \quad (3)$$

The solar direct transmittance  $\tau_e$  and the secondary heat transfer factor of the glazing towards the inside  $q_i$  can be calculated according to EN 410 [20]. Angle dependence of the two parameters is described in [5,6,12].

This paper describes detail calculation method for the mode when the blind is activated. Both the total solar transmittance  $g_t$  and the direct solar transmittance  $\tau_{e,t}$  of the double glazing with external blind are calculated by the equations below. Direct solar transmittance  $\tau_{e,t}$  will be used to compare with the calculated results by BSim.

The total solar transmittance of the glazing with external solar protection device is given by equation (4) [7,8]:

$$g_t = \tau_{e,B}g + \alpha_{e,B} \frac{G}{G_2} \tau_{e,B}(1-g) \frac{G}{G_1} \quad (4)$$

where

$$\alpha_{e,B} = 1 - \tau_{e,B} - \rho_{e,B} \quad (5)$$

$$G_1 = 5W / (m^2 \cdot K) \quad (6)$$

$$G_2 = 10W / (m^2 \cdot K) \quad (7)$$

$$G = \left( \frac{1}{U_g} + \frac{1}{G_1} + \frac{1}{G_2} \right)^{-1} \quad (8)$$

The solar direct transmittance of the whole façade with external solar protection devices is determined by equation (9) [7,8]:

$$\tau_{e,t} = \frac{\tau_e \tau_{e,B}}{1 - \rho_{e,B} \tau_{e,B}} \quad (9)$$

The solar transmittance of the solar protection device  $\tau_{e,B}$  can be divided into direct solar transmittance  $\tau_{S,D}$  and diffuse solar transmittance  $\tau_{S,d}$ . The solar reflectance of the solar protection device  $\rho_{e,B}$  can be divided into direct solar reflectance  $\rho_{S,D}$  and diffuse solar reflectance  $\rho_{S,d}$  (equations (10)–(15) [7,8]). The solar reflectance of the side of the solar protection device facing towards the room  $\rho'_{e,B}$  is the same as the diffuse solar reflectance  $\rho_{S,d}$ .  $\tau_{S,D}$ ,  $\tau_{S,d}$ ,  $\rho_{S,D}$  and  $\rho_{S,d}$  are calculated by equations (10)–(15) [7,8].

$$\tau_{S,D} = \phi_{51}\rho + \phi_{61}\tau + \frac{(Z\phi_{54}\rho' + \phi_{63}\tau)(\phi_{31}\rho + \phi_{41}\tau) + (Z\phi_{63}\tau + \phi_{54}\rho)(\phi_{41}\rho' + \phi_{31}\tau) \cdot Z}{\phi_{34}\rho \cdot (1 - ZZ')} \quad (10)$$

$$\rho_{S,D} = \phi_{52}\rho + \phi_{62}\tau + \frac{(Z\phi_{54}\rho' + \phi_{63}\tau)(\phi_{32}\rho + \phi_{42}\tau) + (Z\phi_{63}\tau + \phi_{54}\rho)(\phi_{42}\rho' + \phi_{32}\tau) \cdot Z}{\phi_{34}\rho \cdot (1 - ZZ')} \quad (11)$$

$$Z = \frac{\phi_{34}\rho}{1 - \phi_{34}\tau} \quad (12)$$

$$Zl = \frac{\phi_{34}\rho'}{1 - \phi_{34}\tau} \quad (13)$$

$$\tau_{s,d} = \phi_{21} + \frac{(\phi_{23}\rho + \phi_{24}\tau)(\phi_{31} + Zl\phi_{41}) + (\phi_{24}\rho' + \phi_{23}\tau)(\phi_{41} + Z\phi_{31})}{\phi_{34}\rho \cdot (1 - ZZl)} \cdot Z \quad (14)$$

$$\rho_{s,d} = \frac{(\phi_{23}\rho + \phi_{24}\tau)(\phi_{32} + Zl\phi_{42}) + (\phi_{24}\rho' + \phi_{23}\tau)(\phi_{42} + Z\phi_{32})}{\phi_{34}\rho \cdot (1 - ZZl)} \cdot Z \quad (15)$$

The method calculates the solar properties of the venetian blind considering the incident angle of the solar radiation and the slat angle of the blind. The calculation is conducted in 2D (Fig. 1 [7,8]), assuming that the reflection of the solar radiation along the slats is neglected, which means the radiation moves in the surface perpendicular to the façade surface. Therefore, only the solar altitude angle is taken into account and there is no reflectance along the slat length of the blind.  $H$  is the distance between the slats of the blind;  $W$  is the width of the slats of the blind;  $\alpha$  is the solar altitude angle;  $\beta$  is the tilt angle of the slats of the blind; the numbers 1–6 stand for different surfaces used to calculate the view factors [7,8]. For example,  $\phi_{ij}$  is the view factor from surface  $i$  to surface  $j$ . Fig. 1

Based on this assumption, the view factors between the surfaces 1–6 are calculated with ray tracing method every time step according to the dimension of the slat, the solar altitude angle and the slat angle. Equations (16)–(27) below calculate the simplified view factors.

$$\phi_{51} = \frac{\text{Degrees}\left(\arctan \frac{H \cdot \cos \beta}{H \cdot \sin \beta + W \cdot \frac{m}{2}}\right)}{180} \quad (16)$$

$$\phi_{52} = \frac{\text{Degrees}\left(\arctan \frac{H - \sin \beta \cdot \frac{m}{2}}{\cos \beta \cdot \frac{m}{2}}\right) + \beta}{180} \quad (17)$$

$$m = \frac{H}{\cos \beta \cdot \tan \alpha + \sin \beta} \quad (18)$$

$$\phi_{54} = 1 - \phi_{51} - \phi_{52} \quad (19)$$

$$\phi_{31} = \frac{\text{Degrees}\left(\arctan \frac{H \cdot \cos \beta}{H \cdot \sin \beta + \frac{W}{2}}\right)}{180} \quad (20)$$

$$\phi_{32} = \frac{\text{Degrees}\left(\arctan \frac{H - \sin \beta \cdot \frac{W}{2}}{\cos \beta \cdot \frac{W}{2}}\right) + \beta}{180} \quad (21)$$

$$\phi_{41} = \phi_{32} \quad (22)$$

$$\phi_{42} = \phi_{31} \quad (23)$$

$$\phi_{34} = 1 - \phi_{31} - \phi_{32} \quad (24)$$

$$\phi_{24} = \frac{\text{Degrees}\left(\arctan \frac{W \cdot \cos \beta}{W \cdot \sin \beta + \frac{H}{2}}\right)}{180} \quad (25)$$

$$\phi_{23} = \frac{\text{Degrees}\left(\arctan \frac{W - \sin \beta \cdot \frac{H}{2}}{\cos \beta \cdot \frac{H}{2}}\right) + \beta}{180} \quad (26)$$

$$\phi_{21} = 1 - \phi_{23} - \phi_{24} \quad (27)$$

### 3.2. Hourly model of building

The simplified model of façade with different controlled elements was also integrated with a simple hourly model defined in EN 13790 [18] calculating the energy performance and indoor comfort. Fig. 2 [18] shows the network and heat flow of the simulated zone. Full sets of equations for the simple hourly method are shown below [18].

The heat flow rates from the internal loads and solar heat sources  $\phi_{\text{int}}$  and  $\phi_{\text{sol}}$  are split into the air node  $\theta_{\text{air}}$  and internal surface node  $\theta_s$ . The indoor air temperature  $\theta_{\text{air}}$  and the energy demands of heating and cooling can be calculated by the simplified method. Detailed equations are shown in Annex C in EN 13790 [18].

### 3.3. Calculation of daylight level

The daylight level at the reference point in the room can be calculated by equations (28) and (29).

$$E_v = \tau_e \times SF_1 \times K_D \times \phi_D + \tau_d \times SF_2 \times K_d \times \phi_d + \tau_d \times SF_3 \times K_d \times \phi_R \quad (28)$$

$$E_{v-s} = \tau_{e,t-D} \times SF_4 \times K_D \times \phi_D + \tau_{e,t-d} \times SF_4 \times K_d \times \phi_d + \tau_{e,t-d} \times SF_4 \times K_d \times \phi_R \quad (29)$$

In BSim [16] the relative illuminance in the room is specified in relation to the current solar radiation on the window, with the ratio being called the solar light factor SF, which must not be confused

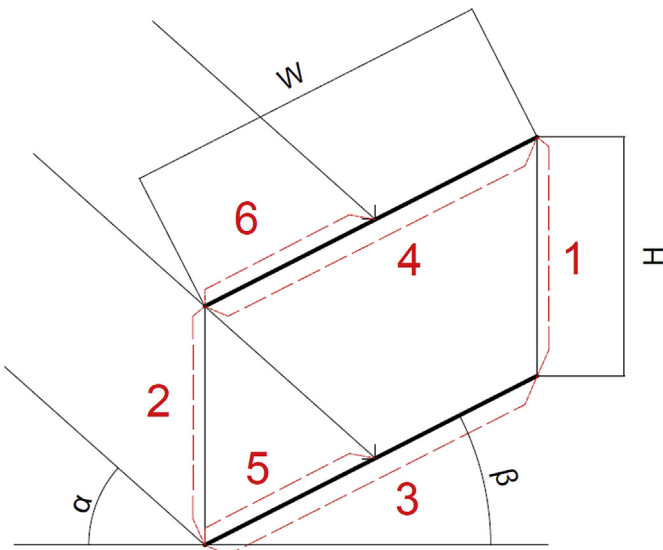


Fig. 1. Schematic presentation of a venetian blind [7,8] (surfaces 1 to 6 refer to the view factor  $\phi_{ij}$ ).



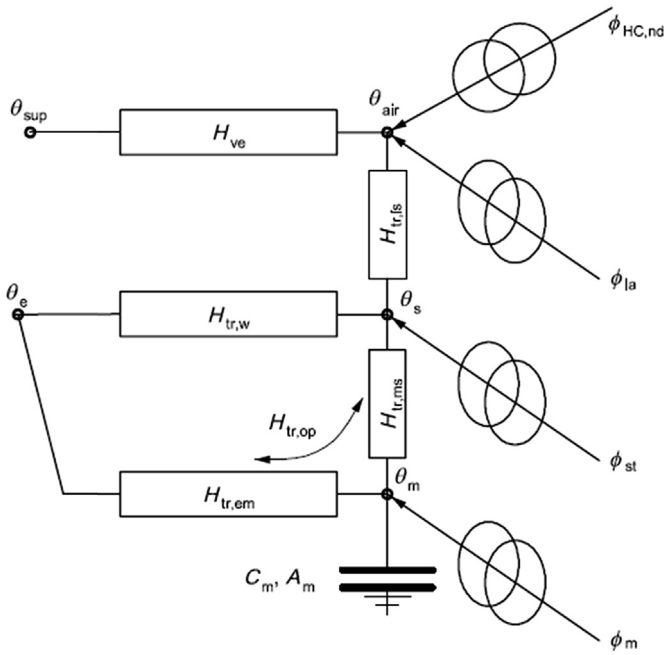


Fig. 2. Analogue electrical network of heat flow of the simulated zone.

with the daylight factor (DF). The solar light factor SF [16] at a point on a given plane is defined as the ratio of the illuminance at the point to the illuminance outdoors on the surface of the facade, without any shadows. The illuminance at a point cannot be described by a single value of the solar light factor, but must be divided into different contributions as follows:

- SF1 the solar light factor for direct sunlight (direct light)
- SF2 the solar light factor for light from the sky (diffuse light from the firmament)
- SF3 the solar light factor for reflected light
- SF4 the solar light factor for the window, when this is equipped with sunshades.

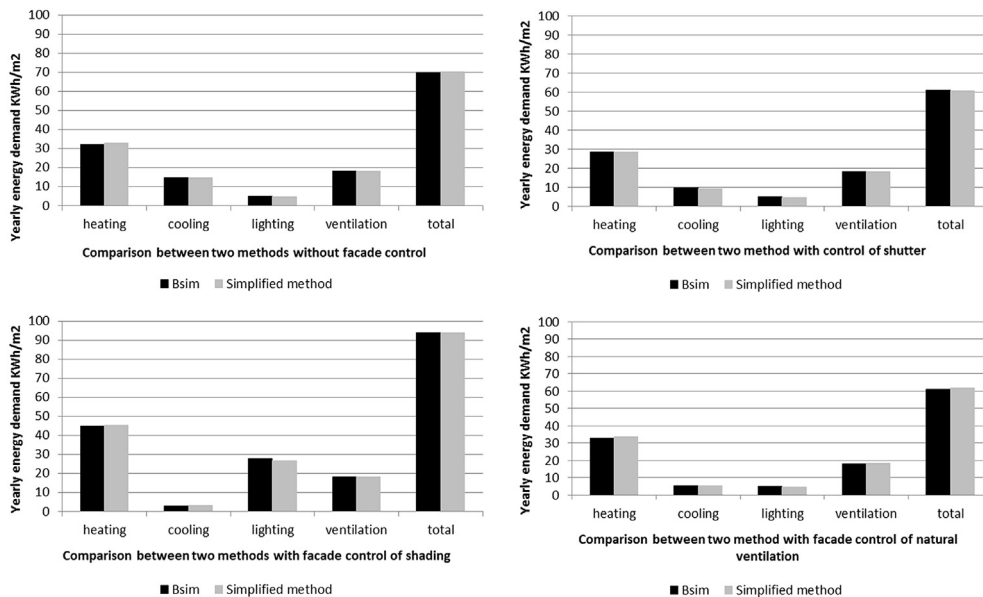


Fig. 3. Comparisons of energy demand of the room on the four control conditions.

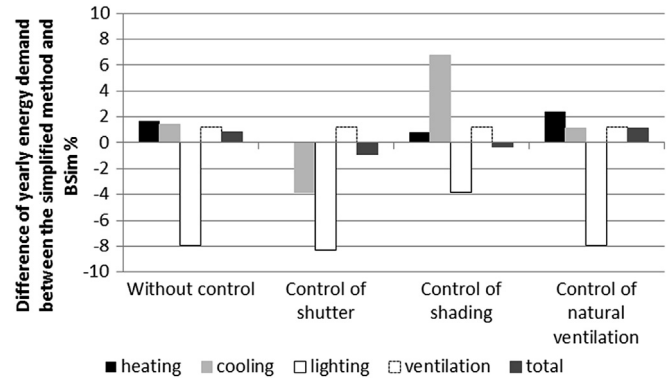


Fig. 4. Difference of energy demand on the four control conditions between the two methods.

Solar light factors  $SF_1, SF_2, SF_3$  and  $SF_4$  can be obtained from BSim [16].

#### 4. Result

Figs. 3 and 4 show the comparison on the yearly energy demand under the four control conditions between the simplified method and BSim. According to the figures, compared with BSim, the energy demands for heating calculated by the simplified method are overestimated under all the four control conditions. The heating demand under the control of the natural ventilation calculated by the simplified method has the biggest difference of approximately 2.4% compared with that calculated by BSim.

Compared with BSim, the energy demands for cooling are overestimated by the simplified method under all the four control conditions except control of shutter. The cooling demands calculated by the simplified method under the control of solar shading have the biggest difference of around 6.8% of that calculated by BSim. The differences can be explained by the different inputs of heating and cooling loads calculated according to different principles of the two methods.

**Table 3**  
Comparison of the result between the simplified method and BSim.

Model	MBE	MBE (%)	RMSE	RMSE (%)	R square
Reference condition (without facade control)					
Indoor air temperature °C	0.177	0.930	0.884	4.020	0.932
Solar transmittance (W/m <sup>2</sup> )	0.451	-1.440	5.175	6.404	0.997
Daylight illuminance (Lux)	94.700	4.866	220.090	12.737	0.980
Control of night shutter					
Indoor air temperature °C	0.163	0.849	0.704	3.278	0.935
Solar transmittance (W/m <sup>2</sup> )	0.268	-1.294	8.748	8.348	0.993
Daylight illuminance (Lux)	239.621	10.010	374.511	17.480	0.947
Control of solar shading					
Indoor air temperature °C	0.305	1.446	0.842	4.024	0.911
Solar transmittance (W/m <sup>2</sup> )	-1.045	-5.688	4.078	11.318	0.996
Daylight illuminance (Lux)	11.712	7.084	115.084	14.733	0.990
Control of natural ventilation					
Indoor air temperature °C	0.061	0.387	0.845	3.948	0.919
Solar transmittance (W/m <sup>2</sup> )	0.564	-1.374	5.229	6.470	0.997
Daylight illuminance (Lux)	95.792	4.924	220.300	12.749	0.980

The energy demand for lighting under all the control conditions is underestimated by the simplified method, with the difference of up to -8.3% compared with BSim. The difference is bigger than that of the heating, cooling and ventilation, which is because it is difficult to have quite similar prediction of daylight level around the value of 250 lux (the set-point of lighting). Being turned on or off of the lighting devices can be significantly influenced by the prediction of the daylight level at the reference point.

The total energy demand and the energy demand for ventilation between the two methods are similar with the difference of less than ±2%.

Table 3 shows the overview comparison (Values of MBE, RMSE and R<sup>2</sup>) between the two methods on the parameters of indoor environment under the four control conditions: indoor air temperature; solar transmittance through the façade; indoor daylight level on the chosen point. In all the four control conditions, difference of daylight level between the two methods is significantly higher than other parameters, with the average values of MBE and

RMSE at around 6% and 14%, respectively. The results of the other two parameters under all the four control conditions are similar between the methods, with the values of MBE within ±6% and RMSE within 12%, respectively.

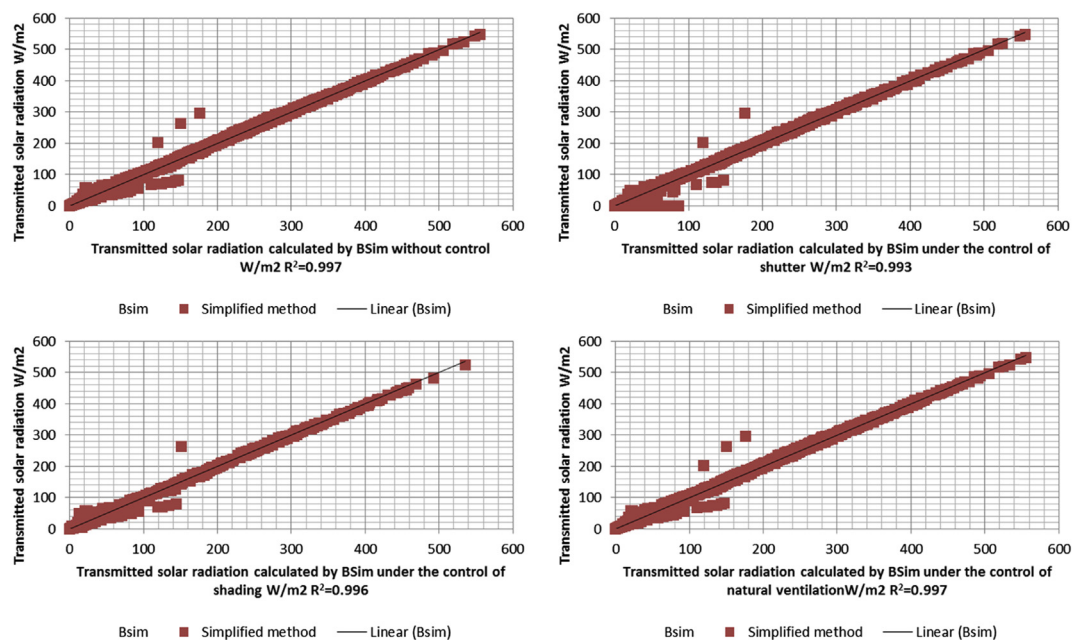
Figs. 5–7 present the calculated results by the simplified method for all the parameters under the four control conditions as a function of the corresponding results calculated by BSim. The result shows that, under the condition of façade without function control, the calculated results of the simplified method have acceptable agreement with that of BSim software in terms of both the indoor air temperature and the solar transmittance through the façade, with the values of R<sup>2</sup> at 0.932 and 0.997.

The comparison shows that during most of the time the illuminance level at the chosen point, in the simplified method, are similar to the results of BSim with R<sup>2</sup> of 0.980. One explanation for the remaining differences could be that the light transmittances of the two methods might not be exactly the same at different incident angle. Nevertheless, the difference of the predicted results between the two methods is regarded as accepted.

Under the condition of façade with the control of night shutter, the indoor air temperature is overestimated by the simplified method, with the value of R<sup>2</sup> at 0.935. The difference can be explained by the different input of the heating and cooling needs of the two methods. The results of solar transmittance are similar between the two methods (R<sup>2</sup> = 0.993). The illuminance level at the chosen point is overestimated by the simplified method at most of the time (R<sup>2</sup> = 0.947).

Under the conditions of the façade with the control of shading and natural ventilation, the results of the indoor air temperature and the solar transmittance are similar between the two methods. However, the illuminance level is slightly overestimated by the simplified method at most of the time.

The simplified method is exclusively developed for evaluating the performance of intelligent or controlled façade design for office buildings. Therefore, the inputs and simulation possibilities for control strategies of façade are detailed, completed and can be updated. It is possible to change the parameters of the rest parts of the building except façade if the users need. Otherwise, they are set



**Fig. 5.** Comparison on the parameter of transmitted solar radiation between the two methods under the four controlled condition.

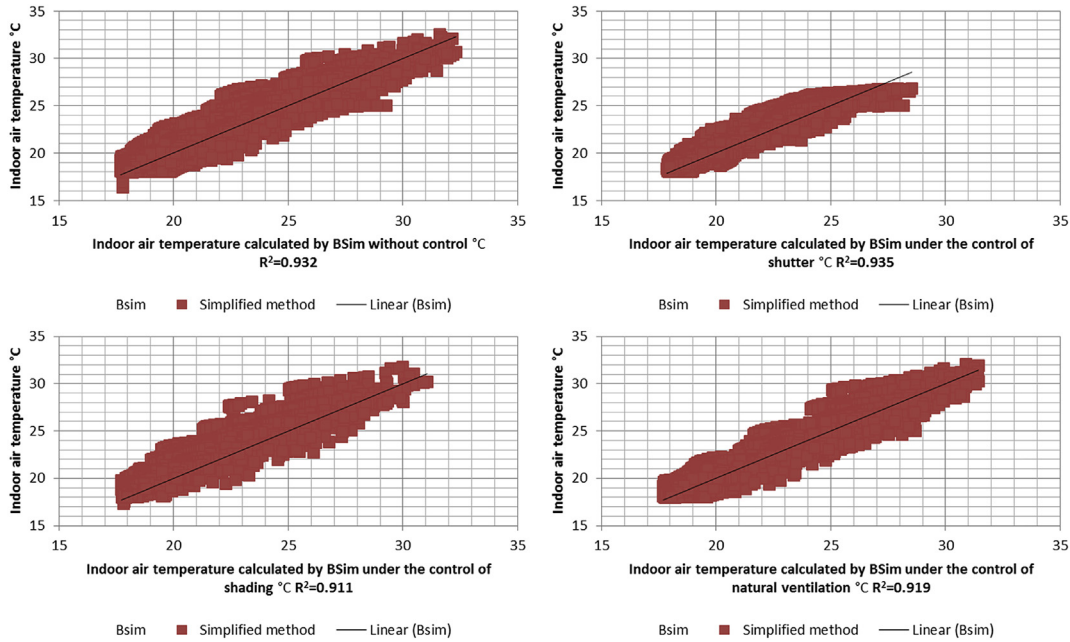


Fig. 6. Comparison on the parameter of indoor air temperature between the two methods under the four controlled condition.

as normal office conditions with pre-inputted parameters and set points, which makes it simple and less time consuming to investigate only the properties of building façade.

### 5. Conclusion

In order to investigate the performance of the façade with different control strategies, we developed a simplified method to simulate several energy and comfort parameters of the room under different control conditions. The evaluation of the results by the Danish building simulation tool BSim showed good correlation for indoor air temperature and solar transmittance and acceptable correlation for illuminance level, energy demands of heating, cooling, lighting and ventilation between the simplified method

and BSim. The authors rated the simplified method as a reasonable reliable tool for the early stages of an office building design process, since the model is based on hourly calculation of an office in the whole reference year.

According to all the comparisons, the correlation between the results of the simplified method and that of BSim is relatively high. Some differences are caused by the different inputs of heating and cooling needs calculated according to different principles of the two methods. In general these differences were regarded as having minor importance and therefore the method is acceptable for further simulations.

In addition, simple to input, quick to get results and flexible enough to model new control strategies will be a great advantage for the beginning of design process.

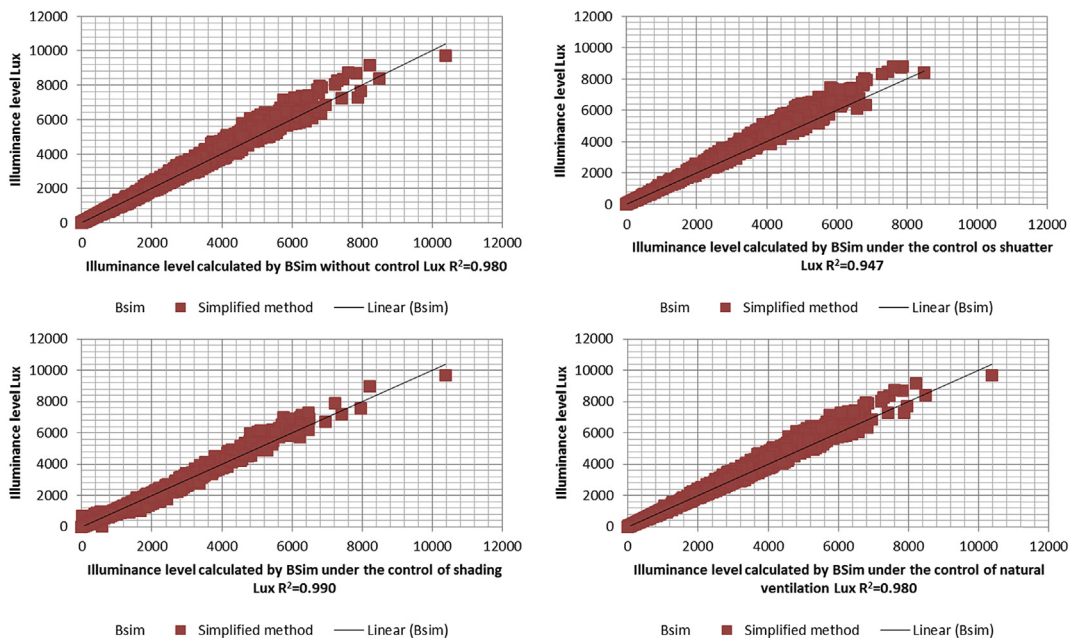


Fig. 7. Comparison on the parameter of daylight level on the reference point between the two methods under the four controlled condition.

For the future work, the simplified method should also be confirmed by experimental assessments and should be tested with other solar shading systems.

### Acknowledgements

This paper is based on research conducted in a PhD project supervised by Senior Researcher Kim Wittchen, Danish Building Research Institute (SBI) and Professor Per Heiselberg, Department of Civil engineering both at Aalborg University, Denmark. The PhD is part of the Strategic Research Centre for Zero Energy Buildings at Aalborg University and financed by the Danish aluminium section of The Danish Construction Association, Aalborg University and The Danish Council for Strategic Research, under the Programme Commission for Sustainable Energy and Environment.

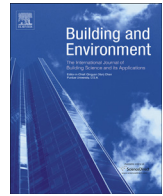
### Nomenclature

$g$	is the total solar transmittance of glazing [dimensionless];
$\tau_e$	is the solar direct transmittance of the glazing [dimensionless];
$q_i$	is the secondary heat transfer factor of the glazing towards the inside [dimensionless];
$g_t$	is the total solar transmittance of glazing and solar protection device [dimensionless];
$\tau_{e,B}$	is the solar transmittance of the solar protection device [dimensionless];
$\alpha_{e,B}$	is the solar absorptance of the solar protection device [dimensionless];
$G_1$	5 W/(m <sup>2</sup> K);
$G_2$	10 W/(m <sup>2</sup> K);
$\rho_{e,B}$	is the solar reflectance of the side of the solar protection device facing the incident radiation [dimensionless];
$U_g$	is the thermal transmittance of glazing [W/(m <sup>2</sup> K)];
$\tau_{e,t}$	is the total solar transmittance of glazing and solar shading [dimensionless];
$\rho_e$	is the solar direct reflectance of the side of the glazing facing the incident radiation [dimensionless];
$\rho'_e$	is the solar direct reflectance of the side of the glazing facing away from the incident radiation [dimensionless];
$\rho'_{e,B}$	is the solar reflectance of the side of the solar protection device facing away from the incident radiation [dimensionless];
$\tau_{S,D}$	is the direct solar transmittance of the blind system [dimensionless];
$\rho_{S,D}$	is the direct solar reflectance of the blind system to the exterior [dimensionless];
$\phi_{ij}$	is the view factor from zone $i$ to zone $j$ [dimensionless];
$\tau$	is the transmittance of the blind material [dimensionless];
$\rho$	is the reflectance of the blind material on the side of blind facing the incident radiation [dimensionless];
$\rho'$	is the reflectance of the blind material on the side of blind facing away from the incident radiation [dimensionless];
$\tau_{S,d}$	is the diffuse solar transmittance of the blind system [dimensionless];
$\rho_{S,d}$	is the diffuse solar reflectance of the blind system to the exterior [dimensionless];
$H$	is the distance between the slats of the blind [mm];
$W$	is the width of the slats of the blind [mm];
$\alpha$	is the solar altitude angle [°];
$\beta$	is the tilt angle of the slats of the blind [°];
$E_v$	is the illuminance level on the chosen point with the glazing façade [Lux];
$E_{v-s}$	is the illuminance level on the chosen point with the façade of glazing and solar shading [Lux];

$\phi_D$	is the direct solar radiation on the south vertical façade [W];
$\phi_d$	is the diffuse solar radiation on the south vertical façade [W];
$\phi_R$	is the reflected solar radiation on the south vertical façade [W];
$K_D$	is the luminous efficacy of direct radiation [lumen/W];
$K_d$	is the luminous efficacy of diffuse radiation [lumen/W];
$\tau_d$	is the diffuse solar transmittance of the glazing [dimensionless];
$SF_1$	is the solar light factor for direct sunlight (direct light) [dimensionless];
$SF_2$	is the solar light factor for diffuse sky light (diffuse light from the firmament) [dimensionless];
$SF_3$	is the solar light factor for reflected light [dimensionless];
$SF_4$	is the solar light factor for the window when fitted with shading [dimensionless];
$\tau_{e,t-D}$	is the direct solar transmittance of the façade with glazing and solar shading [dimensionless];
$\tau_{e,t-d}$	is the diffuse solar transmittance of the façade with glazing and solar shading [dimensionless];
$\phi_{int}$	is the heat flow rate from internal [W];
$\phi_{sol}$	is the heat flow rate from the solar heat sources [W];
$\theta_m$	is the temperature of the mass [°C];
$\theta_s$	is the temperature of the internal surface [°C];
$\theta_{air}$	is the temperature of the indoor air [°C];

### References

- Selkowitz SE. Integrating advanced facades into high performance buildings; 2001.
- Selkowitz SE, Aschehoug O, Lee ES. Advanced interactive facades-critical elements for future Green buildings?; 2003.
- Wienold J. Dynamic simulation of blind control strategies for visual comfort and energy balance analysis; 2007. pp. 1197–204.
- Gomes MG, Santos AJ, Rodrigues AM. Solar and visible optical properties of glazing systems with venetian blinds: numerical, experimental and blind control study. *Build Environ* 2014;71:47–59.
- Karlsson J, Roos A. Modelling the angular behaviour of the total solar energy transmittance of windows. *Sol Energy* 2000;69:321–9.
- Kuhn TE. Solar control: a general evaluation method for facades with venetian blinds or other solar control systems. *Energy Build* 2006;38:648–60.
- EN. 13363-1. Solar protection devices combined with glazing-calculation of solar and light transmittance-Part 1: simplified method; 2007.
- EN. 13363-2. Solar protection devices combined with glazing-calculation of total solar energy transmittance and light transmittance-Part2: detailed calculation method; 2005.
- Petersen S, Svendsen S. Method and simulation program informed decisions in the early stages of building design. *Energy Build* 2010;42:1113–9.
- Nielsen TR. Simple tool to evaluate energy demand and indoor environment in the early stages of building design. *Sol Energy* 2005;78:73–83.
- Wong J, Li H. Development of a conceptual model for the selection of intelligent building systems. *Build Environ* 2006;41:1106–23.
- Liu M, Wittchen KB, Heiselberg P, Winther FV. Development of simplified and dynamic model for double glazing unit validated with full-scale facade element. *PLEA*; 2012. Lima Peru-Opportunities, Limits & Needs.
- Liu M, Wittchen KB, Heiselberg PK, Winther FV. Development of a simplified and dynamic method for double glazing façade with night insulation and validated by full-scale façade element. *Energy Build* 2013;58:163–71.
- Liu M, Wittchen KB, Heiselberg PK, Winther FV. Development and sensitivity study of a simplified and dynamic method for double glazing facade and verified by a full-scale facade element. *Energy Build* 2014;68:432–43.
- Li DH. A review of daylight illuminance determinations and energy implications. *Appl Energy* 2010;87:2109–18.
- Wittchen KB, Johnsen K, Grau K. BSIM user's guide. Hørsholm, Denmark: Danish Building Research Institute; 2005.
- DOE U. EnergyPlus. Input output reference: the encyclopedic reference to EnergyPlus input and output. USA: Department of Energy; 2010.
- ISO EN. 13790. Energy performance of buildings—calculation of energy use for space heating and cooling (EN ISO 13790: 2008). Brussels: European Committee for Standardization (CEN); 2008.
- Montgomery DC. Design and analysis of experiments. John Wiley & Sons; 2008.
- CEN EN. 410. Glass in building—determination of luminous and solar characteristics of glazing; 1998. Bruxelles.



# Verification of a simplified method for intelligent glazed façade design under different control strategies in a full-scale façade test facility – Preliminary results of a south facing single zone experiment for a limited summer period



Mingzhe Liu <sup>a, \*</sup>, Kim Bjarne Wittchen <sup>a</sup>, Per Kvols Heiselberg <sup>b</sup>

<sup>a</sup> Danish Building Research Institute (SBI), Aalborg University, A.C. Meyers Vænge 15, 2450 København SV, Denmark

<sup>b</sup> Department of Civil Engineering, Aalborg University, Sohngaardsholmsvej 57, 9000 Aalborg, Denmark

## ARTICLE INFO

### Article history:

Received 16 June 2014

Received in revised form

9 September 2014

Accepted 13 September 2014

Available online 19 September 2014

### Keywords:

Simplified method

Intelligent façade

Night shutter

Venetian blind

Natural ventilation

Façade control

## ABSTRACT

The research aims to verify a simplified calculation method for intelligent glazed facade under different control strategies (night shutter, solar shading and natural ventilation). The method is developed to simulate the energy performance and indoor environment of an office room installed with intelligent facades. The calculation results of heating and cooling needs are verified by experimental data collected in a full-scale test facility (Cube) with south-facing façade at Aalborg University (DK) during summer period from 18th to 22nd June 2014. According to the results of the comparison, the calculated air temperature has good agreements with the measurements, with the  $R^2$  value of 0.8. Additionally, the total cooling energy consumptions measured in the experiment are 30% lower than the calculated. The experiment was conducted in the test facility with only south-facing façade and during a short summer period, which limits the verification of the method.

When using water system in the chilled beam to cool down test room, it needs to be noticed that the forward water temperature should be controlled not to be higher than the air temperature of the test room when there is no cooling need in the test room; otherwise the chilled beam will release heating to the test room, which could influence the accuracy of the result.

National Instrument (NI) CompactRIO is used to acquire measured data from different sensors and send signal to control building services like ventilation, heating, cooling and artificial lighting. The whole process is realized with the help of Labview.

© 2014 Elsevier Ltd. All rights reserved.

## 1. Introduction

Given highly glazed facades are more and more popular in modern buildings, solar heat load and light transmittance through facades in summer and the heat transmittance through them in winter are of great importance to the energy consumption and indoor environment of high performance buildings. To decrease the energy demand and improve the indoor comfort of buildings, intelligent façades with controlled façade elements is one of the effective solutions [1,2]. Appropriate control of all these technologies (night shutter, solar shading and natural ventilation, etc.) can greatly reduce the heating and cooling load and optimizes the

visual and thermal comfort in a building. A simplified method has been developed to compare energy performance of different control strategies and optimize the entire system in the early stage of building design [3–6]. Comparisons have been conducted between the simplified method and Danish Building Simulation Tool BSim [7,8]. However, its accuracy still needs to be evaluated by experimental measurements in full scale test facility.

Experiments have been conducted to verify parts of the simplified method like methods for double glazing and glazing with insulated shutter [3–5]. Other parts (method for blind, etc.) and the holistic system of the method also need to be verified by experimental measurements. Experiments have been conducted by researchers to evaluate methods or performance of different façade elements (blind and shutter, etc.) [9–20]. Advantages of setup and method in these experiments have been studied to be made use of

\* Corresponding author. Tel.: +45 99407234.

E-mail address: [ml@civil.aau.dk](mailto:ml@civil.aau.dk) (M. Liu).

in this experiment. The room model in the simplified method is developed according to EN 13790 [21], of which the general criteria and validation procedures are shown in EN 15265 [22]. Previous experiments have been implemented in the same facility to investigate performance of different building elements [23,24].

The experiment test is designed and implemented specifically for evaluating the accuracy of the simplified method, which is necessary for future application of the method on predicting the energy and comfort performance of intelligent facades of different control strategies.

The purpose of this study is to verify the accuracy of the simplified methodology by comparing its calculation results with experimental measurements. The paper describes the full-scale test facility used for the experiment in Aalborg University (Cube) [23,24]. The setup, instruments, procedure and the results of the experiment are also demonstrated in the paper.

## 2. Description and research method

The simplified method of intelligent glazed façade is developed to calculate the energy and comfort performance of buildings with intelligent façade controlling insulated shutter, venetian blind, natural ventilation and night cooling. Energy consumption (heating, cooling, lighting and ventilation) and indoor operative temperature are calculated by the method under different control strategies. The façade part of the method is developed to be integrated into BSim and BE10 to fulfil their functions of simulating different control strategies, but the entire method can also work independently. Capability of hourly calculation of an office room in the whole reference year and flexibility of modelling new control strategies make the method a great advantage in the design and certification of buildings with intelligent façade. It is named simplified method because of its simple one zone room model according to the simple hourly model in EN ISO 13790, which has only one control point for thermal mass, surface and indoor air each. Therefore, the calculation of the indoor air and thermal mass is homogenous, but this limitation can be improved when integrating the façade part of the method into BSim or BE10. The method has been described and presented in Refs. [3–6]. The experimental verification of the method is presented in this paper.

Fig. 1 shows the structure of the simplified method. The core part of the method is the algorithms of façade elements (red dish

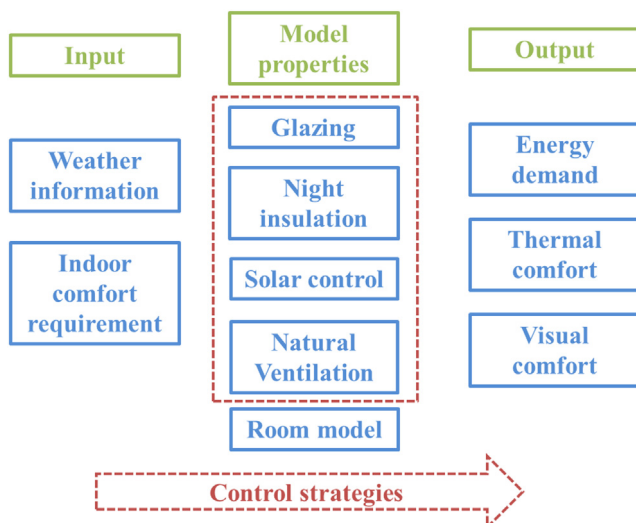


Fig. 1. Structure of the simplified method.

frame), which contains algorithms of different façade elements: double glazing unit (triple glazing unit), insulated shutter, solar shading (venetian blind), natural ventilation and night cooling. By setting the input of weather data and indoor comfort requirements, the parameters of energy demand, thermal comfort and visual comfort will be calculated. The method is flexible to evaluate different control strategies.

The simplified method is compared with Danish building simulation tool BSim on calculating the yearly energy consumption (heating, cooling, lighting and ventilation) and indoor environment parameters (indoor air temperature, solar transmittance and daylight level on the reference point) under different control strategies that exist in BSim. According to all the comparisons (Fig. 2), difference of energy calculation between the two methods is below 10%.

Fig. 3 presents the calculated results by the simplified method for indoor air temperature under the four control conditions as a function of the corresponding results calculated by BSim. The result shows that, under the condition of façade with different control, the calculated results of the simplified method have acceptable agreement with that of BSim software in terms of the indoor air temperature, with the average value of  $R^2$  at 0.92.

The purpose of this study is to evaluate the accuracy of the simplified method in terms of calculating the energy and comfort parameters of the test room. The verification of the simplified method is implemented by the measurements performed in the test facility “The Cube” at Aalborg University. The indoor air temperatures and heating and cooling loads were measured during a summer period at the end of June 2014 (18th–22nd), and the calculations by the simplified method are conducted through all the time the measurements were implemented.

## 3. Experiment setup

The measurements are implemented in the full-scale test facility (The Cube at Aalborg University [23,24]) (Fig. 4) consisting of one south-facing test room with the internal dimension of  $2.76 \times 2.7 \times 3.65 \text{ m}^3$  (H × W × D). The glazed facade system faces south and has a dimension of  $2.76 \times 1.6 \text{ m}^2$ . All the enclosures of the test room except the south façade are surrounded by a guarded zone to minimize heat transfer through the enclosures. The entire heat capacity of the test room is 1700,000 J/K (47 Wh/Km<sup>2</sup>).

The glazing type used in the experiments is a double glazing unit with a 22 mm argon-filled cavity and low-E coating on the internal pane. The air-tightness between the test room and outdoor has been tested by performing a blower door test, both in over- and under-pressure. The infiltration rate has been measured and is

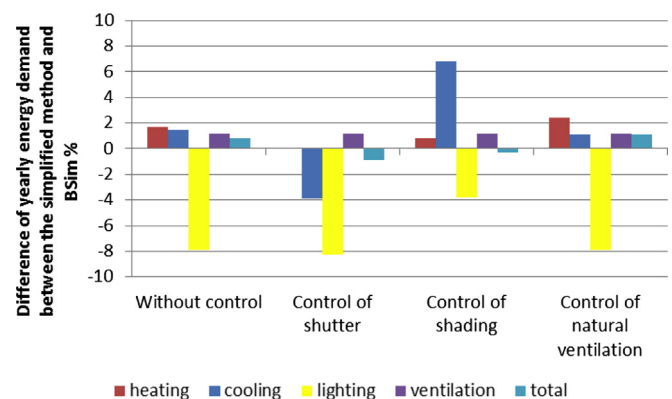


Fig. 2. Difference of energy demand on the four control conditions between the two methods.

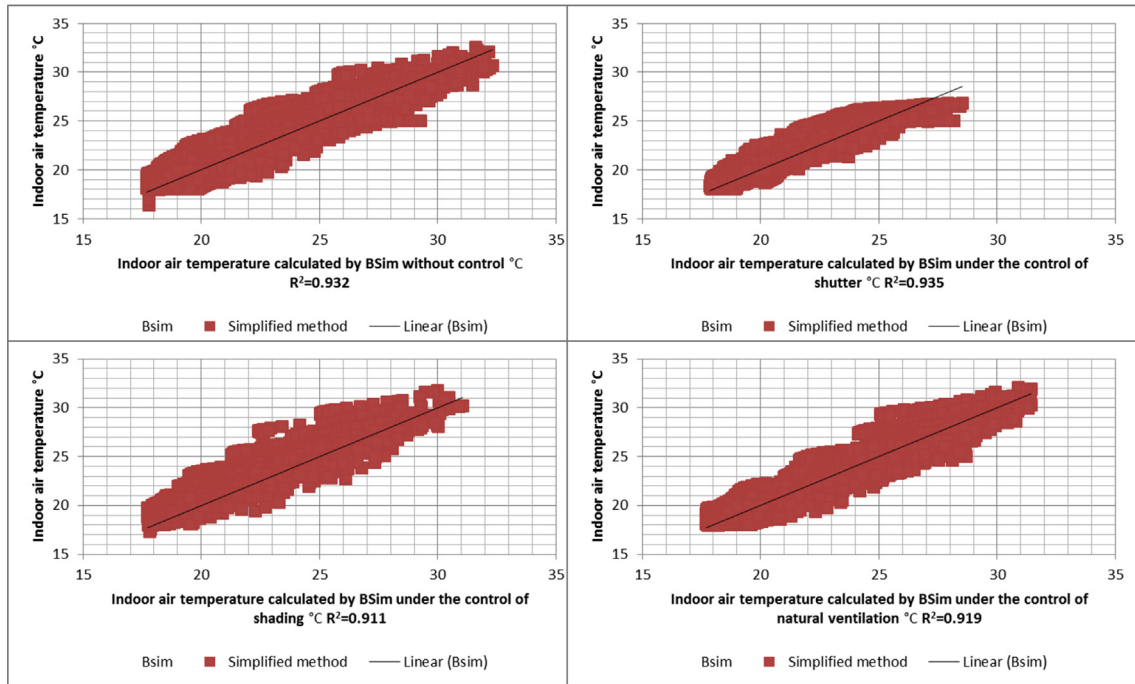


Fig. 3. Comparison on the parameter of indoor air temperature between the two methods under the four controlled condition.

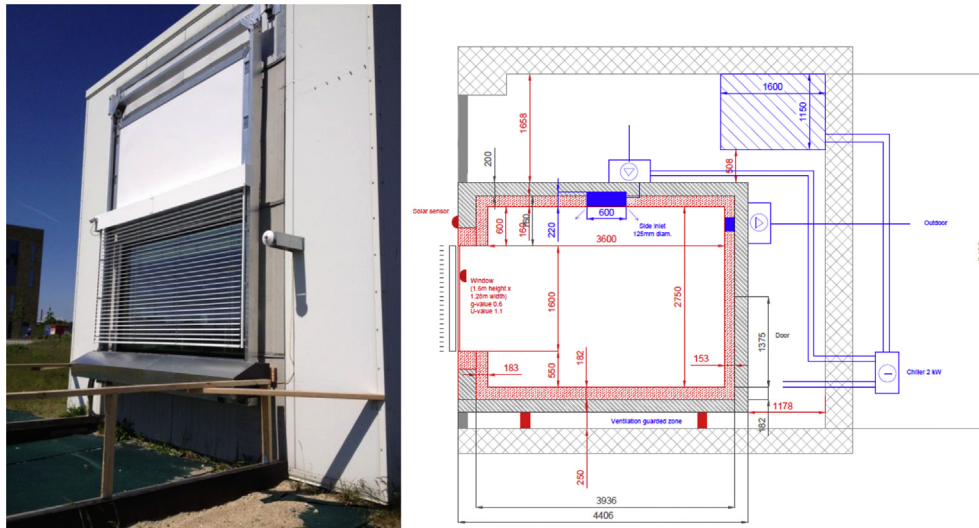


Fig. 4. Full-scale test facility in Aalborg University-Cube. (Left: test facility, Right: section).

below 0.3 L/s.m<sup>2</sup>floor at 50 Pa. The layout of the double glazing unit is shown in Table 1. The measurements of the indoor air temperature of the test room are conducted in the end June 2014 (18th–22nd).

The surrounding internal surfaces of the room are built up of 15 mm plywood and are painted white, apart from the floor, which

is made of 150 mm concrete. The heat loss due to infiltration is minimized to 0.09 l/s per square metre at average by sealing all joints with silicon.

Fig. 5 shows the setup of the entire system to collect measured data from different sensors and to control different elements and devices. All the instruments can be integrated and controlled

Table 1  
Layout and material of the double glazing façade.

Element	Thickness (mm)	$\lambda$ (W/m.K)	$\rho$ (kg/m <sup>3</sup> )	$C_p$ (J/kg.K)	$\epsilon_1$ LW (-)	$\epsilon_2$ LW (-)
Outer pane	5.9 ± 0.1	1.0 ± 0.1	2300 ± 10	840 ± 50	0.84 ± 0.05	0.03 ± 0.01
Cavity	12.0 ± 1.0	0.017 ± 0.005	1.64 ± 0.10	522 ± 30	–	–
Inner pane	5.9 ± 0.1	1.0 ± 0.1	2300 ± 10	840 ± 50	0.84 ± 0.05	0.84 ± 0.05

together according to different measurements. The system is flexible and visible to implement different control strategies by ourselves.

### 3.1. Measurements

Table 2 shows the parameters that are measured by different sensors to be used to calculate the heating and cooling energy needs. All the measured data are averaged every 10 min.

To measure the air temperature in the room, five columns of thermocouples have been installed in the test room: one in the middle and one in the centre of each wall (60 cm away from the south and north wall, and 25 cm away from the west and east wall). Temperatures are measured using thermocouples type K, which are calibrated with a reference thermocouple [24,25]. The thermocouples measure the air temperature at 0.1, 0.6, 1.1, 1.7 and 2.65 m high with an accuracy of  $\pm 0.1$  K. In order to decrease the influence of radiation on the measurement of air temperature, the thermocouples are silver-coated and protected by a mechanically ventilated silver shield.

Irradiance is measured using two CM21-pyranometers and one CM22-pyranometer. CM22 is placed on the top of the cube to measure the global irradiance on a horizontal surface. CM21 pyranometers are placed inside and outside the glazing, measuring irradiance on the vertical surface both on the external façade and into the test room.

The measurement of the air flow through the ventilation system is performed using an orifice plate located before the inlet (accuracy of the air change rate:  $\pm 7.5\%$ ).

**Table 2**  
Measurements of the parameters used in the simplified method.

Description	Measurements from sensors
Internal heat load (manikin + artificial lighting)	Power meters of manikin and artificial lighting
Solar heat gain into the room	Pyranometer inside CM21
Air flow rate	Orifice plate
Inlet air temperature	Thermocouple (inlet position)
Outdoor air temperature	Thermocouple (outdoor)
Heating or cooling load (+Heating; -Cooling)	Heating: Power meter; Cooling: Water temperature sensor and flow meter

The cooling released by the active chilled beam is measured by a combination of flow meters and temperature sensors. Cooling load of the active chilled beam can be calculated according to the water flow rate and the temperature difference between the forward and return water flow. The accuracy of the measurement has been estimated to  $\pm 0.9$  L/h for the flow meters and  $\pm 0.057$  K for the Pt-500 sensors.

The heats released from the manikin, the artificial lighting and the electrical heater are measured by power meters to be used in the calculation and validation as the internal load from people, lighting and heating load.

### 3.2. Control of building services

A blind is used to prevent glare problems during the occupied hours and to reduce the solar transmittance through the façade during the unoccupied hours. The tilt angle of the blind depends on

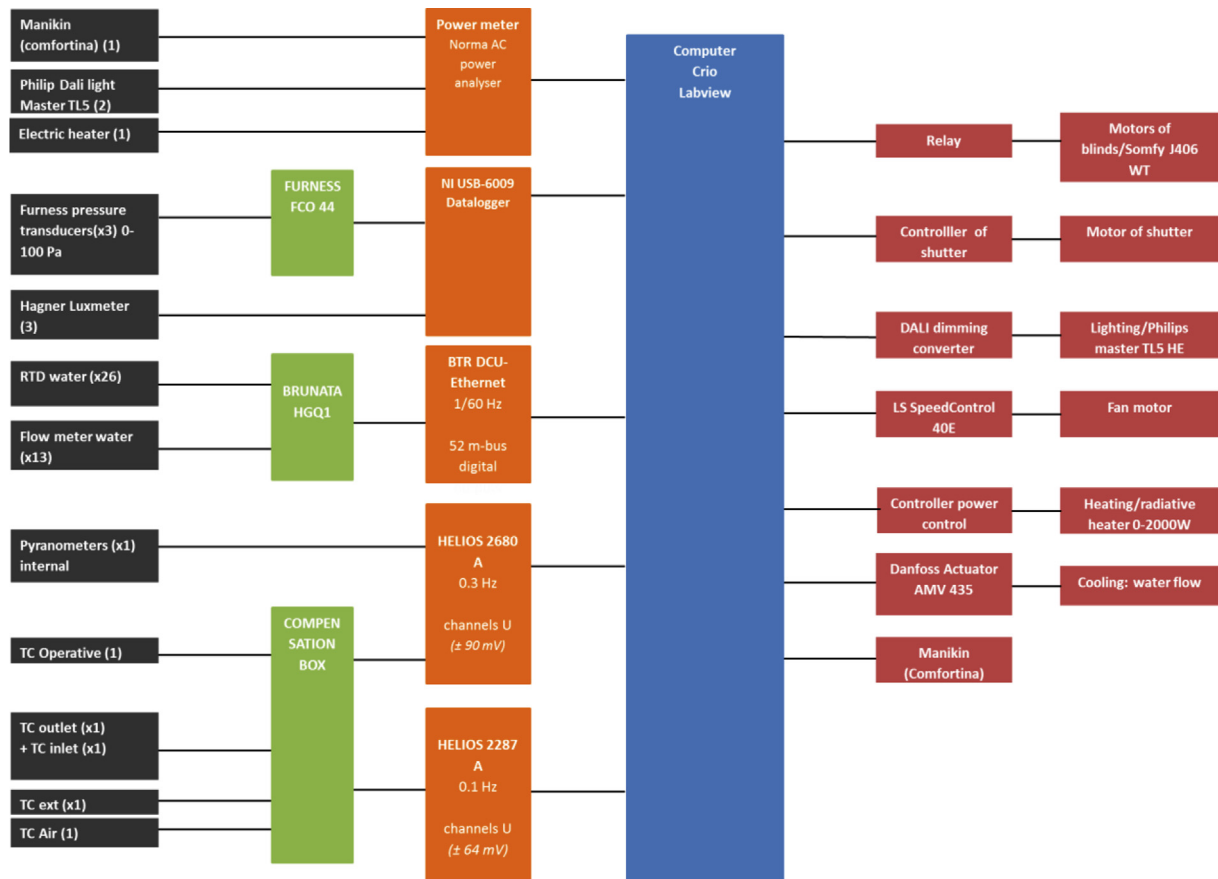


Fig. 5. Experiment setup and structure of the connection of measurement instruments and control devices.



its functions. The tilt angle of the blind during occupied hours is calculated by Equation (1) from previous research [6] to cut the direct solar radiation, which both improve the visual comfort and maximize the daylight transmittance into the room.

$$\beta = \arccos \left[ \frac{\frac{H}{W} \times \tan \alpha + \sqrt{\tan^2 \alpha - \left(\frac{H}{W}\right)^2 + 1}}{\tan^2 \alpha + 1} \right] \quad (1)$$

Where  $\beta$  is the angle between the slat and the horizontal plan.  $\alpha$  is the solar altitude angle.  $H$  is the distance between the slats.  $W$  is the width of the slats.

During unoccupied hours, the blind is controlled to be closed if the indoor air temperature is above 24 °C. The blind is scrolled up if it is not set at cut-off angle or closed position.

The glazed façade is open when the indoor temperature exceeds 23 °C. The control is active only when the outdoor temperature is lower than the indoor temperature and the outdoor temperature is above 12 °C, preventing cold draft in the room. In the real situation, the natural ventilation rate is calculated according to wind speed, wind direction, temperature difference between indoor and outdoor and some other parameters. The calculation is not focus in this paper. The ventilation rate is assumed to be 2 l/s per m<sup>2</sup>, which is equal to around 2.6 air change rate per hour (ACH) assuming the height of the room is 2.7m [26].

The night cooling control is active during unoccupied hours in terms of opening the window if the average outdoor air temperature between 12:00 and 17:00 is above 21 °C and the indoor air temperature is higher than the outdoor air temperature. The control of night cooling can precool the room and help to balance the cooling peak during the day time. In order not to overcool the room so that the indoor air temperature in the morning is too low, the night cooling is inactivated when the indoor air temperature is below 14 °C. However, it is reactivated when the indoor air temperature comes back to 17 °C.

In order to exactly know the cooling amount from the control of natural ventilation and night cooling, they are not activated by importing air from outside but by chilled beam. When the natural ventilation or night cooling is needed, the amount of cooling load caused by them is calculated according to the assumed air flow rate and the temperature difference between indoor and outdoor and outputted by controlling the chilled beam. Therefore, the total cooling power measured is the sum of natural cooling (natural ventilation or night cooling) and mechanical cooling.

Heating and cooling installations are controlled to secure the set-point temperature in the office space. The heating and cooling needs for the office room in every time step (hour) can be calculated by the simplified model according to hourly heat gain and heat lost. The set points for heating and cooling are 20 °C and 25 °C, respectively. Detailed equations for calculating the heating and cooling needs are shown in the EN 13790 [21] and in a previous paper [6]. Artificial lighting of the office building has on-off control during occupied hours according to the illuminance level at the reference point mentioned before. The lighting control is included in all the cases. The set point of the lighting is 300 Lux. The calculation of the illuminance level at the reference point is described in a previous paper [6].

The room is heated by a maximum 2 kW electrical convective heating system controlled to heat the air to keep the air temperature stable. Output of the heating power is calculated by the simplified method and realized by PI control from computer and Compact RIO. There are other internal heat sources like artificial lighting and manikin in the room.

The test room is cooled down using the active chilled beam with the efficiency of 0.85. The unit is located in the middle of the ceiling and has dimensions of 0.6 × 0.6 m. The cooling is controlled using Danfoss AME435 actuator. The achieved indoor air temperature is between 20 °C and 25 °C.

The fresh air is provided from the guarded zone through the same unit as the active chilled beam. When the cooling is performed by the active chilled beam, the inlet consequently has two functions (cooling and ventilation inlet). The air change rate can vary between 1 up to 4 ACH controlled according to the speed of the fan. A circular outlet is located at the top of the north wall (diameter 125 mm). The extraction rate of the outlet is controlled so that there is no over- or under-pressure between the guarded zone and the experimental room.

In order to simulate an office worker, a thermal manikin has been placed closed to the south wall, on an open chair. The manikin is made of a fibreglass shell covered with 0.3 mm diameter nickel wires, which are sequentially used to heat the manikin (accuracy on the heat flow ± 1%) and to measure and control the skin temperature (accuracy ± 0.2 K). The thermal manikin corresponds to a 1.7 m tall woman and is divided into 17 parts, which can be controlled and measured individually (Comfortina [23]).

#### 4. Result

Fig. 6 shows measured weather data and internal loads (upper two charts) and comparison between the measured and calculated indoor air temperature, heating and cooling powers (bottom two charts) during the experiment period, where the positive value means heating and negative value means cooling. The calculated results of cooling power generally have the same tendency as the measurements but with some fluctuations. However, the simplified method overestimates the cooling power compared with the measurements during some periods. The reason of this is the disagreement between the calculated and measured indoor air temperature around 23 °C, which causes the overestimation of cooling by activation of natural ventilation in the calculation shown in Fig. 6. The calculated indoor air temperature reduces simultaneously as the overestimation of the cooling power, which reasonably results from the activation of natural ventilation.

The difference between the calculated and measured cooling load is also caused by the slow reaction of the system. Fig. 6 shows the calculated cooling load by the simplified method (red line), the measured cooling load in the experiment (blue line) and the requested cooling load which is calculated during the experiment by the control system to be released to the room (green line). It shows that in some period the measured cooling load cannot reach the amount by the calculation of the control system before the requested cooling output drops down, which results in the overestimation of cooling load and the total cooling consumption by the simplified method.

The accuracy of the model is validated through the  $R^2$ -value [27]. This value indicates the comparison between the measured and the calculated results at each time step and evaluates the level of accuracy of the method. The  $R^2$  value is not only a measure of how well the pattern of the model follows the pattern of the measurements, but also a measure of accuracy determining the error at each time step.

Equations (2)–(4) show the calculation of the  $R^2$  value. Where  $y_i$  is the measured value;  $f_i$  is the calculated value;  $\bar{y}$  is the mean of the measured value.

$$R^2 = 1 - \frac{SS_{err}}{SS_{tot}} \quad (2)$$

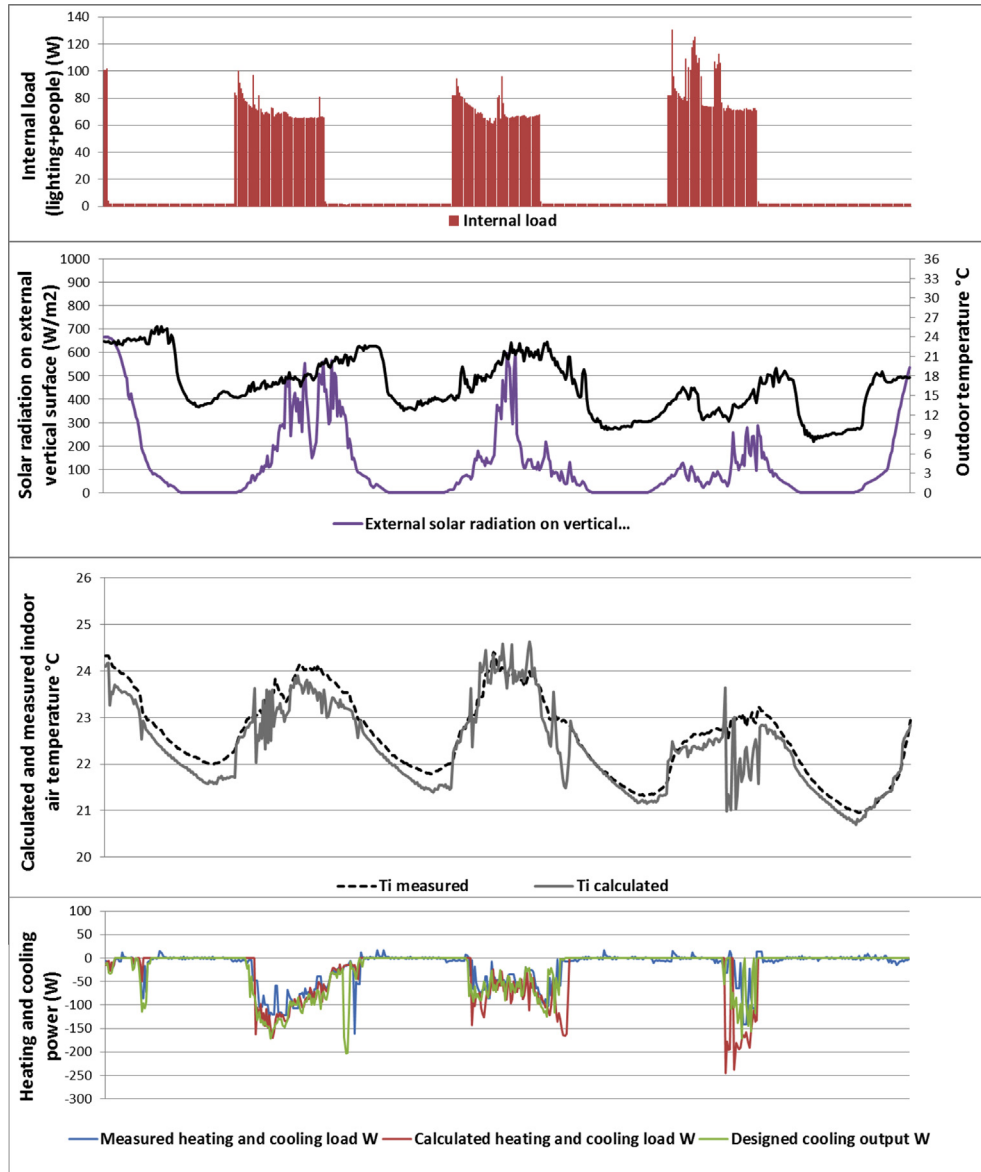


Fig. 6. Experiment results.

$$SS_{err} = \sum_i^n (y_i - f_i)^2 \quad (3)$$

$$SS_{tot} = \sum_i^n (y_i - \bar{y})^2 \quad (4)$$

Fig. 7 shows the linear regression of the calculation results of heating, cooling power and indoor air temperature by the simplified method. According to the figure, the comparison between the calculation results and the measurements is expressed with  $R^2$  value, which is 0.34 and 0.8 for energy power and air temperature, respectively.

Apart from this, the disagreement could be resulted from different reasons. The calculation is conducted assuming homogeneous thermal mass in the test room, but the real situation is that half of the thermal mass is contributed by the tiles lying on the floor. The efficiency of the chilled beam and the difference between the calculation and measurement on the solar transmittance could also influence the calculation of the heat balance. The shield factor

of the façade caused by the external frame holding the blind and insulation could also influence the calculation of the solar heat gain. The disagreement can also be caused by the uncertainty of the measurements.

Fig. 8 shows the comparisons between the measured and calculated total energy consumptions of heating and cooling in the test room during the entire experimental period. The cooling energy consumption measured in the experiment is 30% lower than the calculated by the simplified method, while the requested cooling output is 20% lower than the calculated. There is tiny amount of heating consumption in the experiment due to the temperature difference between water temperature in the chilled beam and air temperature in the room. Its effect has been decreased to the minimum.

### 5. Conclusion and future work

A new simplified calculation method has been developed to predict the energy and comfort performance of intelligent glazed facades with different control strategies. It can make whole year

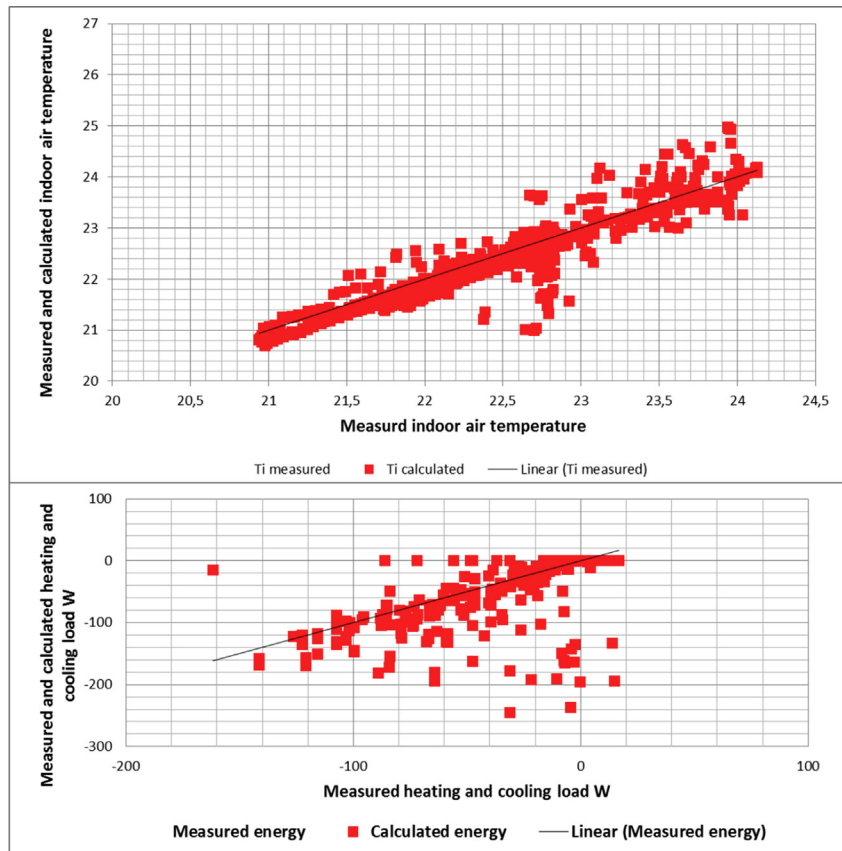


Fig. 7. Comparison between measured and calculated heating and cooling power and indoor air temperature.

simulation at different time steps. According to the results of the comparison, the calculated air temperature has good agreements with the measurements in Danish climate, with the  $R^2$  value of 0.8. Additionally, the total cooling energy consumption measured in the experiment is 30% lower than the calculated by the simplified method.

The experiment method and setup is advanced enough to be implemented in complex experiments that require the integration of different measurement instruments and building services into a holistic system, especially when the measured data is needed to control other devices.

However, there are some limitations in the method and the experiment. The verification can only present the accuracy of the

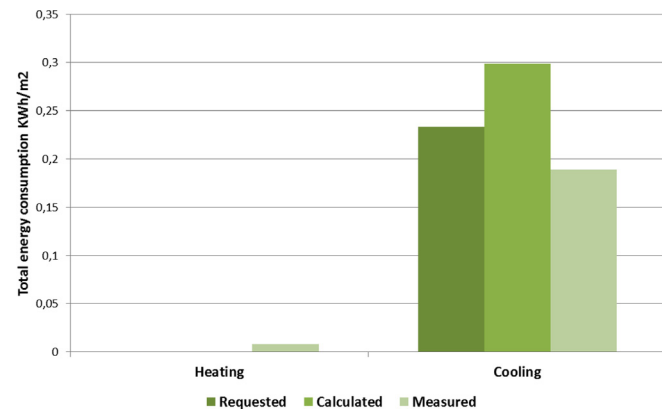


Fig. 8. Comparison between the calculated and measured energy consumptions during the experiment period.

method in one zone building. More work need to be done for multi zone buildings to evaluate the influences of heat and mass transfer between different zones. The accuracy of verification of the method is limited because of the homogenous room model. Additionally, the test facility is categorised as light building, which could limit the verification of the method. More work need to be done in buildings with different levels of heat capacity. The façade of the test facility faces south, more tests on other orientation need to be done. The test was conducted in a short summer period, which limits the verification on the yearly energy calculation and accuracy of the method in other seasons.

Additionally, the user needs to be careful when using water system in the chilled beam to cool down test room. The forward water temperature should be controlled not to be higher than the air temperature of the test room when there is no cooling need in the test room, otherwise the chilled beam will release heating to the test room, which could influence the accuracy of the result.

## Acknowledgements

This paper is based on research conducted in a PhD project supervised by Senior Researcher Kim Wittchen, Danish Building Research Institute (SBI) and Professor Per Heiselberg, Department of Civil engineering both at Aalborg University, Denmark. The PhD is part of the Strategic Research Centre for Zero Energy Buildings at Aalborg University and financed by the Danish aluminium section of The Danish Construction Association, Aalborg University and The Danish Council for Strategic Research, under the Programme Commission for Sustainable Energy and Environment.

## References

- [1] Selkowitz SE. Integrating advanced facades into high performance buildings. 2001.
- [2] Selkowitz SE, Aschehoug O, Lee ES. Advanced interactive facades-critical elements for future green buildings?. 2003.
- [3] Liu M, Wittchen KB, Heiselberg P, Winther FV. Development of simplified and dynamic model for double glazing unit validated with full-scale facade element. PLEA. Lima Peru-Opportunities, Limits & Needs; 2012.
- [4] Liu M, Wittchen KB, Heiselberg PK, Winther FV. Development of a simplified and dynamic method for double glazing facade with night insulation and validated by full-scale facade element. Energy Build 2013;58:163–71.
- [5] Liu M, Wittchen KB, Heiselberg PK, Winther FV. Development and sensitivity study of a simplified and dynamic method for double glazing facade and verified by a full-scale facade element. Energy Build 2014;68:432–43.
- [6] Liu M, Wittchen KB, Heiselberg PK. Development of a simplified method for intelligent glazed facade design under different control strategies and verified by building simulation tool BSim. Build Environ 2014;74:31–8.
- [7] Wittchen KB, Johnsen K, Grau K. BSim – user's guide. Hørsholm, Denmark: Danish Building Research Institute, Aalborg University; 2000–2011.
- [8] Aggerholm S, Grau K. Bygningers energibehov- SBI-anvisning 213. Hørsholm, Denmark: Building Research Institute, Aalborg University; 2008.
- [9] Gomes MG, Santos AJ, Rodrigues AM. Solar and visible optical properties of glazing systems with venetian blinds: numerical, experimental and blind control study. Build Environ 2014;71:47–59.
- [10] Petersen S, Svendsen S. Method and simulation program informed decisions in the early stages of building design. Energy Build 2010;42:1113–9.
- [11] Nielsen TR. Simple tool to evaluate energy demand and indoor environment in the early stages of building design. Sol Energy 2005;78:73–83.
- [12] Wong J, Li H. Development of a conceptual model for the selection of intelligent building systems. Build Environ 2006;41:1106–23.
- [13] Schult JM. Isolerende Skodder [Insulating shutters]. in Danish with a summary in English. Report no. 202. Technical University of Denmark, Thermal Insulation Laboratory; 1990.
- [14] Winter J. Practical assessment of window shutters for night insulation and solar shading for domestic buildings, New Zealand.
- [15] Nicol K. The thermal effectiveness of various types of window coverings. Energy Build 1986;9:231–7.
- [16] Zaheer-Uddin M. Dynamic effects of thermal shutters. Build Environ 1990;25:33–5.
- [17] Saelens D. Energy performance assessment of multiple-skin facades [Ph.D. dissertation]. Leuven: Laboratory for Building Physics, K.U. Leuven; 2002.
- [18] Pal S, Roy B, Neogi S. Heat transfer modelling on windows and glazing under the exposure of solar radiation. Energy Build 2009;41:654–61.
- [19] Noh-Pat F, Xamán J, Álvarez G, Chávez Y, Arce J. Thermal analysis for a double glazing unit with and without a solar control film (SnS–CuS) for using in hot climates. Energy Build 2011;43:704–12.
- [20] Breitenbach J, Lart S, LaËngle I, Rosenfel JIJ. Optical and thermal performance of glazing with integral venetian blind. Energy Build 2001;33:433–42.
- [21] ISO EN. 13790. Energy performance of buildings–calculation of energy use for space heating and cooling (EN ISO 13790: 2008). Brussels: European Committee for Standardization (CEN); 2008.
- [22] EN 15265. Energy performance of buildings- calculation of energy needs for space heating and cooling using dynamic methods-General criteria and validation procedures. 2007. Brussels.
- [23] Jérôme LD. Energy flow and thermal comfort in buildings/comparison of radiant and air-based heating & cooling systems [PhD thes. 2013. is], Aalborg.
- [24] Kalyanova O, Heiselberg P. Experimental set-up and full-scale measurements in “The Cube”. DCE, Technical Reports, nr. 034. Aalborg: Aalborg University, Department of Civil Engineering; 2008.
- [25] Artmann N, Vonbank R, Jensen RL. Temperature measurements using type K thermocouples and the Fluke Helios Plus 2287A Datalogger. DCE Technical Reports, nr. 52. Aalborg: Aalborg University, Department of Civil Engineering; 2008.
- [26] Larsen TS, Heiselberg PK. Single-sided natural ventilation driven by wind pressure and temperature difference. Energy Build 2008;40:1031–40.
- [27] Montgomery DC. Design and analysis of experiments. 7th ed. Hoboken, N.J.: John Wiley & Sons; 2009.

1 **Control strategies for intelligent glazed façade and their**  
2 **influence on energy and comfort performance of office buildings**  
3 **in Denmark**

4  
5 Mingzhe Liu<sup>a,\*</sup>, Kim Bjarne Wittchen<sup>a</sup>, Per Kvols Heiselberg<sup>b</sup>

6 <sup>a</sup> Danish Building Research Institute (SBI), Aalborg University, A.C. Meyers Vænge 15, 2450  
7 København SV, Denmark

8 <sup>b</sup> Department of Civil Engineering, Aalborg University, Sohngaardsholmsvej 57, 9000 Aalborg,  
9 Denmark

10 \* Corresponding author. Tel.: +45 99407234.

11 E-mail address: [ml@civil.aau.dk](mailto:ml@civil.aau.dk).

12 Abstract

13 The research aims to develop control strategies for intelligent glazed façades and investigate the  
14 influence of different control strategies on energy and comfort performance of office buildings. The  
15 intelligent glazed façade is capable of controlling the thermal transmittance, solar transmittance and  
16 mass transmittance by controlling shutters, blinds and openings. The façade and building services are  
17 designed and controlled holistically to optimize the indoor comfort (thermal, visual comfort and indoor  
18 air quality) and minimize the energy demand by heating, cooling, lighting and ventilation. The study is  
19 conducted numerically with the help of a simplified hourly calculation method developed to calculate  
20 yearly energy and comfort performance of the office room with the intelligent façade. The simplified  
21 method is verified by both the Danish building simulation tool BSim and experimental test in the full  
22 scale test facility at Aalborg University (Cube).

23 The results show that the yearly primary energy demand of an office building with the intelligent  
24 glazed façade can be reduced by around 60 % compared with the same room without the intelligent  
25 façade. With the help of the intelligent glazed façade, buildings can more easily comply with the future  
26 Danish building class 2020 according to building regulation BR10. The comfort performance of the  
27 building can also be improved by the intelligent glazed façade.

28 **Keywords:** intelligent glazed façade, venetian blind, window shutter, façade control, solar  
29 transmittance, natural ventilation, night cooling, thermal comfort, energy demand

### 30 **1. Introduction**

31 Glazed facades are widely used in modern buildings because of their higher light transmittance and  
32 better outside view for the users. However, their solar and thermal properties also have significant  
33 effects on both the energy consumption and the indoor comfort of buildings. In order to improve the  
34 performance of glazed facades, improve the indoor comfort level and fulfil the future energy  
35 regulation, the intelligent façade or the facades with controls of different technologies are being  
36 investigated and developed. Different characteristics of a façade can be dynamic and controlled  
37 according to both the requirement of the indoor environment and changes of the outdoor weather  
38 conditions.

39 The nature of challenges and possibilities of achieving intelligent facades are discussed in [1-3]. It  
40 is concluded that smarter building operation is necessary to meet the goal of lower energy  
41 consumption and better indoor comfort, and control systems need to integrate strategies that support all  
42 aspects of complex façade functions. Research are conducted to investigate the performance of the  
43 control of solar shading [4-9]. Existing models of control patterns for occupant-shading interactions in  
44 office buildings and their influence in terms of energy demand are reviewed in [10]. Energy  
45 performance and visual comfort are investigated for eleven control strategies. The potential of dynamic  
46 solar shading is quantified in [11] with the simulated results from an investigation of three different  
47 solar shading types. It shows that the annual energy demand can be reduced by 16 % for a south-facing

48 façade using dynamic shading. The difference between static and dynamic control of interior and  
49 exterior blind systems in office buildings is addressed in [12]. It shows that optimal control can  
50 achieve energy savings of 7 %-17 % compared with manual control and without blind control.  
51 Additionally, the energy performance of blind systems can be significantly improved by applying  
52 daylighting control. The impact of glazing area, shading device properties and shading control on  
53 building cooling and lighting energy use in perimeter spaces are evaluated in [13]. It is found that  
54 shading control accounted for a 50 % decrease in annual cooling energy demand compared with the  
55 case without shading. Although electric lighting demand is increased, the total annual energy demand  
56 is still reduced by 12%. The impact of management strategies for external mobile shading and cooling  
57 by natural ventilation is focus in [14]. It is concluded that the control modes have to be carefully  
58 selected with regard to building's characteristics and local weather conditions.

59 A comprehensive analysis is presented in [15, 16] to study the balance between daylighting benefits  
60 and energy requirements (control of solar gains) in perimeter office spaces with interior roller shades  
61 taking into account glazing properties, shading properties and control together with window size,  
62 climate and orientation integrating daylight and thermal needs. It reveals that windows occupying 30-  
63 50 % of the façade can actually result in lower total energy consumption for most cases with  
64 automated shading [15, 16]. It also points out the best designs for each orientation and location based  
65 on both daylighting and thermal results. It is shown in [17] that both cooling energy and fan electrical  
66 energy are saved with the help of well-designed natural ventilation systems compared with mechanical  
67 cooling and ventilation. It is possible to save the cooling energy between 13 and 44kWh/m<sup>2</sup> per year at  
68 Stuttgart, Turin and Istanbul, and additionally savings in fan ventilation electrical energy can be  
69 around 4kWh/m<sup>2</sup> per year.

70 The previous studies focus on the investigation of the controlling of one or more of the façade  
71 elements separately. It is necessary to conduct investigations on a holistic control of both façade

72 system and building services including different technologies. The influence of the control strategies is  
73 evaluated on both the energy consumption and the indoor comfort level.

74 Therefore, the study is performed to develop appropriate and holistic control strategies for the  
75 intelligent glazed façade containing different functions (solar shading, window shutter, natural  
76 ventilation and night cooling) and being integrated with building services (heating, cooling, ventilation  
77 and lighting) to optimize the comfort performance and minimize the energy demand of buildings. The  
78 paper shows the development of the optimized control strategies for intelligent façades and their  
79 improvement on the indoor comfort and energy performance.

## 80 **2. Description and research method**

81 The study is to develop the control strategies for different technologies of intelligent façades. The  
82 control of façades and building services are integrated together and developed for both occupied and  
83 unoccupied hours.

84 The final control strategies are selected after evaluating their influences on the energy and comfort  
85 performance of buildings. The influences of the different control strategies are investigated by a  
86 simplified calculation method [22] assuming being used in an office building. The comfort  
87 performance is evaluated by operative temperature according to the comfort classes given in EN 15251  
88 [18]. The office building was built in Buddinge Denmark in 2013 with a total heated area of around  
89 8000 m<sup>2</sup> and glazing ratio of the entire façade of around 40 %. Figure 1 shows one plan of the  
90 building. The window areas of south, north east and west facades are 514 m<sup>2</sup>, 661 m<sup>2</sup>, 339 m<sup>2</sup> and 376  
91 m<sup>2</sup>, respectively. The glazing type used in the building is a double glazing unit with a 15 mm argon-  
92 filled cavity and low-E coating on the internal pane. The total infiltration rate used in the simplified  
93 method is 0.06 l/(sm<sup>2</sup>). Table 1 shows the input values of the setups and indoor conditions for the  
94 simplified method. Both the heat and cooling loads are assumed to release 100% to the indoor air, and  
95 the indoor illuminance level is measured at the reference point on the working plane (height of 0.85m)



96 which is 1 m from the façade on the centreline of the room. The lighting of the entire room is  
97 controlled by this sensor.

## 98 **Figures 1**

## 99 **Tables 1**

100  
101  
102 The study is conducted theoretically and numerically with the help of a simplified method  
103 developed to calculate the energy and comfort performance of the room with controlled façade [19-  
104 22]. The method can calculate the dynamic properties of different elements of the façade and is also  
105 integrated with the hourly model calculating the performance of whole building according to EN  
106 13790 [23]. Therefore, the simplified model is able to calculate the energy demands (heating, cooling,  
107 lighting and ventilation) and the indoor environment (indoor air temperature, solar transmittance  
108 through the façade and the indoor illuminance level on a chosen point) of the building with façade of  
109 different control strategies. The simplified method is verified by the simulation results from a dynamic  
110 building simulation tool BSim [25] and the experimental data collected in the full-scale test facility in  
111 Aalborg University (cube) [19-22, 24]. The hourly calculations are conducted through the whole year  
112 with the weather data of Danish Reference Year (DRY) [25].

### 113 **2.1. Influence of different control strategies**

114  
115  
116 The calculations on the energy and comfort performance of the office building are conducted for  
117 different control conditions:

- 118 • Façade without any control (present);
- 119 • Control of night shutter;
- 120 • Control of night shutter+ control of solar shading;
- 121 • Control of night shutter+ control of solar shading+ control of natural ventilation;
- 122 • Control of night shutter+ control of solar shading+ control of natural ventilation+ control of  
123 night cooling;

124 • Control of night shutter+ control of solar shading+ control of natural ventilation+ control of  
125 night cooling+ control of lighting.

126 The control strategies of different technologies are added one by one to show the improvement on the  
127 energy and comfort performance step by step.

128

## 129 **2.2. Use of intelligent glazed façade to comply with future energy standards in Denmark**

130

131 The building showed before is designed to comply with the Danish building regulation of BR10 with  
132 primary energy consumption lower than around 72kWh/m<sup>2</sup>/year [26]. Danish government has energy  
133 requirements for future new buildings. They are defined as low energy class 2015 and building class  
134 2020 [26] with yearly primary energy demand of around 41kWh/m<sup>2</sup> and 25kWh/m<sup>2</sup>, respectively. A  
135 study is conducted to investigate if the building after design changes complies with the future building  
136 class 2020 [26]. Design changes include improving the thermal properties or using intelligent glazed  
137 façade. Table 2 shows the thermal properties of the present and changed buildings assumed to comply  
138 with standards of BR10 and building class 2020. They are not required specifically by the standards  
139 but taken as the levels within the limitations that fulfil each standard.

140

### **Table 2**

141

## 142 **2.3. Investigation of influence of ratio of glazing part on the energy consumption**

143

144 Influences of the ratio of the glazing part to the entire facade on the energy performance are studied for  
145 the office building with both a static façade solution and intelligent glazed façade solution. The glazing  
146 ratio of facades is limited because there should be a certain fraction of frame. However, theoretical  
147 calculations are conducted for ratio of glazed façade from 10 % to nearly 100 % (fully glazed).

148

**149 3. Control strategies**

**150** Figures 2 and 3 show the developed control strategies of the intelligent glazed façade for all the  
**151** controlling technologies during both the occupied and unoccupied hours.

**152** **Figures 2 and 3**

**153** The detailed setup of the different control technologies are described below.

**154 3.1. External shutter**

**155** An external shutter is installed and activated to cover the glazed façade outside office hours. Table 3  
**156** shows the layout and the properties of glazing with the external shutter. The theoretical calculation is  
**157** based on the thermal properties of the shutter, not considering the design and realization of  
**158** construction.

**159** **Table 3**

**160** The control of external shutter is active during the unoccupied hours when the indoor air temperature  
**161** is below 18 °C. The shutter is controlled as a function of the energy balance across the façade. The  
**162** evaluation in the calculation is performed by the heat loss and the solar gains through the facade,  
**163** excluding infiltration. In order to realize the use of the external shutter technology requires the  
**164** measurement of internal and external temperature, incident irradiance, and the calculation of internal  
**165** loads.

**166** **Equation (1)**

167 Where  $\phi_{\text{façade}}$  is heat flow through the façade.  $\phi_{\text{sol}}$  is the solar radiation on the glazed façade.  $g_g$  is the  
168 solar transmittance of the window, which is 0.4.  $U_g$  is the U-value of the window, which is 1.1  
169  $W / (m^2 \cdot K)$ .  $T_i$  is the indoor air temperature.  $T_o$  is the outdoor air temperature.  $g_{g+\text{shutter}}$  is the solar  
170 transmittance of the glazing together with the shutter, which is 0.  $U_{g+\text{shutter}}$  is the U-value of the glazing  
171 together with the shutter, which is lower than  $0.5 W / (m^2 \cdot K)$ .

### 172 3.2. Glare and solar control by blind

173 A blind is used to prevent glare problems during the occupied hours and to reduce the solar  
174 transmittance through the façade during the unoccupied hours. The tilt angle of the blind depends on  
175 its functions. The tilt angle of the blind during occupied hours is calculated by equation (2) from  
176 previous research [22] to cut the direct solar radiation, which both improve the visual comfort and  
177 maximize the daylight transmittance into the room.

#### 178 Equation (2)

179 Where  $\beta$  is the angle between the slat and the horizontal plan.  $\alpha$  is the solar altitude angle.  $H$  is the  
180 distance between the slats.  $W$  is the width of the slats.

181 During unoccupied hours, the blind is controlled to be closed if the indoor air temperature is above 24  
182 °C. The blind is scrolled up if it is not set at cut-off angle or closed position.

### 183 3.3. Natural ventilation

184 The glazed façade is open when the indoor temperature exceeds 23 °C. The control is active only when  
185 the outdoor temperature is lower than the indoor temperature and the outdoor temperature is above 12  
186 °C, preventing cold draft in the room. In the real situation, the natural ventilation rate is calculated  
187 according to wind speed, wind direction, temperature difference between indoor and outdoor and some  
188 other parameters. The calculation is not focus in this paper. The ventilation rate is assumed to be 1 l/s  
189 per  $m^2$ , which is equal to around 1.5 air change per hour (ACH) assuming the height of the room is  
190 2.7m [27].

### 191 **3.4. Night cooling**

192 The night cooling control is active during unoccupied hours in terms of opening the window if the  
193 average outdoor air temperature between 12:00 and 17:00 is above 18 °C and the indoor air  
194 temperature is higher than the outdoor air temperature. The control of night cooling can precool the  
195 room and help to balance the cooling peak during the day time. In order not to overcool the room so  
196 that the indoor air temperature in the morning is too low, the night cooling is inactivated when the  
197 indoor air temperature is below 14 °C. However, it is reactivated when the indoor air temperature  
198 comes back to 17 °C.

### 199 **3.5. Heating and cooling**

200 Heating and cooling installations are controlled to secure the set-point temperature in the office space.  
201 The heating and cooling needs for the office room in every time step (hour) can be calculated by the  
202 simplified model according to hourly heat gain and heat losses. The set points for heating and cooling  
203 are 20 °C and 25 °C, respectively. Detailed equations for calculating the heating and cooling needs are  
204 shown in the EN 13790 [23] and in a previous paper [22].

### 205 **3.6. Lighting**

206 Artificial lighting of the office building has on-off control during occupied hours according to the  
207 illuminance level at the reference point mentioned before. The lighting control is included in all the  
208 cases. The set point of the lighting is 300 Lux. The calculation of the illuminance level at the  
209 reference point is described in a previous paper [22].

210

## 211 **4. Result**

212 The primary energy demand of the building is reduced from approximately 72kWh/m<sup>2</sup>/year to  
213 63kWh/m<sup>2</sup>/year by improving the building from standard of BR10 to building class 2020 but still using  
214 the static façade (figure 4). However, the energy performance is still far away from the requirement of  
215 building class 2020. With the help of the control of night shutter, the heating energy is reduced by

216 10kWh/m<sup>2</sup>/year, lowering the total energy demand 17 % compared with that of the building without  
217 any control strategies. The cooling energy is greatly reduced by 24kWh/m<sup>2</sup>/year by adding the control  
218 of the blind. The total energy demand of the façade with the control for night shutter and blind is  
219 32kWh/m<sup>2</sup>/year, which is 9kWh/m<sup>2</sup>/year lower than the requirement of low energy class 2015. The  
220 energy performance of the building is optimized further by adding the control for natural ventilation  
221 and night cooling. The annual energy demand of the building under all the control strategies reaches  
222 approximately 25kWh/m<sup>2</sup>/year, which is 40% of the energy use of the building without any façade  
223 control. Therefore, there is a potential that the energy demand for mechanical ventilation can be  
224 reduced using the control of natural ventilation, which is not counted in this paper.

#### 225 **Figure 4**

226  
227 The comfort performance of the building is also improved using different control strategies compared  
228 with the static façade. Figure 5 shows the time percentage of the different comfort classes specified  
229 according to EN 15251. The total time percentage of comfort class I and class II is increased from 21  
230 % to 64 % of the occupied hours by conducting control strategies. In addition, the comfort class IV  
231 which is not recommended for indoor comfort was shorted to 7 % of the occupied hours. The indoor  
232 set points of air temperature are set at the same value for the different control strategies, so the  
233 operative temperature of the office is optimized by using façade control strategies.

#### 234 **Figure 5**

235 Even though the properties of the building elements except the façade are improved from the standards  
236 of BR10 to 2020, the energy performance of the building does not comply with the requirements of  
237 total energy demand of 2020 with the static façade (figure 6). The energy demand of the building of  
238 BR10 with the intelligent glazed façade is lower than that of the building of 2020 with the static  
239 façade. The building complies with the building class 2020 with both the improved thermal properties  
240 from BR10 to 2020 and the intelligent façade. It is reasonable that the energy demand for lighting

241 increases when the blind control is introduced because that the blind makes the light transmittance of  
242 the façade lower than that without the blind.

243 **Figure 6**The energy performances of the building with different glazing ratios for both the static  
244 façade and the intelligent façade are shown in figures 7 and 8. The less the glazing ratio of the static  
245 façade is, the better the energy performance. The building with a 20 % glazing ratio of the static glazed  
246 façade has the lowest energy demand approximately 50kWh/m<sup>2</sup>/year. With the intelligent glazed  
247 façade, the glazing ratio having the lowest energy demand is 40 %. Additionally, even with 100% of  
248 glazing in the façade, it still has significantly lower energy demand compared to the static façade with  
249 a glazing ratio of 20 %. The building with an intelligent glazed façade with glazing ratio of 90 %  
250 complies with the energy requirement of 2015. The advantages of the intelligent glazed façade make it  
251 possible for modern office buildings to have higher glazing ratios of the façade without increasing the  
252 energy demand quite much, which is desired because of good daylight condition and better view.

### 253 **Figures 7 and 8**

## 254 **5. Conclusion**

256 The energy consumption of the building is greatly reduced by approximately 40 % when using the  
257 intelligent glazed façade instead of a static façade in the climate of Denmark.

258 Together with the improvement of the thermal properties of other building elements, the building  
259 installed with the intelligent glazed façade can comply with the energy requirements of the building  
260 class 2020, which cannot be fulfilled by the building with the static façade.

261 The facade glazing ratio with the lowest energy consumption is increases to around 40 % for the  
262 building with the intelligent glazed façade compared with that of 10 % for the building with a static  
263 façade. At a glazing ratio of 90 %, the building with the intelligent façade still complies with the  
264 energy requirement of low energy class 2015 with an energy consumption of 38kWh/m<sup>2</sup>/year.

265 In the future, the improvements of the intelligent glazed façade need to be investigated on office  
266 buildings of other climates outside Denmark. Additional, it can also be used for residential buildings,

267 in which the control strategies need to be modified, as the building type is heating dominated in the  
268 Danish climate in contrast the office building which is cooling dominated.

269

270

## 271 **Nomenclature**

272  $\phi_{facade}$  is the difference of the net heat gains between the façade with glazing only and the façade  
273 with glazing and night shutter [ $W/m^2$ ];

274  $\phi_{sol}$  is the total solar radiation on the glazed facade [ $W/m^2$ ];

275  $g_g$  is the solar transmittance of glazed facade [-];

276  $U_g$  is the thermal transmittance of glazing [ $W / (m^2 \cdot K)$ ];

277  $T_i$  is the indoor air temperature of the room [ $^{\circ}C$ ];

278  $T_o$  is the outdoor air temperature [ $^{\circ}C$ ];

279  $g_{g+shutter}$  is the solar transmittance of glazed façade together with night shutter (0) [-];

280  $U_{g+shutter}$  is the thermal transmittance of glazed façade together with night shutter [ $W / (m^2 \cdot K)$ ];

281  $H$  is the distance between the slats of the blind [mm];

282  $W$  is the width of the slats of the blind [mm];

283  $\alpha$  is the solar altitude angle [ $^{\circ}$ ];

284  $\beta$  is the tilt angle of the slats of the blind [ $^{\circ}$ ];

285

## 286 **Acknowledgements**

287 This paper is based on research conducted in a PhD project supervised by Senior Researcher Kim

288 Wittchen, Danish Building Research Institute (SBI) and Professor Per Heiselberg, Department of Civil

289 engineering both at Aalborg University, Denmark. The PhD is part of the Strategic Research Centre



**290** for Zero Energy Buildings at Aalborg University and financed by the Danish aluminium section of The  
**291** Danish Construction Association, Aalborg University and The Danish Council for Strategic Research,  
**292** under the Programme Commission for Sustainable Energy and Environment.

### **293** References

- 294** [1] Selkowitz SE. Integrating advanced facades into high performance buildings. 2001.
- 295** [2] Selkowitz S, Aschehoug O, Lee ES. Advanced Interactive Facades-Critical Elements for Future  
**296** Green Buildings? 2003.
- 297** [3] Lee ES, DiBartolomeo DL, Rubinstein FM, Selkowitz SE. Low-cost networking for dynamic  
**298** window systems. *Energy Build* 2004;36:503-13.
- 299** [4] Skelly M, Wilkinson M. The Evolution of Interactive Facades: Improving Automated Blind  
**300** Control. *Whole Life Performance of Facades* 2001:129-42.
- 301** [5] Foster M, Oreszczyn T. Occupant control of passive systems: the use of venetian blinds. *Build*  
**302** *Environ* 2001;36:149-55.
- 303** [6] Gomes MG, Santos A, Rodrigues AM. Solar and visible optical properties of glazing systems  
**304** with venetian blinds: Numerical, experimental and blind control study. *Build Environ*  
**305** 2014;71:47-59.
- 306** [7] Fuliotto R, Cambuli F, Mandas N, Bacchin N, Manara G, Chen Q. Experimental and numerical  
**307** analysis of heat transfer and airflow on an interactive building facade. *Energy Build* 2010;42:23-  
**308** 8.
- 309** [8] Chan A. Effect of adjacent shading on the thermal performance of residential buildings in a  
**310** subtropical region. *Appl Energy* 2012;92:516-22.
- 311** [9] Palmero-Marrero AI, Oliveira AC. Effect of louver shading devices on building energy  
**312** requirements. *Appl Energy* 2010;87:2040-9.

- 313** [10] Da Silva PC, Leal V, Andersen M. Influence of shading control patterns on the energy  
**314** assessment of office spaces. *Energy Build* 2012;50:35-48.
- 315** [11] Nielsen MV, Svendsen S, Jensen LB. Quantifying the potential of automated dynamic solar  
**316** shading in office buildings through integrated simulations of energy and daylight. *Solar Energy*  
**317** 2011;85:757-68.
- 318** [12] Kim D, Park C. Manual vs. optimal control of exterior and interior blind systems. 2009:1663-70.
- 319** [13] Tzempelikos A, Athienitis AK. The impact of shading design and control on building cooling  
**320** and lighting demand. *Solar Energy* 2007;81:369-82.
- 321** [14] Van Moeseke G, Bruyère I, De Herde A. Impact of control rules on the efficiency of shading  
**322** devices and free cooling for office buildings. *Build Environ* 2007;42:784-93.
- 323** [15] Shen H, Tzempelikos A. Daylighting and energy analysis of private offices with automated  
**324** interior roller shades. *Solar Energy* 2012;86:681-704.
- 325** [16] Shen H, Tzempelikos A. Sensitivity analysis on daylighting and energy performance of  
**326** perimeter offices with automated shading. *Build Environ* 2012.
- 327** [17] Schulze T, Eicker U. Controlled natural ventilation for energy efficient buildings. *Energy Build*  
**328** 2012.
- 329** [18] EN 15251: Indoor environmental parameters for assessment of energy performance of buildings-  
**330** addressing indoor air quality, thermal environment, lighting and acoustics, 2007.
- 331** [19] Liu M, Wittchen KB, Heiselberg PK, Winther FV. Development of a simplified and dynamic  
**332** method for double glazing façade with night insulation and validated by full-scale façade  
**333** element. *Energy Build* 2013;58:163-171.
- 334** [20] Liu M, Wittchen KB, Heiselberg P, Winther FV. Development of Simplified and Dynamic  
**335** Model for Double Glazing Unit Validated with Full-Scale Facade Element. PLEA 2012 Lima  
**336** Peru-Opportunities, Limits & Needs.

- 337 [21] Liu M, Wittchen KB, Heiselberg PK, Winther FV. Development and sensitivity study of a  
338 simplified and dynamic method for double glazing facade and verified by a full-scale facade  
339 element. *Energy and Buildings* 2014;68:432-443.
- 340 [22] Liu M, Wittchen KB, Heiselberg PK. Development of a simplified method for intelligent glazed  
341 facade design under different control strategies and verified by building simulation tool BSim.  
342 *Building and Environment* 2014;74:31-38.
- 343 [23] ISO EN. 13790: Energy performance of buildings–Calculation of energy use for space heating  
344 and cooling (EN ISO 13790: 2008). European Committee for Standardization (CEN), Brussels  
345 2008.
- 346 [24] Kalyanova O, Heiselberg P. Experimental Set-up and Full-scale measurements in the ‘Cube’  
347 2008.
- 348 [25] Wittchen KB, Johnsen K, Grau K. BSIM User’s guide. Danish Building Research Institute,  
349 Hørsholm, Denmark 2005.
- 350 [26] Building Regulations (BR10). The Danish Ministry of Economic and Business Affairs, Danish  
351 Enterprise and Construction Authority, Copenhagen, Denmark 2010.
- 352 [27] Larsen TS, Heiselberg PK. Single-sided natural ventilation driven by wind pressure and  
353 temperature difference. *Energy and Buildings* 2008;40:1031-1040.

354 **Figure captions**

- 355** Figure 1: Figure of the building in Buddinge used as case study.
- 356** Figure 2: Control strategies for office room with external blind during occupied hour.
- 357** Figure 3: Control strategies of office room with external blind during unoccupied hour.
- 358** Figure 4: Energy demand of the office building under different control strategies.
- 359** Figure 5: Percentage of different comfort classes of different control strategies.
- 360** Figure 6: Energy consumptions of the building under different building conditions and different types
- 361** of facade.

362 Figure 7: Energy performance of static façade with different ratio of glazing part under building  
363 standard of 2020.

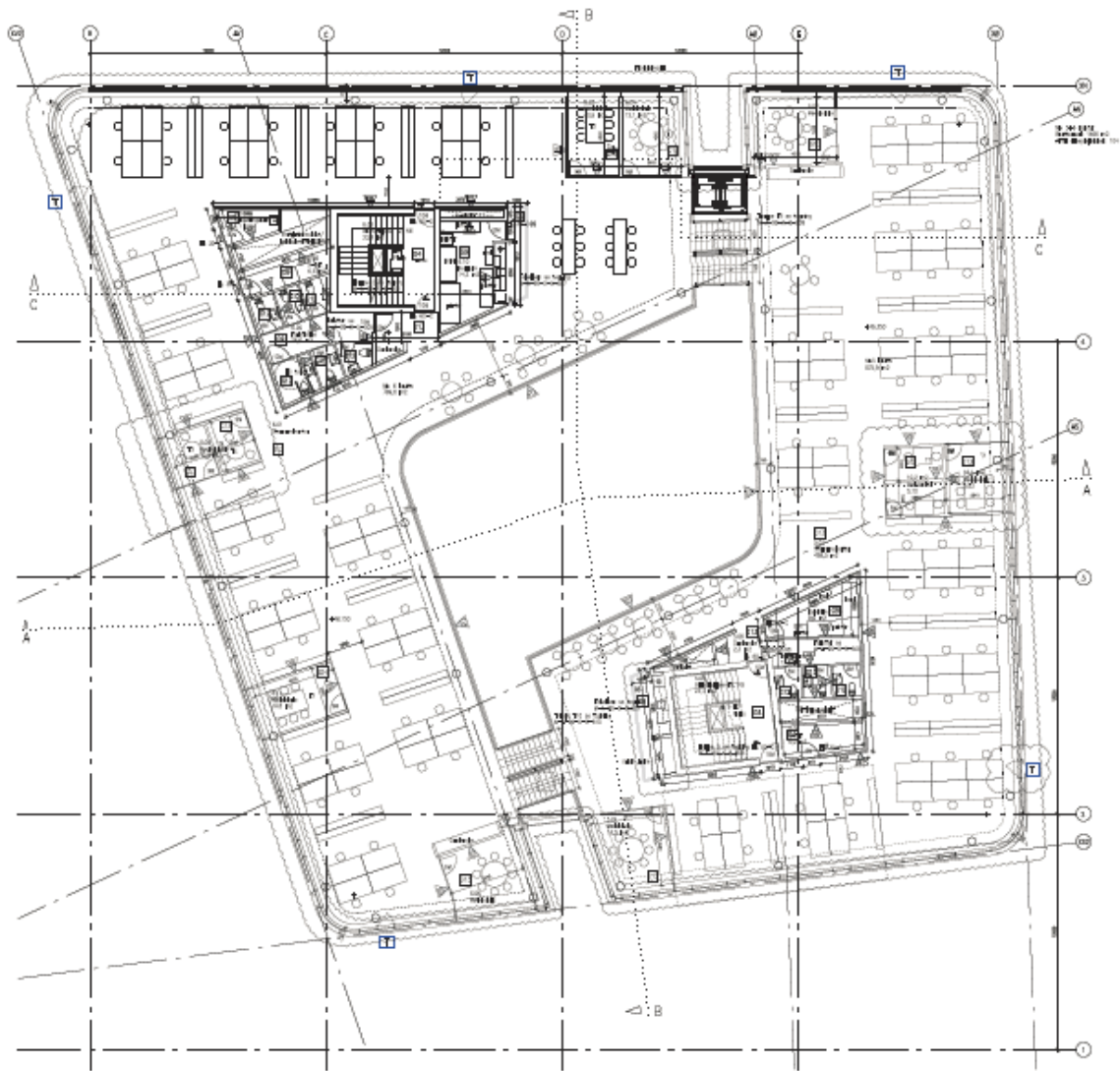
364 Figure 8: Energy performance of intelligent glazed façade with different ratio of glazing part under  
365 building standard of 2020.

366 
$$\phi_{facade} = [\phi_{sol} g_g - U_g (T_i - T_o)] \quad \text{equation (1)}$$
  
$$- [\phi_{sol} g_{g+shutter} - U_{g+shutter} (T_i - T_o)] < 0$$

367 
$$\beta = \arccos \left[ \frac{\frac{H}{W} \times \tan \alpha + \sqrt{\tan^2 \alpha - \left(\frac{H}{W}\right)^2 + 1}}{\tan^2 \alpha + 1} \right] \quad \text{Equation (2)}$$

368

369

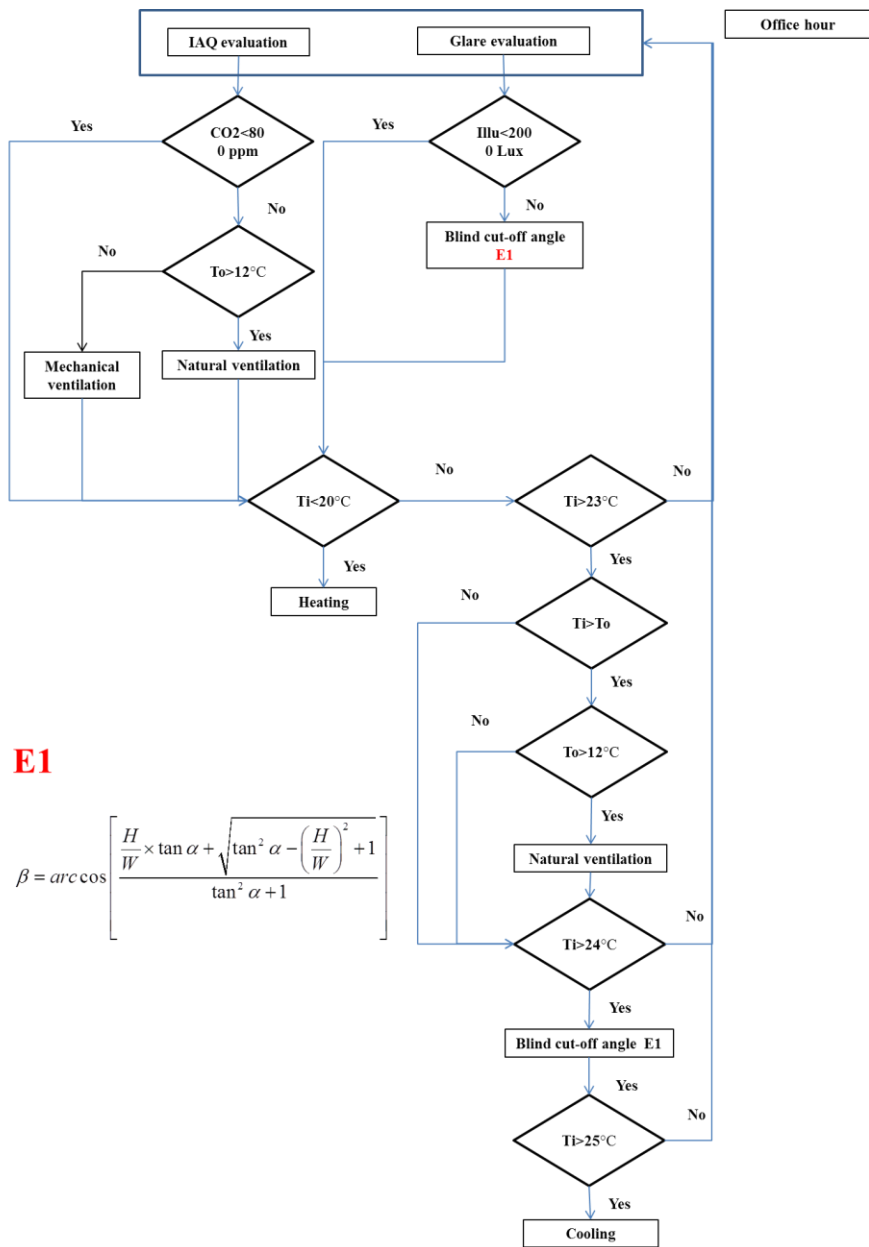


370

371

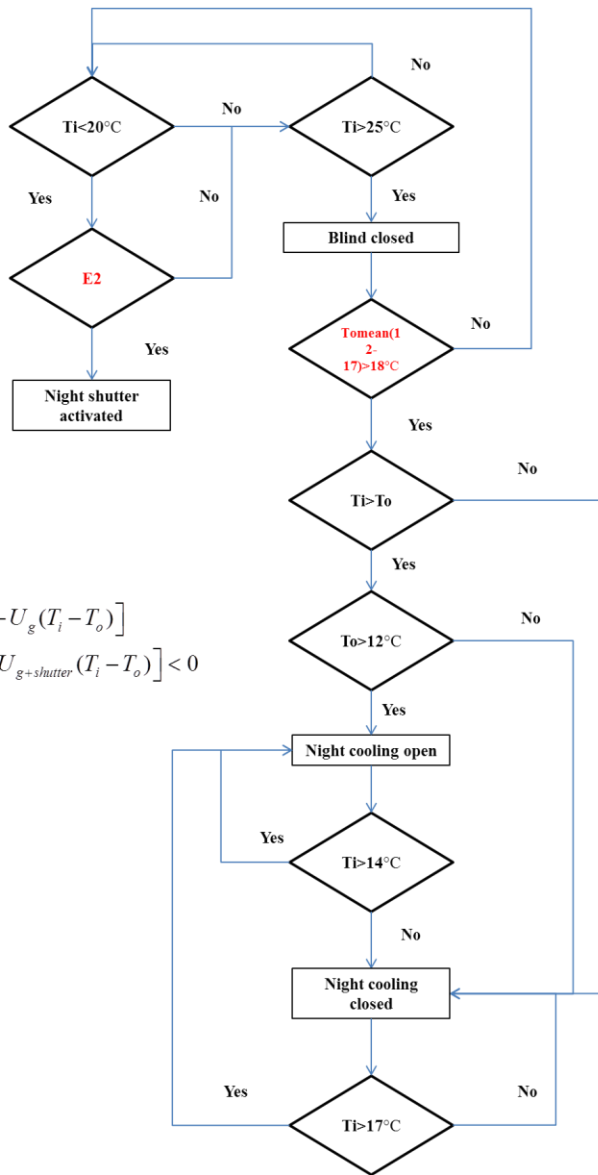
Figure 1: Figure of the building in Buddinge used as case study.

372



373

374 Figure 2: Control strategies for office room with external blind during occupied hour.



**E2**

$$\phi_{facade} = [\phi_{sol} g_g - U_g (T_i - T_o)]$$

$$-[\phi_{sol} g_{g+shutter} - U_{g+shutter} (T_i - T_o)] < 0$$

375

376 Figure 3: Control strategies of office room with external blind during unoccupied hour.

377

378



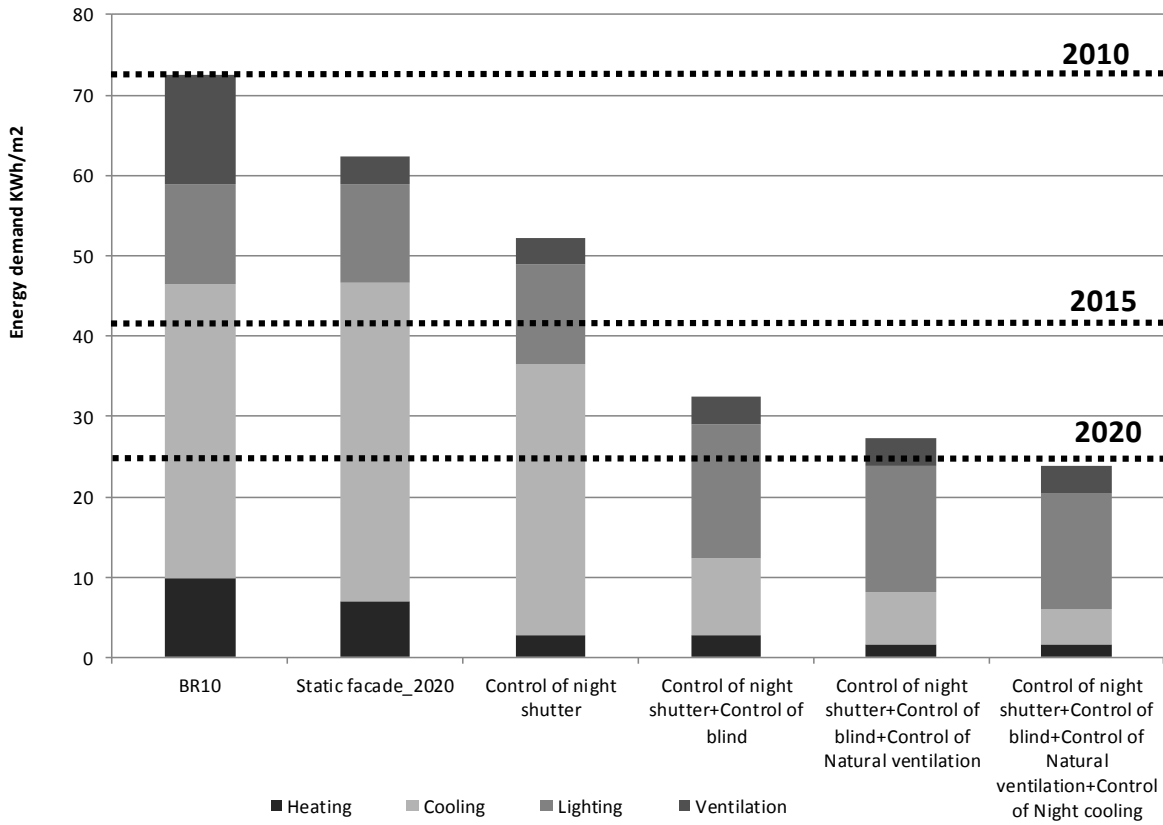


Figure 4: Energy demand of the office building under different control strategies.

379  
380  
381  
382  
383  
384  
385

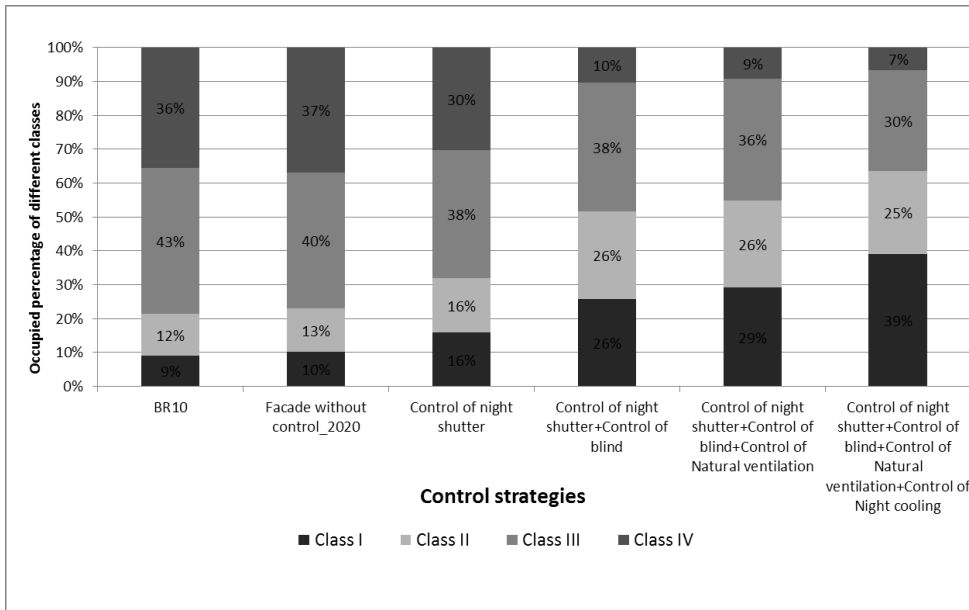
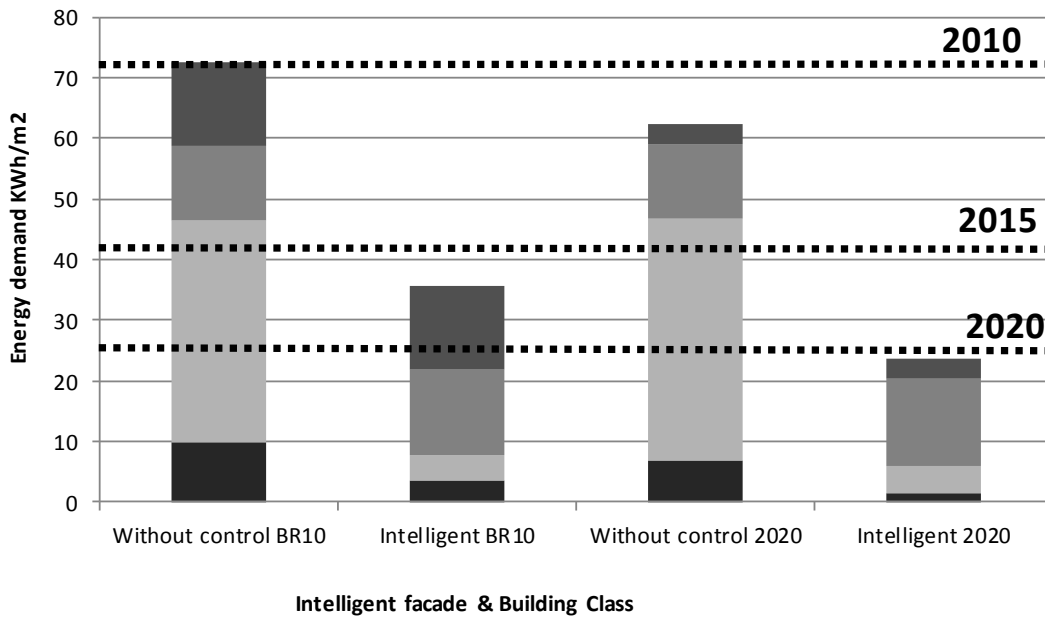


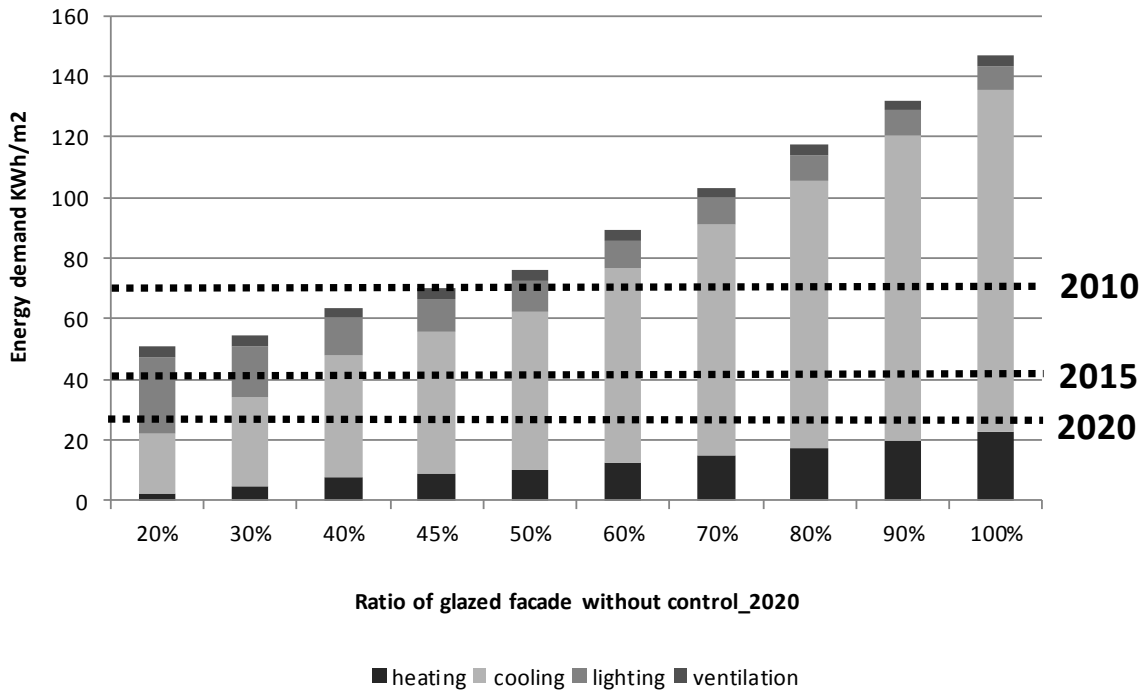
Figure 5: Percentage of different comfort classes of different control strategies.

386  
387  
388



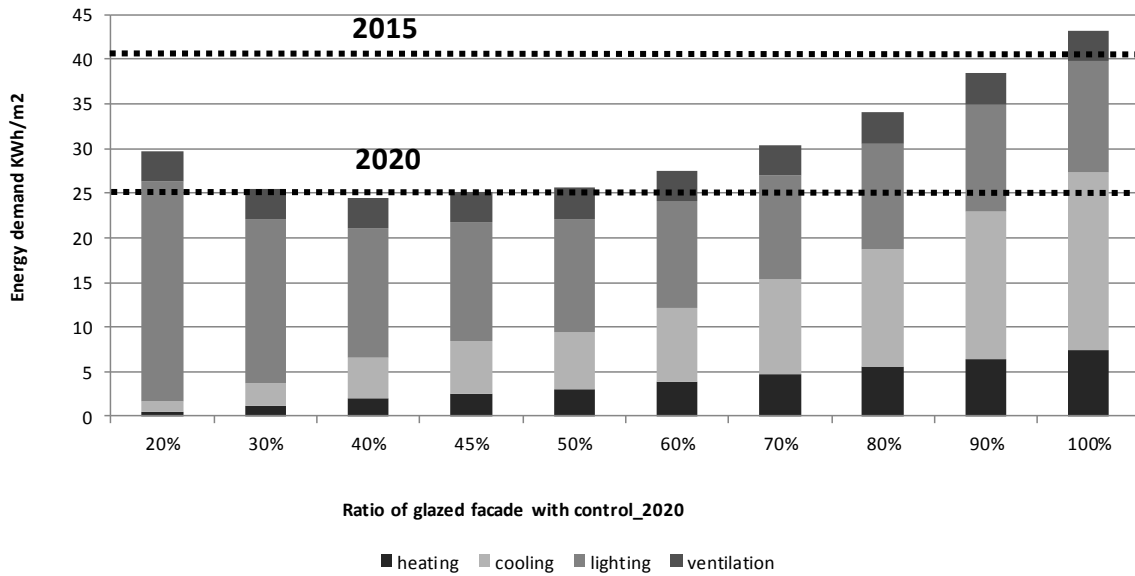
389  
390  
391  
392

Figure 6: Energy consumptions of the building under different building conditions and different types of facade.



393  
394  
395

Figure 7: Energy performance of static façade with different ratio of glazing part under building standard of 2020.



396  
397  
398  
399  
400  
401

**Figure 8: Energy performance of intelligent glazed façade with different ratio of glazing part under building standard of 2020.**

Table 1: Setup of building services and indoor conditions.

Internal load of people	10 W/m <sup>2</sup>
Lighting power (on/off)	6W/m <sup>2</sup>
Setpoint for the heating	20 °C
Setpoint for the cooling	25 °C
Mechanical ventilation rate (office hour)	1.2 l/(sm <sup>2</sup> )
Setpoint of lighting	300 lux

402  
403  
404  
405

Table 2: Properties difference of building for both BR10 and building class 2020.

	BR10	2020
Area (m <sup>2</sup> )	7405	7405
Heat capacity (Wh/Km <sup>2</sup> )	120	120
Office hour	8-17	8-17
Internal load (W/m <sup>2</sup> )	10	10
Heating temp (°C)	20	20
Cooling temp (°C)	25	25
Ventilation (l/sm <sup>2</sup> ) (On office hour)	1.2	1.2
Lighting (W/m <sup>2</sup> ) (on/off 250Lux)	7	7

U-value opaque wall (W/Km <sup>2</sup> )	0.13	0.09
Fan efficiency (kJ/m <sup>3</sup> )	2	0.5
Heat exchange	0.85	0.85
Infiltration (l/sm <sup>2</sup> )	0.06	0.03

406  
407 Table 3: Layout and material of the façade with external insulation.  
408

Position	Material	Conductivity	IR emissivity outdoor	IR emissivity indoor
Outside	Polystyren 100mm	0.05 W/mK	0.09	0.09
Cavity	Air 110mm	-	-	-
Middle	Planilux 4 mm SGG	1 W/mK	0.837	0.837
Cavity	Argon 15 mm	0.017 W/mK	-	-
Inside	PI Tutran 4 mm SGG	1 W/mK	0.04	0.837

409  
410

# Investigation of different configurations of a ventilated window to optimize both the energy balance and the thermal comfort

Mingzhe Liu<sup>a,\*</sup>, Per Kvols Heiselberg<sup>b</sup>, Olena.K. Larsen<sup>b</sup>, L. H. Mortensen<sup>a</sup>, J. Rose<sup>a</sup>

<sup>a</sup> Danish Building Research Institute (SBI), Aalborg University, A.C. Meyers Vænge 15, 2450 København SV, Denmark

<sup>b</sup> Department of Civil Engineering, Aalborg University, Sohngaardsholmsvej 57, 9000 Aalborg, Denmark

\* Corresponding author. Tel.: +45 99407234.

E-mail address: [ml@civil.aau.dk](mailto:ml@civil.aau.dk).

## Abstract

The study in this article investigates 15 ventilated window typologies with different pane configurations and glazing types in climates of four European countries (United Kingdom, Denmark, France and Germany) in order to identify the optimum typology with regard to their energy balance and impact on thermal comfort. There are no shading devices in the ventilated cavity for all the studied typologies. Hourly simulations of the heat balances of the windows are conducted on four days representing different typical weather conditions according to the method described in EN ISO 13790. U and g values used in the calculation method are calculated in WIS software. Additionally, comfort performance is evaluated by inlet air temperature and internal surface temperature of the windows calculated by WIS software.

The results of the study show the energy and comfort performance of different ventilated window typologies and provide optimal ventilated window typologies for climates of these four European

climates. The typologies with solar control or low-E coatings and typologies with double glazing on the outside have better performance in terms of either minimizing the energy consumption or optimizing the thermal comfort. The provided optimal window typologies can be used in residential and commercial buildings for both new constructions and renovations.

Keywords: ventilated window, configuration, energy consumption, thermal comfort

## **1. Introduction**

Houses and apartments are nowadays the most energy intensive sector and their operation takes up to 40% of the total amount of energy use in Europe. Almost 90% of residential building stock were constructed before 1990 and according to the EPBD rating of energy performance most of them fall to D or even F category, which means “unsatisfactory” or “very un-economizing” (Hazucha). The energy saving potential of the existing building stock is considerable and the thermal loss through windows and doors is a key parameter, since it accounts for about 33% of the energy consumption for heating (Hazucha).

Windows have a significant effect on building performance and several aspects have to be taken into account, when developing new concepts for refurbishment (Häkkinen; European Environment Agency). The window industry’s response to the challenge has been to improve thermal envelopes using better insulation materials in frames, improve glass panes as well as reducing air leaks. These solutions have led to a sealing of buildings, including the installation of more fixed pane windows and creating a strong need for ventilation. In many existing buildings mechanical ventilation is very difficult and expensive to provide and there is a need for development of alternative window and ventilation solutions.

Therefore, it is appropriate to investigate different ventilated window solutions in order to identify the most suitable ventilated windows fulfilling the requirements for renovation of European buildings in different climatic conditions. An optimal approach should consider the following aspects: to improve window performance in terms of both the energy consumption and the thermal comfort; to provide ventilation together with heat recovery; to remove solar heat in summer; to improve insulation and provide ventilation heat recovery in winter.

Five window typologies were simulated indicating that better energy performance can be achieved with the help of ventilated window in the subtropical and temperate climate zones (Chow et al., 2006, 2009). Appelfeld et al. (2011) conducted experimental analysis showing that a ventilated window can potentially contribute to energy savings and the ventilated window might be most suitable for window unit with low ventilation rates. Different models and calculation methods have already been developed to investigate the performance of ventilated windows (Carlos et al., 2011; Kamal et al., 2009; Ismail et al., 2005; Ismail et al., 2006; EN 15099, 2003). Carlos et al. (2010) found that ventilated window system act as an efficient heat exchanger using transmission heat losses and solar radiation to preheat ventilation air in real outdoor weather conditions of Portugal. It can reduce the building's heating energy costs and increase the air temperature in the cavity by 10 °C under solar radiation at an average air flow rate of about 19m<sup>3</sup>/h. Three multiple-skin facades with different ventilation strategies are investigated by Saelens et al. (Saelens et al., 2006, 2005, 2002; Manzet al., 2005) showing that both the heating and cooling demand may significantly be improved by implementing control strategies such as controlling the airflow rate and the recovery of air returning from the multiple-skin facades. As study has been conducted by Perez-Grande et al. (2005) showing that the thermal loads of the building can be reduced by blowing the air through the channel. However, more evaluations are needed to identify the most promising ventilated window typology depend on the different climatic conditions and with a unified method.

Therefore, a comprehensive investigation needs to be implemented for different window typologies and both the energy demand and the thermal comfort of the different window typologies need to be evaluated. The study investigates 15 different window typologies (e.g. glazing type, glazing position, coating position and cavity width, etc.) under two different ventilation concepts (heating mode and cooling mode). Energy demand and thermal comfort (internal surface temperature and inlet air temperature of the window typologies) have been calculated under different weather conditions in four European countries and the most energy efficient solution providing acceptable indoor thermal comfort has been identified. After comparison, the optimal window typologies without solar shading systems or other technologies are selected for the climatic conditions of the four countries.

## **2. Description and Method**

The investigations were performed on the 15 different window typologies illustrated in Figure 1. Typology 3 is a closed cavity window and the others are variations of windows with different pane and glazing configurations and a ventilated cavity. In general the typologies were simulated to test the effect of:

- Coating on a single glazing
- Single glazing outside
- Single glazing inside
- Coating position (surface facing inside or surface facing outside)
- Coating type (solar control or Low-E)

**Figure1**



The ventilation concepts shown in Figure 2 are used in the simulation. In summer the active mode is the Cooling mode while in winter the Heating mode is active.

The goal of the cooling mode is to minimize amount of solar radiation passing through the window. For a traditional window configuration some amount of solar radiation striking the window is absorbed in the glazing panes and then transferred to the room by convection and radiation. Natural ventilation through the air gap can cool down the glazing panes and the heated air can be expelled to the outdoors removing some amount of solar radiation. In addition the air to the room is supplied directly from the outside in the cooling mode. The main idea behind the heating mode is minimizing the heating load from the heating system to the room by means of utilization of solar radiation for preheating of the ventilation air. Also the energy losses from the room through the inner skin of the window will return back to the room with the ventilation air. The preheating of the ventilation air will also reduce the risk of draught.

## **Figure 2**

Simulation of the window performance have been carried out for three orientations; north, south and west and for four different locations. The locations are Copenhagen (Denmark), Finningley (United Kingdom), Nice (France) and Würzburg (Germany). The calculations are time consuming, so only these four locations are selected to representing the northern, western, southern and eastern Europe. The results are presented for the individual orientations and discussed. The simulations are performed without solar shading systems.

The weather data is very important for the analysis of the window design and in principle the performance should be evaluated based on hourly values for a whole year. However, for a ventilated window both the U-value and the g-value changes hour by hour and it is a very huge task to calculate these values for every hour during a whole year. Therefore, the performance evaluation in this

investigation is based on calculations performed for four different typical 24 hour periods, i.e. a sunny summer, an overcast summer, a sunny winter and an overcast winter day.

The weather data of the four climates are from EnergyPlus software weather data (EnergyPlus). The methods for choosing the four different days for each of the four different climates are:

- Sunny summer (clear day) - it is chosen to use a 24h-period with a clear sky and with a month-maximum (from 24h-average) temperature for June-July-August.
- Overcast summer - it is chosen to use a 24h-period that include monthly average solar radiation intensity with reasonable part of diffuse solar radiation and with a monthly average (from 24h-average) temperature for June-July-August.
- Sunny winter (clear day) - it is chosen to use a 24h-period with a clear sky and with a month-minimum (from 24h-average) temperature for December-January-February
- Overcast winter - it is chosen to use a 24h-period that include monthly average solar radiation intensity with reasonable part of diffuse solar radiation and with a monthly average (from 24h-average) temperature for December-January-February.

The weather data used for Denmark is illustrated in Figure 3. The Danish weather data reveals large differences in temperatures. Therefore, sunny summer day is in average 8 °C warmer than the overcast summer day and thus the cooling demand will be much higher during the sunny summer day. The opposite is true for the winter period, where the sunny winter day in average is more than 12 °C colder than the overcast winter day, so here the energy demand for heating is dominant for sunny winter. In

overcast days the diffuse radiation is dominant. In sunny days the direct radiation is dominant. South-facing windows have high loads of direct solar radiation in the sunny summer day and the highest load in the sunny winter day. West-facing windows have the highest load of direct solar radiation in sunny summer day. North-facing windows have very low loads of direct solar radiation in summer and none in winter situations.

### **Figure 3**

The French weather data used in the calculations reveal only small differences in temperatures whether it is sunny or overcast, see figure 4. The average temperature in winter is much higher than that of Denmark. For the overcast days the diffuse solar radiation is dominant but with clearly higher effect in summer than in winter. Note that in overcast winter the simulations will be based on purely diffuse radiation and thus the results will be the same for all three window orientations.

There is only very limited direct solar radiation at north-facing windows in summer and no direct solar radiation in winter. For sunny days the direct solar radiation on south-facing windows is much higher in winter than in summer. West-facing windows has the highest load of direct solar radiation in the sunny summer day.

### **Figure 4**

The evaluation of the window typologies is based on achieving the lowest energy consumption of heating and cooling and the best thermal comfort performance in terms of internal surface temperature and inlet air temperature.

## **2.1. Calculation of the energy consumption**

The energy demand for cooling and heating is calculated according to EN/ISO 13790 (EN ISO 13790). The energy balance through the windows is calculated considering heat transmittance, ventilation

losses and the solar gain through the windows. Hourly calculations are implemented for all the typical days.

It must be noted that the monthly method is modified for hourly calculation, and instead of monthly average weather data the hourly values were used (EN ISO 13790).

Calculation procedure is shown below.

Energy need for heating and cooling is given as in Equation 1 and Equation 2.

### **Equation 1**

### **Equation 2**

Heat losses are calculated according to EN ISO 13790 as in Equation 3 and included ventilation losses,  $Q_{ve}$  and transmission losses  $Q_{tr}$ .

### **Equation 3**

Total heat gains are calculated according to EN ISO 13790 and consist of internal heat gains and solar heat gains (Equation 4).

### **Equation 4**

Solar radiation entering the ventilated window depends on solar radiation intensity  $I_s$ , solar properties of glazing and the glazing area, Equation 5. Direct and diffuse solar heat gains are both taken into account.

### **Equation 5**

Gain utilization factor for heating  $\eta_{H,gn}$  and cooling  $\eta_{C,gn}$  are calculated according to pr EN ISO 13790-2005. When calculating  $\eta_{H,gn}$  and  $\eta_{C,gn}$ , the conditioned zone is assumed to be  $1\text{m}^2$  with the

medium type of construction (EN ISO 13790). The U-value of the walls of the conditioned zone is assumed to be low enough so that the heat transfer through the walls can be neglected.

Ventilation heat transfer coefficient and transmission heat transfer coefficient of the window are calculated according to pr EN ISO 13789-2005 (EN ISO 13789) in Equation 6 and 7.

#### **Equation 6**

#### **Equation 7**

During heating mode, U-value is calculated by WIS software. The value integrates both heat transmittance and heat transfer by ventilation through the cavity between two skins (Dijk et al. 1996). During cooling mode, the U-value calculated by WIS stands for the heat transmittance only (Dijk et al. 1996).

## **2.2. Estimation of thermal comfort performance**

The indoor comfort near the window is evaluated by WIS, which can calculate the average surface temperature of all the window layers and the air temperature at centre and exit position of the cavity. During the heating mode, the performance of all the typologies is evaluated by the inlet air temperature at the exit of the cavity and the average internal surface temperature of the glazing. During the cooling mode, the performance is evaluated by the average internal surface temperature of the glazing. The exit air temperature and average internal surface temperature of every typology is the average value of 24 hours. Additionally, the highest hourly internal surface temperature for the sunny summer day and the lowest hourly internal surface and exit temperature of a whole day for the sunny and overcast winter days are presented to compare the comfort performance. During heating mode, the typologies with the higher exit air temperature have lower internal surface temperature because of the heat transfer from indoor environment to the cavity through internal glazing.

### **2.3. Overall evaluation of window typologies**

Each of the selected window typologies has different characteristics, advantages and disadvantages. Some perform well in heating mode, others in cooling mode, while some typologies have an excellent energy performance but provide a poor thermal comfort, etc.

In order to be able compare the different ventilated window typologies, we have defined an overall performance index for each typology by integrating all the performance parameters of energy and comfort together. The following 14 parameters are picked to calculate the index result:

- Heating energy demand in sunny winter;
- Heating energy demand in overcast winter;
- Cooling energy demand in sunny summer;
- Cooling energy demand in overcast summer;
- Lowest temperature of supplied air in sunny winter;
- Average temperature of supplied air in sunny winter;
- Lowest temperature of supplied air in overcast winter;
- Average temperature of supplied air in overcast winter;
- Lowest temperature of internal surface in sunny winter;
- Average temperature of internal surface in sunny winter;
- Lowest temperature of internal surface in overcast winter;
- Average temperature of internal surface in overcast winter;
- Average temperature of internal surface in sunny summer;
- Highest temperature of internal surface in sunny summer.

Index result values of every parameter are from 0 to 1. For the parameters of energy demand in winter and summer and comfort temperature in summer, the index values are calculated with equation:

### **Equation 8**

For all the parameters of comfort temperature in winter, the index values are calculated with equation:

### **Equation 9**

Total index result is calculated equally summing the index value of all the energy parameters and all the comfort parameters (equation 10) and the best solution is the one with the lowest index.

### **Equation 10**

The equations can make sure that the typology which has lower total index result performs better than the typology that has higher total index result. As the main feature of a ventilated window is the improvement of comfort through preheating of ventilation air, the majority of parameters included in the index are comfort related.

## **3. Results and Discussion**

For all four climatic zones the results of the investigation showed that a ventilated window typology can improve the window performance compared to a traditional closed cavity window. It was also found that solar control glass help to block out solar radiation and thus perform well in summer situations, where overheating must be prevented. In addition, windows with two layers of low-emissivity coatings were found to reduce the energy demand for heating in winter seasons.

All simulations showed that the best energy and comfort performance is obtained when the ventilated cavity is on the interior side of the window. The simulations also showed that the double

pane performs slightly better if it has air-argon 10/90 gas in the closed cavity compared to just air and even better with coatings.

According to the calculation, the results of different window typologies have almost the same tendency in different countries and directions, so it is not necessary to show the results of all the countries and for all the directions. Therefore, it has been chosen only to include the calculation results of energy consumption and thermal comfort of the ventilated window typologies facing north in Denmark, facing south in Denmark and facing south in France in this article, see figures 5, 6 and 7.

### **3.1. Performance of ventilated window typologies facing south in Denmark**

In general the energy demand for cooling of south-facing windows in a sunny summer day is the higher than other days. Additionally, the energy demand for heating of south-facing windows in a sunny winter day is higher than the overcast winter day because the outdoor temperature is quite low due to the clear sky and the solar radiation is not high enough in that day to cover the heat loss even for the south-facing windows.

#### **3.1.1. Results for low emissivity coating on a single pane (typologies 1 and 2)**

The calculated energy performance for typologies 1 and 2 are generally better than that of the closed cavity window and especially in the winter situation the energy performance improves significantly. The results are very similar for typologies 1 and 2. Slightly less energy is used, when the single pane with coating is placed internally (typology 1). For a low-emissivity coating it is preferable to place the single glazing on the exterior side. The small difference in the results can emphasize that the placement can be based on best practice in the final design phase.

From the view point of comfort, typologies 1 and 2 have better performance than that of the closed cavity. And typology 1 has the highest inlet air (cavity exit) temperature, while it has a lower internal surface temperature than typology 2 during the heating mode. But for typology 1 both the internal



surface temperatures for a sunny winter day and for an overcast winter day are higher than 14 °C which is above the dew point temperature for normal indoor winter conditions (22 °C and 50% RH).

During the cooling mode typology 1 has slightly lower internal surface temperature than typology 2.

### **3.1.2. Results for single glazing on the outside (typologies 5, 6, 7 and 8)**

The calculated energy performance for typologies 5 and 6 are worse than for the reference case, but neither of them have coatings on the panes. Typologies 7 and 8 have generally a better energy performance than the reference case with typology 8 as the best one. However, for the sunny summer case typology 7 with a low-emissivity coating needs slightly more energy for cooling than the reference case. In general the performance of low-emissivity coating is best in the winter situation, whereas the solar control glass performs best during summer.

The inlet air temperature of all the four typologies is higher than the reference case, which takes air directly from outside. Typologies 7 and 8 have lower inlet air temperature but higher internal surface temperature than typologies 5 and 6 during the heating mode. For the cooling mode, typologies 7 and 8 have slightly higher internal surface temperature. The highest internal surface temperature during summer days of typology 8 is lower than the others as well as the fluctuation of the internal surface temperature is smaller.

### **3.1.3. Results for single glazing on the inside (typologies 9, 10, 11 and 12)**

The calculated energy performance for typologies 9 and 10 are worse than for the reference case, but neither have coatings on the panes. Typologies 11 and 12 have generally better performance than the reference case with typology 12 as the best one. However, for the summer case typology 11 with a low-emissivity coating needs slightly more energy for cooling than the reference case. The solar

control glass in typology 12 has a good effect in reducing the energy demand for cooling in the summer time, but at the same time it increases the heating demand during winter slightly. As found for the typologies with single glazing inside the low-emissivity coating performs best in the winter situation, whereas the solar control glass performs best during summer.

The inlet air temperature for heating mode for all the four typologies is higher than the reference case, which takes air in directly from outside. Typologies 11 and 12 have both higher inlet air temperature and higher internal surface temperature than typologies 9 and 10 during heating mode. For the cooling mode, typologies 11 and 12 have slightly higher internal surface temperature. The highest internal surface temperature during summer days of typology 12 is lower than the others as well as the fluctuation of the internal surface temperature is smaller.

#### **3.1.4. Results for different coating positions (typologies 13, 14 and 15)**

All the results show better performance than the reference case. All results are very similar but the typologies 13 and 14 are marginally better than typology 15. The small difference in results suggests that the placement of the coating should be based on the practical experience, i.e. the coating might be best protected between the double glazing (typology 13) rather than in the ventilated air gap (typologies 14 and 15).

All the results of inlet air temperature are better than the reference case. Typologies 14 and 15 have marginally lower inlet air temperature but slightly higher internal surface temperature than typology 13 during heating mode. For the cooling mode, typologies 14 and 15 have slightly higher internal surface temperature. But the highest internal surface temperature of typology 14 is slightly lower than typologies 13 and 15.

#### **3.1.5. Cross-comparisons between groups**

For low emissivity coating on a single pane it is interesting that typology 15 compared to typologies 1 and 2 shows that only one layer of coating on an internally placed single pane performs worse than a combination of two layers of coating, i.e. the low-emissivity coating on the double glazing improves the design in terms of both energy and comfort performance.

For a single layer of glazing outside the typologies 5, 6, 7 and 8 can be compared to typology 2. Typologies 2 and 7 show very similar results, but as stated above two low-emissivity coatings reduces the energy demand. This could indicate that it may be useful to investigate other combinations of low-emissivity coatings maybe in combination with solar control glass. Both typologies 7 and 8 have worse comfort performance than typology 2 during heating mode and cooling mode.

For a single layer of glazing inside the typologies 9, 10, 11 and 12 can be compared to typology 1. Typologies 1 and 11 show very similar results. Again it is found that one layer of coating reduces the energy demand, but two layers enhance the effect. Both typologies 11 and 12 have higher inlet air temperature during heating mode.

Note that the typology 1 with two low-emissivity coatings performs almost as well as typologies 8 and 12 with solar control glass.

The groups with single glazing outside compared to the group of single glazing inside reveal that a single glazing inside generally gives the best energy performance. However, the variations in the results are relatively small, so if other considerations points to a window typology with the single glazing outside this will also be a good solution.

The comparisons between the groups of the single glazing outside and the single glazing inside also reveal that installing single glazing inside greatly improves the comfort performance in terms of inlet air temperature during heating mode. Typologies with single glazing inside perform slightly better during the cooling mode in the south and west orientation than typologies with single glazing outside.

Cross-comparison of all window typologies show that the energy demand can be reduced by a window typology with a ventilated cavity in combination with an air-argon filled double pane and a low-emissivity coating or solar control glass.

### **Figure 5**

### **3.2. Comparison of performance of window typologies facing south and north in Denmark and facing south in France**

Shown in figures 5 and 6, south-facing typologies in Denmark have higher cooling energy demand than north-facing typologies in Denmark because of the higher solar radiation in sunny summer. Furthermore, the internal surface temperature of all the south-facing typologies are approximately 5 °C higher than that of the north-facing typologies also resulted by the higher solar radiation.

According to figures 5 and 7, the cooling energy demand and the internal surface temperature of the south-facing typologies in both Denmark and France are high in sunny summer because of the higher value of the solar radiation. The cooling energy demand of south-facing typologies in France, however, is higher than that in Denmark in overcast summer because of the higher outdoor temperature in France. Furthermore, the heating energy demand of south-facing typologies in Denmark is much higher than that in France in sunny winter days, which is because of the lower outdoor temperature in sunny winter in Denmark.

### **Figure 6**

### **Figure 7**

### **3.3. Overall performance evaluation of window typologies**

According to the calculated overall evaluation index, see figure 8, typology 12 was in general found to be recommendable for all four countries. Typology 12 has an air-argon filled double pane with solar control glass combined with an interior single pane where the gap between them acts as a ventilated cavity. It performs better in terms of the combination of both the energy demand and the indoor thermal comfort. The only exception is in France on north-facing windows. Here typology 1 was found to perform better.

In all the countries, typologies with solar control glazing like typologies 8 and 12 perform worse in north orientation than in the other two orientations, which is reasonable because solar radiation in the north orientation is less problematic than the other two orientations. Therefore, typology 12 with the internal single pane has only slightly lower index value than that of typology 1 for DKN and UKN. The performance of typology 12 does not vary significantly for different orientations in Germany and United Kingdom.

### **Figure 8**

The current simulations are performed without solar shading systems, so all windows that are exposed to high amount of solar radiation have problems with overheating in summer. This explains why window combinations with solar control glass perform so well in the test.

## **4. Conclusion**

Based on the different sets of calculations with varying typologies for the windows it can be concluded that ventilated windows can be used to reduce the energy demand for cooling and/or heating and improve the indoor comfort performance depending on season.

The position of the single glazing is preferably at the internal side. In terms of energy consumption it is only slightly better than when the glazing is placed externally, but the single glazing at the internal side performs much better in terms of the inlet air temperature.

It is recommended to use a window typology like either typology 12 with an air-argon filled double pane with solar control glass combined with an interior single pane where the gap between them acts as a ventilated cavity or like typology 1 with an air-argon filled double pane with a low-emissivity coating combined with an interior single pane also coated where the gap between them acts as a ventilated cavity. The main strength of typology 12 is the superior summer performance, while typology 1 is recommended because of its better indoor comfort performance. However, typology 13 is also recommended considering its lower cost than typology 1. With only one pane of low-e coating, its energy performance is slightly worse than typology 1, while the comfort performance of typology 1 and 13 are almost the same.

However, it should be emphasized that the present evaluation is limited as it is based on an equal consideration of the four selected typical days. A simplified way to take into consideration how the different window typologies would perform on an annual basis in different climates could be based on weighting factors for the four days “sunny summer”, “overcast summer”, “sunny winter” and “overcast winter”. It would probably still be the same two typologies that would perform best but it might be useful in order to choose among them. Another important factor to consider is that the primary energy factors for cooling and heating may differ significantly, so this can also influence the final choice of the window design, i.e. it is often preferable to use active heating rather than active cooling.

Further research is recommended on combinations of solar control glass and low-emissivity coatings and solar shading devices. Calculations for other locations could be conducted in the future to investigate the performance of different windows.

Typology 12 performs best for almost all window orientations and climates. This is the typology that includes solar control glass and therefore helps to reduce cooling demand during summer. However, most windows will be equipped with movable shading device. In that case, it is useful to continue work with typologies 1 and 2. Finally, window performance may change with installation of solar shading device and therefore it is important to verify performance of preferred window typologies together with shading device.

## Nomenclature

- $Q_{H,nd}$  - is the energy need for heating [kWh]
- $Q_{H,ls}$  - are the total heat losses for the heating mode [kWh]
- $Q_{H,gn}$  - are the total heat gains for the heating mode [kWh]
- $\eta_{H,gn}$  - is the dimensionless gain utilisation factor for heating
- $Q_{C,nd}$  - is the building energy need for cooling [kWh]
- $Q_{C,ls}$  - is the total heat losses for the cooling mode [kWh]
- $Q_{C,gn}$  - are the total heat gains for the cooling mode [kWh]
- $\eta_{C,gn}$  - is the dimensionless gain utilisation factor for cooling.
- $Q_{ls}$  - are the total heat losses [kWh]
- $Q_{tr}$  - are the total transmission heat losses [kWh]
- $Q_{ve}$  - are the total ventilation heat losses [kWh]
- $Q_{gn}$  - are the total heat gains [kWh]
- $Q_{int}$  - is the sum of the internal heat gains over a given period [kWh]
- $Q_{sol}$  - is the sum of the solar heat gains over a given period [kWh]
- $A$  - is the area of each external surface of the annex with a specific orientation [ $m^2$ ]

- $I_s$  - is the global solar radiation intensity for the orientation of the respective dividing surface  
[W/m<sup>2</sup>]
- $I_{dir}$  - is direct solar radiation
- $g_{dir}$  - is g-value of direct solar radiation
- $I_{dif}$  - is diffused solar radiation
- $g_{dif}$  - is g-value of diffused solar radiation
- $H_V$  - is the heat transfer coefficient of ventilation between the ventilated window and the outside atmosphere [W/K]
- $V$  - is the airflow rate
- $\rho_a c_a$  - is the heat capacity of air per volume.
- $H_T$  - is the transmittance heat transfer coefficient of the ventilated window.
- $A_i$  - is the area of the ventilated window [m<sup>2</sup>]
- $U_i$  - is the thermal transmittance of the ventilated window [W/(m<sup>2</sup>·K)]
- $Index_i$  - is the index result of different parameters.
- $F_i$  - is the value of the evaluated typology.
- $F_{lowest}$  - is the lowest value of all the 15 typologies.
- $F_{highest}$  - is the highest value of all the 15 typologies.

## **Acknowledgements**

The research work presented in this article was carried out in the EU FP7-SME supported project CLIMAWIN—An intelligent window for optimal ventilation and minimum thermal loss, Project number 262262.



## References

Appelfeld D., Svendsen S., 2011. Experimental analysis of energy performance of a ventilated window for heat recovery under controlled conditions. *Energy and Buildings*. 43, 3200-3207.

Carlos J. S., Corvacho H., Silva P. D., Castro-Gomes J.P., 2010. Real climate experimental study of two double window systems with preheating of ventilation air. *Energy and Buildings*. 42, 928-934.

Carlos J., Corvacho H., Silva P., Castro-Gomes J.P., 2011. Modeling and simulation of a ventilated double window. *Applied Thermal Engineering*. 31, 93-102.

Chow T., Lin Z., Fong K., Chan L., He M., 2009. Thermal performance of natural airflow window in subtropical and temperate climate zones – A comparative study. *Energy Conversion and Management*. 50, 1884-1890.

Chow T.T., Lin Z., He W., Chan A.L.S., Fong K.F., 2006. Use of ventilated solar screen window in warm climate. *Applied Thermal Engineering*. 26, 1910-1918.

Dijk D. V., Goulding J., 1996. WIS Reference Manual-Advanced Windows Information System.

EN 15099, November 2003. Thermal performance of windows, doors and shading devices-Detailed calculations.

EN ISO 13789, Thermal performance of buildings-Transmission and ventilation heat transfer coefficients-Calculation method, 2005.

EN ISO 13790, Energy performance of buildings-Calculation of energy use for space heating and cooling (2008).

Häkkinen T. (ed.), Sustainable refurbishment of exterior walls and building facades, Final report, Part

A – Methods and recommendations, Espoo 2012. VTT Technology 30. 303 p. + app. 40 p.

Hazucha, J., Guidelines for complex renovations, Centrum pasivního domu, Czech Republic, This guidebook was developed in the framework of the IEE project “PASS-NET”.

[http://apps1.eere.energy.gov/buildings/energyplus/?utm\\_source=EnergyPlus&utm\\_medium=redirect&utm\\_campaign=EnergyPlus%2Bredirect%2B1](http://apps1.eere.energy.gov/buildings/energyplus/?utm_source=EnergyPlus&utm_medium=redirect&utm_campaign=EnergyPlus%2Bredirect%2B1)

Ismail K.A.R., Henríquez J.R., 2005. Two-dimensional model for the double glass naturally ventilated window. *International Journal of Heat and Mass Transfer*. 48, 461-475.

Ismail K.A.R., Henríquez J.R., 2006. Simplified model for a ventilated glass window under forced air flow conditions. *Applied Thermal Engineering*. 26, 295-302.

Kamal A.R. Ismail, Carlos T. Salinas, Jorge R. Henriquez, 2009. A comparative study of naturally ventilated and gas filled windows for hot climates. *Energy Conversion and Management*. 50, 1691-1703.

Manz H., Frank T., 2005. Thermal simulation of buildings with double-skin facades. *Energy and Buildings*. 37, 1114–1121.

Pérez-Grande I., Meseguer J., Alonso G., 2005. Influence of glass properties on the performance of double-glazed facades. *Applied Thermal Engineering*. 25, 3163–3175.

Saelens D., 2002. Energy performance assessment of single storey multiple skin facades, Ph.D. Thesis, Catholic University Leuven, Belgium.

Saelens D., Roels S., Hens H., 2005. Optimization of the energy performance of multiple-skin facades. Ninth international IBPSA Conference, Montréal, Canada.

Saelens D., Roels S., Hens H., 2006. Strategies to improve the energy performance of multiple-skin

facades. Building and Environment. doi:10.1016/j.buildenv.2006.06.024.

Share of total energy consumption by fuel in 2007, European Environment Agency, published on 15 April 2010 <http://www.eea.europa.eu/data-and-maps/figures/share-of-total-energy-consumption>.

### **Figure captions**

Figure 1: The 15 different window typologies used in this study.

Figure 2: Illustration of the ventilation concepts: Cooling mode (left) and Heating mode (right).

Figure 3: Danish weather data for the four selected typical days. (OSDK: overcast summer Denmark; SSDK: sunny summer Denmark; OWDK: overcast winter Denmark; SWDK: sunny winter Denmark.)

Figure 4: French weather data for the four selected typical days. (OSFR: overcast summer France; SSFR: sunny summer France; OWFR: overcast winter France; SWFR: sunny winter France.)

Figure 5: Energy demand and thermal comfort results of all the window typologies for south facing orientation in Denmark.

Figure 6: Energy demand and thermal comfort results of all the window typologies for north facing orientation in Denmark.

Figure 7: Energy demand and thermal comfort results of all the window typologies for south facing orientation in France.

Figure 8: Overall evaluation index results of all the window typologies, orientations and climatic conditions.

$$Q_{H,nd} = Q_{H,ls} - \eta_{H,gn} \cdot Q_{H,gn} \text{ Equation 1}$$

$$Q_{C,nd} = Q_{C,gn} - \eta_{C,ls} \cdot Q_{C,ls} \text{ Equation 2}$$

$$Q_{ls} = Q_{tr} + Q_{ve} \text{ Equation 3}$$

$$Q_{gn} = Q_{int} + Q_{sol} \text{ Equation 4}$$

$$I_s \cdot g \cdot A = (I_{dir} \cdot g_{dir} + I_{dif} \cdot g_{dif}) \cdot A \text{ Equation 5}$$



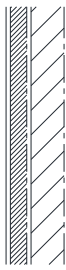

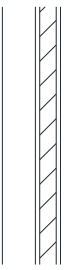
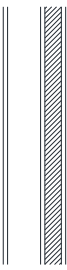









$$H_V = \rho_a \cdot c_a \cdot V \text{ Equation 6}$$

$$H_T = A_i \cdot U_i \text{ Equation 7}$$

$$Index_{i\_energy} = \frac{F_{i\_energy} - F_{lowest\_energy}}{F_{highest\_energy} - F_{lowest\_energy}} \text{ Equation 8}$$

$$Index_{i\_comfort} = \frac{F_{i\_comfort} - F_{highest\_comfort}}{F_{lowest\_comfort} - F_{highest\_comfort}} \text{ Equation 9}$$

$$Index_{total} = \frac{Index_{i\_energy}}{4} + \frac{Index_{i\_comfort}}{10} \text{ Equation 10}$$

Typ 1	Typ 2	Typ 3	Typ 4	Typ 5	Typ 6	Typ 7	Typ 8
							
Typ 9	Typ 10	Typ 11	Typ 12	Typ 13	Typ 14	Typ 15	
							






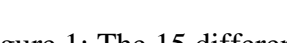
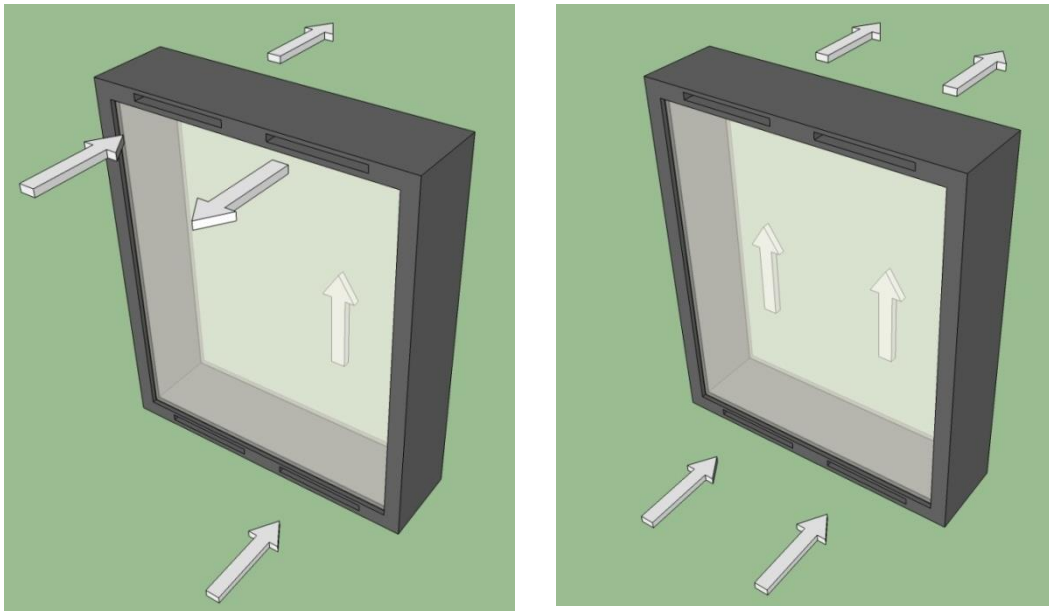
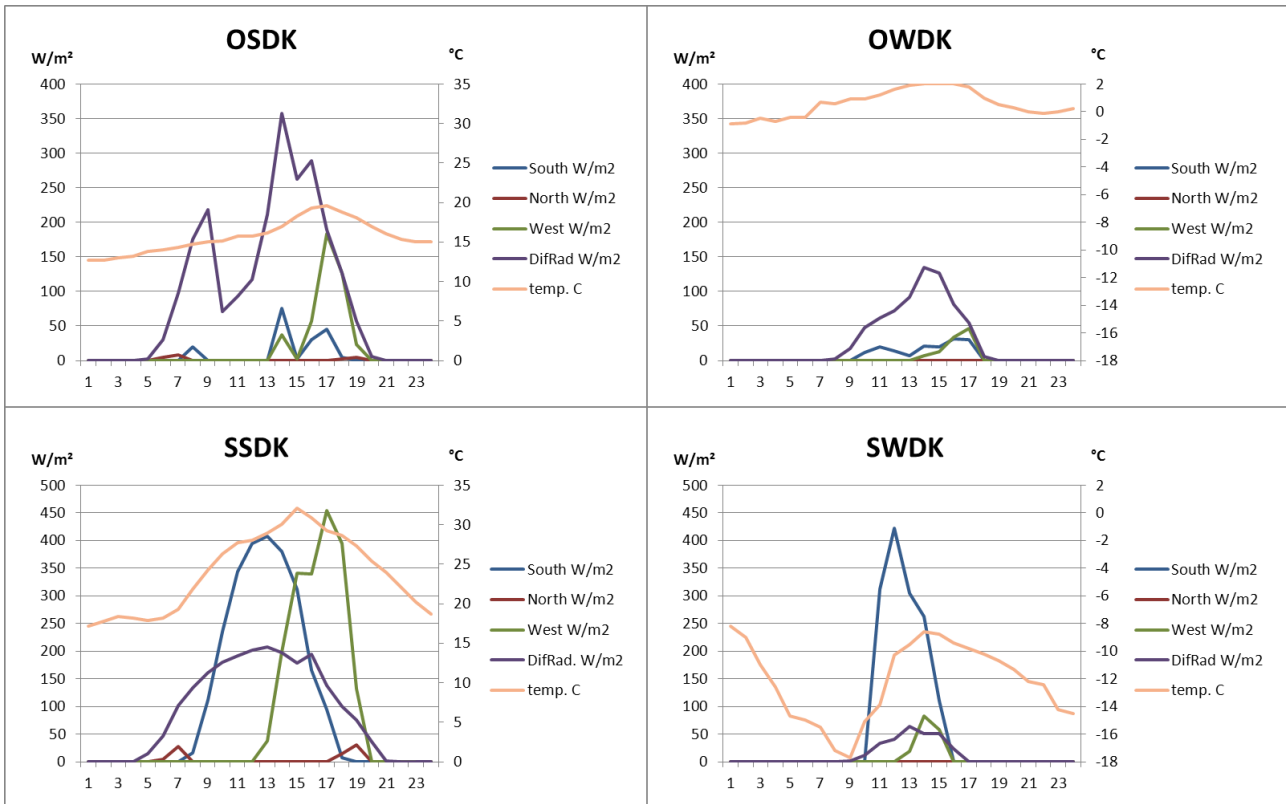
-  Closed cavity, air
-  Ventilated cavity
-  Glass
-  Closed cavity, air-argon 10/90
-  Low-E coating
-  Solar control glass coating

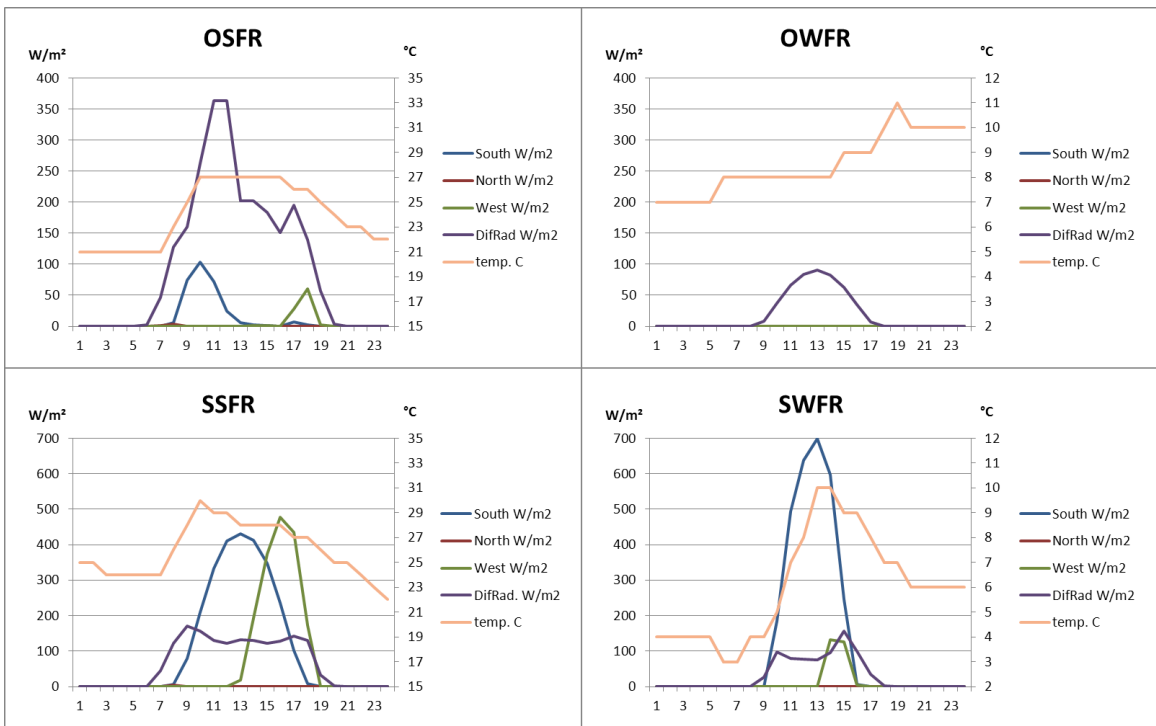
Figure 1: The 15 different window typologies used in this study.



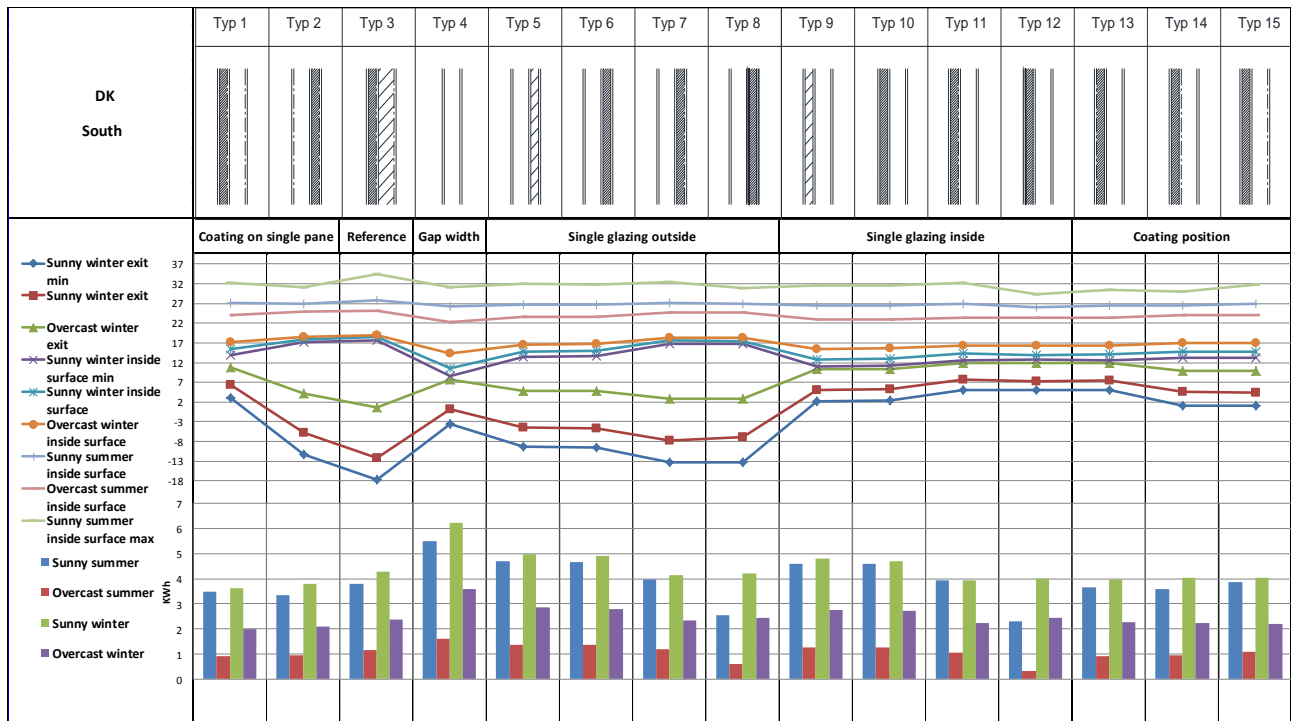
**Figure 2: Illustration of the ventilation concepts: Cooling mode (left) and Heating mode (right).**



**Figure 3: Danish weather data for the four selected typical days. (OSDK: overcast summer Denmark; SSDK: sunny summer Denmark; OWDK: overcast winter Denmark; SWDK: sunny winter Denmark.)**



**Figure 4: French weather data for the four selected typical days. (OSFR: overcast summer France; SSFR: sunny summer France; OWFR: overcast winter France; SWFR: sunny winter France.)**



**Figure 5: Energy demand and thermal comfort results of all the window typologies for south facing orientation in Denmark.**

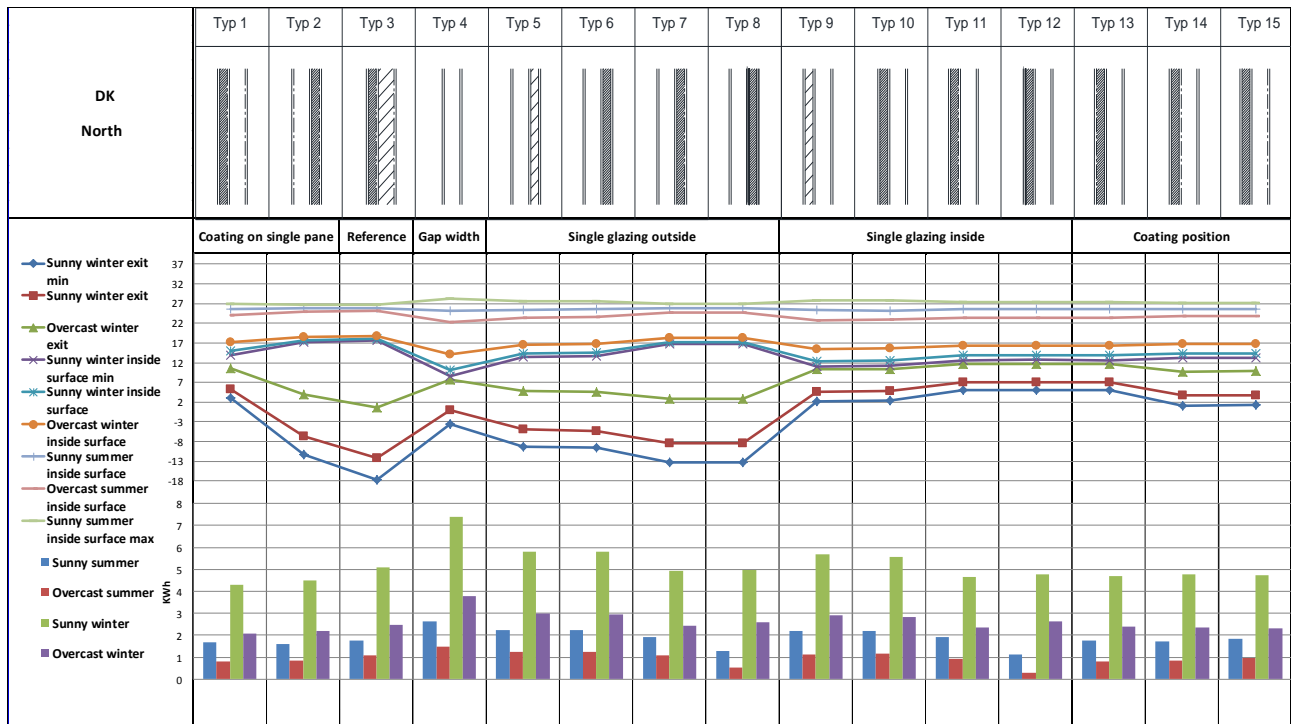


Figure 6: Energy demand and thermal comfort results of all the window typologies for north facing orientation in Denmark.

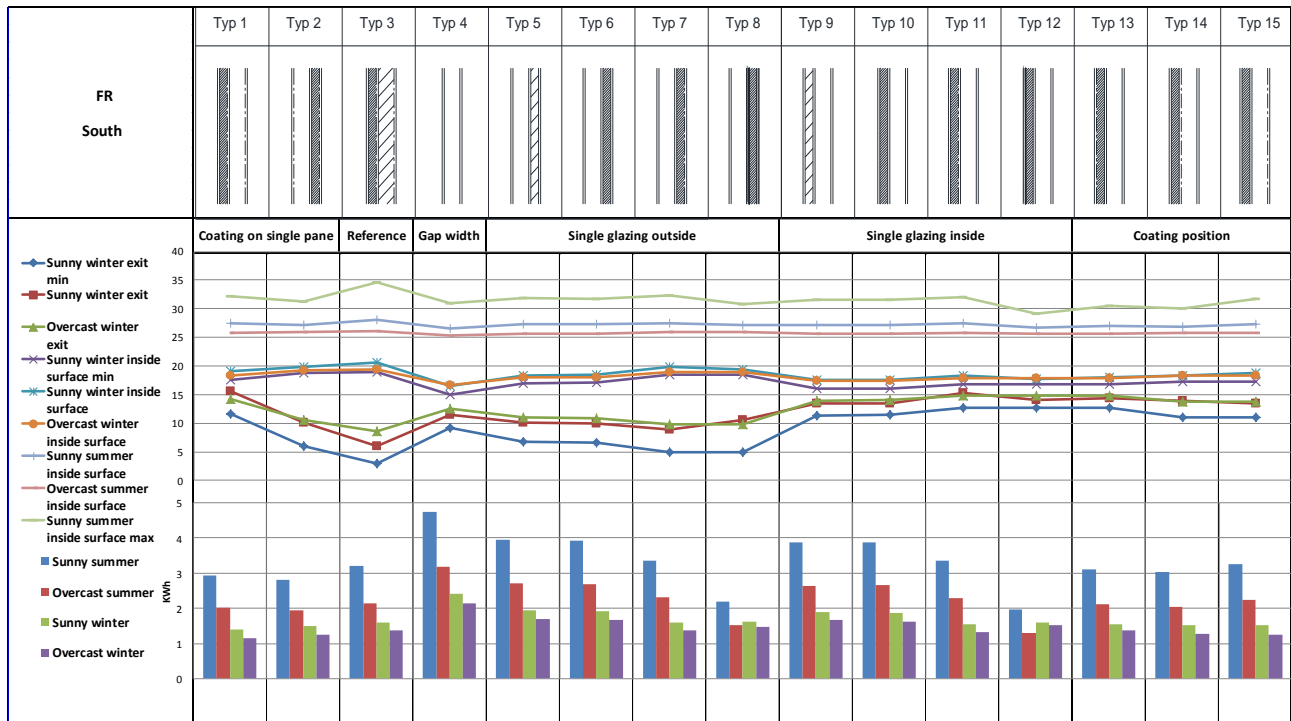
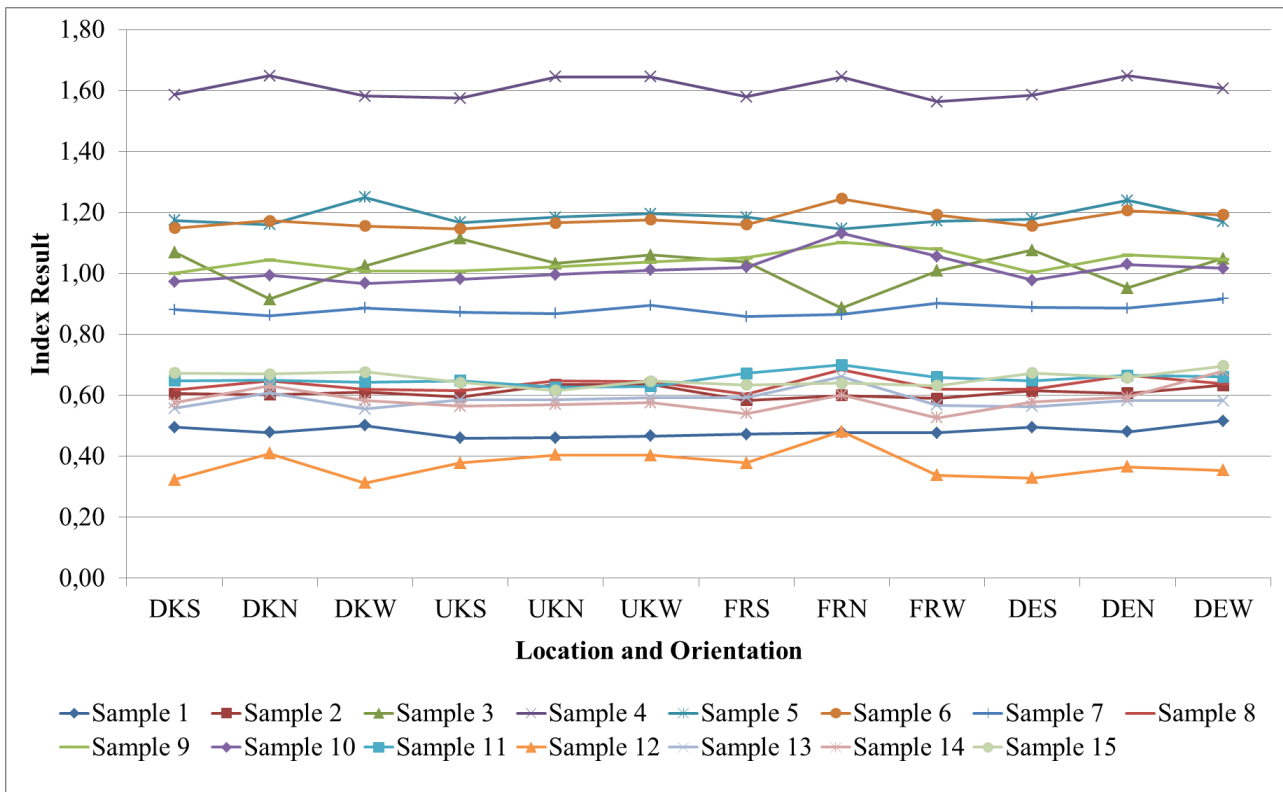


Figure 7: Energy demand and thermal comfort results of all the window typologies for south facing orientation in France.





**Figure 8: Overall evaluation index results of all the window typologies, orientations and climatic conditions.**